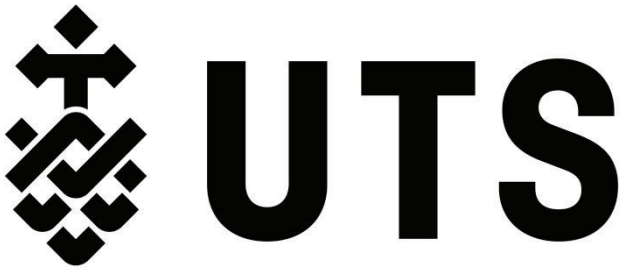

The Potential of exosomal RNAs as biomarkers for Prostate Cancer

Samuel Brennan

Doctor of Philosophy C02031

April 2018

Biosafety Approved: 2003-02-R-G

CONFIDENTIAL THESIS

The following thesis should be treated as confidential and examined as such.

The subject matter shows a potential commercial opportunity and forms part of a UTS invention disclosure #DISC-UTS-000443.

It is further requested that no copies of the thesis are placed in the UTS library or made publicly available for a period of at least 12 months following the thesis submission date.

All copies of the student thesis should be returned to the student's supervisor Dr Rosetta Martiniello-Wilks, apart from (1) copy (preferably in electronic format) that should be stored by the Research and Innovation Office with the above invention disclosure.

CERTIFICATE OF ORIGINAL AUTHORSHIP

I certify that the work in this thesis has not previously been submitted for a degree nor has it been submitted as part of requirements for a degree except as part of the collaborative doctoral degree and/or fully acknowledged within the text.

I also certify that the thesis has been written by me. Any help that I have received in my research work and the preparation of the thesis itself has been acknowledged. In addition, I certify that all information sources and literature used are indicated in the thesis.

This research is supported by an Australian Government research Training Program Scholarship.

Signature of Student:

Production Note:
Signature removed prior to publication.

Date:12/4/2018

Acknowledgements

First and foremost I want to thank my parents who built an unshakeable foundation of kindness and curiosity in our home that inspired my love of science and gave me the drive to seriously pursue it. I also want to thank my loving and beautiful partner Jenny who listened with enthusiasm and curiosity to the minutiae of the project itself, and with great sympathy and understanding whenever I was feeling overwhelmed, stupid and hopeless.

I also wish to thank my primary supervisor Dr Gyorgy Hutvagner without whom I could not have finished this project. Many thanks also go to my co-supervisor Dr Rosetta Martiniello-Wilks who gave many, many hours to this project. I also wish to thank Dr Nham Tran for his contributions to my early work. To Dr Aled Clayton, your supervision of my work in 2013 showed me how satisfying science can be at its very best. It was a truly formative experience that I'm very grateful for. Dr Eileen McGowan, your sage advice about everything from experimental design to scientific writing has been absolutely invaluable over the years I've been here. Perhaps most importantly your contagious enthusiasm for science helped me keep my head above water when all I wanted to do was quit.

I also want to thank all my friends, many of whom came through the same arduous process of getting their PhDs alongside me. Pat, having you around the lab made it a fun place to be whether we were turning a critical eye towards some wonky Ct values or to whether or not "Bugatti" is a great piece of rap music (Okay I admit it, it's not). Rosaline you have been a wonderful and stalwart friend throughout our entire university careers and I can't think of a single moment when you weren't there for me!

And this acknowledgement could never be complete without thanking Rob, Sophie, Elliot, Marty, Pam, Pete, Eunji and Ben. You guys have been inspiring me to be the very best person I can be since our days as undergraduates.

Table of Contents

List of Tables and Figures

Abstract

Prostate cancer (PCa) is currently the most diagnosed cancer of Australian men, and the incidence is likely to keep increasing given our ageing population. Compounding this issue is the fact that the available tests are either discouragingly invasive, or lacking in specificity/sensitivity and offer no prognostic information. To overcome these issues we have been profiling the RNA content of exosomes isolated from PCa cell lines and patient body fluid samples including urine, plasma and saliva and have developed a miRNA signature for the diagnosis of early PCa. The large bodies of data also afforded an opportunity to probe the functional potential of exosomal RNAs. This was done using *in silico* methodologies as well as some experiments regarding the role of PCa exosomal RNAs in the tumour microenvironment.

Urine exosomal miRNAs (exomiRs) provided the most robust diagnostic signature found during this project. They also hold some potential as prognostic and treatment response markers for PCa. Furthermore, urinary exomiRs can be harvested from patients in a non-invasive manner which is a significant step forward in the clinical care of PCa. The expression profile of urine exomiRs will be investigated in future experiments on much larger sample sizes to confirm the diagnostic and prognostic potential highlighted by this project. ExomiRs may also have roles in PCa immune evasion with the potential to inhibit the tumour killing and proliferative abilities of cells within the immune system, most likely natural killer cells and dendritic cells. This work needs further biological validation in future experiments. PCa exosomes were also shown to be potent inducers of myofibroblast transdifferentiation which suggests that PCa exosomes are in part responsible for metastatic progression of the disease. However, PCa exomiRs do not appear to be absorbed by recipient cells and do not impact the process of myofibroblast transdifferntiation.

Chapter 1: Introduction

1.1 Prostate Cancer (PCa) incidence, diagnosis and disease management

The prostate is a small exocrine gland located directly below the bladder and surrounds the urethra in the male genitourinary tract. The prostate is responsible for the production of enzymes involved in the liquefaction of semen. The prostate also contains smooth muscle tissue which aids in expulsion of semen during ejaculation. Most PCas (~98%) arise from the glandular cells, and are thus termed adenocarcinoma (1). Surprisingly, the highest incidence of PCa occurs in Australia and New Zealand (Figure 1.1.)

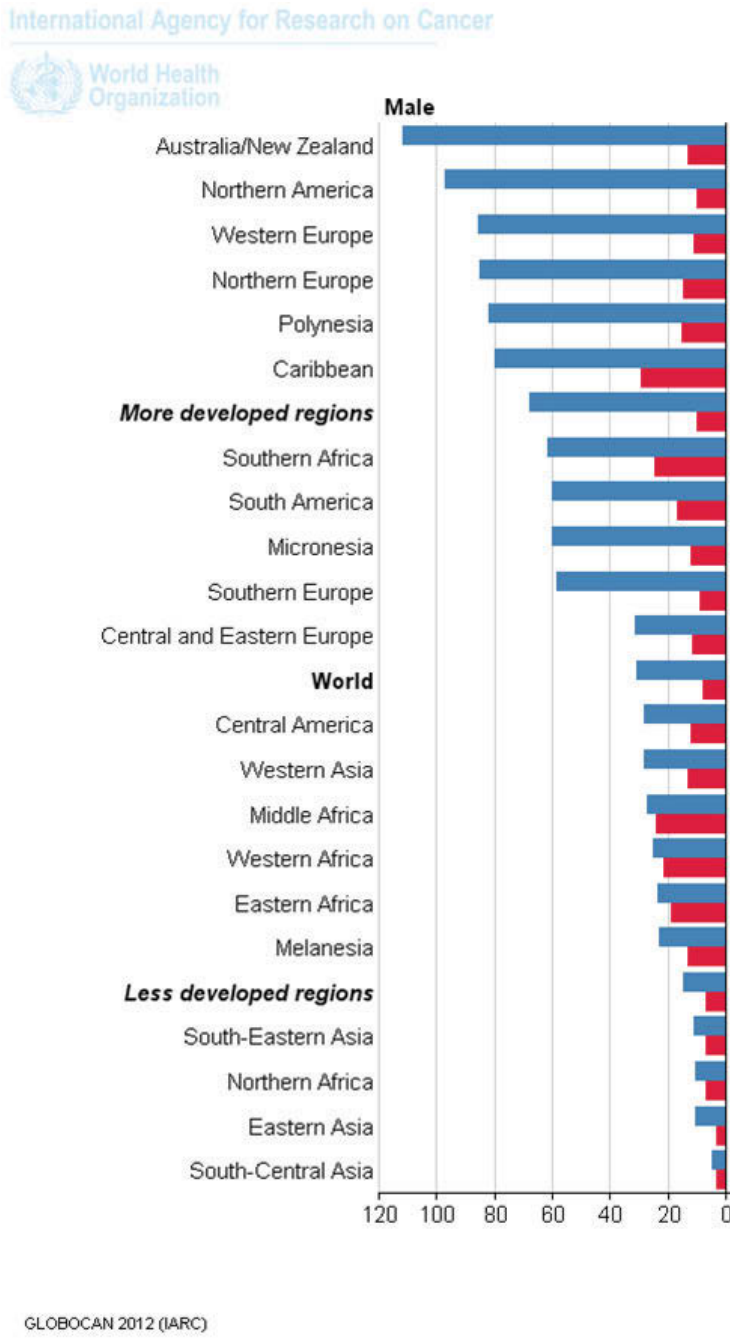

Figure 1.1. 2012 Globocan data showing PCa incidence (Age Standardised Rate).

Estimated Age Standardised Rates of prostate cancer per 100 000 population throughout the world. Australia and New Zealand have the highest incidence rate in the world with 111.6 cases per 100 000 people.

The high frequency of PCa in Australia is largely due to the increased prevalence of screening programs. Blood PSA levels are regularly screened in men. If high PSA levels are detected, men undergo a Digital Rectal Examination (DRE) of the prostate and an invasive prostate biopsy (usually 12 tissue samples (2, 3)) is taken for histological PCa diagnosis by a pathologist. Once a diagnosis has been made, there are several treatments available for early PCa, however advanced PCa that has spread outside the prostate is largely incurable and can only be managed with radiotherapy, chemotherapy or androgen ablation therapy provided the PCa is androgen sensitive (Figure 1.2.).

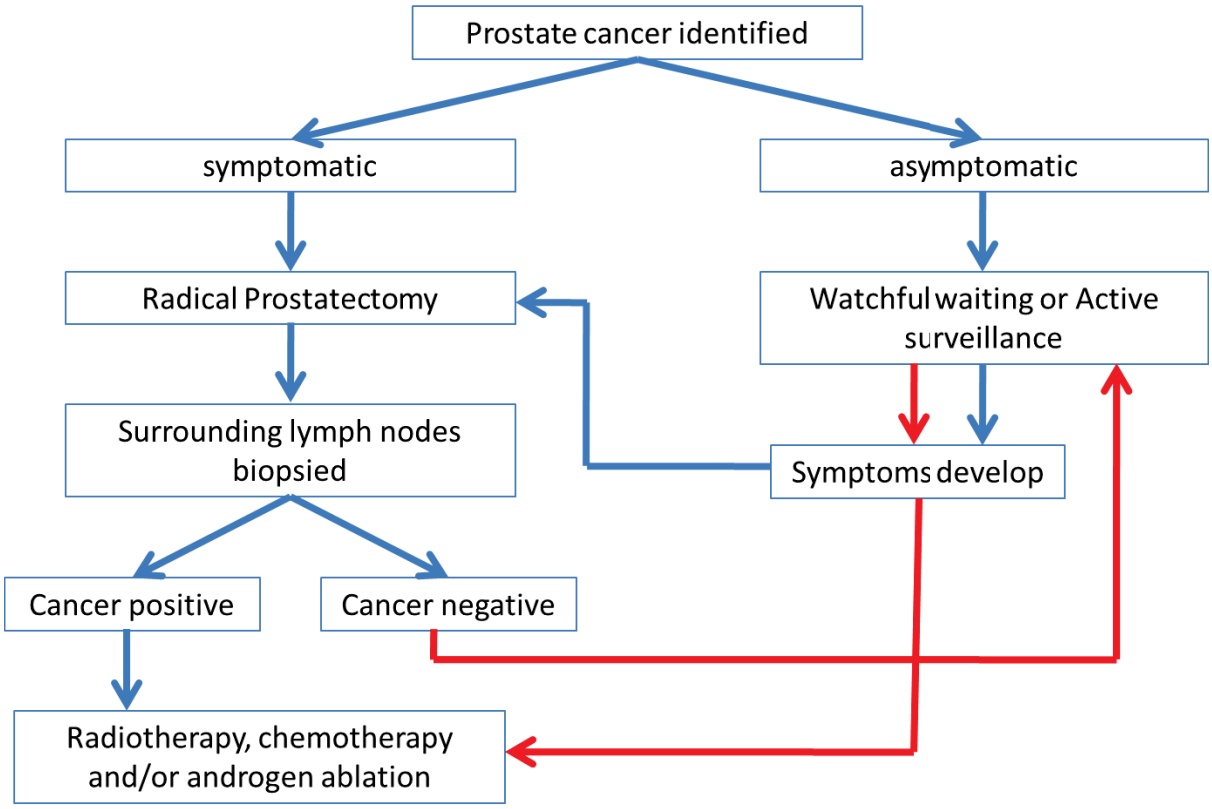

Figure 1.2. Common sequence of PCa treatment.

For organ confined prostate cancer, the most effective treatment is radical prostatectomy sometimes utilising robotic assistance and laparoscopic (keyhole) surgery. During this surgery, biopsies of the surrounding lymph nodes are also made to assess cancer spread, which determines further treatments. If cancer has spread to lymph nodes within the prostate region (blue arrows), radiotherapy is a likely next step and has been shown to increase life expectancy by an average of two years (4). Many men are free of prostate cancer for at least 10 years after radiotherapy, with lower rates of impotence compared to even the best nerve-sparing surgeries (5). Some prostate cancers also respond to androgen ablation therapy, in which testosterone release is inhibited pharmacologically or by removal of the testes which are responsible for the production of testosterone. If the lymph node biopsy is cancer negative, patients undergo medical supervision in case the cancer recurs (red arrows). If PCa does appear elsewhere in the body, radiotherapy, chemotherapy and/or androgen ablation therapy can be administered.

In most cases of PCa, life-threatening disease does not develop rapidly and can be delayed using less aggressive therapies than radical prostatectomy if they are administered early in cancer progression (5). This highlights the need for more sensitive early detection methods to minimise mortality and improve patient outcome.

1.1.2. Future molecular diagnostics for PCa

The current molecular diagnostic for PCa, the Prostate Specific Antigen (PSA) test involves taking blood from a patient and analysing the concentration of circulating PSA. Historically, men with a PSA above 4.0 ng/mL who also have evidence of PCa during their Digital Rectal Exam (DRE) are recommended for further, more definitive diagnostic procedures such as a prostate biopsy. Unfortunately, the PSA test lacks both sensitivity. In an assessment made by the American Cancer Society, sensitivity of detection was reported at a maximum value of 68.8 %. However, this was when looking at aggressive PCa with a high Gleason Score (≥ grade 8). The average sensitivity was actually 32.2% when a more general population of men was analysed (6). The specificity for men with PSA levels between 4.0 ng/mL and 10 ng/mL is however improved when the ratio of free-to-total PSA is used for assessment. This test differentiates between the amount of PSA that is actually free in the plasma versus how much is bound to plasma proteins. Using this approach, 56% of PCa were detected (7), but this level is still low. It has been determined in subsequent assessments that the use of free-to-total PSA is only useful at the extremes of the ratio. The PSA test can also complicated by other health factors such as the presence of Benign Prostatic Hyperplasia (BPH) and bacterial prostatitis (8) , two fairly common conditions in elderly men.

Because of the difficulties interpreting the PSA test caused by low sensitivity, overtreatment has become an issue in the clinical care of PCa. Firstly, not all PCa are life threatening and many may never progress to a point where they even lower the quality of life as Haas and Sakr found when they learned that 80% of men who died at 70 or above were positive for PCa but died of causes unrelated to it (9). The first risk associated with over-diagnosis is the confirmatory prostate biopsy that is a highly invasive procedure with a small risk of infection or prolonged bleeding (10). If the tumour size and grade are considered clinically significant after this procedure (80% of PCa are considered clinically significant (11)) treatment may be attempted. The treatments themselves are responsible for causing urinary incontinence, bowel problems and sexual dysfunction (12-14). Current estimates put over-diagnosis between 23% and 42% of PCa cases largely thanks to PSA use as a screening tool (15).

These data reveal the need for new molecular diagnostics to augment or replace the PSA test with something that offers definitive diagnostic power and potentially the ability to stratify patients according to their risk of developing life-threatening cancer. There are a large number of candidate molecules currently under investigation, but the focus of this thesis will be on noncoding RNAs such as microRNAs and long noncoding RNAs. MicroRNAs in particular are known to exist in stable forms in plasma (16) that can survive for extensive periods of time at -80^{0}C (17). Given the highly specific expression patterns exhibited by microRNAs and long noncoding RNAs in various cancers, they are ideal biomarker candidates. Analysing the expression profiles of PCa cells and their secreted exosomes also offers a unique opportunity to determine potential mechanisms by which these noncoding RNAs contribute to the growth and progression of PCa cells. What follows is an introduction into the origins and functions of noncoding RNAs and their roles in PCa.

1.2. Noncoding RNA structure and function

Noncoding RNAs are transcribed from the genome, but they are rarely translated into protein. However, these RNAs are functional and tissue specific just as their protein coding cousins are. Noncoding RNAs are often found in regulatory roles influencing the amount of specific proteins being produced or by modifying the function of proteins or other RNAs. Noncoding RNAs can also be responsible for contributing to the hallmarks of cancer as laid out by Hanahan and Weinberg (18). There is a huge diversity of structure and function in the field of noncoding RNA, but for the purpose of this dissertation, two main families of noncoding RNA were focused on: MicroRNAs (miRNAs), and long noncoding RNAs (lncRNAs).

1.2.1 The miRNA gene family

The very first miRNA, lin-4 was described as part of an early genetic screen in 1974 (19) in the nematode worm *C. elegans*. It was observed that particular mutants termed "lin-4" showed a very specific set of developmental defects. At this time, little was known about the mechanistic pathway of lin-4, let alone the role of miRNAs. It was not until 1993 that the mechanism by which this set of mutations occurred was first described (20). It was determined that lin-4 was not a protein, but rather a small non-coding RNA which exerted its regulatory effect by an antisense interaction with the 3'UTR of the lin-14 mRNA. It was seven years later that the next small, non-coding regulatory RNA was discovered and its function determined (21). This miRNA is known as let-7 and was also discovered in *C. elegans*. Like lin-4, let-7 is involved in the control of growth and development via antisense RNA interactions with target mRNA molecules. Since its initial discovery, let-7 homologues have been discovered in many different species, including *Homo sapiens* and *Drosophila melanogaster* (22).

The final revelation that miRNAs have a profound regulatory role throughout the animal kingdom came in 2001. Three independent groups (23-25) rapidly expanded the library of known miRNAs and their functions in *C. elegans* and demonstrated the conservation of sequence and function within bilaterian organisms. Since this landmark discovery, thousands of miRNAs have been identified in a vast array of organisms and has led to a significant rise in understanding the complexity of gene regulation in cell biology. Most relevant to this thesis is the fact that many miRNAs have emerged as tumour suppressors or oncogenes(26).

1.2.2. miRNA Biogenesis

Most miRNA genes are transcribed by RNA Polymerase II (27) in the nucleus from intergenic regions, or within the introns of a host gene. The resulting primary miRNA transcript (Pri-miRNA) can be several kilobases long and may contain multiple mature miRNAs. The mature miRNAs themselves are found in stem-loop structures which are recognised by the microprocessor complex which consists of the RNAse III enzyme Drosha (28) and DGCR8, an RNA binding protein (29, 30). These two enzymes catalyse the release of the stem-loop structures, yielding transcripts of approximately 70 nucleotides known as pre-miRNAs. These transcripts harbour the effector miRNA molecule and are transported to the cytoplasm for final biogenesis. Export of the pre-miRNAs occurs via the Ran-GTP dependent exportin-5 pathway (31). This process is outlined in Figure 1.3.

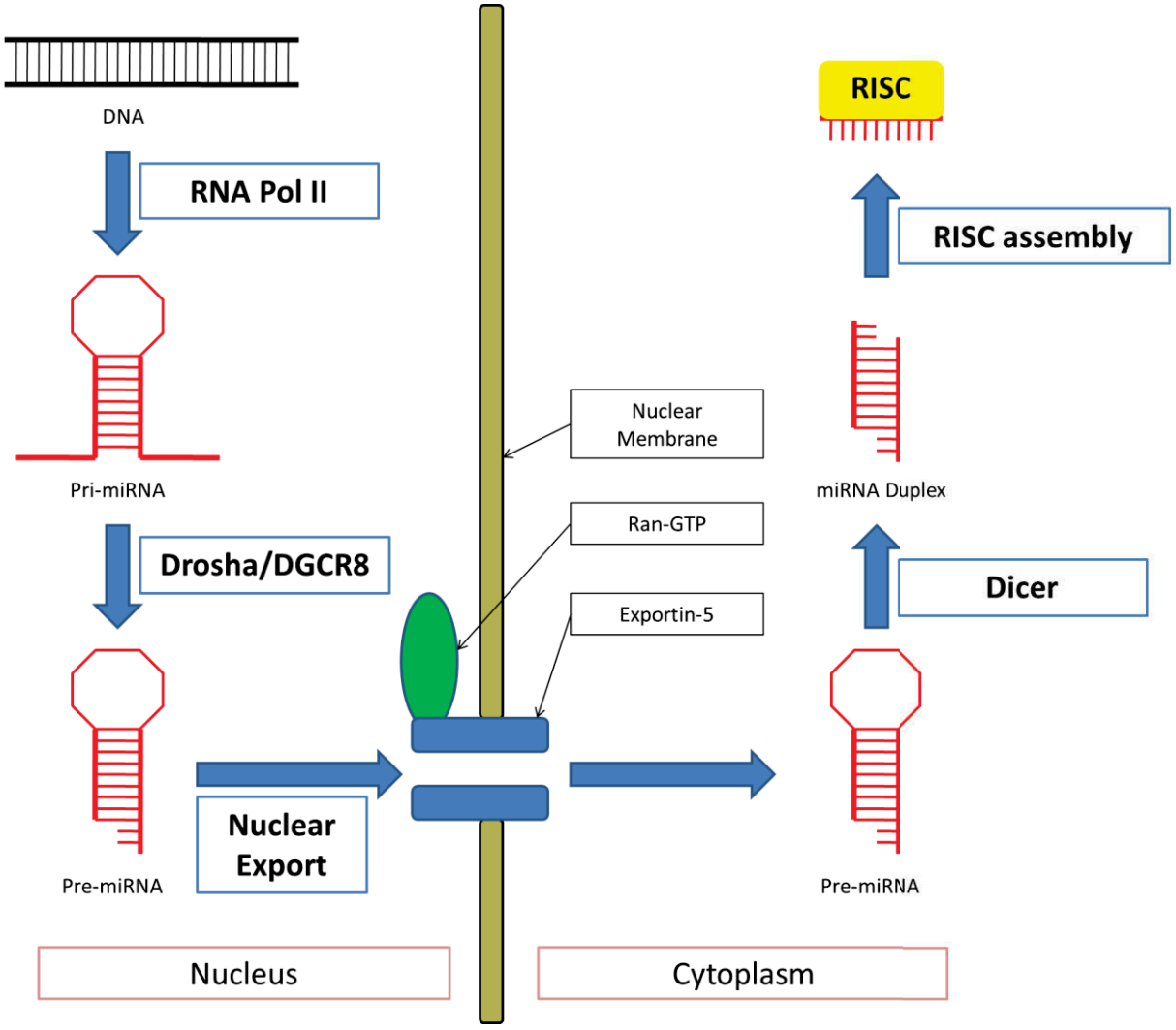

Figure 1.3. miRNA biogenesis in mammalian cells.

RNA Pol II transcribes the miRNA from the genome as a long pri-miRNA with one or more stem loop structures embedded in the transcript. The Microprocessor complex consisting of Drosha and DGCR8 then cleaves out the stem loop structure leaving behind the pre-miRNA. The pre-miRNA is then transported from the nucleus to the cytoplasm via Exportin-5 in a RAN-GTP dependent manner. Once in the cytoplasm, the pre-miRNAs are subject to a final round of RNAse III cleavage, by Dicer (32). This enzyme cleaves the loop from the pre-miRNA, resulting in a 21-22 nucleotide double stranded RNA (dsRNA) molecule with a two nucleotide 3' overhang and a 5' phosphate group. This dsRNA structure is the miRNA duplex which is incorporated into an RNA Induced Silencing Complex (RISC), which mediates gene silencing (see Figure 1.4).

1.2.3 miRNA function

Generally, miRNAs function to inhibit the protein expression of a mRNA transcript or group of transcripts. There are currently three mechanisms by which this is known to occur: Translational repression, mRNA destabilisation and target mRNA cleavage.

1.2.4. miRNAs repress translation and destabilise their target mRNA

It has been proposed that translational repression and mRNA destabilisation are related. This begins with initial translational repression, followed by rapid mRNA degradation which is initiated by deadenylation and removal of the 5' cap (Figure 1.4.) (33). Translational repression is currently thought to occur by two different mechanisms, repression of translation initiation and repression of post-initiation steps (34).

Subsequent to translational repression, mRNA decay is a likely next step for miRNA repressed mRNAs. MRNAs are targeted to degradation pathways via deadenylation, in which the poly-A tail is enzymatically removed. This model involves the recruitment of various other proteins to RISC, by interactions with GW182, an adaptor protein that binds to the minimal RISC, a complex of a miRNA and AGO2 (reviewed in (33, 35)). Once bound to the minimal RISC, GW182 recruits the Carbon Catabolite Repression 4-Negative On TATA-less (CCR4-NOT) complex, which deadenylates RISC bound mRNA transcripts (36). Also essential to deadenylation is Poly-A Binding Protein (PABP), which may mediate translational repression by two mechanisms. Firstly, it may orient the poly-A tail nearer to the CCR4-NOT deadenylation complex, increasing the rate of deadenylation. Furthermore, CCR4-NOT recruits Deadbox Helicase 6 (DDX6) which enhances the degradation of the target mRNA even further (37, 38).

PABP also promotes translation via interactions with ribosomal components (39) and co-factors (40-43), so the immobilisation of PABP by the RISC may prevent the formation of functional ribosomes and thus prevent translation (35). Deadenylation is often followed by decapping, in which the 5' terminal cap (M^7G) is removed from the mRNA by the DCP1/2 complex (44). Once decapped, mRNAs are susceptible to 5' to 3' exonucleolytic digestion by exoribonuclease (Xrn1) which degrades the mRNA (45). Current understanding is that RNA destabilisation accounts for 66 – 90% of observed target mRNA repression (46).

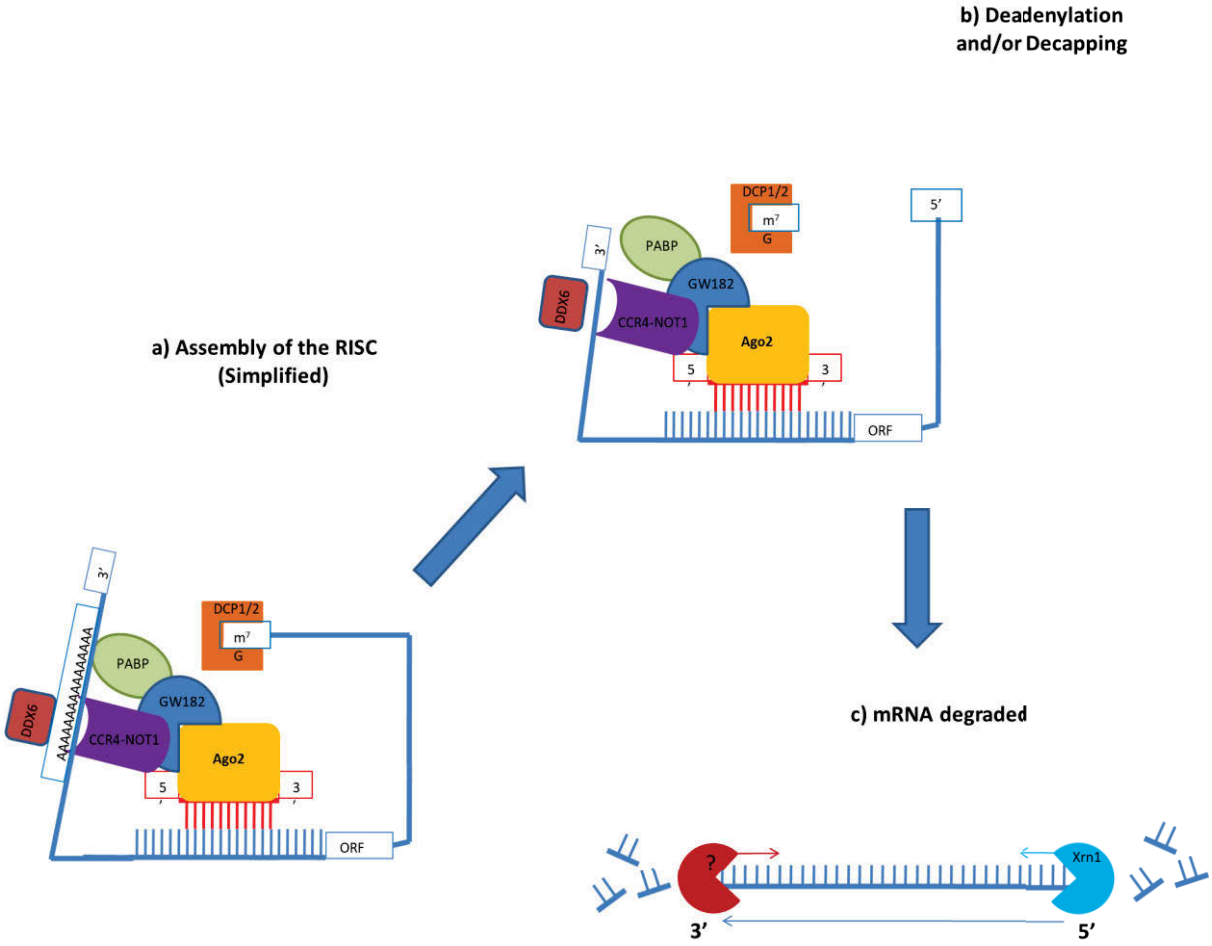

Figure 1.4. Model showing RISC components and activity.

a), The miRNA guides the RISC to its binding site in the 3' UTR of its target mRNA transcript between the poly-A tail at the 3' end and the Open Reading Frame (ORF) towards the 5' end. **b)** AGO2 is the fundamental part of the RISC and is responsible for recruiting other effector enzymes GW182, CCR4-NOT1, PABP and DDX6. The RISC is then able to remove the poly-A tail, and remove the 5' methyl cap which destabilises the mRNA, allowing it to be degraded by exonucleases in **c)**.

1.2.5. miRNAs can cleave target mRNA

Unlike the mechanisms of mRNA degradation, miRNA target cleavage requires a much greater degree of complementarity throughout the miRNA guide strand and its target sequence. Ago2 is able to cleave the miRNA:mRNA complex between nucleotides 10 and 11 of the miRNA strand (47-49). mRNA cleavage is a function of the Ago2 PIWI domain which possesses RNase H activity (50). This mechanism of miRNA directed repression was demonstrated in mouse embryos (49) where miR-196 directed cleavage of HOXB8 mRNA fragments was observed. This mechanism is uncommon in the animal kingdom but is dominant in plant RNA interference (51). Target cleavage due to high complementarity is also exploited in gene knockdown studies to identify the function of a gene or gene set in mammalian systems.

1.2.6. The role of miRNAs in PCa cells

MicroRNAs now have well established roles in cancer development and progression (52-54) but there are 2588 miRNAs mature miRNA sequences currently identified in miRBase, the online repository for all known miRNAs (55). Given this large volume of data, the functions of many miRNAs with respect to cancer biology are yet to be elucidated. Table 1 below summarises the diverse roles of miRNAs identified in PCa at the time of writing and also illustrates the varying influence of these miRNAs. For example, miR-21 regulates such an expansive group of target genes that it has been implicated in almost every aspect of cancer development and progression, while miR-24 has only one validated target and contributes only to apoptosis resistance.

MicroRNA expression may also be tissue specific, or specific to a type or stage of cancer, making them ideal biomarkers. MicroRNA based biomarkers that identify the presence of cancer have been identified in several cancers as well as markers that offer prognostic (outcome) value. This is the case with miR-141, whose presence in serum correlates strongly with the presence of stage 4 (advanced) colon cancer showing poor prognosis (56). MiRNAs with established roles in PCa growth and progression are outlined in Table 1.1.

Table 1.1. miRNAs identified in PCa to date.

Ref.	miRNA	Known Target(s)	miRNA Expression in PCa	Result of miRNA Dysregulation
(57)	miR-let7a	E2F2, CCND2	Under expression	Enhanced cell proliferation
(57)	miR-1	Exportin-6, Tyrosine Kinase 6,	Under expression	Altered actin dynamics
(58)	miR-7	KLF4	Under expression	Enhances PCa stem cell formation
(59)	miR-15a & miR-16	BCL-2, CCND1, WNT3A, VEGF	Under expression	Resistance to apoptosis, enhanced cell proliferation, increased expression of oncogenes, angiogenesis
(60)	miR-23a	PAK6	Under expression	Increased metastatic potential
(57, 61)	miR-34	CDK4, CDK6, Cyclin D1, Cyclin E2, E2F3, BCL-2, SIRT1	Under expression	Increased PCa initiation and progression. Dependent on lack of P53.
(62)	miR-96	-	Under expression	Cancer recurrence after surgery
(63)	miR-99	SMARCA5, SMARCD1	Under expression	Enhanced cell proliferation, Increased PSA production
(57)	miR-101	EZH2	Under expression	Enhanced proliferative and invasive capabilities

(57)	miR-107	granulin	Under expression	Enhanced cell proliferation
(57)	miR-143	MYO6, ERK5	Under expression	Increased cell migration and proliferation
(57)	miR-145	MYO6, BNIP3L->AIFM1, CCNA2, TNFSF10	Under expression	Apoptosis resistance, increased cell migration
(64)	miR-146a	ROCK1, CXCR4	Under expression	Promote metastasis
(57)	miR-148a	MSK1	Under expression	Enhanced cell proliferation, drug resistance
(65)	miR-126*	Prostein	Under expression	Promotion of cell migration and invasion
(57, 59)	miR-205	PRKCE, ZEB2, E2F1, Il-24, IL-32, Cepsilon	Under expression	Apoptosis resistance, enhanced proliferative ability, androgen independence
(66)	miR-296	HMGA1	Under expression	Enhanced cell proliferation and invasiveness
(57)	miR-331-3p	ERBB-2, CDCA5, KIF23	Under expression	Altered signal transduction via the androgen pathway.

(57)	miR-449a	HDAC1	Under expression	Enhanced cell proliferation
(57)	miR-1296	MCM (various)	Under expression	Enhanced cell proliferation
(57)	miR-20a	E2F1-3	Enrichment	Enhanced proliferative capabilities, apoptosis resistance
(57, 59)	miR-21	PDCD4, PTEN, SPRY2, TIMP3, RECK, AKT	Enrichment	Increased cell motility, adhesion , invasiveness and membrane trafficking, apoptosis resistance
(57)	miR-24	FAF1	Enrichment	Apoptosis resistance
(57)	miR-25	E2F1	Enrichment	Apoptosis resistance
(59)	miR-32	BIM, BTG2, PI3KIP1	Enriched	Apoptosis resistance
(67)	miR-100	-	Enrichment	Biochemical recurrence
(59)	miR-106b-25-93	E2F1, $p21^{waf1}$	Enriched	Apoptosis resistance
(57, 59)	miR-125b	Bak1, BBC3, p53, HER2	Enriched	Androgen independence , Apoptosis resistance
(57)	miR-148a	CAND1	Enriched	Enhanced cell proliferation
(59, 68)	miR-221 & miR-222	$P27^{kip1}$, TIMP3	Enriched	Increased proliferative ability, Androgen independence
(69)	miR-373	CD44	Enrichment	Promote metastasis

(70)	miR-let7c	RAS, c-myc, BUB1	Enrichment→Under expression	Transition allows for early C'somal instability and late Enrichment of RAS and c-myc
(68, 70)	miR-218	LAMB3, Paxillin	Enrichment→Under expression	Early Enrichment allows cancer to transform from a localised to metastatic tumour
(70)	miR-100	THAP2, SMARCA5, BAZ2A	Enrichment→Under expression	Early Enrichment allows cancer to transform from a localised to metastatic tumour

1.2.7. The lncRNA gene family

lncRNAs are a much more recent discovery and most lncRNA transcripts are not functionally annotated. However, the emerging information regarding this vast family of noncoding RNA reveals extreme versatility in biogenesis and function with several sub-families emerging that are largely classified by their functional modality.

1.2.8. lncRNAs guide transcriptional repressors and enhancers to genomic loci

Chromatin modifying complexes (CMCs) and the ontologically related DNA methyltransferase enzymes are known to modify chromatin and DNA (71) to activate or deactivate sets of genes that will define cellular identity (72). There is considerable evidence available that places lncRNAs at the centre of these cellular imprinting processes. Specifically, particular gene sets are targeted by lncRNAs.

For example, the EVF-2 lncRNA targets the CMC dlx-2 to the dlx-5/6 enhancer, making EVF-2 an essential coactivator of transcription from this locus (73). AIR on the other hand targets the slc22a3 promoter, recruiting the methyltransferase G9a which represses transcription

from this site (74). It has been suggested by Magistri et al (75) that natural antisense lncRNAs (termed NATs by the authors) are the most common type of lncRNA to participate in cis-regulatory chromatin re-modelling activities, as they frequently regulate the mRNA arising from the sense strand. These lncRNA functions are shown diagrammatically in Figure 1.5.a.

1.2.9. lncRNAs act as armatures for protein complexes

Alongside lncRNA interactions with CMCs, many other types of lncRNA:protein interactions have been demonstrated. In fact, lncRNAs are beginning to answer long standing questions about the structure of many ribonucleoprotein complexes (RNPs) with diverse roles across many cell types (74, 76). Outside of chromatin interactions, lncRNAs have been found to have vital roles in speckles and paraspeckles, sub-nuclear compartments containing RNA splicing machinery (77) and Inosine-substituted mRNA binding proteins (78, 79) respectively. At the heart of Nuclear speckles is MALAT1 (80), while NEAT1 is the fundamental lncRNA component of nuclear paraspeckles (81). Both of these lncRNA components are essential for recruiting the effector proteins of their respective complexes. LncRNAs can also participate in cytoplasmic RNP complexes as evidenced by The NRON lncRNA described by Sharma et al (82). This lncRNA is transcribed from a large intergenic region of chromosome 9 and was shown to modulate NFAT activity, which is a critical determinant of T cell activity. This lncRNA function is shown diagrammatically in Figure 1.5.b.

1.2.10. lncRNAs can induce mRNA editing

Beltran and co-workers demonstrated the interaction between the ZEB2 premature mRNA and a NAT that prevented a particular splicing event in ZEB2 mRNA maturation (83). This NAT overlaps a region of ZEB2 intron that contains an Internal Ribosome Entry Site (IRES) essential for ZEB2 protein expression that would otherwise be spliced out. Therefore, the action of this NAT prevents IRES splicing which allows expression of ZEB2. Although this evidence is extremely convincing, this is an isolated example of lncRNA behaviour. This lncRNA function is shown diagrammatically in Figure 1.6.a.

1.2.11. lncRNAs act as molecular decoys

The first reported lncRNA acting as a molecular decoy was seen between the lncRNA Gas5 and glucocorticoid receptor (GR) (84). Kino and colleagues demonstrate that Gas5 bound the DNA binding motifs in GR in cells starved of nutrients and vital growth factors. The binding of GR by Gas5 produced a competitive inhibition whereby GR was prevented from binding enhancer elements in the promoter of anti-apoptotic genes. Since this time, Linc-MD1 has been shown to soak up miR-133 and miR-135 molecules, preventing them from inhibiting their targets MAML1 and MEF2C. These two transcription factors are essential for muscular differentiation and linc-MD1 expression effects timing of myoblast differentiation (85). This lncRNA function is shown in Figure 1.6.b.

Recently, a new family of lncRNAs were doiscovered that function as molecular decoys. These lncRNAs are known as ecircRNAs and they arise from alternatively spliced exons which form closed circles of RNA instead of the usual lariat structure (86, 87). Jeck et al have shown that approximately 14.4% of transcribed human genes can give rise to ecircRNAs and it is now understood that ecircRNAs are commonplace throughout metazoan organisms (88). These RNAs are highly stable in the cytoplasm, are conserved between mice and humans and are associated with ALU repeats of the genome (87). There are currently two proposed functions of ecircRNA. The first involves an ecircRNA binding to an RNA binding protein in favour of that proteins regular RNA substrate, inhibiting whichever process that RNA:protein pair contributes to. The second modality involves the ecircRNA sequestering a large number of miRNAs. This mechanism has been shown by Memczak et al (89) and Hansen et al (90). Both groups have discovered ecircRNAs that bind large numbers of miR-7 molecules, drastically reducing the repressive action of miR-7. Being molecular decoys, these lncRNAs function in a similar way to that depicted in Figure 1.6.b.

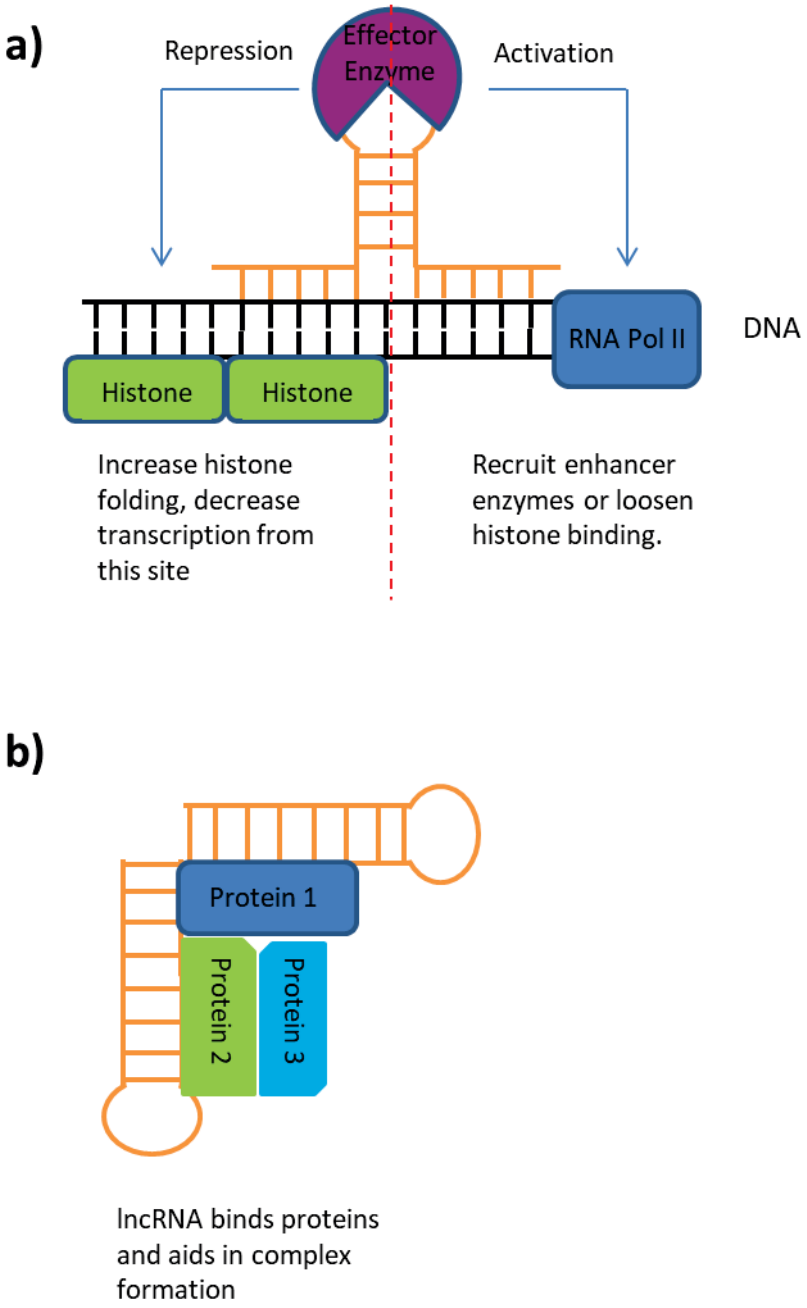

Figure 1.5 a) lncRNAs rescruit chromatin modifying complexes that can activate or repress transcription from genomic loci.

A) This shows the lncRNA transcript recruiting an effector enzyme to specific loci in the genome. The lncRNA:effector enzyme combination can either repress transcription from this locus by causing further tightening of the DNA around the histone molecules, or it can enhance transcription from the site by recruiting transcriptional enhancer enzymes, or enzymes that lessen DNA binding around histone molecules. B**) lncRNAs form structural support for protein complexes** lncRNA binds proteins which provides structural support for protein complexes such as NEAT1 providing structural support for nuclear paraspeckle formation (81).

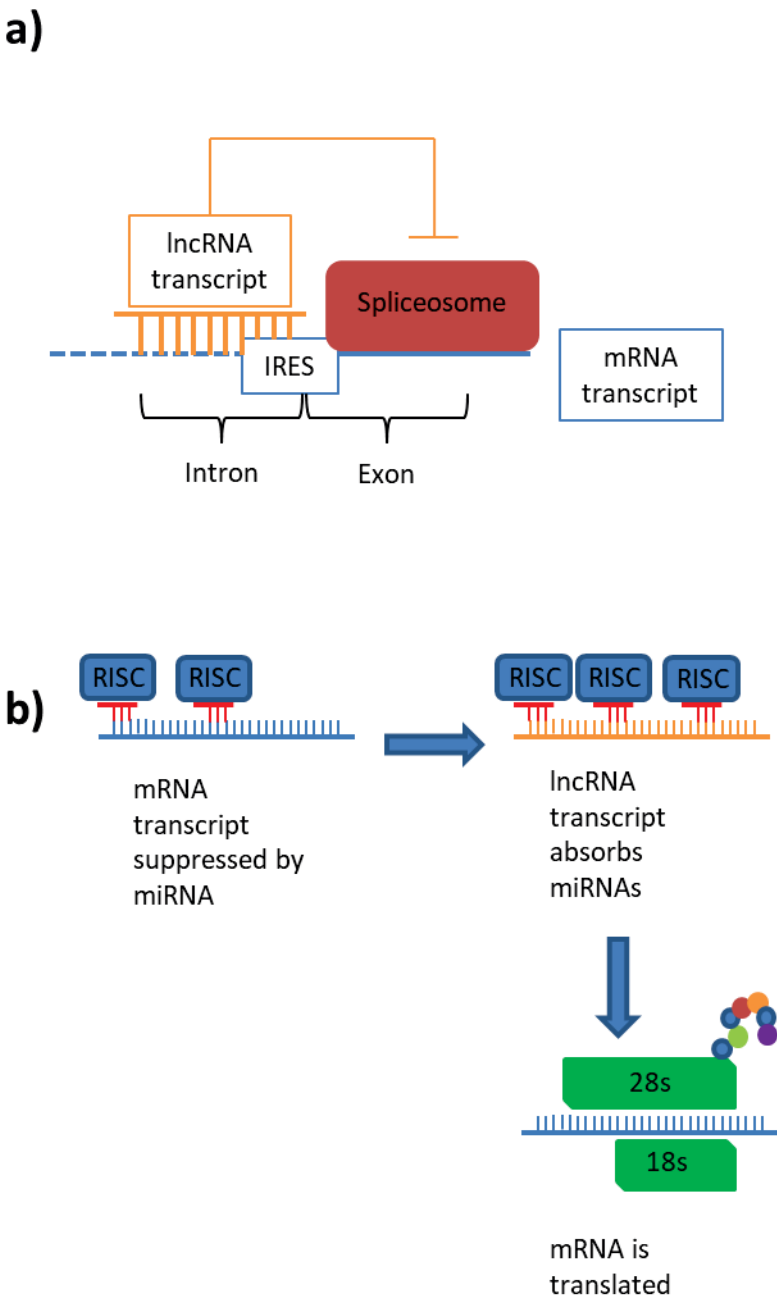

Figure 1.6. a) lncRNAs control splicing function by blocking spliceosome binding sites.

A) lncRNA binds a portion of an immature mRNA transcript which prevents the splicing out of a crucial IRES required for translation of the mRNA. **b) lncRNAs act as molecular decoys by binding miRNAs in favour of target mRNA transcripts** lncRNA molecule contains many binding sites for a particular miRNA. The miRNAs bind to the lncRNA instead of the target mRNA, allowing the mRNA to be translated into protein.

1.2.12. The role of lncRNAs in PCa cells

Given the fact that lncRNAs are much more poorly annotated as a group and that lncRNAs are a relatively recent discovery, fewer lncRNAs have been identified as having a functional role in PCa. However, some lncRNAs have been shown to influence the behaviour of PCa cells and these lncRNAs are outlined in table 1.2.

Table 1.2. PCa lncRNAs

Ref.	lncRNA	Expression in PCa	Link to PCa
(91)	PRNCR1	Enrichment	Affects androgen receptor transactivation activity.
(92)	DD3/PCA3	Enrichment	Elevation of BMCC1 which interacts with RhoA and RhoC genes.
(93, 94)	PCGEM1	Enrichment	Associated with androgen dependence.
(95)	XIST	Enrichment	XIST locus hypomethylation associated with PCa aggressiveness.
(96)	ANRIL	Enrichment	Repression of theINK4b/ARF/INK4a tumour suppressor locus.
(97)	plncRNA-1	Enrichment	Protects cells from apoptosis. Regulates Androgen receptor level.

1.2.13. The potential of noncoding RNAs as PCa diagnostics

The microRNAs in table 1 and the lncRNAs in table 2 all exist within cells and regulate intracellular gene expression. Therefore a diagnostic gene signature can only be generated if the cancer is of sufficient size to be biopsied. By this time the primary prostatic tumour may have spread to surrounding lymph nodes and possibly metastasised to the lungs or bones, severely reducing prognosis at the time of detection. Thus an ideal noncoding RNA based biomarker is expressed at a detectable level very early in cancer development and must be readily available in a stable form in the circulation or other easily accessible body fluid. Additionally, these miRNA signatures must differ between normal and PCa bearing individuals. A growing body of evidence suggests that circulating noncoding RNAs meet these criteria and may be found within exosomes, which are 40-100 nm vesicles and are secreted by all cells.

1.3 Exosomes: biogenesis, function and their roles in PCa

Exosomes carry information around the body in the form of active proteins, mRNAs, lncRNAs and miRNAs. They behave like a hybrid between viral particles and hormones, as they are discrete particles which fuse with target cells to alter that cells behaviour in a specific way (Figure 1.7.). In the case of cancer, exosomal contents are often quite different between the cancer cells themselves and the cell lineage from which they are derived.

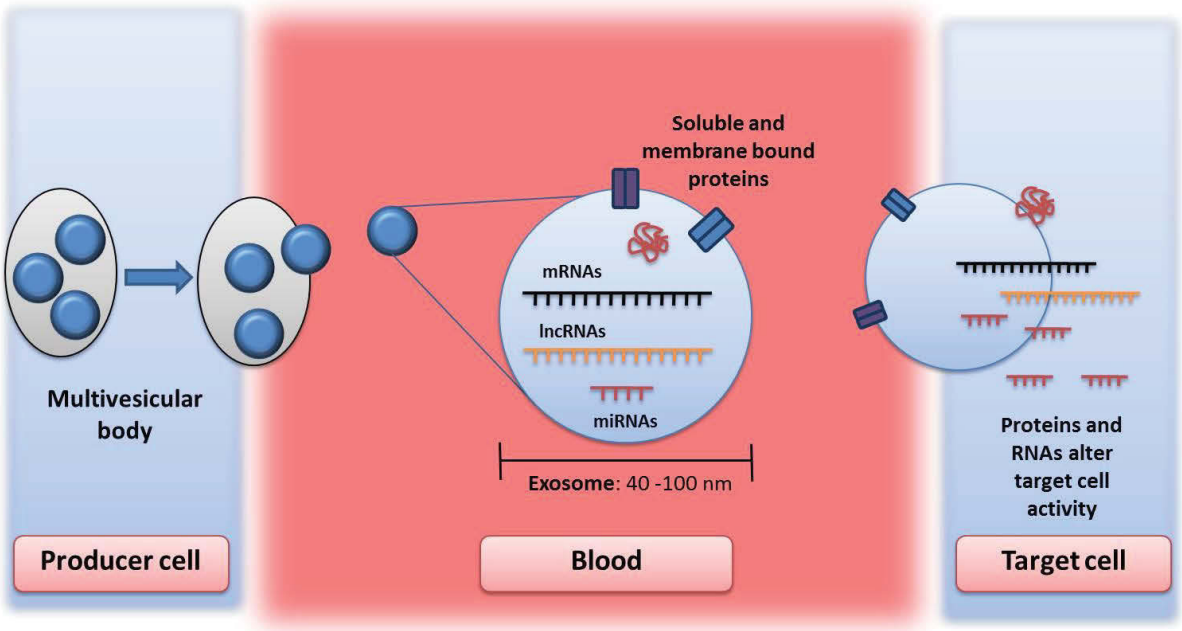

Figure 1.7. Exosome biogenesis, structure and function.

Beginning in the multivesicular body (MVB) of producing cells, exosomes are released into the blood stream which carries them to target cells elsewhere in the body. Exosomes are then able to fuse with target cells and release soluble proteins, mRNAs, lncRNAs and miRNAs into these target cells, while membrane bound exosomal proteins are maintained on the target cells surface. Thus each exosome is a vehicle for horizontal gene transfer and carries the contents representative of the cell from which it originated. This process leads to altered gene expression in target cells (98-100). The ExoCarta database (101) has been established as a repository for proteome and transcriptome data gathered from exosome studies.

1.3.1. Functions of exosomes in cancer

Exosomes are known mediators of cell-to-cell communication and have become of great interest for their potential roles as communicators between the cancer cells and the cells of the body that can influence their growth. These often include cells in the immediate area around the tumour (the stromal microenvironment) that can be influenced to induce growth of new blood vessels into the area to feed the tumours ongoing growth (see section 1.3.2.). Cancer exosomes also direct tumour stroma to become more permeable via the effects of metalloproteinases that degrade the Extracellular Matrix (ECM) allowing the tumour cells to escape the primary site and potentially form metastatic deposits elsewhere in the host body (see section 1.3.2.). Cancer exosomes have also been shown to aid in the formation of pre-metastatic niches that prime specific tissues of the body to receive and support circulating tumour cells to form metastases (section 1.3.3.). Lastly, exosomes can influence the behaviour of the immune system to decrease immune responses to cancer cells and also to cause an accumulation of suppressive or immature immune system cells to tumours.

1.3.2. Cancer exosomes in the stromal microenvironment

The stromal microenvironment is a complex milieu of immune system cells, fibroblasts, vasculature and extracellular matrix (ECM) that is modified by tumour cells during tumour progression (102, 103). One particularly well researched area in which exosomes contribute to stromal remodelling is angiogenesis. All solid tumours must deal with hypoxia once they outgrow their existing blood supply. To overcome this many tumours secrete vascular growth factors such as VEGF to encourage the growth of new blood vessels into the tumour (18). However, exosomes can also communicate with the stromal microenvironment and induce pro-angiogenic responses. For example, hypoxic Glioblastoma cells secrete exosomes which activate receptors (EGFR, VEGFR and EPHA2) on endothelial cells known to elicit an angiogenic response. This resulted in activation of the ERK1/2 MAPK, PI3K and FAK which increased microvascular sprouting from endothelial cells receiving stimulation from hypoxic exosomes (104). Multiple Myeloma cells have also been shown to secrete exosomes that enhance angiogenic responses from endothelial cells. In this case, hypoxic multiple myeloma cells increase their secretion of miR-135b encapsulated in exosomes, which are then taken up by receptive endothelial cells. Once inside, the miR-135b inhibits a repressor of HIF-1α. This de-represses HIF-1α which is then able to induce a pro-angiogenic response (105).

Cancer exosomes can also transfer various cancer phenotypes to nearby untransformed cells, as well as to other cancer cells in the immediate vicinity (106). For example, exosomes released by metastatic melanoma cells can induce an invasive phenotype in primary melanocytes by bringing about epithelial to mesenchymal transition. Xiao et al showed that exosomal let-7i is an essential part of this process as the transfer of exosomal let-7i to primary melanocytes induced expression of well known EMT markers (107). In the case of colon cancer cells, a mutant form of KRAS is secreted in exosomes and can be taken up by normal colon cells. This transfer causes the otherwise normal colon cells to grow more invasively (108).

1.3.3. Cancer exosomes and the pre-metastatic niche

The pre-metastatic niche describes a location in the body where primary tumours are likely to metastasise to. This process largely relies on induced expression of matrix metalloproteinase 9 (MMP-9) by endothelial cells and macrophages (109) and expression of VEGFR-1 on Bone Marrow Derived Cells (BMDCs) , which are recruited to the pre-metastatic site (110). These factors create a supportive environment for circulating tumour cells that allows them to be retained in this tissue where they survive and proliferate into secondary tumours. Exosomes offer an enticing explanation of why certain cancers show clear preferences for what organs they metastasise to, given the presence of cell specific receptors, ligands and RNAs contained within each exosome.

Current thinking on the role of cancer exosomes in pre-metastatic niche formation involves **i)** the processes of increasing vascular permeability to allow circulating tumour cells into specific sites, and **ii)** angiogenesis to support growth of new tumours. For example, the highly metastatic breast cancer cell line MDA-MB-231 secretes exosomes enriched with miR-105. This miRNA can then be absorbed by endothelial cells where it represses the tight junction protein Zona Occludens 1 (ZO-1) (111), which facilitates the exit of cells from the primary tumour site and/or the entry of tumour cells into pre-metastatic niche. Evidence for exosomes as angiogenic stimulators meanwhile comes from renal cancer stem cells. These cells release exosomes that act on lung endothelial cells causing them to express VEGF and MMP-2 which are angiogenic factors previously linked with angiogenesis (112, 113).

1.3.4. Cancer exosomes down-regulate immune responses to tumour antigens

Exosomes, or rather their contents can alter the immune response to cancer via two mechanisms: direct cytotoxicity (Figure 1.8.a); or biased differentiation fate of precursor cells (Figure 1.8.b).

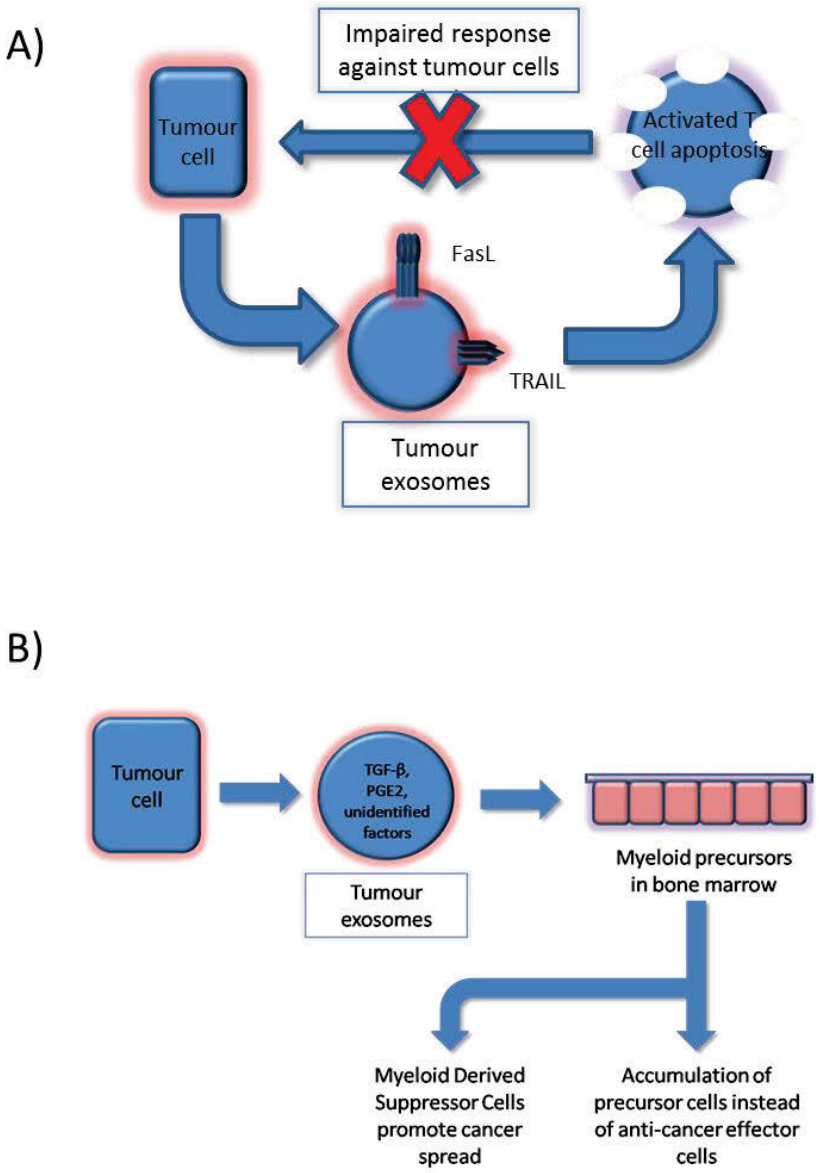

Figure 1.8. Cancer exosomes can induce T cell death and cause accumulation of immature immune cells.

a) Exosomes from several cancers contain FasL and TRAIL which induce apoptosis of activated T-lymphocytes, thus limiting any potential response they may mount against tumour cells (114-116). **b)** Differentiation bias revolves around exosomes of various origin that divert the lymphocyte population to cells that either aid cancer progression or are unable to effect clearance of cancer cells. Breast cancer cells for example release exosomes that force myeloid precursor cells in the bone marrow to produce an aberrant number of secondary myeloid precursors which accumulate in the spleen instead of macrophages that could launch an attack on tumour cells (117). These accumulating myeloid cells were recently determined to be mainly Myeloid derived suppressor cells (MDSCs) (118). The effect of this is two-fold as MDSCs are known to support cancer progression (119), and they are being made at the expense of other anti-cancer effector cells. Melanoma cells also secrete exosomes that inhibit monocyte to dendritic cell differentiation, instead favouring an immunosuppressive phenotype (120).

1.3.5. Exosomal noncoding RNAs as PCa biomarkers and functional agents in extracellular communication

MicroRNAs are highly promising biomarker candidates due to their abundance in bodily fluids and their resistance to degradation (16, 17). The use of miRNA biomarkers is dependent on a differential expression profile involving multiple miRNAs that may offer higher sensitivity than the PSA test, and potentially even prognostic information as well. Exosomes contain many different miRNA species and are easily obtained from several bodily fluids including saliva and urine. This is important because patients are more likely to submit saliva or urine samples instead of the blood sample required for the PSA test, or the invasive tests such as a prostate biopsy. Furthermore, exosomes are readily isolated from these fluids using ultracentrifugation and in future may be isolated using tissue specific surface markers, such as those already identified for prostate exosomes (121). Lastly, detection of cancer exosomes is made easier as cancer cells secrete more exosomes than normal cells (122), and the degree of extra secretion may correlate with aggressiveness (123). Therefore the dynamic range of cancer exosomes versus normal exosomes will presumably be shifted significantly in all fluids, making biomarker detection easier.

Using the approach of identifying exosomal noncoding RNA biomarkers in human body fluids, a range of noncoding exosomal RNA biomarkers have been identified for PCa. For the most part, they are all microRNAs with the exception of lncRNA-p21. These biomarker candidates are outlined in table 1.3.

Table 1.3. Exosomal noncoding RNAs as PCa biomarkers

Cancer Type	Bodily Fluid	Nanovesicle Characterisation	Isolation Method	ExomiR Signature	Reference
prostate cancer	urine	Atomic force microscopy, Zetasizer ZS, CD9 +ve, TSG101 +ve, AGO 1 - 4, -ve	Lectin-induced Agglutination	miR-574-3p, miR-141-5p, miR-21-5p	(124)
prostate cancer	serum	TEM, CD63 marker	Exoquick	miR-141	(125)
metastatic prostate cancer	serum	Nanoparticle tracking analysis (NTA)	total exosome isolation reagent (invitrogen)	miR-375, miR-21, MIr-574	(126)
castration resistant prostate cancer	plasma	NTA	Exoquick	miR-1290, miR-375	(127)
Prostate cancer	urine	None	Norgen Urine Exosome Isolation Kit	lncRNA-p21	(128)

Ahadi et al have also identified a number of lncRNAs that are found in PCa exosomes (129). However due to the poor characterisation of many of the transcripts in this study, they were not included in table 3. They may however become valuable markers once their expression is validated using qPCR.

Investigating the noncoding RNA expression profile of PCa exosomes further offers an exciting opportunity to analyse the potential role of these RNAs in cell to cell communication. Exosomal miRNAs are biologically active and can enact gene silencing when delivered to target cells (98, 105, 130), but the function of PCa exosomal miRNAs in tumour formation and/or expansion remains largely unknown.

The role of exosomal lncRNAs in PCa is even less well explored. However, Ahadi et al have produced some interesting insight into this question. It seems that exosomal lncRNAs harbour large numbers of complementary sites at which miRNAs might bind (129). This suggests that perhaps these lncRNAs are behaving as a carrier for functionally related miRNA families. The lncRNA contains all the necessary structure to retain the miRNAs it carries, and enough room to harbour specific signal motifs to load the lncRNA and its cargo into exosomes in a sequence specific manner. Then once the exosome is taken up by a target cell, the lncRNA disgorges its cargo of miRNAs which perform their repressive functions in this target cell. Unfortunately there is currently no experimental data that tests this hypothesis.

1.4. Hypotheses

The noncoding RNA expression profile of PCa exosomes will be different to that of exosomes derived from normal prostate cells. Detection of this differential expression signature will allow early PCa diagnosis and improve PCa prognosis (outcome).

The noncoding RNA identified in PCa exosomes will have functional implications with respect to the tumour microenvironment, pre-metastatic niche formation and/or immune system regulation.

1.4.1 Aims

1. To determine the noncoding RNA expression profile of normal prostate and PCa exosomes *in vitro* with a focus on differentially expressed and/or known cancer associated miRNAs.
2. To optimise techniques for isolating exosomal RNA from various body fluids.
3. To test the utility of biomarkers identified in aim 1 as diagnostic/prognostic markers using patient body fluid samples.
4. To identify the potential roles of exosomal noncoding RNAs in cancer development and progression using bioinformatics methods. This includes mainly tumour immune evasion strategies, cancer metabolism and changes to the cancer microenvironment

Chapter 2 Abstract:

Affymetrix and Arraystar microarray platforms were utilised to determine the RNA expression profile of prostate cancer exosomes. Transmission Electron Micrographs were taken to assure that exosomes samples were appropriately pure, and bioanalyzer small RNA chips were used to perform qualitative and quantitative analysis of exosomal RNA samples. The most interesting biomarker candidates were then validated using Taqman qPCR assays. The microarray data were also functionally interrogated using Cytoscape and associated plugins to build networks of interacting genes. The microarrays revealed a large number of microRNAs enriched in exosomes secreted by prostate cancer cells. However, most mRNAs and lncRNAs were expressed at lower levels in prostate cancer exosomes. This observation was later supported by the Bioanalyzer data showing that exosomal RNA samples are mostly composed of small RNAs. The TEM images also confirmed that our exosomes samples were quite pure. The functional interpretation of the microarray data also revealed a great many possible functions for exosomal microRNAs. The most important functional possibilities of exosomal microRNA were in immune regulation and hormone metabolism.

2.1.Methods

2.1.1. Cell culture methods for exosome isolation: standard tissue culture

The primary method for exosome isolation from cell culture was very similar to standard tissue culture techniques. However, Foetal Calf Serum (FCS) contains large amounts of exosomes or bovine origin. These exosomes had to be removed prior to cell culture, so each aliquot of FCS was centrifuged at 100 000 xg overnight at 4^0C. This pelleted the FCS exosomes allowing the remaining FCS to be safely decanted into sterile vessels for storage. This was conducted in a class 2 biosafety cabinet to avoid environmental contamination of the depleted FCS.

Once depleted FCS was acquired it was used to make tissue culture media consisting of 10% depleted FCS and 5% pen/strep. All base media contained glutamax as a source of glutamine and are listed in Table 2.1. alongside which cell lines they support. All tissue culture reagents were supplied by GIBCO ® (ThermoFisher Scientific, Waltham, MA, USA). All cells were grown in their respective media at 37^0C and 5% CO_2.

To acquire exosomal RNA at a concentration appropriate for microarrays (50 ng/µL), very large amounts of cells needed to be grown. 5x 175 cm^2 flasks were grown up per cell line and their culture supernatants were removed after the cells reached 70 to 80% confluence as recommended by Thierry et al (131). The Exosomes were then isolated from the culture supernatants by differential ultracentrifugation.

Table 2.1. Details of cell lines used to generate exosome samples

Cell Line	Cell Type	Media	Responsive to Androgens	Reference
LNCaP	Prostate adenocarcinoma isolated from metastatic deposit in lymph node	RPMI	yes	(132)
DU145	Prostate adenocarcinoma isolated from metastatic deposit in brain	RPMI	No	(133)
PC3	Prostate adenocarcinoma isolated from metastatic deposit in bone	RPMI	No	(134)
VCaP	Prostate adenocarcinoma isolated from metastatic deposit in lumbar vertebrae	50% F12, 50% DMEM	No	(135)
PNT2	Normal Prostate epithelium immortalised with SV40	RPMI	yes	(136)

2.1.2. Differential ultracentrifugation

Culture supernatants were collected and either stored at 4^0C for one to five days prior to exosome isolation by ultracentrifugation or frozen at -80^0C and thawed the day before extraction. All exosome preparations were performed using the published protocol (137) illustrated in Figure 2.1.

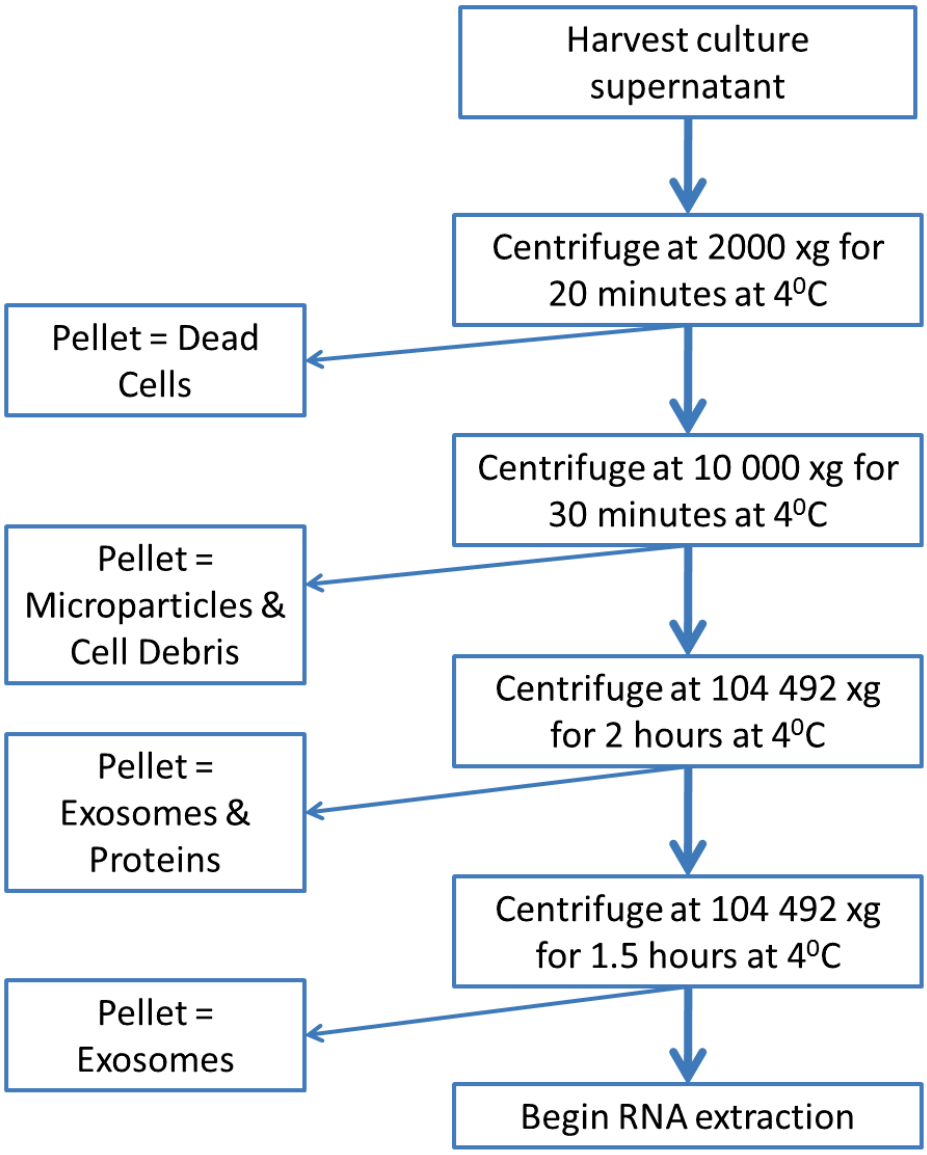

Figure 2.1.Exosome isolation from tissue culture supernatants using differential ultracentrifugation.

Exosome isolation by differential ultracentrifugation (137). To avoid possible contamination of the exosomal microRNA profile with cellular RNA, the principal step in exosome isolation was the removal of dead cells from the CS by centrifugation at 2000 xg for 20 minutes at 4^0C. This would typically yield a small beige pellet at the bottom of the tube. Supernatant was transferred into sterile 75 mL polycarbonate centrifuge tubes (Thermo Fisher Scientific) to remove cell debris and microaprticles at 10 000 xg (9000 rpm for F40L-8x100 rotor) for 30 minutes at 4^0C. The supernatant was transferred to fresh, sterile 75 mL polycarbonate tubes and the volume was topped up to 70 mL with 1x Phosphate Buffered Saline (PBS; Thermo Fisher Scientific). Finally, to pellet the exosomes, the tubes were centrifuged at 104 492 xg for 2 hours at 4^0C. The supernatant was then carefully poured off without disturbing the pellet and the tubes were completely refilled with 70 mL of 1x PBS. The final spin to remove most contaminating proteins was performed at 104 492 xg for 1.5 hours at 4^0C.

2.1.3.Transmission Electron Microscopy

Transmission electron microscopy (TEM) provides extremely high magnification and high resolution images required to qualitatively identify exosomes. In the provided images exosomes were qualitatively identified according to their cup-shaped morphology and size of 100 nm or less. Microparticle fractions were also taken prior to exosome collection and analysed for size and morphology comparisons to the exosome samples. Negative controls were performed by performing TEM on cell media samples that underwent the same exosome isolation procedures as the actual exosome samples. All Electron Micrographs were performed by Dr Lyn Schedlich at the ANZAC research institute at Concord Hospital, Sydney. Due to the difficulty obtaining exosomal samples, one biological sample per cell line per condition (exosomal, ,microparticle, negative control) was submitted for imaging.

2.1.4. RNAzol RT whole RNA extraction from exosomes

RNAzol RT (500 µL) was used to flush the exosome pellet off the wall of the polycarbonate centrifuge tube. Once the pellet was dissolved, the same aliquot of RNAzol RT was used on other exosome pellets derived from the same patient sample and/or cell line as seen in Figure 2.2. This approach allowed the concentration of total RNA from multiple exosome preparations. When the last pellet was dissolved, the lysate was transferred into a 2 mL Eppendorf tube. Using the micropipette, any remaining fluid was removed from the centrifuge tubes and added to the 2 mL tube.

The RNAzol RT whole RNA extraction protocol required the use of a ratio of 1 mL RNAzol:0.4 mL water. Once the water was added, the tubes were Shaken for 15 seconds and incubated at room temperature for 15 minutes prior to centrifugation at 16 000 xg for 20 minutes at 4^0C.

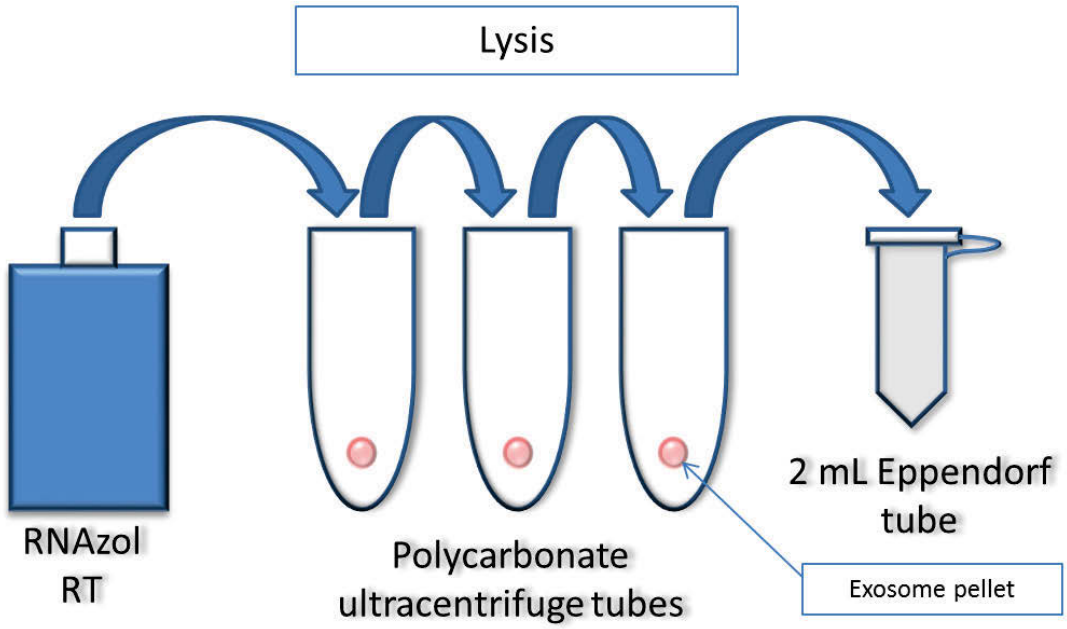

Figure 2.2. Lysis of exosome pellet following differential ultracentrifugation.

Once exosome pellets are acquired from differential ultracentrifugation a 0.5 mL aliquot of RNAzol RT is added to each pellet derived from the same cell line. Once lysis is complete, the exosome lysate is stored in a 2 mL Eppendorf and either stored at -80^{0}C or 0.2 mL of DNAse/RNAse free dH_2O is added to begin the RNA purification process.

Centrifugation yields a blue pellet, visible at the bottom of the 2 mL tube. Supernatant (525 µL) was carefully removed without disturbing this pellet and transferred to a new 2 mL tube. 4-bromoanisole (BAN; 5 µL; Molecular Research Centre Inc.) was then added to the transferred supernatant and this mixture was shaken vigorously for 15 seconds and incubated for 3 – 5 minutes at room temperature before centrifugation at 12000 xg for 15 minutes at 4^0C. This produced a separated blue phase separated at the bottom of the tube and a clear supernatant. Supernatant (400 µL) was then transferred to a new 2 mL tube to which 400 µL of isopropanol (Sigma) and 5 µL of 5 mg/mL glycogen (Invitrogen) was added. This mixture was incubated over night at -20^0C to increase the microRNA yield.

The following day, the samples were centrifuged at 12 000 xg for 15 minutes at 4^0C to pellet the RNA + glycogen. The supernatant was completely removed and the pellet was resuspended in 500 µL of 75% ethanol, prior to centrifugation at 12 000 xg for 15 minutes at 4^0C. After this centrifugation, the ethanol was completely removed, a fresh aliquot of ethanol was added and the sample was centrifuged at 12 000 xg for 15 minutes at 4^0C.

After centrifugation, the ethanol was completely removed leaving the RNA + glycogen pellet. This pellet was dried on a heating block set at 37^0C, prior to resuspension in 10 µL of RNAse/DNAse free H_2O. To completely resuspend the pellet, the sample was incubated at 55^0C for 5 minutes. Once resuspended, the sample was stored at -80^0C.

2.1.5. Agilent Bioanalyzer

The Agilent Technologies (Santa Clara, CA, USA) Bionalyzer 2100 is a microfluidics chip based method used to determine RNA quality and quantity. The chip itself contains 16 wells, with 4 of the wells being reserved for chip setup. This includes applying the gel to the chip and pressurising the gel so that it permeates all of the sample wells. A detection agent is also added along with the standard ladder that allows the Bioanalyzer 2100 software to accurately estimate the size of RNA fragments in the samples. The end result is a virtual electrophoretogram that can be used to identify features RNA samples such as the concentration of RNA and the quality of that sample based on the ratio between the 18S and 28S ribosomal subunits. This quality estimation is known as the RNA Integrity Number (RIN) which is a measure of degradation. A RIN of 10 indicates an extremely high quality sample while a RIN of 1 indicates a totally degraded sample. The Bioanalyzer 2100 software is also capable of estimating the relative miRNA content in a total RNA sample when the Small RNA chip is used.

The small RNA kit (138) was chosen for exosomal RNA analysis as it was able to provide accurate estimates of RNA concentration as well as the percentage of the exosomal RNA sample that was composed of miRNA. This was a valuable piece of information regarding the type of RNA most often found within exosomes.

In order to ensure that all RNA samples sent for array met the correct sample submission criteria (RIN ≥ 8 for cellular RNA samples), the RNA 6000 Nano kit was used to ascertain the RIN for all cellular RNA samples. The exosome samples did not undergo this procedure because RIN relies on the presence of 18S and 28S ribosomal subunits which are not reliably expressed in exosomal RNA samples.

2.1.6.Quantitative real time Polymerase Chain Reaction (qPCR) methods

The first step in establishing an expression profile from an RNA sample is to reverse transcribe that RNA sample into cDNA which results in the amplification of all mRNA transcripts or specific mature miRNA transcripts. cDNA is also substantially more stable than RNA. To perform reverse transcription, Taqman small RNA reverse transcriptase kits (Life Technologies, Carlsbad, CA, USA) were used to reverse transcribe miRNA and Taqman reverse transcriptase kits were used to reverse transcribe mRNA (Life Technologies). To reverse transcribe miRNA, 50 ng of total RNA was used. To reverse transcribe mRNA, 500 ng of total RNA was used. All other steps were performed in accordance with the manufacturers instructions (139). Once cDNA samples were acquired, they were diluted 1:4 with PCR clean dH_2O (GIBCO ®).

The next step is to perform the actual qPCR itself. Every qPCR reaction presented in this chapter was performed using the methodology outlined in Table 2.2. below. All Taqman probes used in this chapter are detailed in Table 2.3.

Table 2.2. Standard method used for 1x qPCR reaction

Reagent	Volume (µL)
Taqman master mix (2x)	2
Taqman probe	0.5
cDNA	1
dH_2O	0.5
Total	4

Table 2.3. Taqman primers/probes used for qPCR

Taqman Primer/Probe Name	Assay ID
miR-362	002117
miR-125b	000449
miR-30a	000416
miR-126*	0004451
miR-149*	002164
miR-1228	002919
miR-1228*	002763
miR-1246	477881_mir
miR-92b*	002343
Let-7i	002221
GAPDH	Hs02786624_g1

Apart from the modifications to the volume of the reagents, all other steps were performed in accordance with the manufacturers protocol (139). Each gene expression assay was performed in triplicate, and the average Ct was calculated from the three Ct values. Next, the delta Ct (ΔCt) value was calculated which is a measure of the difference in expression levels between the gene of interest (GOI) and the endogenous control (EC). Once the ΔCt was calculated, the ΔΔCt was calculated which measures the difference in expression levels between two cell types/experimental conditions. In this experiment, the difference measured was between the GOI in PCa exosomes versus the same GOI in PNT2 (normal prostate exosomes). The formula used to calculate the ΔΔCt was: ΔCt(PCa exosomes) – ΔCt (PNT2 exosomes). Fold-changes were then calculated between PCa exosomes and PNT2 exosomes using the formula $2^{-\Delta\Delta Ct}$.

2.1.7. Microarray analysis of exosomal RNA samples

All Affymetrix miRNA microarrays were performed under contract at the Ramaciotti centre at the University of New South Wales. The miRNA microarray was performed using the Affymetrix Human GeneChip 2.0 and given the difficulty in acquiring exosomal RNA, one exosome and one cell sample per cell line was sent away for analysis.

All Arraystar mRNA/lncRNA microarrays were performed under contract by Arraystar themselves. The Arraystar Human lncRNA microarray V2.0 was used for this analysis. As with the miRNA microarray, one exosomal RNA sample and one cellular RNA sample per cell line was sent off for microarray.

2.1.8. Exosomal RNA microarray analysis

The Partek® Genomics Suite (St Louis, MI, USA) was purchased to analyse the microarray data. Specifically, this software allowed the identification differentially expressed miRNAs in normal prostate and cancerous prostate exosomes and cells. This allowed for identification of candidate biomarker RNAs that were specifically packaged into exosomes by PCa cells compared to prostate epithelial cells. *In silico* functional studies could also be performed on any RNAs found to be preferentially packaged into PCa exosomes. Exosomal miRNAs were selected for this type analysis given the dominance of small RNAs in exosomes. These analyses were conducted using the miRBase and Cytoscape platforms to integrate miRNAs with their target mRNAs. Details of this procedure can be found in section 2.1.11. Figure 2.3. shows the basic workflow used to complete a typical microarray analysis in this study.

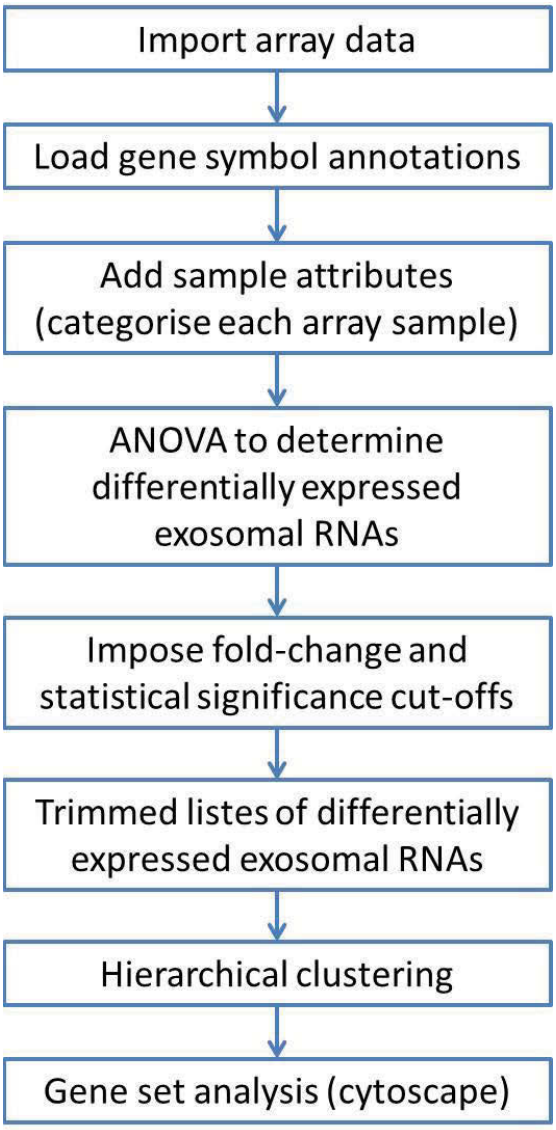

Figure 2.3. Exosomal RNA microarray analysis workflow using Partek Genomic Suite and Cytoscape.

The first step was to import the raw array data and combine the chip data with the gene symbol annotations from an annotation file provided by the array manufacturer. Sample attributes were added to define experimental conditions. For example, DU145 samples were given the attribute “PCa” and PNT2 was assigned the attribute “normal”. An ANOVA was then performed to detect differential expression between the sample attributes and fold-change and statistical significance limits were imposed to identify the most aberrantly expressed exomiRs. From these lists, hierarchical clustering analyses were performed to ascertain whether the exomiRs within these lists provided enough information to differentiate one attribute group from another e.g. “PCa” from “normal”. Gene set analysis was then performed using Cytoscape, a process detailed in Figure 2.4.

2.1.9. ANOVA to determine differentially expressed exosomal RNAs

The primary step in determining which exosomal RNAs were differentially expressed involved loading gene symbol annotations and defining the sample category by adding sample attributes, which are key biological feature of the array sample. For example, DU145, PC3, LNCaP and VCaP cells are cancerous while PNT2 cells are not, hence these samples could be compared by separating them into these attributes. Several sample attributes were defined and ANOVA comparisons performed between them as follows: **i)** PCa exosomal RNAs versus PCa Cellular RNAs, **ii)** PCa exosomal RNAs versus PNT2 (normal prostate) exosomal RNAs, **iii)** exosomal RNAs from androgen independent PCa cell lines (PC3, DU145, VCaP)versus exosomal RNAs from androgen dependent cell lines (LNCaP, PNT2). These analyses allowed us to determine which exosomal RNAs were differentially expressed in cancer exosomes vs normal prostate exosomes and putatively assign functions to PCa exosomal RNAs. This was all included as part of the Partek Genomics Suite workflow which was used to perform this analysis.

Once the ANOVAs were completed, differentially expressed exoRNAs were identified and sub-populations of exoRNAs could be segregated into their own lists according to the fold-change or the statistical significance. This proved necessary as the Arraystar microarray platform contains probes for all known mature lncRNAs and mRNAs which generated a list of 60000 unique expression levels in each sample. These lists were extensively culled by changing the statistical significance cut-offs until somewhere between 50 and 100 exosomal RNAs remained. This was not always possible however as can be seen from looking at Tables 7 and 8 in appendix 1. There are approximately 500 mRNAs and 500 lncRNAs that are at least 2-fold differentially expressed between cells and exosomes with a statistical significance of $P<0.001$, the most stringent statistical cut-off imposed during this experiment.

2.1.10. Hierarchical clustering

Hierarchical clustering was performed in the analyses of i), ii) and iii) described in section 2.1.9. This type of clustering used differentially exosomal RNAs to discriminate between various sample attributes. For example, any differentially expressed exosomal RNAs from androgen independent cells should cause all samples within the androgen independence sample attribute to separate into the same hierarchy.

2.1.11. Cytoscape methods

Cytoscape is a free, Java based platform for visualising and interpreting networks of biological data (140). Further augmenting the abilities of Cytoscape are the many plugins available to bring together data from a great many protein interaction databases(141). All differential expression was reduced to just the Enriched exosomal RNAs, as output from Partek. Enriched exosomal RNAs are presumably enriched and packaged into exosomes at some energy cost to the cell, which implies functional significance. Therefore, we pursued only the Enriched exosomal RNAs in our cytoscape analyses. Specific steps regarding the analysis of each species of Enriched exosomal RNAs (miRNAs, mRNAs and lncRNAs) are outlined in the following subsections.

2.1.12. Cytoscape analysis of Enriched exosomal RNAs

The first step for analysis of Enriched exosomal miRNAs (exomiRs) involved merging these miRNAs with their target mRNA strand. This was necessary because to exert any function in a recipient cell, the exomiRs must first be absorbed then repress the function of the target mRNAs within the target cell. To align our Enriched exomiRs with their target mRNAs, we input the top 10 Enriched exomiRs into TargetScan. This produced a list of potential target genes for each miRNA. The list was then ranked in order of increasing Context score, which is a measure of the likelihood of an interaction occurring between a miRNA and mRNA (142), regardless of the evolutionary conservation of that miRNA family. The top 100 targets according to Context score were selected for further analysis in Cytoscape. The final number of potential target genes input into Cytoscape was around 900. This was to prevent overcomplicating the resulting network and to focus on the genes most likely to be effected by the absorption of miRNAs by target cells.

Within this list of likely target genes for each Enriched exomiR of interest, we searched for interactions at the protein level, assuming that exomiRs would have knocked down the levels of specific proteins by repressing/destabilising their respective mRNA transcripts.

Importing mRNA data from Partek to Cytoscape revolved around a different assumption to that of exosomal miRNAs. It was assumed that any mRNAs packaged into exosomes would be absorbed by their target cell and were actively transcribed soon after. We therefore imported mRNA gene symbols directly into Cytoscape. lncRNAs however were not analysed by Cytoscape because of the general lack of functional annotations available for the vast majority of statistically significant exosome packaged lncRNAs the microarray revealed. Furthermore, there were very few lncRNAs found to be Enriched in PCa exosomes.

With these caveats in mind, a broad workflow suitable for analysing large gene sets was developed and is outlined in Figure 2.4.

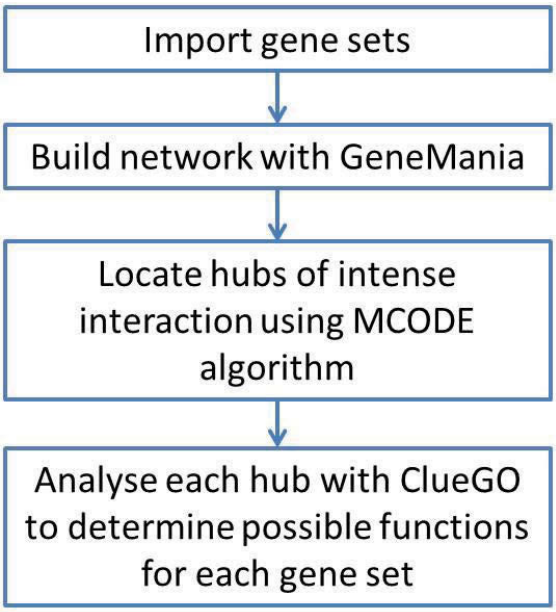

Figure 2.4. Gene set analysis using Cytoscape and associated plugins.

The first of these common steps was use of the Cytoscape plugin Genemania (143). This plugin takes lists of Human Gene symbols and accesses databases of interactions within this list and other closely related genes. This data is presented in the form of a network made up of nodes and edges. Each node represents a gene and each edge (link between nodes) represents some kind of interaction between the genes. Once Genemania has supplied an often very large network of interacting genes, the MCODE algorithm (144) is employed to search for hubs of interaction within the larger network. Each MCODE subnetwork is output and stored in a separate file for ontological (functional) analysis. To perform the ontological analysis, the ClueGO plugin is used (145). ClueGO takes genes from a network or a list and ascribes known functions to this set of genes which ultimately offers insight into the potential functions of each set of genes identified by MCODE.

2.2. Results

2.2.1. Quality of exosomes isolated using differential ultracentrifugation

Before isolating any RNA from exosome samples, qualitative analysis was required to show that these samples did in fact contain exosomes. TEM was the chosen method as it offered superb resolution and was already an established method for ascertaining exosome sample quality. The exosome samples contained particles that were of approximately 100 nm or less and most importantly, they had the classic cup-shaped morphology that is characteristic of exosomes. However there was contamination with a small number of pareticles > 100 nm as well as some very small particles <40 nm. This shows that the population of particles being isolated is actually more of a general extracellular vesicle population than a totally pure exosome population. However, there were no techniques available to us at the time to purify the samples any further.

The microparticle fractions showed particles generally of 200 nm or larger, but there were some exosomes that precipitated in this fraction. The RPMI with 10% depleted FCS image showed that no exosomes or microparticles can be isolated from the pure cell culture media. It can therefore be assumed that all exosomes extracted from the culture supernatants must have been produced by the cells growing in it. The TEM images are presented in Figure 2.5 and 2 samples for exosomes, microparticles and depleted media were assessed.

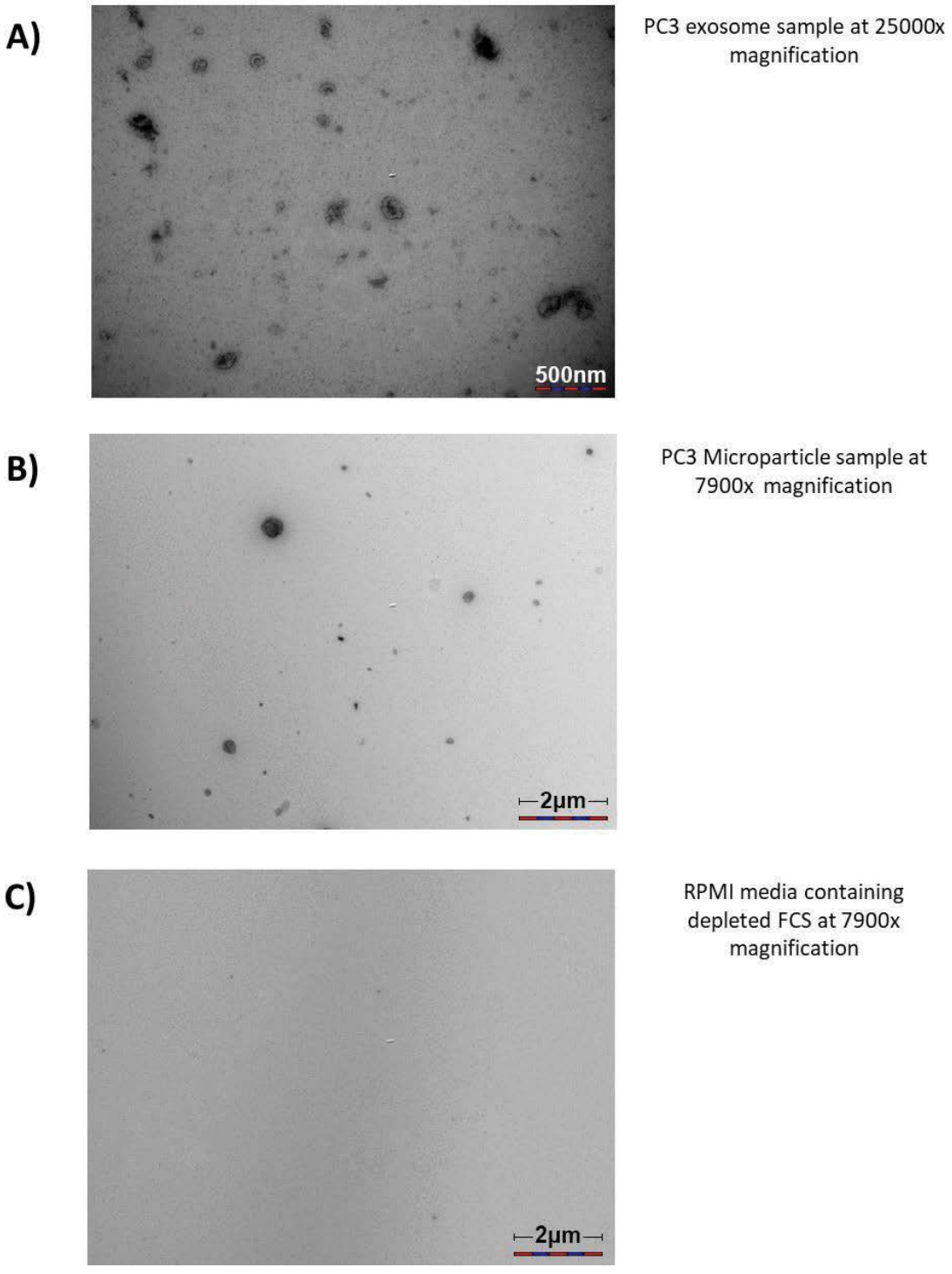

Figure 2.5. TEM images of typical exosome, microparticle and cell culture media samples. Exosomes were isolated from tissue culture supernatants using differential ultracentrifugation. Samples were then fixed on TEM slides and subjected to microscopic analysis. **A)** Representative image of an exosome sample. Particles had cup-shaped morphology and were approximately 100 nm or smaller. **B)** Microparticles taken prior to exosome isolation. Particles are generally larger 200 nm although some exosomes still precipitated. **C)** Image taken from RPMI media containing 10% depleted FCS. No particles are visible in this sample.

2.2.2. Qualitative analysis of exosomal RNA samples using an Agilent Bioanalyzer

Once it was certain that our differential ultracentrifugation method was suitable for isolating pure samples of exosomes, RNA was isolated from these exosome samples. The purpose of this experiment was to better understand the types of RNA present in exosomes. For this reason, small RNA chips were used as it was known from previous work in our lab that exosomes contained predominantly small RNAs. This proved very interesting as the bioanalyzer software estimated that approximately half of the RNA in the exosomal RNA samples was miRNA (Figure 2.6.).

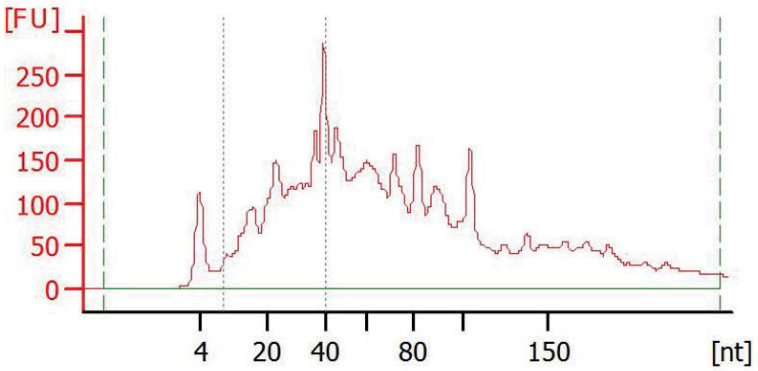

Exosomal RNA
46% miRNA
3765 pg/µL

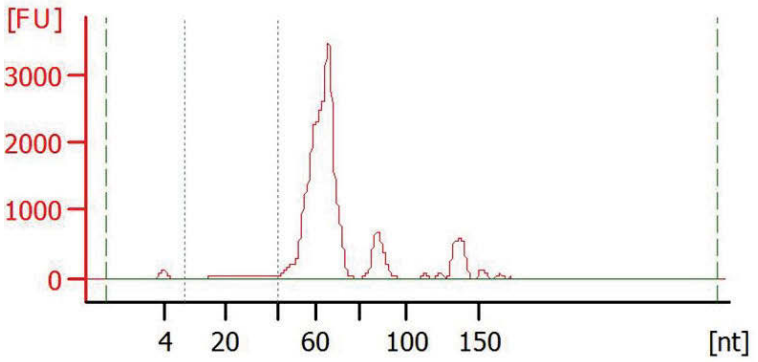

Cellular RNA
8% miRNA
938 pg/µL

Figure 2.6. Bioanalyzer 2100 data showing Small RNA content of exosomes vs cells.

Representative Bioanalyzer 2100 readouts from exosomal and cellular RNA samples collected using a small RNA chip. Exosome samples were isolated from tissue culture supernatants using differential ultracentrifugation. Cell samples were acquired by treating the cells remaining in the tissue culture flasks with TrypLE reagent for 5 minutes at 37^0C. This dissociated the cells from the flask. The dissociated cell solution was then diluted to a final volume of 15 mL using 1x DPBS and spun at 1000 rpm for 5 minutes. The supernatant was drained off the cell pellet which could then undergo RNA extraction. The RNA samples were isolated using RNAzol RT and the RNA concentrations were normalized to 50 ng/µL using a Thermo-Fisher Nanodrop, prior to loading RNA samples on to the small RNA chip. The Bioanalyzer 2100 software was then able to estimate the amount of miRNA present in each sample. It showed that exosomes contain mostly small RNAs with around 46% being miRNAs. This experiment was performed in triplicate for exosome and cellular samples.

2.2.3. MicroRNA microarray based expression analysis reveals differential expression profiles between PCa exosomes and normal prostate exosomes

The purpose of this experiment was to show that the expression profile of microRNAs was different to that of the cells that secreted them. This was important as it would demonstrate that exosomes are loaded with specific species of miRNA and not merely a mirror of cellular miRNA expression. It would also imply that these miRNAs are of functional significance, as cells are unlikely to invest energy in packaging specific miRNAs that do not confer some kind of survival advantage to the cell. The results of this analysis revealed that cellular and exosomal miRNA profiles are highly different to one another with 23 miRNAs being differentially expressed at statistically significant levels. In fact, the cellular and exosomal profiles cluster entirely separately of one another as can be seen in Figure 2.7. The identity of the miRNAs and their expression levels in PCa exosomes compared to PCa cells can be found in Table 1 of the appendix section. Note that one sample from each cell line was used to generate this data for all hierarchical clustering data presented in this chapter.

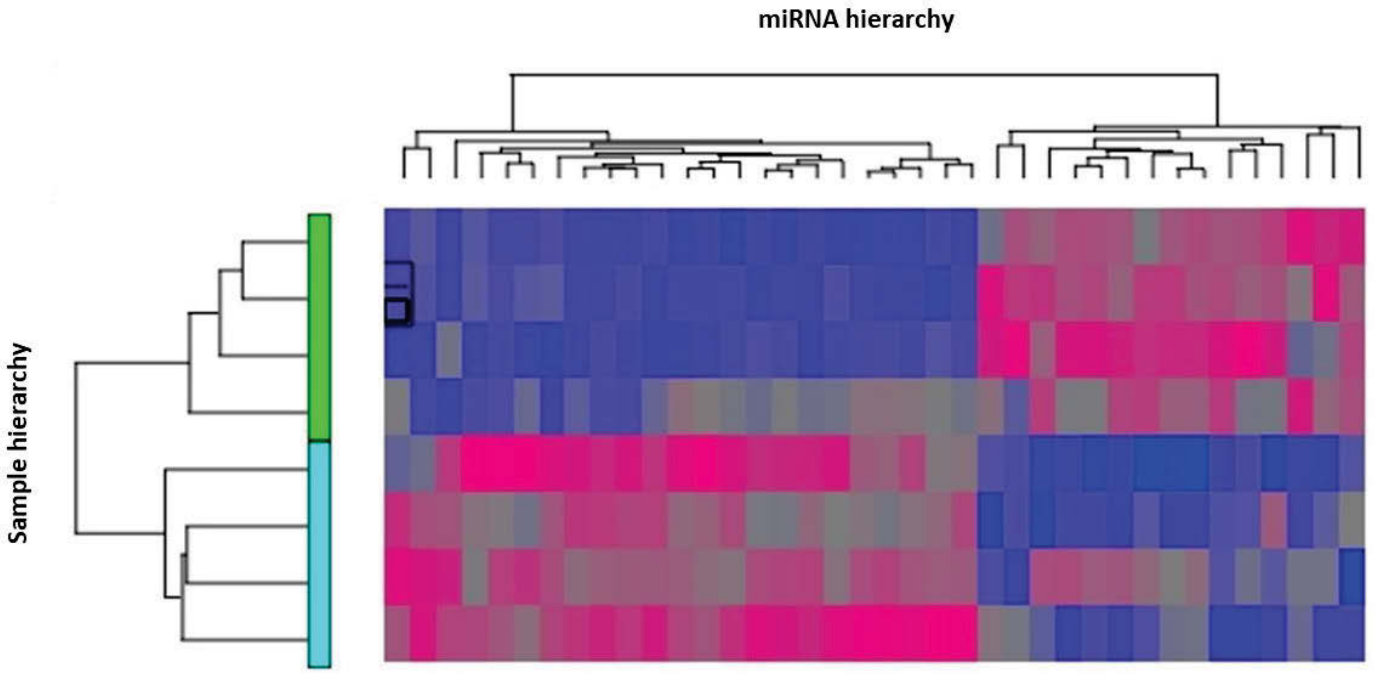

Figure 2.7. Comparison between exosomal miRNA and cellular miRNA expression profiles.

Hierarchical cluster diagram contrasting PCa cells and the exosomes they secreted. Exosomes were isolated from tissue culture supernatants using differential ultracentrifugation. RNA was then isolated using RNAzol RT and the RNA concentrations were normalised to 50 ng/µL prior to loading samples onto an Affymetrix miRNA microarray GeneChip 3.0. All differential exomiR expression was statistically significant ($P<0.05$) with fold changes of greater than 2 or less than -2 This hierarchical clustering diagram shows that exosomes and cells have very different microRNA expression profiles. The dendrogram on the left hand side shows that the cellular (green box) miRNA profiles are different from the exosomal miRNA profile (cyan box) because the first branch in the hierarchy separates these two groups. The top dendrogram indicates the individual miRNAs that contribute to the profile and shows how these profiles differ. The profiles themselves are visible on the diagram as pink (highly expressed) or blue (low expression level) rectangles that correspond to a sample source (Y-axis) and a specific miRNA (X-axis).

Having confirmed that exosomal and cellular miRNA profiles are significantly different from one another, two differential expression analyses were performed amongst the exosomal miRNA profiles. The first was to identify differentially expressed exomiRs between the cancer profiles and the PNT2 (normal prostate epithelia) profile. The second analysis was to determine whether exomiR profiles could be used to differentiate between androgen dependent and independent states of the parent cell line. Both tests were positive, showing that PCa exosomes can be differentiated from normal prostate exosomes, and that the androgen dependence status of the parent cell can be identified using differentially expressed exomiRs. These data are presented in Figure 2.8. and Figure 2.9. Tables 2 and 3 in the appendix section contain the identities of all exomiRs that make up these profiles.

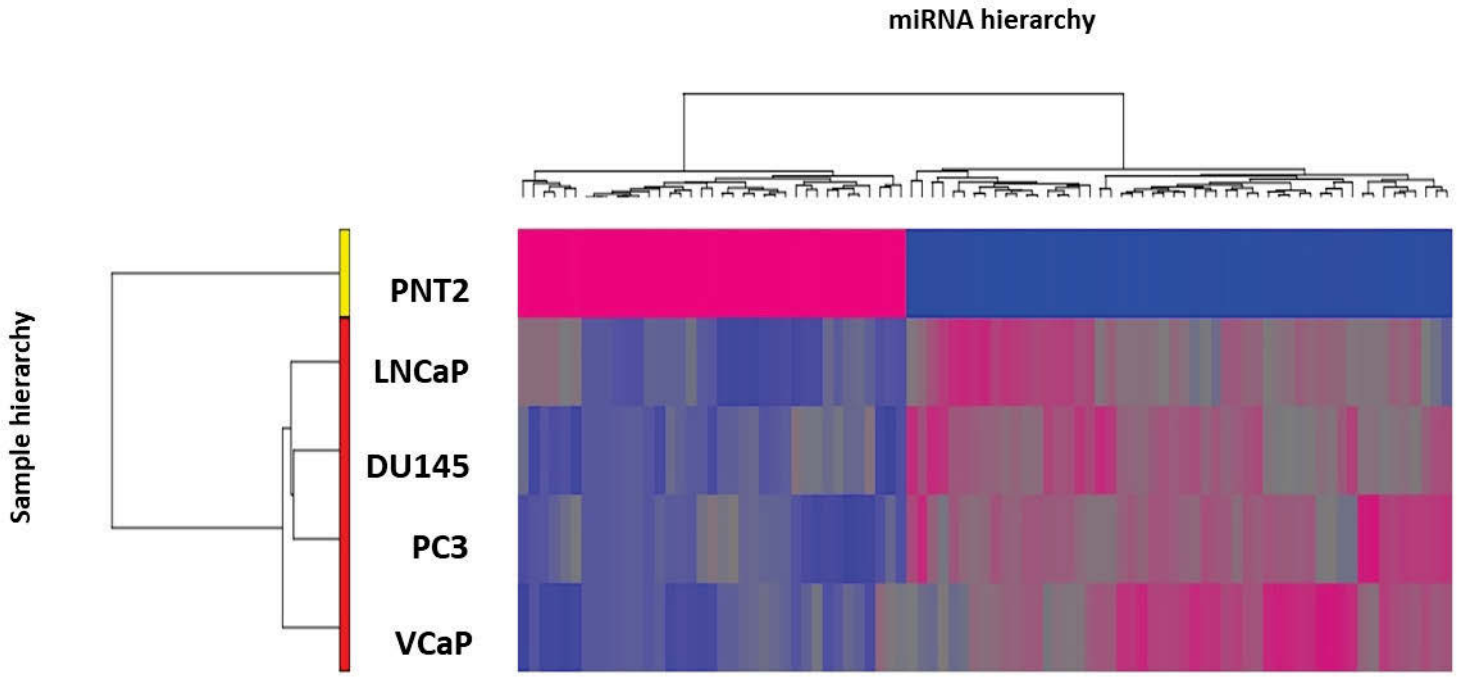

Figure 2.8. Hierarchical clustering diagram of exomiRs differentially expressed between normal prostate exosomes (PNT2) and PCa exosomes.

Exosomes were isolated from tissue culture supernatants using differential ultracentrifugation. RNA was then isolated using RNAzol RT and the RNA concentrations were normalised to 50 ng/µL prior to loading samples onto an Affymetrix miRNA microarray GeneChip 2.0. All differential exomiR expression was statistically significant ($P<0.05$) with fold changes of greater than 2 or less than -2. The dendrogram on the left hand side shows that the Pca exomiRs (LNCaP, DU145, PC3 and VcaP) segregated into one cluster while PNT2 exomiRs form their own cluster. Pink areas on the cluster diagram represent a highly expressed exomiR while blue indicates a lowly expressed exomiR

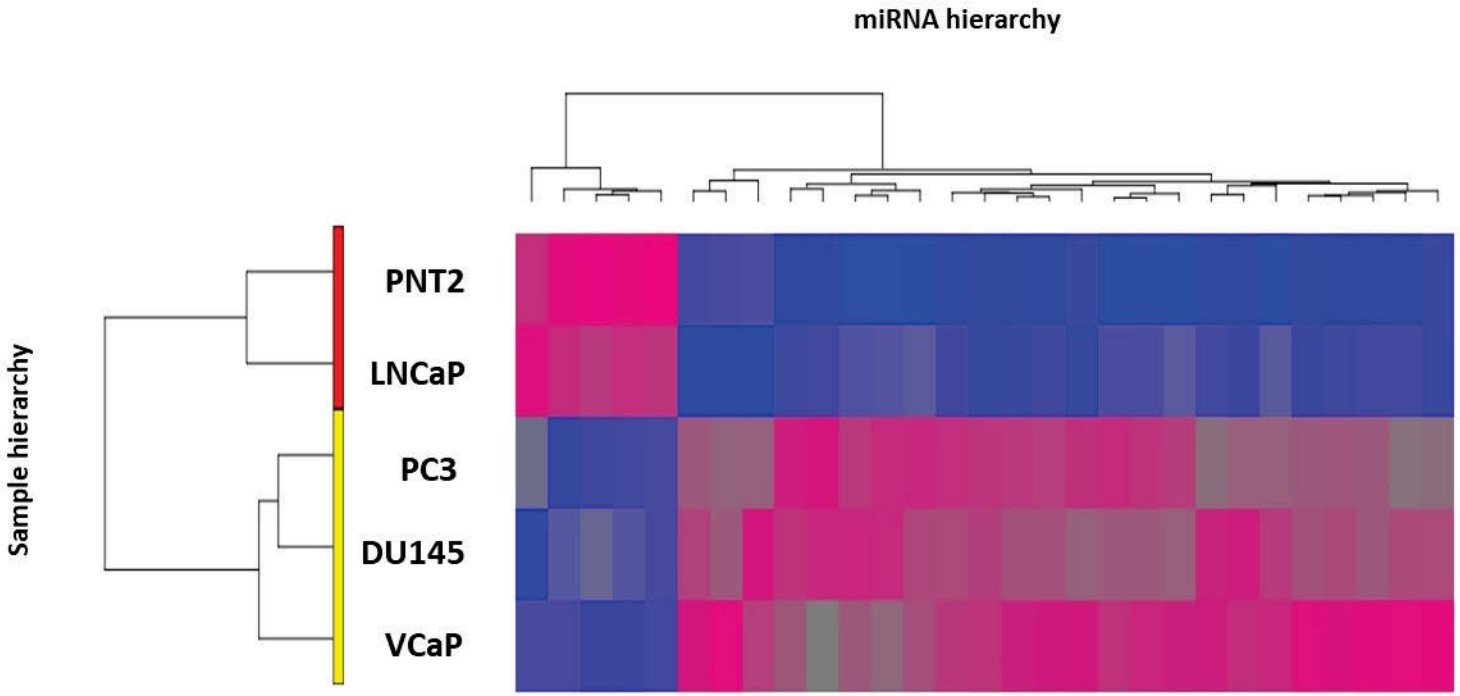

Figure 2.9. Hierarchical clustering diagram of exomiRs differentially expressed between androgen dependent and androgen independent exosomes. Hierarchical clustering diagram of exomiRs differentially expressed between exosomes secreted by androgen dependent cells (red box) and androgen independent cells (yellow box). Exosomes were isolated from tissue culture supernatants using differential ultracentrifugation. RNA was then isolated using RNAzol RT and the RNA concentrations were normalised to 50 ng/µL prior to loading samples onto an Affymetrix miRNA microarray GeneChip 2.0. All differential exomiR expression was statistically significant ($P<0.05$) with fold changes of greater than 2 or less than -2. The dendrogram on the left hand side shows that the exomiR profiles from androgen responsive cell lines (PNT2 and LNCaP) segregate into a cluster separate from the androgen independent exomiR profiles (PC3, DU145 and VCaP). Pink areas on the cluster diagram represent a highly expressed exomiR while blue indicates a lowly expressed exomiR.

2.2.4. Gene ontology analysis of enriched PCa exomiRs using Cytoscape

Once differential expression profiles were established, the enriched PCa exomiRs were analysed further for their potential functional roles. The enriched PCa exomiRs were the only ones analysed because it was assumed that miRNAs packaged at some energy expense to the cell were the most likely to hold functional significance. To perform the analysis, the top 10 most highly enriched PCa exomiRs (according to the miRNA microarray, see Table 2 in appendix section) were merged with the top 100 genes they are likely to target. Using the GeneMANIA plugin for Cytoscape, this list of roughly 800 genes (there were many genes targeted by more than one exomiR) was interrogated for interactions. This produced a massive network containing over 2000 known or putative interactions amongst the input gene set. To simplify things, the MCODE plugin was used to search the network for interaction hubs, areas particularly dense with interactions (termed “edges” by Cytoscape). One particularly interesting interaction hub (termed MCODE PCa Cluster 2) was discovered and is presented in Figure 2.10.

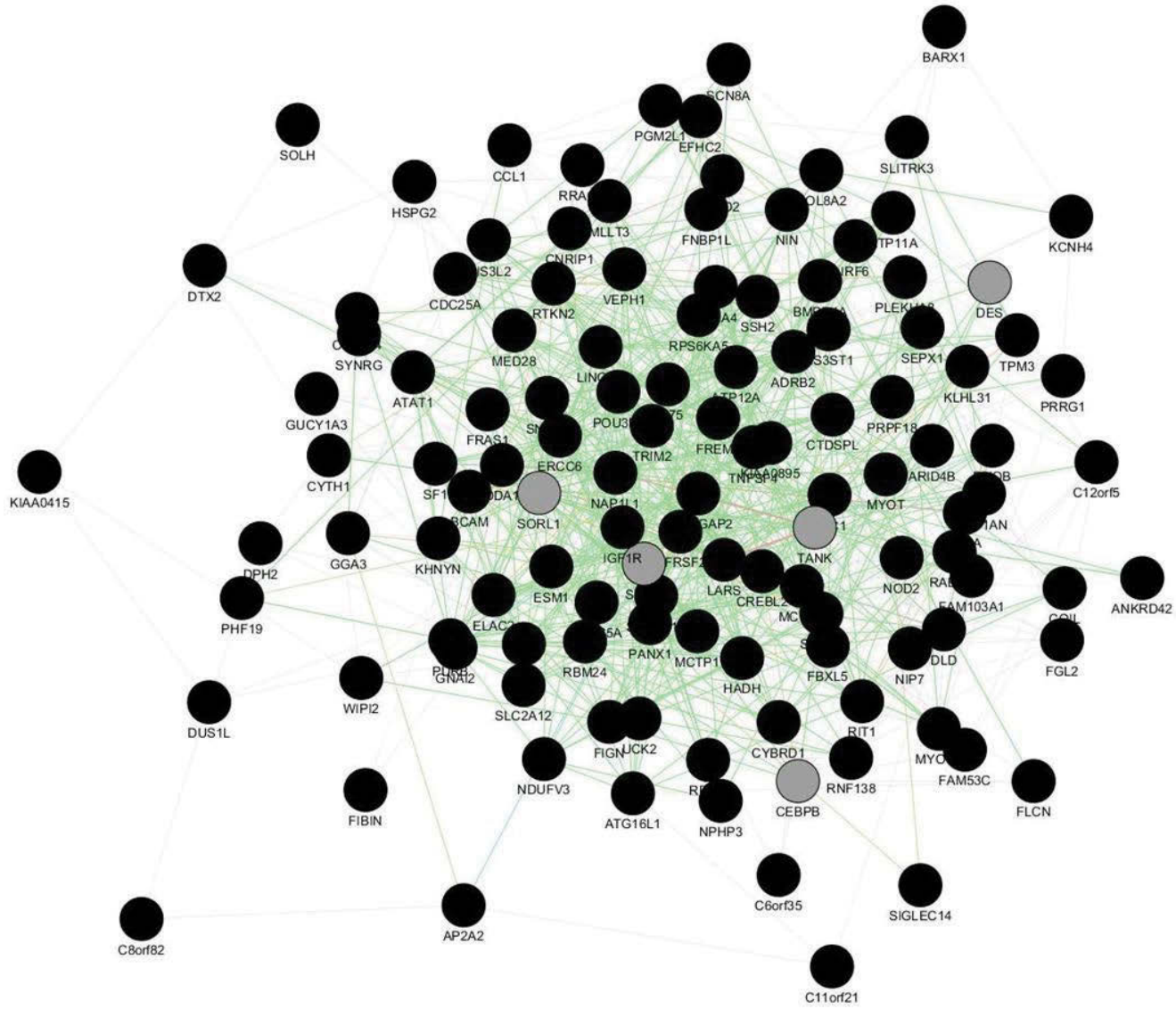

Figure 2.10. MCODE PCa Cluster 2, genes targeted by miRNAs that are highly concentrated in PCa exosomes. Interaction hub taken from a larger network of genes using the MCODE algorithm. The top ten miRNAs most highly enriched in PCa exosomes were merged with their most likely target genes using TargetScan 5.2. The top 100 target genes of each exomiR were then selected using the context score. This large list (approximately 900 potential target genes) was then interrogated for interactions using GENEMania, a Cytoscape plugin. Black nodes represent genes that are known or predicted targets of exomiRs enriched in PCa exosomes. Grey nodes are genes known to interact heavily with genes in the black nodes and were selected for inclusion in the network automatically, using the GeneMANIA plugin. There are a total of 122 nodes (proteins likely to be down-regulated by the absorption of highly expressed PCa exomiRs) in the network. There are 888 edges (lines between the nodes that represent protein-protein interactions) amongst these genes.

This interaction hub was deemed particularly interesting as it contained genes mainly involved in immunological processes. This would suggest that the top 10 PCa exomiRs are involved in dampening immunological function, one of the main functional modalities suggested for exosomes secreted by cancerous cells (146). These gene ontologies are presented below in Table 2.1.

Table 2.4. MCODE PCa Cluster 2, immunological processes targeted by PCa exomiRs

MCODE PCa cluster 2 gene ontology
regulation of cytokine secretion
positive regulation of adaptive immune response based on somatic recombination
of immune receptors built from immunoglobulin superfamily domains
positive regulation of protein secretion
regulation of gliogenesis
positive regulation of cytokine secretion
interleukin-10 production
interleukin-2 production
regulation of interleukin-10 production
regulation of interleukin-2 production
cytokine production involved in immune response
positive regulation of production of molecular mediator of immune response
positive regulation of leukocyte mediated immunity
toll-like receptor 5 signaling pathway
positive regulation of lymphocyte mediated immunity

toll-like receptor 10 signaling pathway
toll-like receptor TLR1:TLR2 signaling pathway
regulation of T cell mediated immunity
toll-like receptor TLR6:TLR2 signaling pathway
regulation of cytokine production involved in immune response
regulation of JUN kinase activity
positive regulation of JUN kinase activity
positive regulation of cytokine production involved in immune response
regulation of glial cell differentiation
cytokine secretion
positive regulation of adaptive immune response

The same process of integrating enriched exomiRs with their target genes and subsequently building a network from this information was also applied to the androgen independence associated exomiRs. This analysis yielded two dense interaction hubs which are presented in Figure 2.11. and Figure2.12. The ontologies for the gene sets in the interaction hubs are presented in Table 2.5. and Table 2.6. respectively.

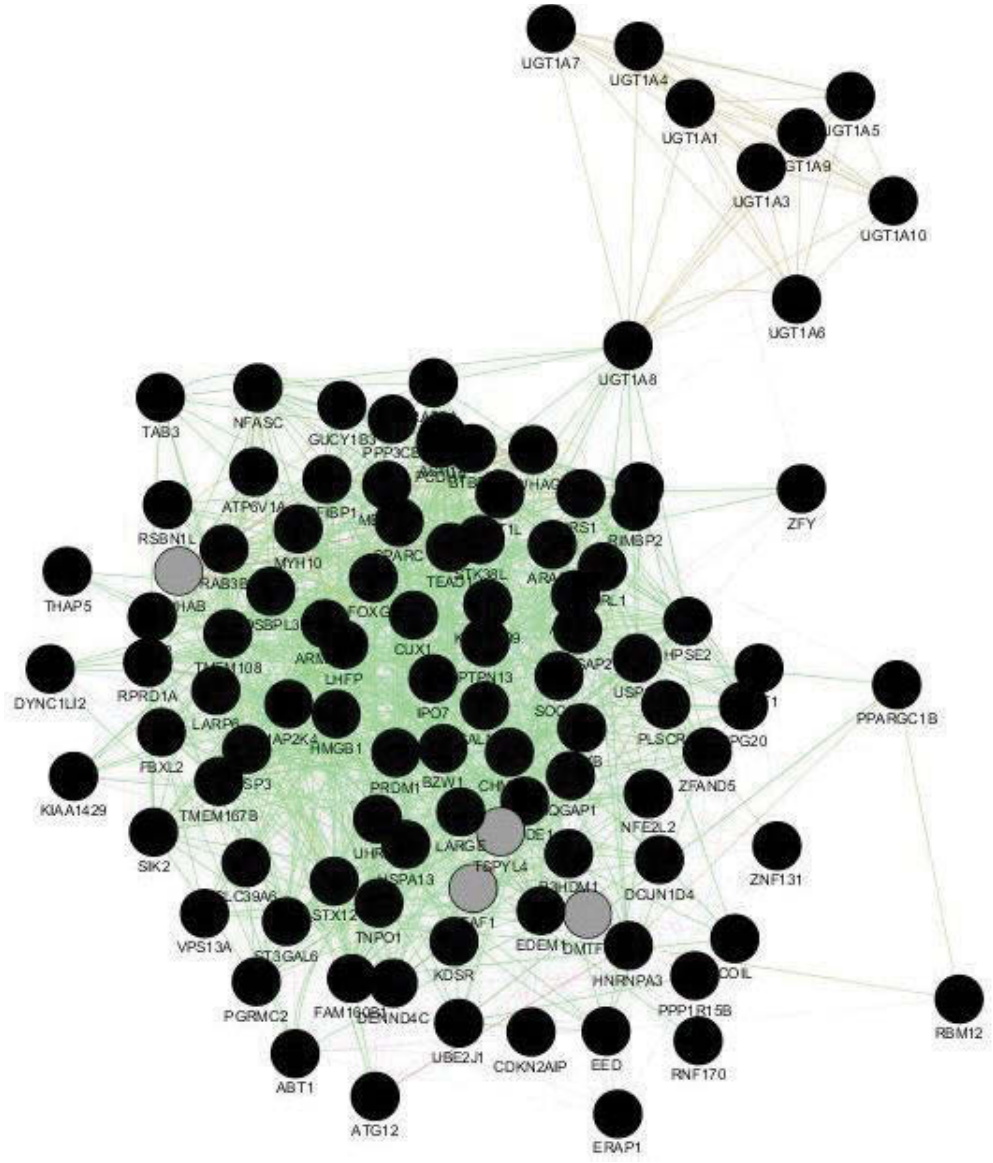

Figure 2.11. MCODE androgen independence cluster 1, targets of exomiRs secreted by androgen independent PCa cells.

Interaction hub taken from a larger network of genes using the MCODE algorithm. The top ten miRNAs most highly enriched in PCa exosomes were merged with their most likely target genes using TargetScan 5.2. The top 100 target genes of each exomiR were then selected using the context score. This large list (approximately 900 potential target genes) was then interrogated for interactions using GENEMania, a Cytoscape plugin. Black nodes represent genes that are known or predicted targets of exomiRs enriched in PCa exosomes. Grey nodes are genes known to interact heavily with genes in the black nodes and were selected for inclusion in the network using the GeneMANIA plugin. There are a total of 104 nodes (proteins likely to be down-regulated by the absorption of exomiRs secreted by androgen independent PCa) in the network. There are 1321 edges (lines between the nodes that represent protein-protein interactions) amongst these genes.

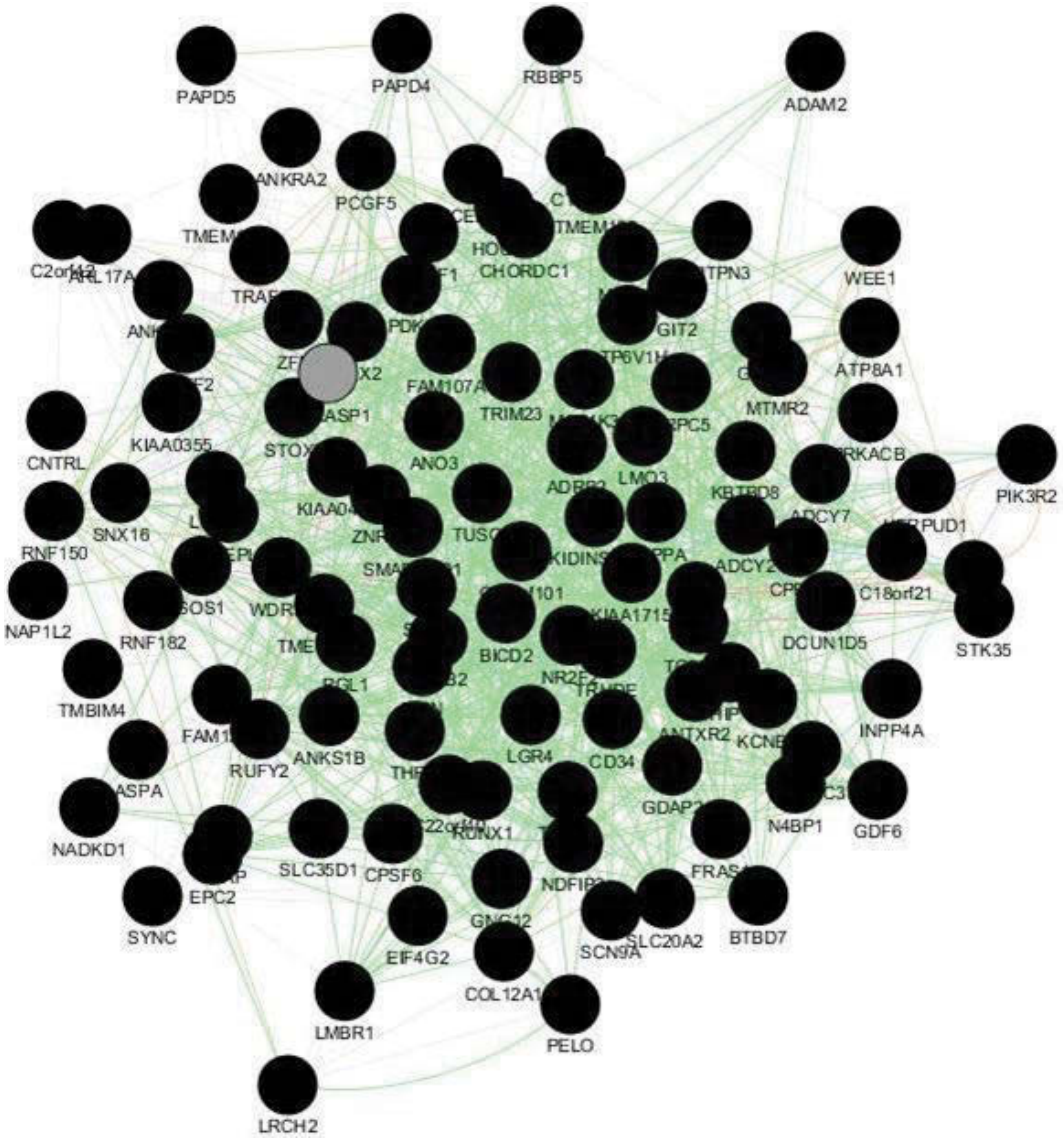

Figure 2.12. MCODE androgen independence cluster 2, targets of exomiRs secreted by androgen independent PCa cells.

Interaction hub taken from a larger network of genes using the MCODE algorithm. The top ten miRNAs most highly enriched in PCa exosomes were merged with their most likely target genes using TargetScan 5.2. The top 100 target genes of each exomiR were then selected using the context score. This large list (approximately 900 potential target genes) was then interrogated for interactions using GENEMania, a Cytoscape plugin. Black nodes represent genes that are known or predicted targets of exomiRs enriched in PCa exosomes. Grey nodes are genes known to interact heavily with genes in the black nodes and were selected for inclusion in the network using the GeneMANIA plugin. There are a total of 113 nodes (proteins likely to be down-regulated by the absorption of exomiRs secreted by androgen independent PCa) in the network. There are 1280 edges (lines between the nodes that represent protein-protein interactions) amongst these genes.

Separate ontology searches were then performed to determine the most likely functions of each cluster. Cluster 1 was mostly associated with various metabolic processes and toll-like receptor signaling (also an immunological function) as seen in Table 2.2. Cluster 2 was mostly associated with cell cycle regulation and developmental genes. This data is summarized in Table 2.3.

Table 2.5. MCODE androgen independence cluster 1 gene ontology analysis

MCODE androgen independence cluster 1 gene ontology
glucuronate metabolic process
toll-like receptor 5 signaling pathway
toll-like receptor 10 signaling pathway
toll-like receptor TLR1:TLR2 signaling pathway
toll-like receptor TLR6:TLR2 signaling pathway
pigment metabolic process
retinoic acid metabolic process
positive regulation of lymphocyte differentiation
flavone metabolic process
cellular glucuronidation
retinoid metabolic process
flavonoid glucuronidation
uronic acid metabolic process
isoprenoid metabolic process
xenobiotic glucuronidation
terpenoid metabolic process
flavonoid metabolic process

Table 2.6. MCODE androgen independence cluster 2 gene ontology analysis

MCODE androgen independence cluster 2 gene ontology
pathway-restricted SMAD protein phosphorylation
salivary gland morphogenesis
endosome to lysosome transport
regulation of morphogenesis of a branching structure
positive regulation of phospholipase C activity
regulation of cartilage development
phosphatidylinositol 3-kinase signaling
regulation of phosphatidylinositol 3-kinase signaling
cellular response to glucagon stimulus
positive regulation of phosphatidylinositol 3-kinase signaling
metanephric nephron development
regulation of phospholipase C activity
collagen fibril organization
negative regulation of cellular catabolic process
regulation of chondrocyte differentiation
response to glucagon
exocrine system development
activation of MAPKK activity
fluid transport
epithelial to mesenchymal transition
early endosome to late endosome transport
water transport
vacuolar transport
neuron fate commitment
negative regulation of epithelial cell proliferation
lysosomal transport
adenylate cyclase-activating G-protein coupled receptor signaling pathway
salivary gland development
maternal process involved in female pregnancy

2.2.5. mRNA and lncRNA microarray based expression analysis reveals differential expression profiles between PCa exosomes and normal prostate exosomes

As with the microRNA expression analysis, it was first confirmed that cellular and exosomal expression profiles could be differentiated from one another. This turned out to be the case as a large number of RNAs were differentially expressed using the most stringent statistical method available, the false discovery rate algorithm (FDR). These data are presented in Figure 2.13 and Figure 2.14. Tables 4 and 5 in the appendix section contain all the mRNAs and lncRNAs respectively that make up these profiles.

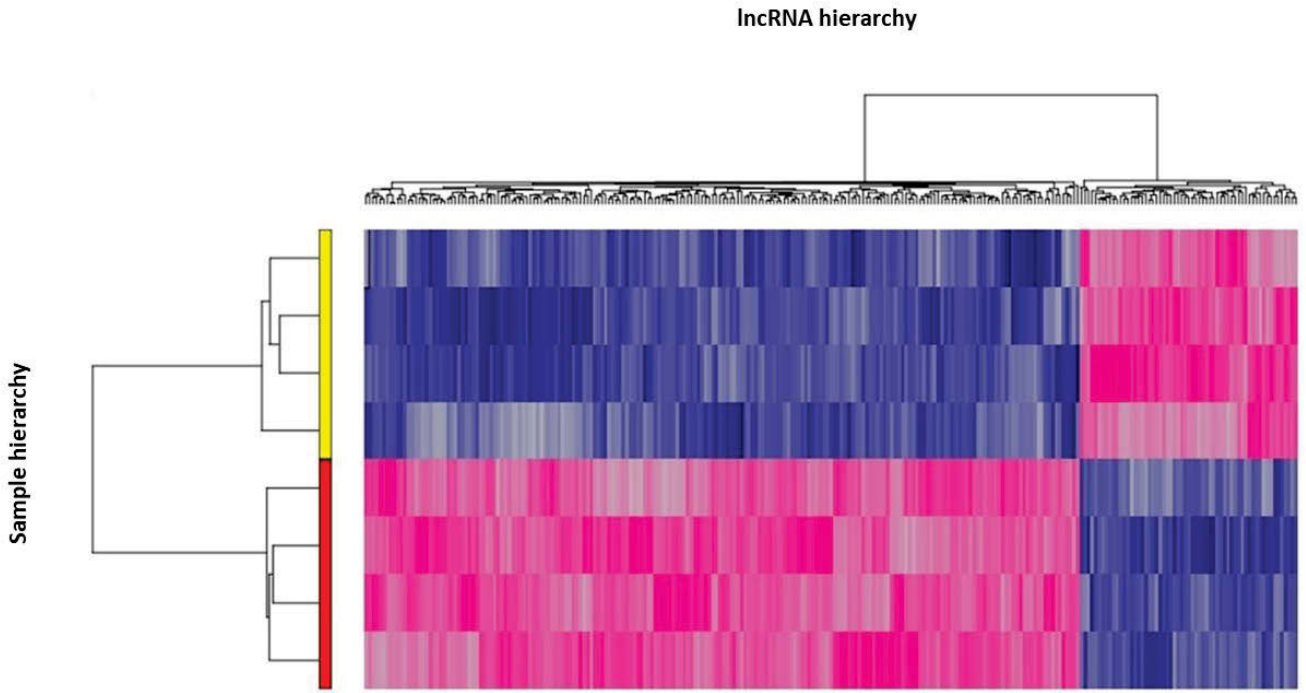

Figure 2.13. Comparison of lncRNA expression profiles between PCa exosomes and PCa cells.

Hierarchical clustering diagram of exosomal mRNAs differentially expressed between PCa cells and PCa exosomes. Exosomes were isolated from tissue culture supernatants using differential ultracentrifugation. RNA was then isolated using RNAzol RT and RNA samples were normalized to 50 ng/µL before being analysed on the ArrayStar microarray platform for mRNA and lncRNA. All differential mRNA expression was statistically significant (FDR<0.05) with fold changes of greater than 2 or less than -2. The dendrogram on the left indicates that PCa cellular and exosomal mRNA expression profiles form separate clusters indicated by the yellow bar (PCa exosomal mRNAs) and the red bar (PCa Cellular mRNAs). On the diagram itself, pink rectangles indicate a mRNA that is more highly expressed, while blue indicates a mRNA that is expressed at lower levels.

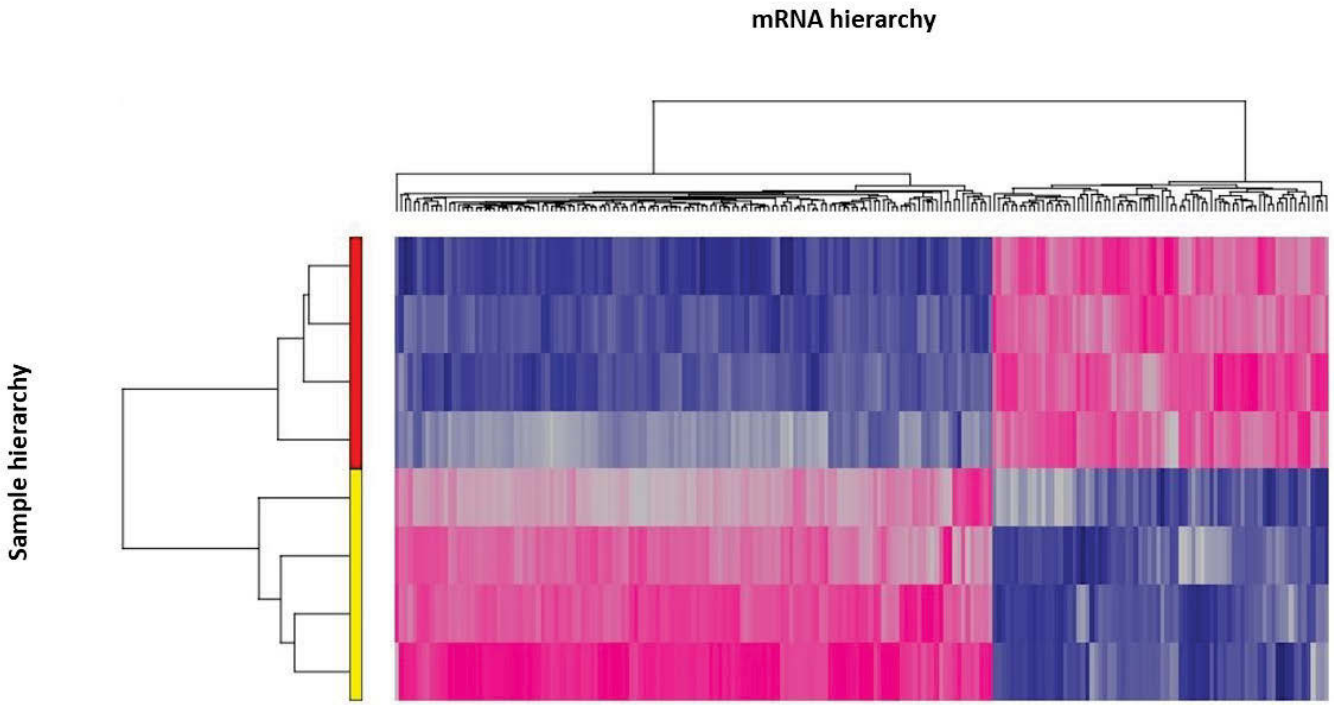

Figure 2.14. Comparison between exosomal mRNA and cellular mRNA expression profiles.

Hierarchical clustering diagram of exosomal mRNAs differentially expressed between PCa cells and PCa exosomes. Exosomes were isolated from tissue culture supernatants using differential ultracentrifugation. RNA was then isolated using RNAzol RT and RNA samples were normalized to 50 ng/µL before being analysed on the ArrayStar microarray platform for mRNA and lncRNA. All differential lncRNA expression was statistically significant (FDR<0.05) with fold changes of greater than 2 or less than -2. The dendrogram on the left indicates that PCa cellular and exosomal lncRNA expression profiles form separate clusters indicated by the yellow bar (PCa exosomal lncRNAs) and the red bar (PCa Cellular lncRNAs). On the diagram itself, pink rectangles indicate a mRNA that is more highly expressed, while blue indicates a mRNA that is expressed at lower levels.

Knowing that exosomal mRNA and lncRNA expression profiles were indeed unique, exosomal expression profiles were analysed further. This yielded similar results to the previous analysis in that most mRNAs and lncRNAs were expressed at lower levels in PCa exosomes, this time relative to normal prostate exosomes. These data are presented in Figure 2.15 and Figure 2.16. Tables 6 and 7 in the appendix section contain all the mRNAs and lncRNAs respectively that make up these profiles.

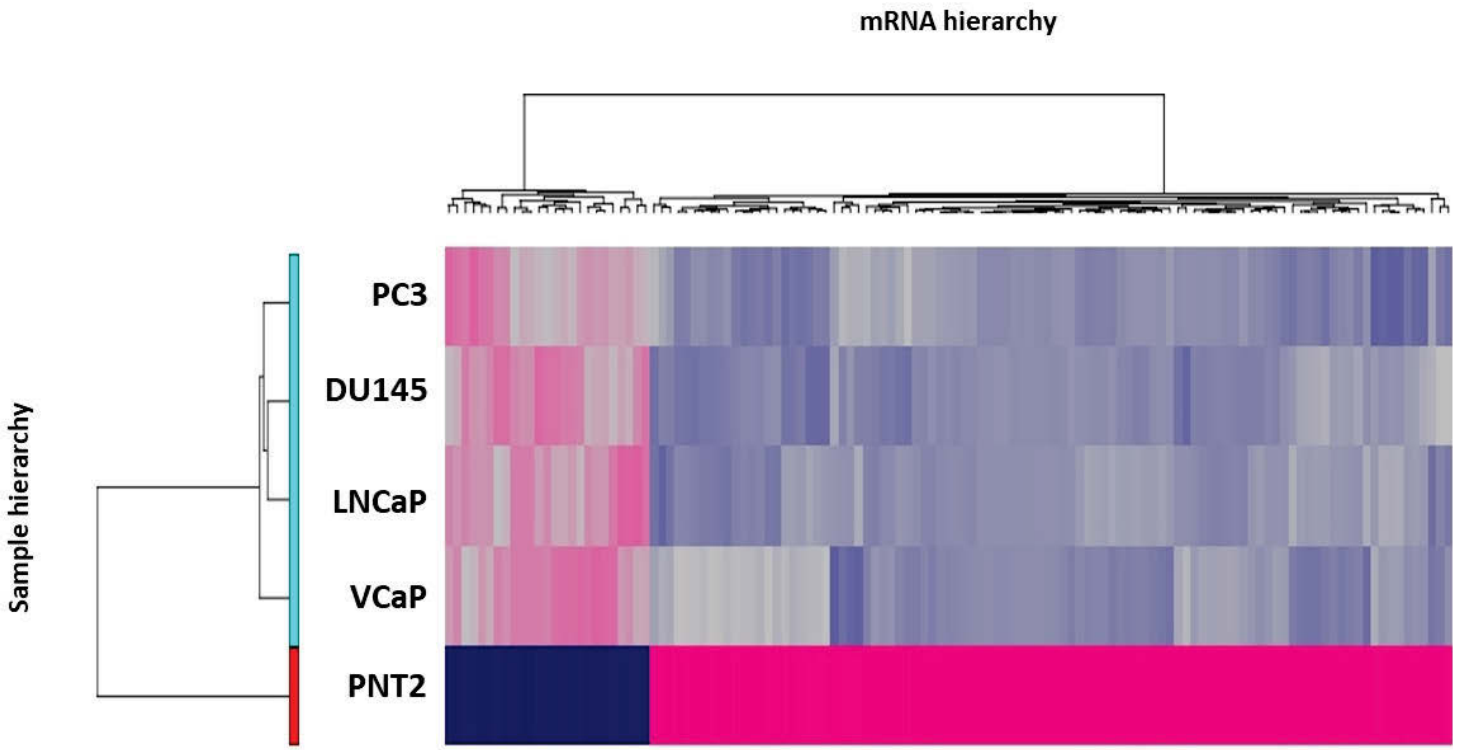

Figure 2.15. Hierarchical clustering diagram of exosomal mRNAs differentially expressed between normal prostate exosomes (PNT2) and PCa exosomes. Hierarchical clustering diagram for exosomal mRNA. Exosomes were isolated from tissue culture supernatants using differential ultracentrifugation. RNA was then isolated using RNAzol RT and RNA samples were normalized to 50 ng/µL before being analysed on the ArrayStar microarray platform for mRNA and lncRNA. The majority of mRNA are packaged at lower concentrations in PCa exosomes (PC3, DU145, LNCaP, VCaP). All differential exosomal RNA expression was statistically significant ($P<0.01$) and all fold changes were either >2 or <-2.

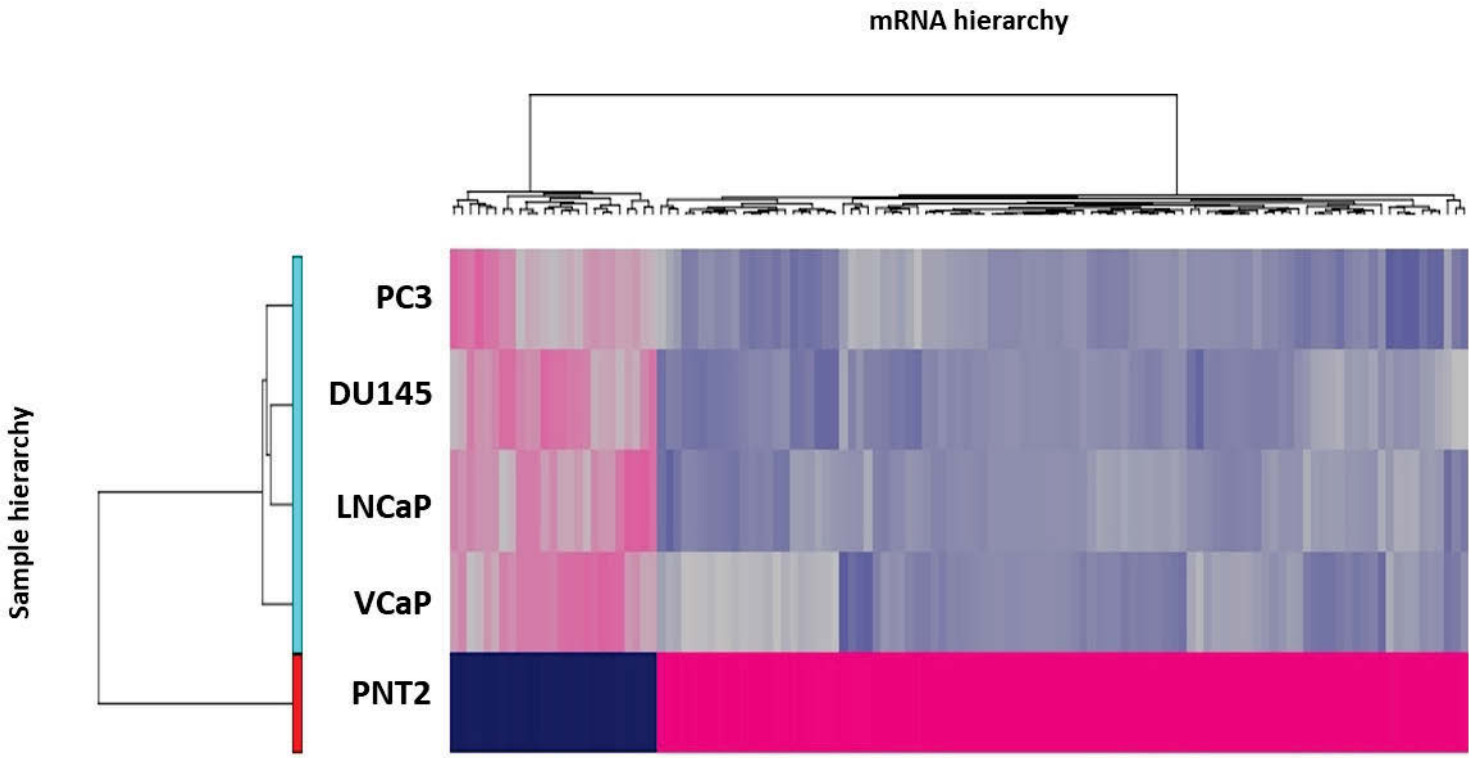

Figure 2.16. Hierarchical clustering diagram of exosomal lncRNAs differentially expressed between normal prostate exosomes (PNT2) and PCa exosomes. Hierarchical clustering diagrams for exosomal lncRNA. Exosomes were isolated from tissue culture supernatants using differential ultracentrifugation. RNA was then isolated using RNAzol RT and RNA samples were normalized to 50 ng/µL before being analysed on the ArrayStar microarray platform for mRNA and lncRNA. The majority of lncRNAs are packaged at lower concentrations in PCa exosomes (VCaP. PC3, DU145, LNCaP). All differential exosomal RNA expression was statistically significant ($P<0.01$) and all fold changes were either >2 or <-2.

Androgen dependence status was also investigated using exosomal mRNAs and lncRNAs. This was performed in much the same manner as with the exomiRs and yielded similar results. The differential expression profile was enough to distinguish androgen dependent cells from androgen independent cells. However, as had become the trend with exosomal mRNA and lncRNA, most of these RNAs were packaged at lower concentrations in exosomes secreted by androgen independent cells. These data are presented in Figure 2.17 and Figure 2.18. Tables 8 and 9 in the appendix section contain the mRNAs and lncRNAs respectively that make up these profiles.

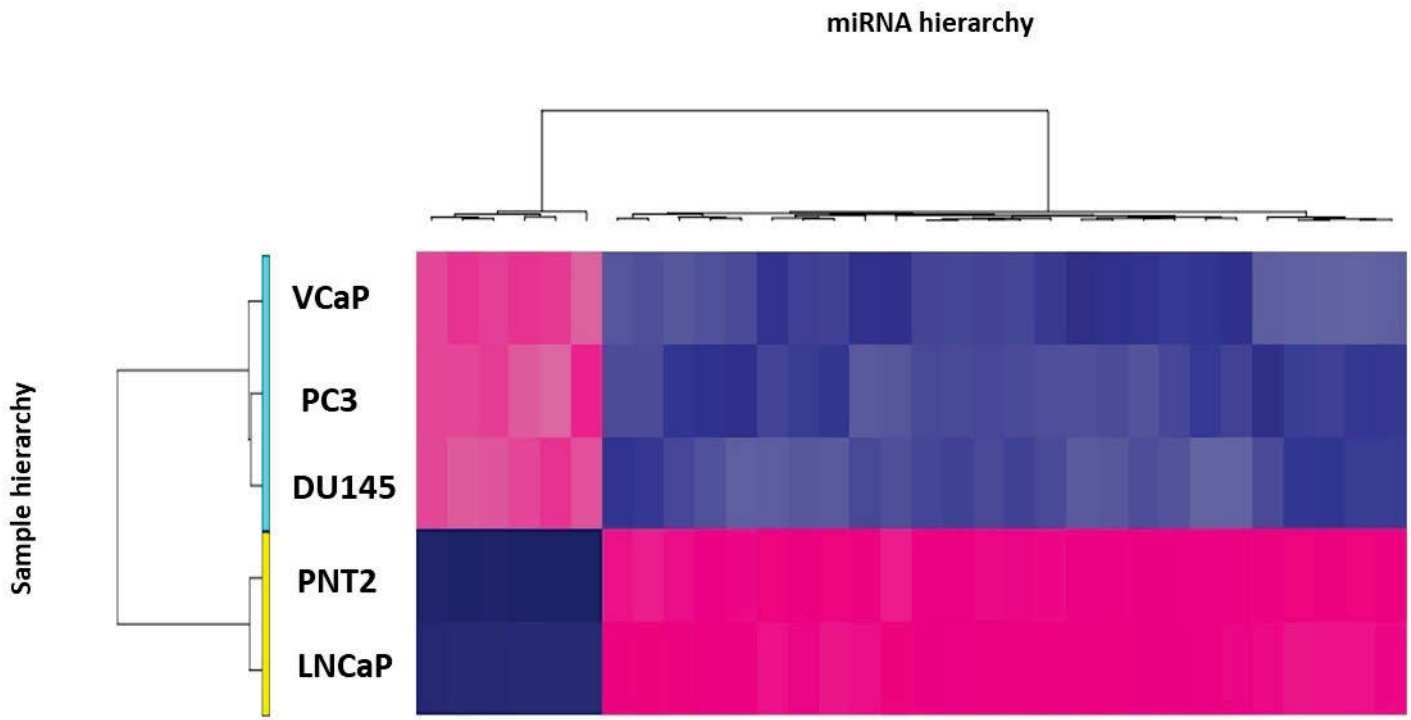

Figure 2.17. Exosomal mRNAs Secreted by androgen independent PCa cells.

Hierarchical clustering diagram for mRNAs in exosomes secreted androgen dependent cells compared to androgen independent cells. Exosomes were isolated from tissue culture supernatants using differential ultracentrifugation. RNA was then isolated using RNAzol RT and RNA samples were normalized to 50 ng/µL before being analysed on the ArrayStar microarray platform for mRNA and lncRNA. Most mRNAs are packaged at lower concentrations in exosomes secreted by androgen independent cells (VCaP, PC3, DU145). All differential exosomal mRNA and lncRNA expression was highly statistically significant ($P<0.001$) and all fold changes were either >2 or <-2.

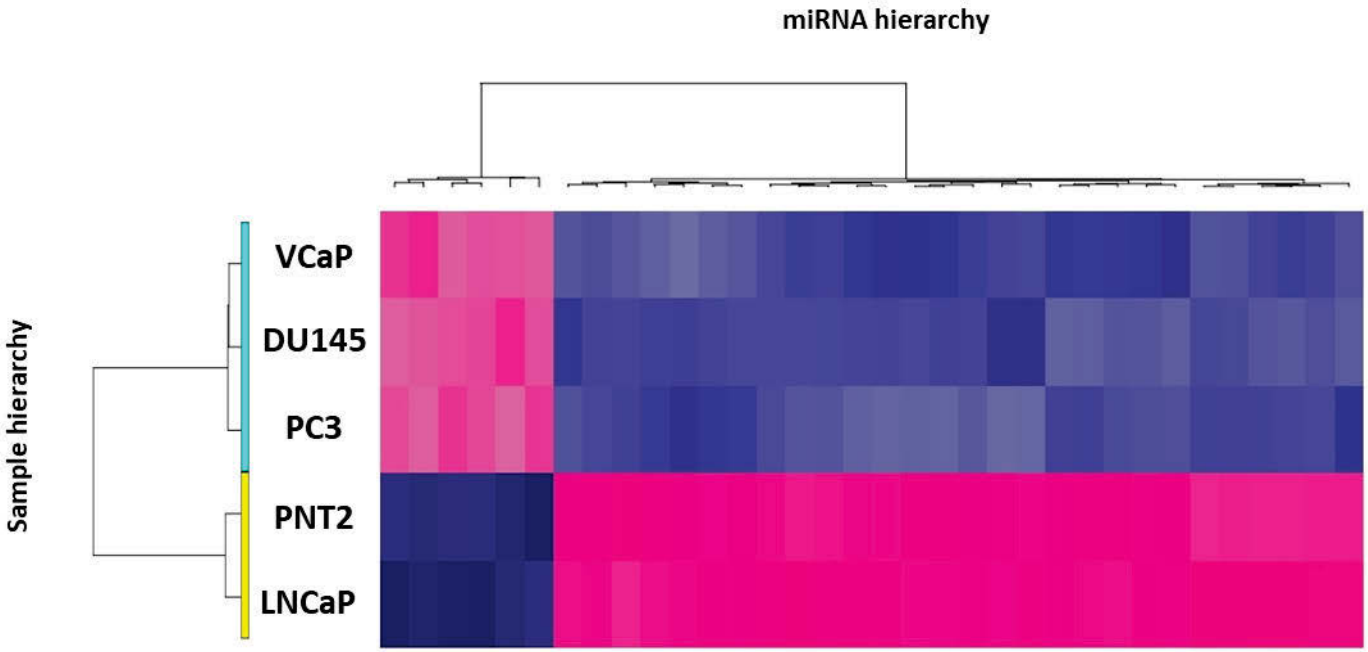

Figure 2.18. Exosomal lncRNAs Secreted by androgen independent PCa cells.

Hierarchical clustering diagram for lncRNAs in exosomes secreted androgen dependent cells compared to androgen independent cells. Exosomes were isolated from tissue culture supernatants using differential ultracentrifugation. RNA was then isolated using RNAzol RT and RNA samples were normalized to 50 ng/µL before being analysed on the ArrayStar microarray platform for mRNA and lncRNA. Most lncRNAs are packaged at lower concentrations in exosomes secreted by androgen independent cells (VCaP, DU145, PC3). All differential exosomal mRNA and lncRNA expression was highly statistically significant ($P<0.001$) and all fold changes were either >2 or <-2.

2.2.6. Selecting the most promising biomarker candidates to be tested for diagnostic and prognostic ability in patient samples

Several things were considered when developing the panel of biomarkers that would be validated by qPCR and subsequently tested in human samples. The first decision was to not use any lncRNAs as biomarker candidates. These types of RNAs were much less abundant in exosomes as both the Bioanalyzer 2100 data (Figure 2.6.) and the ArrayStar microarray data (Figures 2.12. and 2.13.) confirmed, and the descriptive data surrounding lncRNAs was also very poor at the time. These types of RNA are also longer and less stable than miRNAs, meaning they are more likely to degrade before any analysis can be performed. This is of critical importance if any of these biomarker candidates were to enter mainstream medical use, as a biomarker susceptible to decay may be degraded in transit to a diagnostic pathology centre.

The exomiR biomarker candidates that were ultimately selected had to meet two critical criteria. The first was that the miRNA had to be more concentrated in PCa exosomes than in normal prostate exosomes. This is because the increased packaging suggests some sort of benefit or functionality for that particular miRNA in the context of PCa. Enriched exomiRs also are more likely to be detected in complex biological samples such as plasma which contains exosomes from a large number of tissues. This likely means a low signal to noise ratio will be achieved when analysing exomiR samples from this source. A highly concentrated exomiR is therefore more likely to be detected in this scenario.

The novelty of the exomiR biomarker candidates was also an important consideration from a patent perspective. If the biomarkers presented in this thesis did turn out to offer strong diagnostic and/or prognostic potential, they may form the basis of a patentable diagnostic technique. An exomiR that has been already associated with PCa and is published in a scientific journal is considered public domain and therefore not patentable. Unpublished, novel exomiRs therefore offered an more straightforward path to a patented diagnostic technique. At the time this work was performed, almost no data existed regarding star strand miRNA expression in PCa cells or their exosomes. Several highly expressed star-strand exomiRs were therefore selected for inclusion in the panel of candidate biomarkers.

The biomarker candidates that were selected for qPCR validation and possible further testing in human samples were: miR-362, miR-125b, miR-30a, miR-126*, miR-149*, miR-1228, miR-1228*, miR-1246, let-7i and GAPDH. GAPDH was selected for inclusion in the biomarker candidate panel as it turned out to be very highly expressed in PCa exosomes but not PNT2 exosomes.

2.2.7. Validation of biomarker candidate exomiRs by qPCR

qPCR was a required step to validate the differential expression of the potential biomarkers from the microarray. This is because microarrays are prone to false positive errors which need to be eliminated before using precious patient samples. The first step in validating the most promising array findings with qPCR was to identify an endogenous control gene. An effective endogenous control gene must be stably expressed in exosomes regardless of the cell of origin, and the condition of the cells secreting the exosomes. Once an endogenous control gene was identified, further exosome samples were isolated from the cell lines and their RNA extracted. The RNA samples were reverse transcribed into cDNA and molecular probes for the genes of interest identified in the microarray analysis were used on the cDNA samples to ensure that the biomarker candidates were true positives.

2.2.8. Identification of an endogenous control gene for use as a loading control in future experiments

This is an essential part of any qPCR based experiment as it is used to detect errors and to appropriately normalise the results for an accurate interpretation of the data (147, 148). Normally a constitutively expressed gene is selected for use as the reference gene. However, at the time this experiment was performed there was no information available regarding an appropriate constitutively expressed endogenous control, so a number of common reference genes (GAPDH, ACTB, U44, U75) were tested, except for 18S as the Bioanalyzer was not able to detect 18S in the exosomal sample. MiR-92b*, which was originally suspected to be a biomarker candidate was also tested and it performed admirably as an endogenous control as it t exhibited the least variation in expression across all cell lines. The data are presented in Figure 2.19.

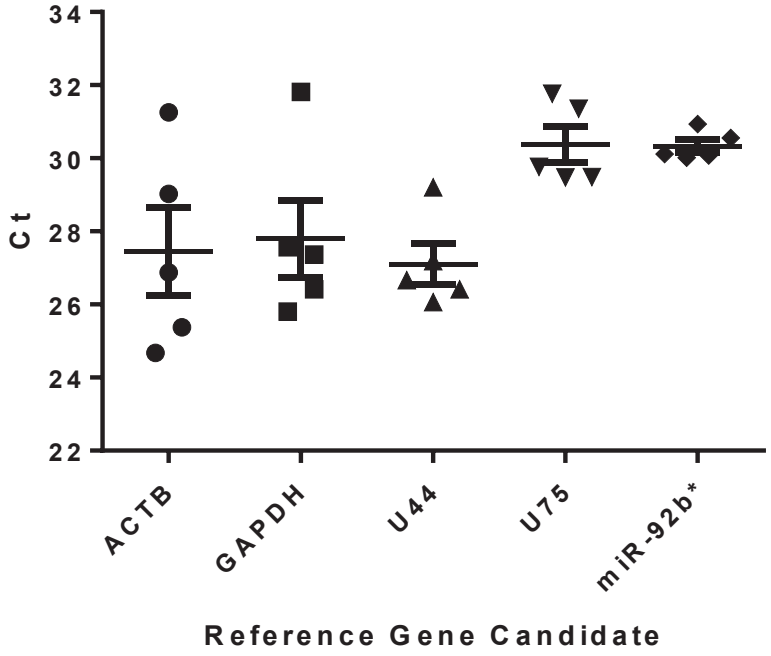

Figure 2.19. Candidates for endogenous control genes in PCa and PNT2 exosomes.

Exosomes were isolated from tissue culture supernatants (n = 5) using differential ultracentrifugation. RNA was then isolated using RNAzol RT and RNA samples were normalized to 100 ng/µL before undergoing reverse transcription using Taqman primers for the RNAs listed in the above Figure. The reverse transcribed samples were then analysed on the Quantstudio 12k Flex platform. Each gene expression assay was performed in triplicate. Only miR-92b* showed stable expression (around ct = 30) across all cell lines. It was used in all subsequent experiments as a reference gene.

2.2.9. qPCR validation of the differential expression profiles of biomarker candidates

Given the low number of enriched mRNAs and lncRNAs in PCa exosomes, miRNAs became the majority focus of all further analyses. A panel of 9 of the most highly enriched exomiRs and one mRNA were validated using qPCR. This was performed using one exosomal RNA sample from each cell line. Each of these genes except for miR-362 and miR-30a were significantly enriched across all PCa cell lines, a highly encouraging sign that these exosomal RNAs would make good biomarkers *in vivo* as well. This data is presented in Figure 2.20.

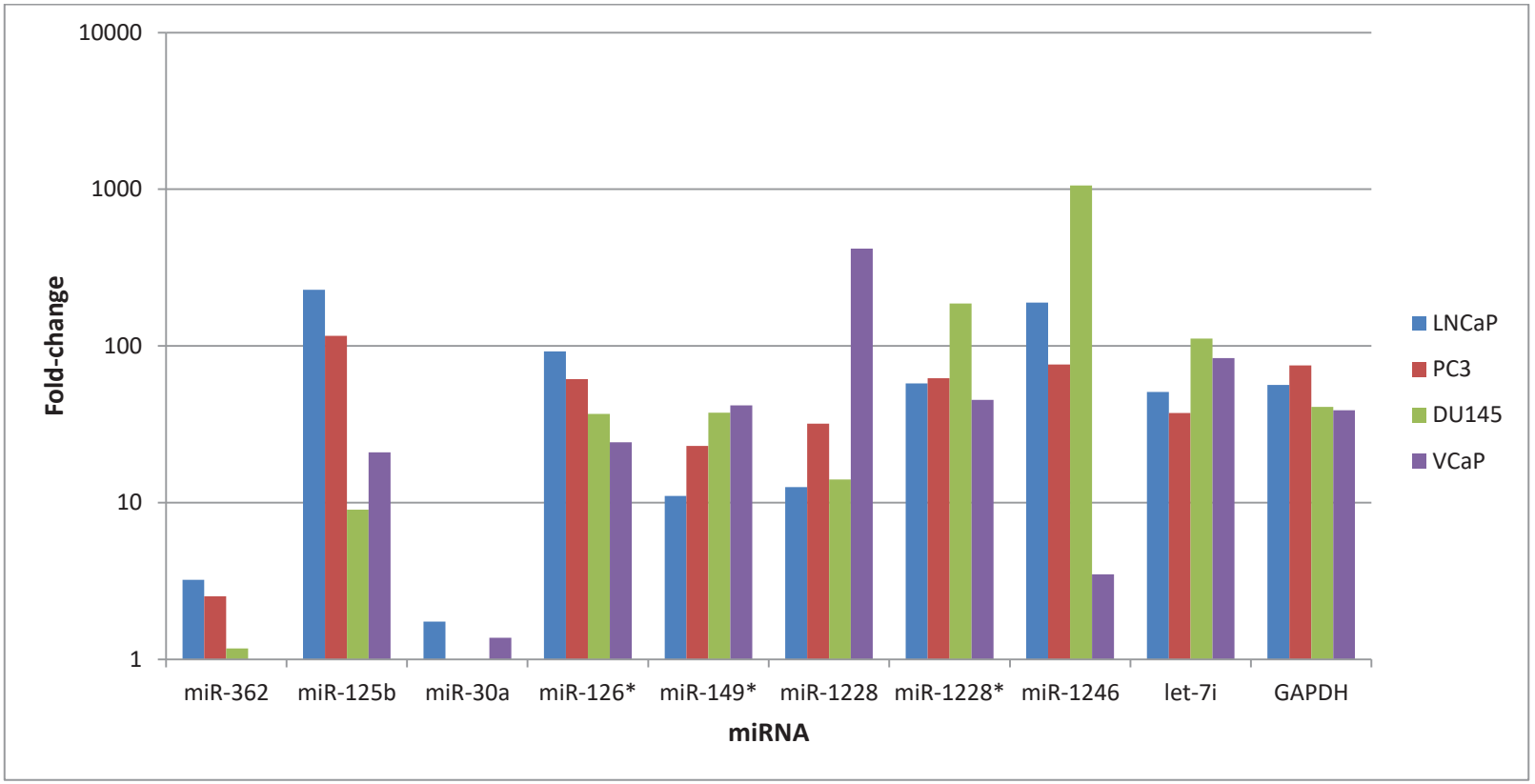

Figure 2.20. qPCR validation of the differential expression profiles of biomarker candidates.

Exosomes were isolated from tissue culture supernatants using differential ultracentrifugation. RNA was then isolated using RNAzol RT and RNA samples were normalized to 100 ng/µL before undergoing reverse transcription using Taqman primers for the miRNAs listed in the above Figure. The amplified samples were then analysed on the Quantstudio 12k Flex platform miR-362 and miR-30a proved to be poor biomarkers as they were not enriched in exosomes from all PCa cell lines. However, all the other candidates are enriched in exosomes from PCa cells versus PNT2 exosomes, and all have very large fold-changes.

2.3. Discussion

2.3.1. Analysis of Exosomal morphology and RNA content confirms that differential ultracentrifugation isolates exosomes that are enriched with small RNAs

Because of the large and still increasing variety of micro and nanoparticles that can be isolated from human body fluids, exosome samples must always be assessed for purity in any experimental workflow involving these particles. Given the very different origins of other particles of similar size such as microparticles, apoptotic bodies etc, contamination of an exosome sample with significant quantities of these particles would greatly influence the RNA expression profile and undermine the reliability of any expression profile generated. To circumvent this issue, Transmission Electron microscopy was performed to ensure that all exosome samples obtained from tissue culture supernatants were free from other non exosomal particles. These results were encouraging as all particles were of approximately 100 nm and appeared with the cup shaped morphology described by Théry et al (137), the highest standard of exosome characterisation at the time this experiment was performed. Furthermore this method is still widely used today with a great variety of published data supporting the use of this technique in exosome quality control. However, in most modern exosome experiments TEM is coupled with other techniques that look at surface markers. This information was not available at the time but exosomal surface markers were more thoroughly assessed in chapters 3, 4 and 5.

The RNA quality itself also had to be considered before performing any laborious and expensive microarray profiling procedures. If RNA is degraded due to environmental contamination or sample specific RNAse activity, then low copy number RNAs may be lost and an inaccurate profile will be generated. Given the small amount of information available regarding exoRNA attributes available at the time, The Agilent Bioanalyzer 2100 RNA pico chips were selected to perform this analysis. These chips were able to determine very precisely the amount of RNA in a sample, and could also provide an estimate of the proportion of the sample made up by small RNA. The latter was of particular relevance given the promising results performed earlier in our laboratory, in which we showed that exomiRs could be used to differentiate between cancerous and non-cancerous cells.

Interestingly, the miRNA content of exosomes is largely composed of small RNA less than 200 nucleotides in length and approximately 50% of exosomal RNA is made up of miRNA in particular. This is in line with other publications that have covered exosomal RNA content. For example, Kogure et al showed in 2011 that their exosomal RNA samples derived from hepatocellular carcinoma cell lines were largely composed of miRNA, and showed that these exomiRs could exert functions in other related cell lines (100). ExomiRs have also been thoroughly examined in our lab and others as biomarkers for many different disease states (see Vlassov et al for review (149)).

Knowing that exosomes are enriched with miRNAs, most of the biomarker candidates revealed later in this chapter are exomiRs. Also, most of the exoRNA functionality proposed in this chapter comes from looking at these differentially expressed miRNAs and their potential target genes.

2.3.2. Exosomal miRNA expression is different to that of the parent cell

This discovery has been fundamental to all of the functional analyses performed throughout this project. It shows clearly that the parent cell lines are capable of packaging unique contents into their exosomes and do not merely reflect the contents of the parent cell in the way microparticles do. It also suggests that the most selectively packaged exomiRs are functional, especially those that are enriched in the exosome versus the parent cell, as cells are unlikely to package anything at all unless it offers some survival advantage to them. This is particularly relevant in cancer biology given the constant barriers to growth faced by cancer cells, such as nutrient and oxygen starvation and/or attack by the immune system.

This finding is also fully in line with literature regarding the specifically packaged content of exosomes, cancer derived exosomes in particular. For example, it has been demonstrated that colorectal cancer cells secrete exosomes containing known metastatic factors and signal transduction related proteins which may aid in metastatic processes (150). Sanchez et al have also recently shown that PCa bulk and stem cell populations secrete different exomiRs that function cooperatively on stromal cell populations to enhance local invasion and even distant metastasis (151). This is further supported by Willms et al who showed that melanoma cell lines release distinct subpopulations of exosomes (152). Exosome content can even be hijacked by infectious diseases as has been seen in patients suffering from Japanese encephalitis (153), various parasitic infections (154) and even in the animal kingdom in cows that secrete prion proteins in exosomes (155).

Given this control that cells can exert over their exosomal content, it is likely that exosomal content, in particular exomiRs can perform many biological functions that are relevant to cancer growth and aggression. Their differential expression also justifies the intense scrutiny upon exomiRs and other exosomal constituents as biomarkers for various disease states including cancer.

2.3.3. PCa exomiRs may promote immune evasion

It has been known for some time that cancer exosomes can influence most of the hallmarks of cancer (see Kanada et al (156) and Meehan and Vella (157) for reviews), a set of biological features that are unique to cancer growth and development (18, 158). Among these hallmarks is immune system evasion, which covers any process in which cancer cells may evade detection or inhibit the tumour killing ability of the immune system. As exosomes are highly mobile within the host body, they are an attractive explanation for system-wide repression of anti-tumour immune system functions. There are three broad modalities by which cancer exosomes have been shown to inhibit anti-tumour immune responses, i) inhibit cytotoxic effector cell functions, ii) killing of activated effector cells, iii) inhibition of anti-tumour related cytokines.

The first to demonstrate that cancer exosomes can have immunomodulatory effects were Clayton and Tabi (159), who revealed that tumour exosomes bearing various NKG2D ligands actively reduce the proportion of activated killer T-cells (CD8+) and reduce their ability to kill antigen bearing target cells. They went on to show that the NKG2D ligands in conjunction with exosomal TGFβ1 were responsible for the loss of killing function in CD8+ T-cells and Natural Killer cells (NK cells) (160). NK cell function was also down-regulated by NKG2D ligand expressing Leukaemia and lymphoma exosomes as demonstrated by Hedlund et al (161), and the same exosomal NKG2D ligands have also been associated with castration resistant PCa as the circulating CD8+ and NK cells of patients with this stage of disease had lower levels of NKG2D (162). Given the known anti-tumour effects mediated via the NKG2D receptor (163), it is unsurprising that this receptor is actively down-regulated by cancer exosomes.

It has also been shown that LNCaP exosomes can induce apoptosis in T-cells, thanks to the presence of FasL on the exosome surface (164). A similar process has also been observed in melanoma cells (114), colorectal cancer cells (115), oral cancer (116) and most recently, renal carcinoma (165). The loss of these anti-tumour effector cells would of course allow the cancer cells to grow unencumbered by immune attack.

Cancer exosomes can also indirectly inhibit anti-tumour T-cell responses by influencing the behaviour of myeloid derived suppressor cells (MDSCs). These cells are described as a heterogeneous, immature myeloid cell population known to participate in immune regulation under normal and pathological conditions (166). They are also known to migrate to tumour sites and inhibit both adaptive and innate anti-tumour responses by preventing IL-2 secretion that would stimulate expansion of anti-tumour effector cells, and by secreting IL-10, TGFβ or arginase. These 3 cytokines induce expansion of Treg cells which suppress inflammatory processes necessary for immune attack on tumour cells, and these cytokines are themselves directly suppressive of an inflammatory response, instead favouring the promotion of a non-inflammatory Th2 immune phenotype that can promote cancer progression (167). Furthermore Exosomes enriched with Hsp70 on their membranes have been shown to activate MDSCs through interaction with Toll-like Receptor 2 (TLR2). Gobbo et al showed that Hsp70 is often high on the surfaces of cancer derived exosomes compared to matched healthy tissue, highlighting the importance of MDSCs to cancer biology (168).

In the context of our own gene ontology results from Cytoscape, NKG2D, cytokine secretion and MDSCs all give rise to interesting exomiR based immune evasion hypotheses. For example, stimulation of NKG2D on NK cells by dendritic cells is known to induce secretion of IFN-γ and TNF-α, which both exhibit anti-tumour effects although with some potentially pro-tumorigenic properties depending on cellular context (169, 170). As cytokine secretion is among the cellular processes targeted by our exomiR set, it is possible that secretion of these cytokines is inhibited by exosome absorption by NK cells. Regarding PCa however, the potential attack on NK cell function extends beyond the NKG2D pathway down-regulation described above. Given that NK cells are known to enhance differentiation of dendritic cells (DCs) into their potent antigen presenting form (via action of IFN-γ and TNF-α), it is possible that exomiRs are also dampening the NK cells ability to promote DC maturation. Given that dendritic cells are being explored as a cell therapy alternative in PCa (171) this is an enticing hypothesis. However there is unfortunately no data regarding this at the time of writing.

Another potentially exomiR dependent immune evasion mechanism revolves once more around inhibiting cytokine secretion. In the context of PCa, cytokine secretion is highly relevant to NK/DC crosstalk. The interaction between these cells and the adaptive immune system can promote a sustained and effective anti-tumour response. For example, activated NK cells can kill tumour cells resulting in more antigen presentation by mature DCs, leading to more recruitment of tumour-specific CD8+ T-cells (172). It is here that IL-2 in particular is very important, given its role in the clonal expansion of these CD8+ T-cells capable of directly attacking tumour cells (173). IL-2 is also important in NK cell function (174) and dendritic cell function (173). Our data suggests that PCa exomiRs target genes involved in the secretion of IL-2 which would dampen both innate and adaptive anti-tumour responses.

The toll-like receptor targeting ability of our PCa exomiRs is another mechanism by which tumour immune evasion may occur. Although TLR molecules are thought to be important on the cancer cells themselves, they are an important part of anti-tumour responses mounted by the immune system (175). TLR2 and TLR4 agonists have in fact been used for some time in the treatment of bladder cancer (176) and TLR1 and TLR2 agonists have improved CD8+ responses to glioma in a mouse model (177). Both of these processes involve the TLR2 receptor to some extent and Li et al have recently shown that hepatocellular carcinoma cells can recruit MDSCs to the tumour site only when loss of TLR2 receptor allowed for increased IL-18 secretion by surrounding hepatocytes (178). It is therefore possible that PCa exomiRs target TLR2 on surrounding stromal tissue and on CD8+ T-cells to hinder anti-tumour responses.

2.3.4. ExomiRs secreted by androgen independent PCa may alter flavonoid and retinoid metabolism leading to testosterone disinhibition and immunosuppression

As PCa becomes more aggressive and invasive, they often alter their metabolism to circumvent their reliance on testosterone availability by modifying the activity of Androgen Receptor (AR), increasing its expression level and secreting their own hormones in an autocrine manner (179). We also performed exomiR analyses on our androgen independent (AI) cell lines (VCaP, DU145 and PC3), to uncover potential roles in the altered metabolism of this advanced, aggressive form of PCa. The most relevant biological features potentially effected by AI-exomiRs are the flavonoid and retinoic acid (RA) metabolic processes.

Flavonoids for example are associated with a lowered risk of prostate cancer in populations that have high levels of these compounds in their diets, usually from fruits and vegetables (180). Flavinoids have also been explored as anti-cancer therapies (181). Natural terpenoids (182) and isoprenoids (183) also have anti-cancer activities and are being explored as complements to chemo or other anti-cancer therapies . Dietary flavones are also associated with a decrease in testosterone secretion (184) making these compounds ideal targets for AI-exomiRs to seek out. This is unsurprising knowing that metabolic processes for these compounds hinge upon the expression of genes from the UGT1 locus which is heavily targeted by the top 10 Enriched PCa exomiRs. This locus is known to be deleted or mutated in many prostate cancers that recur after the initial radical prostatectomy (185). If PCa cells are able to decrease the synthesis of these compounds in other cells, or alter their own metabolism of these compounds, they may be able to remove an inhibitory signal from their environment.

Another enticing explanation for the targeting of these various metabolic processes comes once more from the potential impact on the immune system. It has been known for some time that vitamin A, the precursor to RA, is essential for immune system functions ranging from leukocyte proliferation and differentiation to eliminating parasitic, bacterial and viral infections (186). In the context of PCa, it is possible that reducing the amount of Retinoic acid in the tumour microenvironment that dendritic cells would fail to present antigen and adequate co-stimulatory signals to T-cells (187), likely resulting in a subdued response to cancer antigens. RA stimulated DCs have also been shown to more effectively provide proliferative signals to induce a Th1 response (188) which is known to favour anti-tumour activities. Furthermore, RA stimulated DCs can home better to malignancy (189), and are

better able to induce T-cell homing through production of stimulatory cytokines (190). RA also seems to have the ability to reduce tumour infiltration by MDSCs (191) which as discussed in the previous section, is a fundamental step in tumour immune evasion. Synthesising all of this information, it is possible that through targeting multiple elements of the immune system and the tumour microenvironment to hamper secretion and response of RA, that the tumour itself can reduce any antigen specific responses.

2.3.5. Messenger and long noncoding RNAs are relatively rare in PCa exosomes

The data presented in this chapter show that the vast majority of mRNAs and lncRNAs are found in cells, not exosomes (Figure 2.7). This is not surprising given the fact that exosomes are highly enriched with smaller RNA species as can be seen from our own data (Figure 2.2) and also from deep sequencing of exosomal RNAs which revealed that approximately 43% of detectable exosomal RNA is composed of miRNA (192). Further supporting this is our finding that PCa exosomes contain lower levels of mRNA and lncRNA than exosomes from the normal prostate PNT2 cell line (Figure 2.8) and this trend was repeated when looking at androgen independent cell lines (Figure 2.9).

This is not to say however that exosomal mRNAs and lncRNAs are irrelevant to exosome function. A recent hypothesis put forward by Ahadi et al may explain why there is a greater abundance of miRNA in exosomes while still providing a reason for lncRNAs to present. The authors suggest that some of the miRNAs most enriched in PCa exosomes are transported by lncRNAs that harbour many seed region sequences for these miRNAs. Essentially, the lncRNAs are behaving as a bus for certain families of miRNAs. This “bus” is long enough to contain other sequences and/or RNA secondary structures to be recognised by exosome loading machinery, which then loads the bus lncRNA into the exosome (129). The potential of mRNAs as miRNA transporters remains unexplored but is worthy of further interest as it may help explain the enrichment of yet other miRNA families in exosomes. It is also necessary to determine the exact mechanism by which bus lncRNAs acquire their miRNA cargo, and how this cargo is loaded into the exosome.

However, given the general lack of functional annotations for lncRNAs, these exosomal RNA species were ignored in further functional analyses. Also given the very small number of Enriched exosomal mRNA and lncRNA, these RNA species were dropped from further biomarker experiments. All further experiments were performed on exomiRs only.

2.3.6. Validation of exomiR biomarkers *in vitro*

QPCR validation of miRNA expression was a fundamental step in proving that exomiRs of interest were actually enriched in all PCa exosome samples. This is because of the low reproducibility inherent to microarrays and because of the low sample input and low expression levels of many miRNAs (193-195). Most of the exomiRs chosen from the microarray were indeed enriched in PCa exosomes compared to PNT2 exosomes (Figure 2.10) as they were at least 2-fold enriched in PCa exosomes, and most were ≥ 10-fold enriched. However,miR-362 and miR-30a performed poorly in the validations. This is unfortunate for miR-362 in particular as it was one of few exomiRs that was also highly enriched in androgen independent PCa exosomes, making it a possible prognostic marker. Both of these exomiRs were dropped from further analyses.

The next challenge was to take this panel of PCa associated exomiRs and test their utility as biomarkers using exosomes isolated from the various bodily fluids of PCa patients, with the intention of patenting this panel. The first step down this path involved optimising exosome isolations from bodily fluids, in particular using better exosome characterisation methods that became widely used after 2012, the year in which the work in this chapter was performed. These experiments are described in the next chapter.

Chapter 3 abstract:

Prior to testing the utility of our PCa cell line exosomal microRNA biomarker panel for PCa patient liquid biopsies, efficient methods of exosome isolation and RNA extraction from biological fluids including Urine, Plasma and Saliva needed to be developed within the lab. It is important that sufficient exosomes are extracted providing the nanogram quantities of good quality RNA (100 – 200 ng total RNA at a concentration of ≥15 ng/µL) required for detailed miRnome qPCR profiling. When this study was initiated, few commercially available reagents or methods were available. Many different methods were explored including ultrafiltration, exosome capture or precipitation, ultracentrifugation or a combination of these methods. The solution to isolate exosomes and their RNA from Plasma involved the use of a recently released ExoRNeasy kit from Qiagen. Exosome isolation from Urine involved particle size exclusion and ultrafiltration to remove most contaminating proteins followed by ultracentrifugation to pellet the exosomes. This isolation method was validated using Nanosight to measure particle size and abundance, and the DELFIA Europium assay to determine the presence of canonical exosome surface markers. Both of these tests showed that our isolation method gives pure exosome samples.

3.1. Introduction to Exosome Isolation Methodologies

3.1.1. Challenges of isolating exosomes from body fluids

Exosomes can be isolated from the majority of human body fluids, but differences in the concentration and type of other biomolecules found in these fluids can complicate isolation of pure exosomes. However, in recent years there has been an explosion of both published methods and commercially available kits for isolation of exosomes from various body fluids. Currently there are many trade-offs involved when selecting a technique for exosome isolation as a single, robust technique for all fluids does not yet exist. This is mainly due to the hugely varying complexity of human body fluids in terms of concentration, the presence of other contaminating particles and other confounding factors such as proteins known to sequester exosomes. These challenges must be overcome to isolate pure exosomes samples from the bodily fluid of interest. All current "state of the art" techniques for exosome isolation from human body fluids are described and compared in the following sections. Broadly, exosome isolation techniques fall under the following categories. i) differential ultracentrifugation, ii) ultrafiltration, iii) aggregation agents, iv) Size exclusion chromatography, v) immune-isolation, vi) microfluidic capture

3.1.2. Differential Ultracentrifugation (DU)

This has been the gold standard technique available for exosome isolation since the first publication on this topic by Théry et al (137). In their guide to isolation from body fluids, the authors describe a protocol similar to that available for tissue culture supernatants, with the added modifications of diluting the viscous body fluids and increasing the length and speed of certain ultracentrifugation steps. Since this publication, many variations have appeared in the literature at any number of steps. The most common deviation from the original protocol is the inclusion of a filtration step as a replacement for the 12 000 x g spin aimed at removing microvesicles and other non exosomal particles. The speed of the final exosome precipitation spin is the other common variation, but are generally of 110 000 x g or higher.

The main advantage of differential ultracentrifugation is that it is such a well established protocol and ultracentrifuge facilities are a common feature of most research labs. However, this technique is quite laborious taking the better part of a day to complete the exosome isolation and is not a high throughput technique given the limited number of positions available in the average ultracentrifuge rotor. Furthermore, ultracentrifuges are a relatively rare piece of equipment in most clinical settings. These features limit the usefulness of differential ultracentrifugation as part of a clinical diagnostic process.

3.1.3. Ultrafiltration (UF)

This technique was developed to meet the increasing need to concentrate and subsequently isolate exosomes from large numbers of patient Urine samples that differential ultracentrifugation could not perform in a timely manner (196). This group was able to isolate exosomes from as little as 0.5 mL of Urine as revealed by the presence of TSG101 and AQP2 (Exosomal surface markers that identify exosomes originating from the kidney, detected by Western blot) being retained in the filter unit. Channavajjhala et al went on to confirm that this isolation method was most appropriate for the isolation of exomiRs by using a larger starting volume of Urine (25 mL) and incubating the retentate with DTT. Up to 93% of the RNA isolated from exosomes using this method was miRNA (197). Given these findings and the fact that the prostate is in constant contact with Urine, ultrafiltration is an appropriate method for isolating urinary exomiRs and potentially diagnosing conditions of the urogenital system.

An ultrafiltration method based on affinity purification and ultrafiltration is also available for serum and plasma as a commercial kit, ExoRNeasy from Qiagen. This kit provides an extremely rapid turn around from serum/Plasma samples to Extracellular Vesicle (EV) RNA in a matter of hours and can be easily scaled to the number/volume of samples. However, in a recent paper by Enderle et al, it was shown that this kit isolates a more general population of EVs, not just exosomes as evidenced by the larger than expected sizes found in both Scanning Electron Microscope (SEM) and Nanoparticle Tracking Analysis (NTA) (198). Although this method does provide good yields of intact EV RNA, it cannot be considered as pure exomiR given the inclusion of these larger particles. Nonetheless these EV RNA may have diagnostic potential and are worthy of further analysis.

Norgen Biotek Corp has also recently released a range of commercial kits for exosome isolation from Plasma and Urine, based on spin columns containing a proprietary resin to capture exosomes. The information provided for this product shows particles of the expected size but gives no information on the presence or absence of exosomal markers. This product is also very new and the only publication to make use of any of these products did not provide any commentary on the quality of exosome samples isolated using this kit (199).

3.1.4. Aggregation Reagents (AR)

Aggregation reagents are simpler again than ultrafiltration, but are applicable to a greater variety of human body fluids. The most common of the aggregation reagents seen in literature is ExoQuick which is commercially available from SBI (System biosciences, Palo Alto, USA). The principle behind ExoQuick is that their proprietary polymer facilitates the precipitation of exosomes at a low speed in 30 minutes. Most published literature reports minimal if any modifications to the manufacturers protocol, but there are also some modified protocols using standard ExoQuick reagents in the literature for isolation from particular body fluids. For example, Zlotogorski-Hurvitz et al optimised their protocol for isolation of exosomes from human Saliva and concluded that ExoQuick was an effective method (200). Ravi et al (201) and Alvarez (202) have also reported their own ExoQuick methods for isolating exosomes from Urine and also came to the conclusion that it is an effective product. The issue with the use of Exoquick and other related products such as miRCURY EX (Exiqon), Total exosome isolation reagent (Invitrogen) and Exospin (Cell Guidance Systems) to name a few, is their tendency to pull down other larger particles and proteins, or the available product data contains no analysis of exosomal markers.

Recently however, Samsonov et al have published an agglutination method for urinary exosomes based on the interaction between saccharide residues on the exosomes and lectin molecules. Similar to commercially available aggregation kits, samples are first cleared with low to moderate speed centrifugations (200 x g, then 15000 x g) before incubation with concanavalin A and the final, exosome precipitating spin at 20 000 x g (124). This group provided extremely convincing evidence for the quality and content of their exosomes meeting the most up to date requirements for exosome identification (203).

3.1.5. Size Exclusion Chromatography (SEC)

The purpose of this technique is to remove the majority of protein contaminants that can co-precipitate with exosomes in UC and AR based techniques. This technique is in fact often preformed after UC to greatly enhance the purity of an exosome sample without resorting to the incredibly laborious sucrose gradient method. SEC is somewhat limited in its uses due to the low throughput of samples bottlenecking at the UC stage, and the lengthy set up and elution procedures involved in SEC itself. The first group to use SEC in this manner were Rood et al, who performed SEC after UC on Urine and found that it substantially enhanced detection of exosomal proteins, relative to either UC alone or UF (204). Muller et al followed the same method to show that UC-SEC is an effective method for serum/Plasma exosome isolation also, providing high yields of intact, functional exosomes (205). Böing et al also performed a single-step SEC from Plasma that was highly effective at isolating EVs with minimal contamination from Plasma proteins and lipoproteins. These particles were within the expected size range for exosomes and bore both CD63 and CD9 (206).

3.1.6. Immunoaffinity based methods (IA)

Immunoaffinity refers to any method that utilises exosomal surface proteins to selectively precipitate exosomes from body fluid(s). The most common immunoaffinity methodologies involve magnetic beads coated with antibodies against canonical exosome tetraspanin molecules such as CD63, CD81 and CD9. Recently, Zarovni et al performed a thorough assessment of plate and bead based immunocapture techniques utilising these markers, with great success (207). Although these markers are not limited to expression on exosomes, careful pre-clearing methods such as low speed centrifugation and/or nanomembrane filtration can remove other particles that express these tetraspanins before exosome precipitation. The other notable exosomal marker used in IA isolations is EpCAM, that has proven useful in isolating exosomes from blood Plasma (208) and tumour ascites (209). Bead based EpCAM exosome isolation has also been specifically optimised by Kim et al who were able to increase the uptake of EpCAM onto the beads by 40% and practically eliminated non-specific protein binding to the beads (210). Others however have been more stringent, selecting markers to isolate exosomes secreted by a particular tissue as was the case with Mizutani et al who used PSMA coated magnetic beads to isolate prostate specific exosomes (211) and Hong et al who used CD34 to isolate acute myeloid leukaemia blast exosomes (212).

More recently, Chen et al developed an IA method using specially treated filter paper as an inert substrate to which anti-CD63 antibodies can be attached to specifically trap exosomes. The apparatus proposed is simple and cheap to build, has a low sample volume requirement (as low as 72 µL), is easy to use and is quite effective at capturing exosomes. They were also able to isolate small but useable amounts of RNA and protein from their Plasma and aqueous humour samples (213). Since their initial publication, Chen et al have managed to lower the sample input to 10 µL (214).

3.1.7. Immunoaffinity - Microfluidic hybrid Devices (IA-MD)

Microfluidic devices for the isolation of exosomes are a relatively recent development. The first foray into this field came in the form of a hybrid IA-MD device, which trapped exosomes sourced from tissue culture inside the device using anti-CD63 antibody. The exosomes could then be lysed for RNA or visualised in SEM (215). More recently, He et al have utilised a similar hybrid IA-MD technique to specifically isolate lung cancer exosomes from a minute volume of Plasma. They were able to demonstrate extremely efficient capture of exosomes, and noted that their method maintained the physical integrity of their exosomes more so than standard DU (216). Kanwar et al demonstrated similarly high utility on their ExoChip platform, another IA-MD device. Also using CD63 as their capture antibody, they were able to isolate highly pure populations of exosomes from serum and isolate enough exosomal RNA to perform an Openarray analysis of 754 human mature miRNAs (217). Since this development, Zhao et al have designed and tested ExoSearch for the diagnosis of Ovarian cancer from as little as 10 µL of Plasma (218).

These devices are all incredibly promising avenues of exosome isolation for diagnostic purposes. They are extremely efficient at isolating exosomes taking as little as 100 minutes to complete the assay yielding diagnostically useful information (216).

3.2. Chapter Methods

3.2.1. Body fluid sample pre-processing and storage conditions

All body fluid samples were stored at -80^{0}C as soon as they reached the lab. After this, there were several different processing steps depending on the fluid. For instance, Urine was first centrifuged at 2000 x g for 20 mins at 4^{0}C to remove any cells or large debris. The supernatant was then vacuum filtered using a 0.2 µm PES filter membrane. The filtrate was then pipetted into 45 mL aliquots for freezing until ready for use. Doing this first simplified downstream analyses greatly while still keeping freeze thaw cycles to a minimum.

Plasma processing went through several rounds of optimisation before a simple and robust pre-processing method was settled upon, and these optimisations are described in 3.4.1 to 3.4.7. Common to all pre-processing methods however was the immediate centrifugation of Plasma samples at 3400 x g for 20 mins at 4^{0}C to remove platelets and other large debris. Most often, the Plasma was then simply frozen at -80^{0}C prior to use with the Qiagen ExoRNeasy kit. However, in earlier incarnations, the Plasma was filtered through a 0.2 µm PES membrane to remove microparticles and other large non-exosomal particles from the samples. The samples were then stored at -80^{0}C until ready for use. Théry et al (137) suggested diluting filtered Plasma 1:2 with DPBS, but this proved to be an unnecessary step as optimisations went on.

Saliva posed the most significant challenge given the presence of oral bacteria and food detritus in every sample, and the presence of Salivary enzymes that may degrade exosomal proteins if stored long term. Saliva is also a highly viscous fluid. So the first step was to dilute Saliva 1:2 with a mix of 1x DPBS and protease inhibitor. The protease inhibitor came in tablet form which was to be used at 1 tablet per 100 mL. The saliva samples themselves came in 5 mL aliquots which were then diluted to a final volume of 10 mL prior to storage. The samples were then centrifuged at 2000 x g for 20 mins at 4^{0}C and the supernatant was passed through a 0.2 µm PES filter membrane. Saliva samples were then stored at -80^{0}C until ready for further analysis.

3.2.2. DELFIA Europium assay to detect canonical exosomal marker proteins

To probe purified exosomal samples for the presence of exosome specific markers, the DELFIA Europium assay was used. The first step was to add 100 µL of an exosome sample to a well on a high protein binding Optiplate (Perkin Elmer, Waltham, MA, USA). Duplicate samples were required per sample and per marker (to assay a Urine sample for CD9, TSG101 and AGO2, a total of 600 µL of exosome sample was required). Once the samples were added to the plate, it was covered with parafilm and stored overnight at 4^0C. The next day, all liquid was removed from the plate and all wells were washed with 300 µL of 0.1% BSA in 1x DPBS. The wells were then blocked with 300 µl of 1.0% wt/vol BSA in 1x DPBS. Blocking was performed for 2 hours at room temperature on a plate shaker.

Next, primary antibodies (see table 3.1) were added to relevant wells. Antibody dilutions were performed according to the manufacturer's instructions in 0.1% BSA DPBS solution. 100 ng of primary antibody was added to each relevant well and the plate was again covered with Parafilm and incubated at room temperature for 2 hours on a plate shaker. Once this incubation was completed, all liquid was removed from the plate and each well was washed with 0.1% BSA DPBS solution three times. The secondary antibody (see table 3.1.) was diluted in 0.1% BSA DPBS solution to 100 ng/mL, and 100 µL was added to each well. The plate was covered once more with Parafilm and incubated at room temperature for 1 hour.

All liquid was removed from the plate and this time the plate was washed three times with DELFIA wash buffer (Perkin Elmer). The strepatavidin-Europium chelate was then diluted 1:1000 in DELFIA assay buffer and 100 µL was added to each well. The plate was covered and incubated at room temperature for 45 minutes on the plate shaker. Then, all liquid was removed from the plate and a further 6 washes were performed using the DELFIA wash buffer once more. Finally, the development solution was added to each well and the plate was incubated at room temperature for 5 minutes. Time resolved fluorescence (TRF) reading was then performed using a Tecan m100 pro plate reader. This protocol was typically performed in technical duplicate per sample.

Table 3.1. Antibodies used.

Antibody	Primary or Secondary	Catalog No.	Dilution Used
Rabbit monoclonal [EPR5702] to CD63	Primary	ab134045	1:1000
Rabbit monoclonal [EPR2949] to CD9	Primary	ab92726	1:1000
Rabbit monoclonal [EPR7130(B)] to TSG101	Primary	ab30871	1:1000
Rabbit monoclonal [EPR10411] to Ago2 / eIF2C2	Primary	ab186733	1:1000
Goat anti-rabbit H&L (biotin)	Secondary	ab97049	1:5000

3.2.3. Measuring particle size and concentration in exosomal samples using the Nanosight

The Nanosight (Nanosight Ltd., Salisbury, UK) is an instrument used to track nanoscale particles. The tracking of these particles allows for computation of particle size and accurate estimation of particle concentration. To do this, a sample containing purified particles is injected into a thin chamber with a laser passing through the sample horizontally. The particles scatter laser light which is detected by a camera/microscope combination. This is the basis of particle tracking. The particle's Brownian motion is then tracked by the Nanosight software and the speed of Brownian motion is used to calculate a particle's size.

All samples taken from patients were routinely diluted 1:1000 to bring the particle count within the dynamic range of the instrument (1 x 10^8/mL to 10 x 10^9/mL). The final dilution was recorded and used later for calculating the concentration of the stock exosome sample.

Once dilutions were performed, 0.3 mL of the diluted sample was drawn up and injected into the sample chamber of the Nanosight. The laser was then activated and the camera was focused on the "thumbprint region" (219). A 60 second video of the particles was then recorded. At this point the syringe was pushed to flush some of the sample through the sample chamber. A second and third video was recorded and the Nanosight software automatically analysed all three videos estimating average particle size and concentration in the original sample (220). Between samples, the sample chamber was flushed through with 0.5 mL of 1x DPBS to remove all particles that might contaminate subsequent analyses.

3.2.4. Isolation of exosomal RNA from human body fluids

At the time the experiments presented in this chapter were performed, there was no method in scientific literature or on the market that could reliably isolate RNA samples of sufficient quality and quantity for qPCR. As such, many different techniques were used throughout this chapter. Each following sub-chapter contains a full description of the RNA isolation method used for that experiment.

3.2.5. Quantitative Real Time Polymerase Chain Reaction (qPCR) to measure relative expression levels of potential biomarker exomiRs

All PCR and qPCR procedures performed in this chapter were performed exactly as in section 2.1.6, except for a minor modification to the final qPCR volume. This modification is described by the contents of table 3.2. The primer/probe assays are presented in table 3.3.

Table 3.2. 1x qPCR reaction mix

Reagent	Volume (µL)
Taqman master mix (2x)	2
Taqman probe	0.5
cDNA	1
dH_2O	0.5
Total	4

Table 3.3. Taqman miRNA primer/probe sets

Taqman Primer/Probe Name	Assay ID
miR-125b-2*	002158
miR-1228	002919
miR-145*	002149
miR-92b*	002343
miR-1228*	002763
miR-126*	0004451
miR-149*	002164
miR-22	000398
miR-25	000403
miR-106b	000442
Let-7i	002221

Apart from the modifications to the volume of the reagents, all other steps were performed in accordance with the manufacturers protocol (139). Each gene expression assay was performed in triplicate, and the average Ct was calculated from the three Ct values. If a Ct value was >35 however, the result was excluded as any detection after Ct 35 is likely a false positive. Next, the delta Ct (ΔCt) value was determined which is a measure of the difference in expression levels between the gene of interest (GOI) and the endogenous control (EC). Once the ΔCt was known, the ΔΔCt was calculated which measures the difference in expression levels between two cell types/experimental conditions. In this experiment, the difference measured was between the GOI in PCa exosomes versus the same GOI in PNT2 (normal prostate exosomes). The formula used to determine the ΔΔCt was: ΔCt(PCa exosomes) – ΔCt (PNT2 exosomes). Fold-changes were then calculated between PCa exosomes and PNT2 exosomes using the formula $2^{-\Delta\Delta Ct}$. However, in section 3.3. fold-changes were determined using the formula $2^{-\Delta Ct}$ In accordance with the recommendations of Strivak et al when performing qPCR experiments without a control condition (221).

3.3. Exosome Isolation From Body Fluids: Pilot Study

3.3.1. Exosome isolation methods

For the pilot study, Plasma, Urine and Saliva samples were all processed under similar conditions using Amicon (Millipore, Billerica, MA, USA) 100 KDa ultrafilter units. The resulting RNA samples from each isolation were then subjected to qPCR analysis for miRNAs that were previously determined to be highly expressed in PCa exosomes by miRNA microarray (see table 2 in appendix section) and by qPCR analysis prior to functional experiments performed in chapter 5. Let-7i was of particular relevance given that it is strongly associated with PCa exosomes (222, 223). The miRNAs used for all pilot study analyses were miR-106b, let-7i, miR-25 and miR-22. The precise methodology for each fluid is outlined in Figure 3.1.

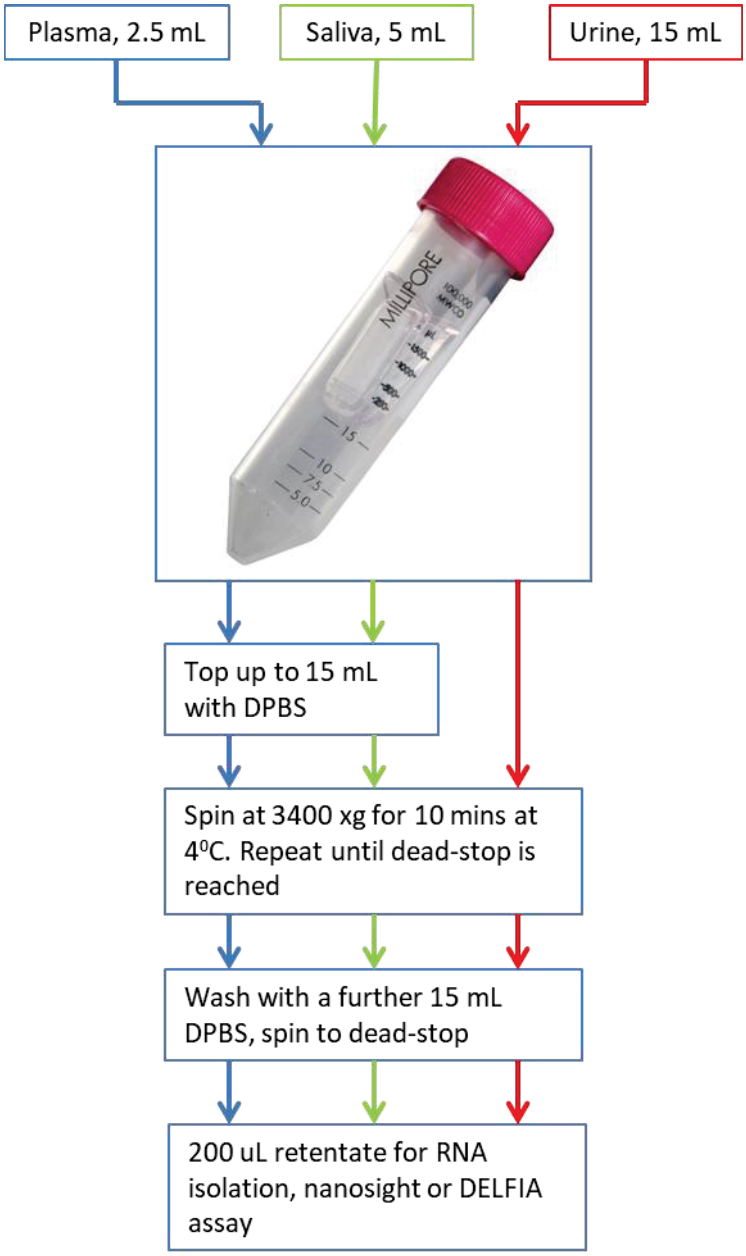

Figure 3.1. Pilot study: exosomal RNA isolation from different human body fluids.

The maximum volume of the ultrafilter units was 15 mL. As Urine was the most dilute fluid, a full 15 mL was used. Plasma and Urine however were significantly more concentrated, so lower starting volumes were used and simply topped up to 15 mL with 1x DPBS. All tubes were then centrifuged at 3400 x g for 10 mins at 4^0C. 15 mL of DPBS was added and centrifugation was repeated. Then 200 µL of retentate was removed and lysed with RNAzol-RT to acquire exosomal RNA. At least 3 biological replicates were preformed per sample type.

3.3.2. Pilot Study: urinary exosome isolation and miRNA expression

The purpose of this experiment was to test a method Adopted by our Movember GAP Urine collaborator Dr Jeremy Clark (Cancer genetics, University of East Anglia, UK) and published by Cheruvanky et al (196) to isolate exosomal RNA from Urine. This involved ultrafiltration of small (15 mL) samples of Urine and RNA extraction from the small volume of retained fluid containing exosomes, known as the retentate. Although we were able to extract sufficient amounts of RNA from our Urine samples and amplify PCa exosome associated miRNAs, we found that consistency of RNA concentration and Ct values varied significantly between Urine samples taken from the same donor as we had access to several samples taken at different times form the same donor. Exosomal expression levels of miR-106B, let-7i, miR-25 and miR-22 were analysed in this experiment. Mir-92b* was used as an endogenous control as it was previously identified as the most reliable exosomal endogenous control gene (see figure 2.19.). The qPCR amplification results are shown below in Figure 3.2.

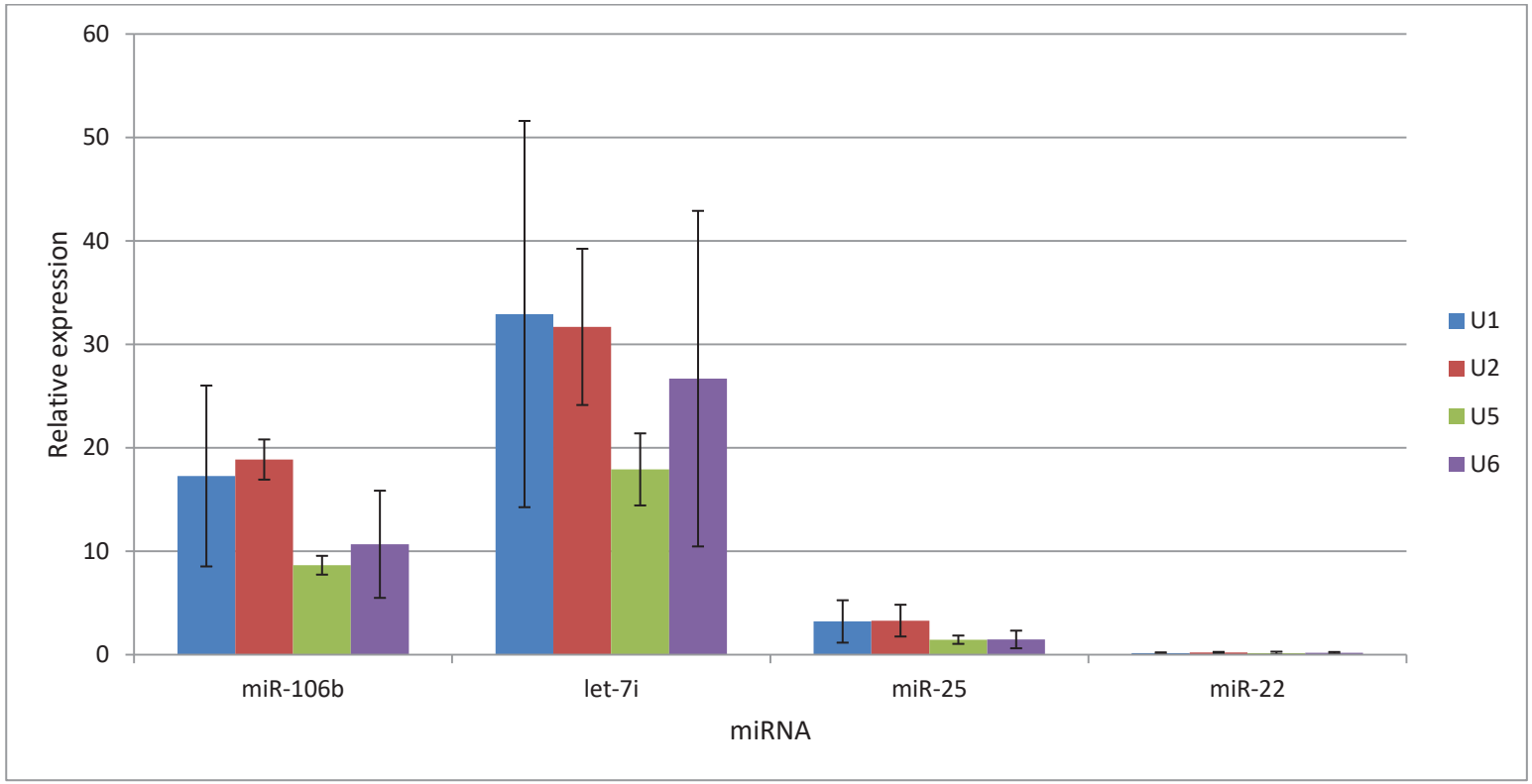

Figure 3.2. Expression levels of PCa exomiRs in exosomes isolated from human Urine.

Urine exosome samples were isolated by subjecting 15 mL of pre-filtered (0.2 µm) Urine to ultrafiltration using Amicon 100 KDa filtration devices spun at 3400 x g at 4^0C for 10 mins. RNA was isolated from 200 µL of retentate using RNAzol-RT and the resulting RNA samples were normalized to 50 ng/µL using a Thermo-Fisher Nanodrop. Normalised RNA samples were then amplified for miR-106b, let-7i, miR-25, miR-22 and miR-92b* using the Applied Biosystems high capacity reverse transcriptase kit. Four biological replicates were performed and are labelled U1 U2 U5 and U6 (RNA concentrations were too low in U3 and U4). MiR-106b and let-7i are both highly enriched relative to miR-92b* while miR-25 and miR-22 were barely detectable. Reproducibility was a serious problem when isolating Urine using this technique.

3.3.3. Pilot study: Plasma exosome isolation and miRNA expression

The purpose of this experiment was to try and adapt the ultrafiltration method used to isolate urinary exosomes to do the same from Plasma samples. Unfortunately this technique appeared to be highly inappropriate. Although RNA could be isolated from the samples and this RNA could be amplified sufficiently for qPCR, the samples appeared highly contaminated with protein. It took up to several hours to reduce the volume from the initial 15 mL to <400 µL (compared to a single 10 minute spin when isolating exosomes from urine samples), and the retentate that remained was extremely viscous, cloudy and yellow which suggested extreme contamination with Plasma proteins and potentially other small particles that came through the initial 0.2 µm filter. Also, the Nanosight profiles indicated the least pure samples obtained in any of the pilot studies (see Figure 3.6.). A great deal of optimisation would be required to obtain pure exosomal samples from Plasma. Figure 3.3. shows the miRNA expression analysis from the Plasma samples.

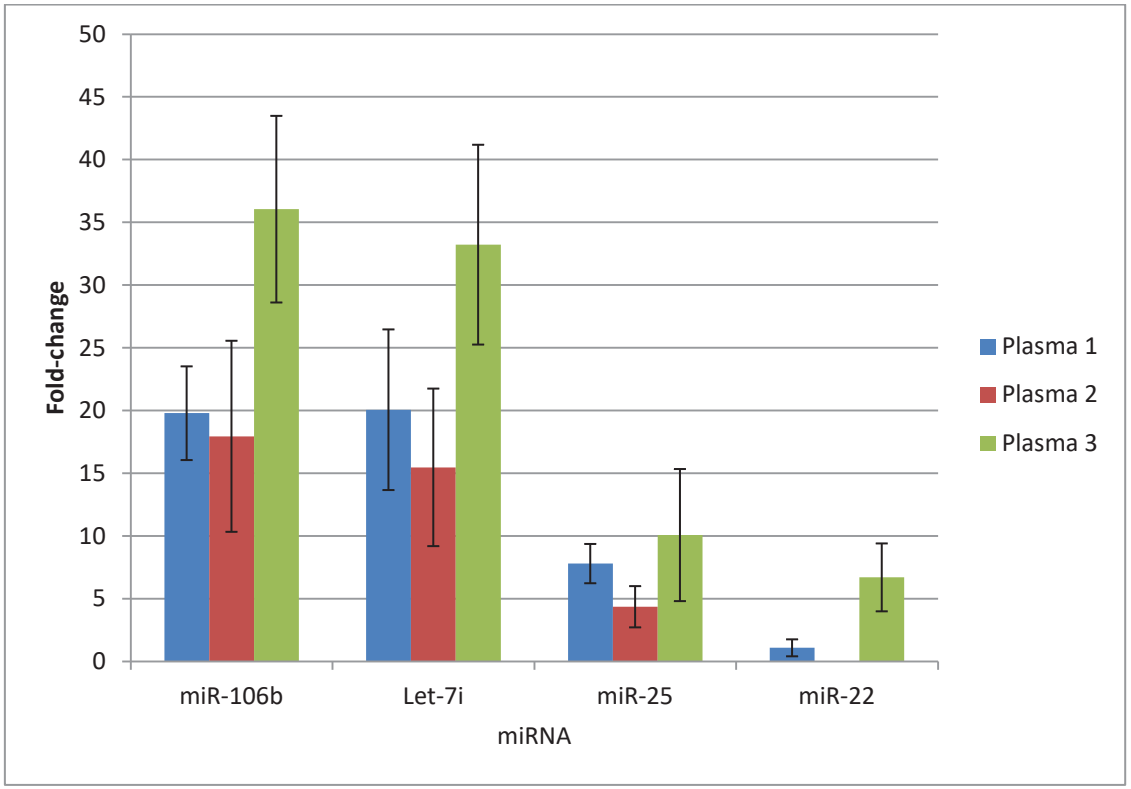

Figure 3.3 Expression of PCa exomiRs in exosomes isolated from human Plasma.

Analysis of ultrafiltered Plasma RNA. Plasma exosome samples were isolated by subjecting 5 mL of pre-filtered (0.2 µm) Plasma to ultrafiltration using Amicon 100 KDa filtration devices spun at 3400 x g at 4^0C for 10 mins. RNA was isolated from 200 µL of retentate using RNAzol-RT and the resulting RNA samples were normalized to 50 ng/µL using a Thermo-Fisher Nanodrop. Three biological replicates were performed. Normalised RNA samples were then amplified for miR-106b, let-7i, miR-25, miR-22 and miR-92b* using the Applied Biosystems high capacity reverse transcriptase kit. MiR-92b* was used as the endogenous control as per previous experiments. MiR-106b, let-7i and miR-25 were all easily detected, but miR-22 was difficult to detect. Reproducibility was a major issue using this technique of isolating exosomes from Plasma.

3.3.4. Pilot study: Saliva exosome isolation and miRNA expression

Saliva was the third and final fluid taken from our patients and required the most pre-processing (see section 3.1.1.). The Saliva samples were subjected to the protocol presented in Figure 3.1. It was relatively easy to perform the ultrafiltration steps themselves, but the RNA yields were quite small and of poor quality with low 260/280 and 260/230 ratios according to the Nanodrop (data not shown). There was sufficient RNA to amplify several miRNAs, but interestingly, let-7i was not detectable in these samples. This is strong evidence that exosomes of prostate origin cannot be recovered from Saliva, given the association of this miRNA with prostate exosomes (222). The results are shown in Figure 3.4.

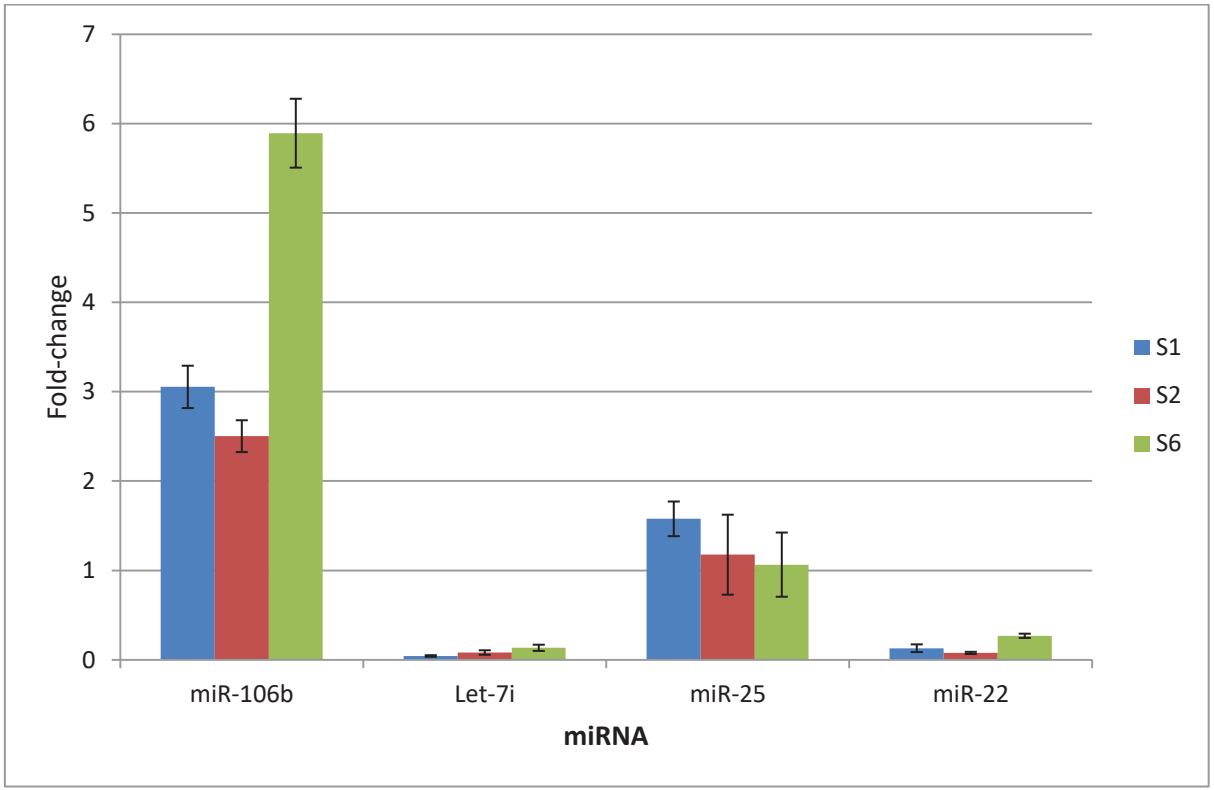

Figure 3.4. Expression of PCa exomiRs in exosomes isolated from human Saliva.

Analysis of exomiRs from Saliva. Saliva exosome samples were isolated by subjecting 15 mL of pre-filtered (0.2 µm) Saliva to ultrafiltration using Amicon 100 KDa filtration devices spun at 3400 x g at 4^0C for 10 mins. RNA was isolated from 200 µL of retentate using RNAzol-RT and the resulting RNA samples were normalized to 50 ng/µL using a thermo-fisher Nanodrop. Three biological replicates were performed. Normalised RNA samples were then reverse transcribed for miR-106b, let-7i, miR-25, miR-22 and miR-92b* using the Applied Biosystems high capacity reverse transcriptase kit. MiR-92b* was used as the endogenous control per previous experiments. MiR-106b was easily detectable in Saliva, but none of the other candidates could be reliably detected. The absence of let-7i is of particular concern because this would indicate a lack of exosomes originating from prostate tissue.

3.3.5. Pilot study: determination of exosome sample purity isolated from body fluids

The pilot studies showed that RNA isolation and qPCR amplification is possible from all three body fluids tested. However, there were large variations in miRNA expression level recorded between samples, and even within replicate measurements made from the same sample. Because of this it was decided to analyse the purity of these exosome samples to determine whether these samples were contaminated with other particles and proteins. The DELFIA Europium assay system was utilised to probe for canonical exosome surface marker proteins and the Nanosight was used to determine particle size and concentration. DELFIA analysis was performed on duplicate samples from each body fluid. Nanosight analysis was performed on single exosome samples from each body fluid.

The DELFIA assay was performed looking at markers CD9 and CD63, two canonical exosomal surface markers (131). The assays showed that CD9 was detectable across all samples, although less strongly in Plasma than either Urine or Saliva (Figure 3.4). CD63 was less detectable in all samples and was not detected at all in the Plasma samples, further suggesting that ultrafiltration alone is a very poor method for isolating exosomes from Plasma. The Nanosight results support this assertion as they show vast numbers of smaller particles (≤ 65 nm) that are inconsistent with exosomes. Saliva samples contained particles that were somewhat larger than expected and in very small quantities relative to either Urine or Plasma. The Urine samples however were of expected or similar size throughout all samples tested and were within acceptable concentration limits. The DELFIA Europium assay data are shown in Figure 3.5. and the Nanosight data are shown in Figure 3.6. Due to the extremely limited sample volume available, only on biological replicate was tested.

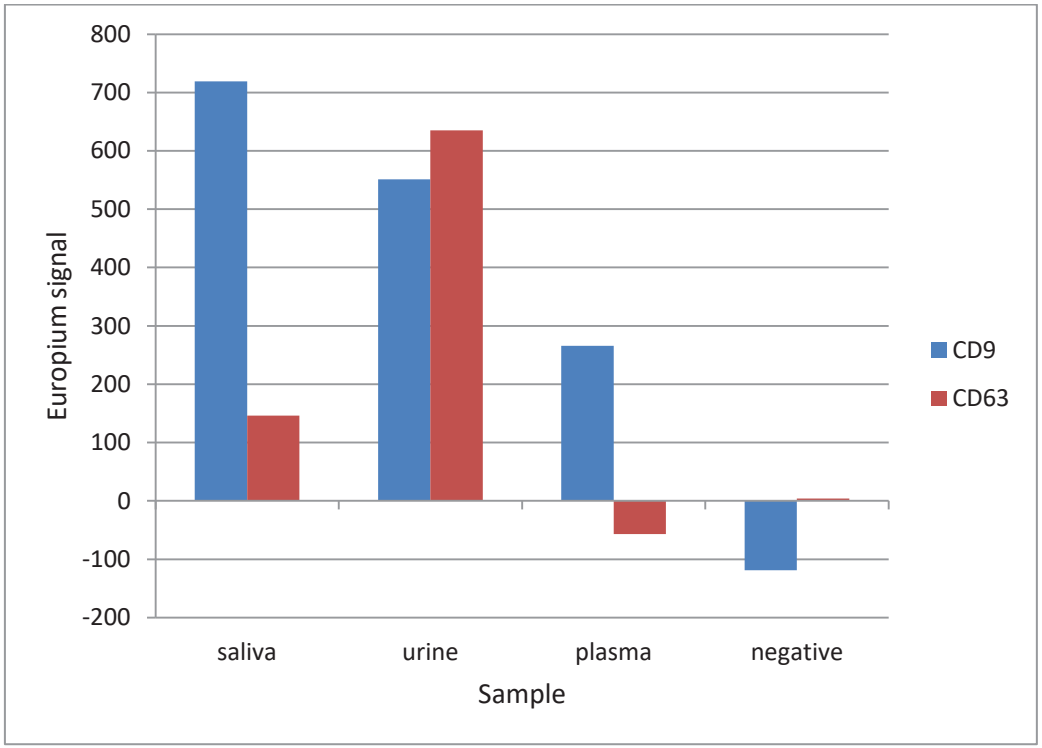

Figure 3.5. Detection of exosomal markers in ultrafiltered body fluid Samples.

Qualitative analysis of exosome samples isolated from different fluids by ultrafiltration using exosomal markers CD9 and CD63. Both markers are detectable above background levels in Saliva and Urine, but CD63 was not detectable in Plasma samples. This strongly suggests that ultrafiltration is a poor method of exosome purification from Plasma.

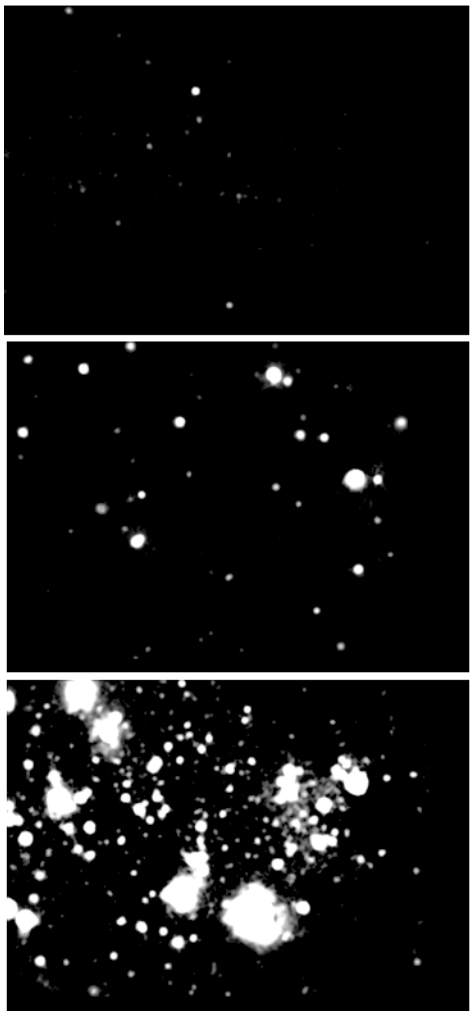

a)	Saliva
Particle count (xE^8/mL)	1.59
Mode particle size (nm)	135

b)	Urine
Particle count (xE^8/mL)	4.17
Mode particle size (nm)	95

c)	Plasma
Particle count (xE^8/mL)	27.12
Mode particle size (nm)	59

Figure 3.6. Determining the purity of exosomal samples isolated by ultrafiltration.

Qualitative analysis of exosome samples isolated from different fluids by ultrafiltration. **a)** Nanosight data for Saliva. Very low particle count and particles are slightly larger than expected. **b)** Nanosight data for Urine. Better particle count than Saliva and mean particle size is consistent with exosomes. **c)** Nanosight data for Plasma. Very high particle count and mean particle size is smaller than expected. This strongly suggests that the sample is highly contaminated with other particles, further confirming that ultrafiltration is unsuitable for purification of exosomes from Plasma.

3.4. Optimising Exosomal RNA Isolation from Human Plasma

3.4.1. Optimising exosomal RNA isolation from Plasma exosomes: volume for ultrafiltration

Given the difficulty in acquiring acceptable concentrations of RNA for qPCR in the pilot study, a new approach was taken. The aim of this experiment was to identify the amount of Plasma from which at least 15 ng/µL of exosomal RNA could be extracted reliably. Volumes of 1 mL, 2.5 mL and 5 mL were processed according to 3.2.1. and RNA was extracted. Resulting RNA quantities were assessed using a Nanodrop (Thermo-Fisher). The volume that produced a sample with the highest yield above 15 ng/µL was considered the most successful sample. The experiment was performed in biological triplicate at each volume (3 Plasma samples, each tested at 1 mL, 2.5 mL and 5 mL filtration volumes). The results are presented in Figure 3.7.

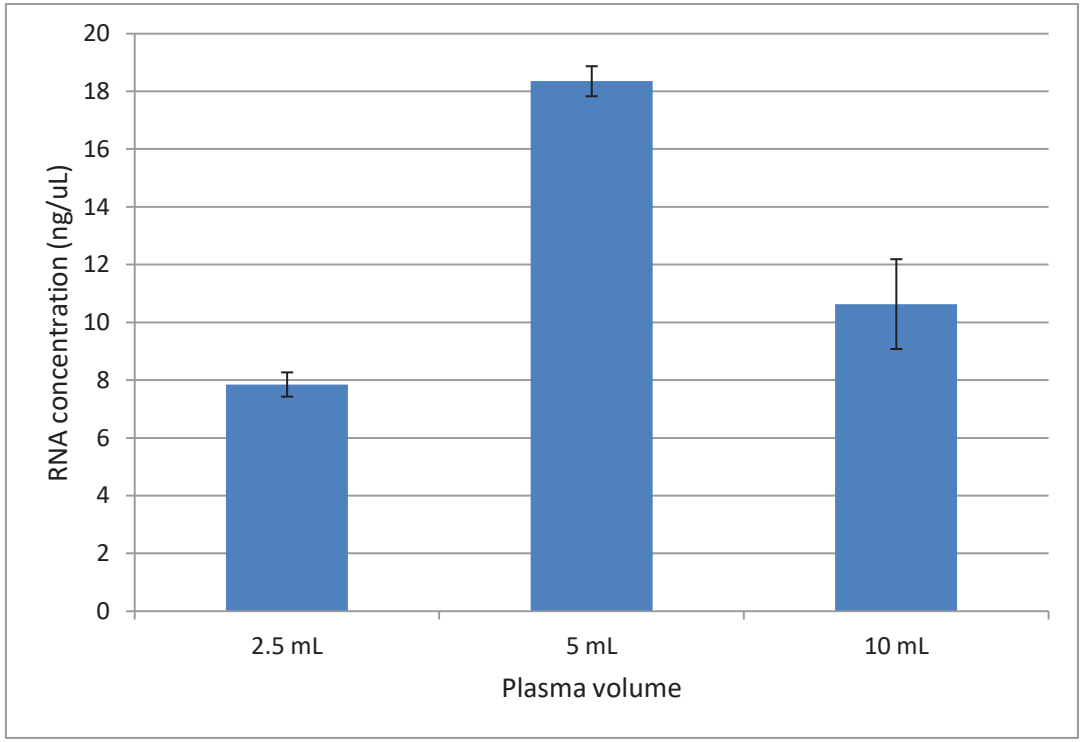

Figure 3.7. Determining RNA concentration per Plasma volume.

RNA concentrations acquired from different starting volumes of Plasma using ultrafiltration. Exosome samples were isolated from Plasma by ultrafiltration through Amicon 100 KDa filter units spun at 3400 x g, 4^0C until approximately 200 µL remained. RNA was then isolated from 200 µL of retentate using RNAzol-RT. RNA concentration was then assessed using a Thermo-fisher Nanodrop. All volumes gave lower than desired yields (less than 20 ng/µL). However, the 5 mL starting volume was consistently the closest to this value. 3 biological replicates were performed for each condition. Error bars are +/- standard deviation.

3.4.2. Optimising exosomal RNA isolation from Plasma exosomes: lysis conditions for retentates

This optimisation step was performed to ascertain whether RNA yields could be increased by attempting to lyse exosomes that were trapped on the membrane of the Amicon ultrafiltration units. 5 mL starting volumes were selected and were topped up to 15 mL using 1x DPBS. The samples were then centrifuged at 3400 x g for 15 minutes at 4^0C. This centrifugation step was performed as many times as necessary to leave a final volume of approximately 200 µL of retentate. Three different lysis conditions were then tested: i) retentate only, ii) membrane only by incubating at 37^0C for 10 minutes on a plate shaker, iii) retentate first, then the same aliquot of RNAzol was used to treat the membrane (same conditions as step ii). 500 µL RNAzol was used for each condition. The condition that returned the highest RNA yield was considered the most successful. The experiment was performed in technical triplicate and the results are presented in Figure 3.8.

Unfortunately, the RNA yield was not increased by exposing the ultrafilter membrane to RNAzol-RT. In fact, this seemed to decrease the yield of RNA that could be acquired from an ultrafiltered Plasma sample possibly due to excess Plasma protein trapped on the membrane entering the RNA isolation reaction. The RNAzol-RT may also have been absorbed into the membrane and not recovered which would also have lowered the yield.

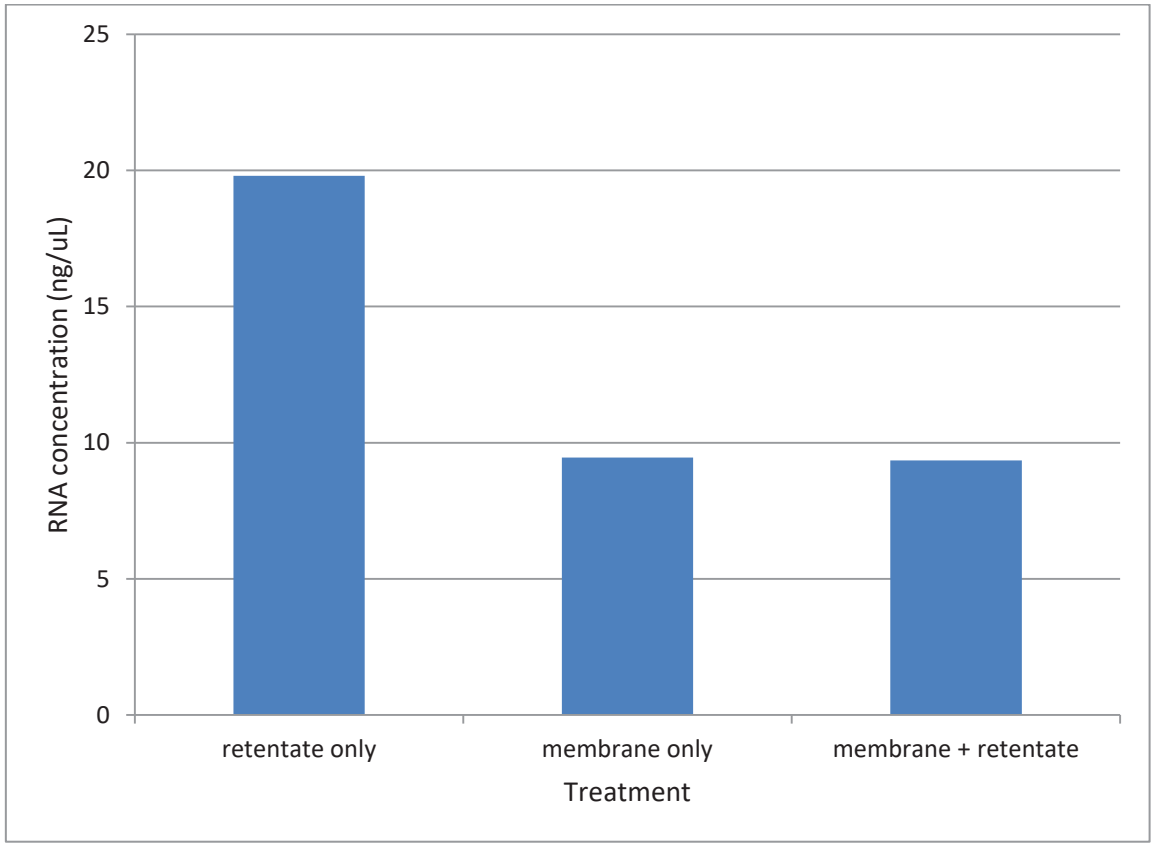

Figure 3.8. Comparing RNA concentrations acquired from retentates and filtration membranes .

RNA isolations from ultrafiltration of 5 mL of Plasma. Exosomes were isolated from 5 mL samples of Plasma using ultrafiltration using Amicon 100 KDa filter units spun at 3400 x g, 4^0C until approximately 200 µL remained. RNA was then isolated from the retentate only, filter membrane only or by using the same volume of RNAzol-RT to extract RNA from the retentate and the filter membrane. Isolating from only the retentate was the most effective way of isolating RNA from ultrafiltered Plasma. However, the yield was still poor.

3.4.3. Optimising exosomal RNA isolation from Plasma exosomes: ultrafilter Molecular Weight Cut-Off (MWCO)

Another important factor regarding exosome sample purity discovered in the pilot study was that the Plasma exosome samples were highly contaminated with Plasma proteins as indicated by the viscosity and yellow colouring of these samples. The next step in optimising exosome isolation from Plasma was a head to head comparison between the RNA yields acquired using higher MWCO ultrafilter units with the hope of allowing more Plasma proteins to be removed from the sample without lowering the RNA yield too far. The experiment was performed using 100 KDa, 300 KDa and 100 KDa MWCO ultrafilter units. 5 mL volumes of Plasma were used as per the findings in section 3.3.1. Unfortunately, RNA samples acquired from all the ultrafilter units failed to achieve concentrations of ≥15 ng/µL. This may be because the larger MWCO allowed some exosomes to cross the filter (being discarded) or it may have been that some RNA being recovered was not exosomal in origin as it is well known that Plasma contains stable miRNAs that are bound by AGO2. It could also have been that particles were depleted at earlier stages of Plasma processing. Regardless, these data led us to believe that each MWCO was approximately equally efficient at capturing Plasma exosomal RNA. The experiment was performed in biological triplicate and the results are shown in Figure 3.9.

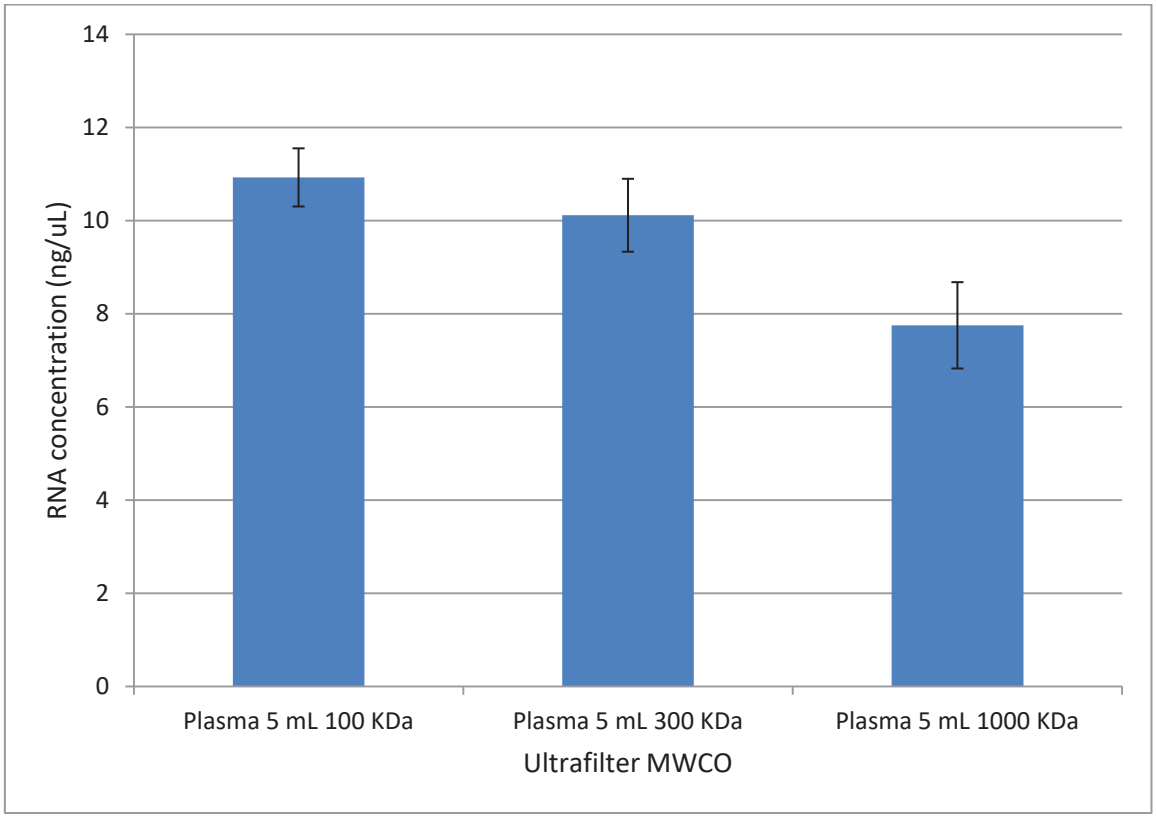

Figure 3.9. Effect of ultrafilter MWCO on the amount of RNA that can be recovered from retentates after ultrafiltration.

Exosomes were isolated from 5 mL Plasma volumes using Amicon filter units with 100 KDa, 300 KDa or 1000 KDa MWCO filter units. Each unit was spun at 3400 x g, 4^0C until approximately 200 µL retentate remained. RNA was then isolated from 200 µL of retentate using RNAzol-RT. RNA concentration was assessed using a Thermo-fisher Nanodrop. The 100 KDa unit retained the most RNA, followed by the 300 KDa unit and the 1000 KDa units performed the worst. However, the yields were so low across the board that this was not deemed significant grounds for selecting one pore size over the other. 4 biological replicates were performed per condition and error bars represent +/- standard deviation.

3.4.4. Optimising exosomal RNA isolation from Plasma: Are particles containing RNA being depleted at any stage of exosome isolation?

Given the very poor, largely unusable RNA yields obtained so far, it was decided to investigate if RNA could be isolated in significant quantities from pre-processing steps such as platelet pellets and the initial 0.2 µm filtration that was performed to remove large particles from the plasma sample prior to further exosome isolation steps. All previously tested ultrafilter MWCO units were also re-tested in this experiment and an ultracentrifugation step was added post- ultrafiltration to try and further purify Plasma exosomes by precipitating them. This methodology is presented in the flow chart in Figure 3.10.

Very low yields were extracted from both the platelet pellet and the 0.2 µm membrane, suggesting that most of the RNA available in Plasma is not lost during these steps. The 100 KDa ultrafiltration gave higher RNA yields than it had in previous experiments, reaching as high as 30 ng/µL. However, there was still substantial variability in RNA yield as evidenced by the large error bars seen in Figure 3.11. The 300 KDa and 1000 KDa ultrafiltration units produced lower concentrations of RNA as was expected from previous experiments. The addition of an ultracentrifugation step post-ultrafiltration drastically reduced this concentration even further. The experiment was performed in biological triplicate for all samples. These data are presented in Figure 3.11.

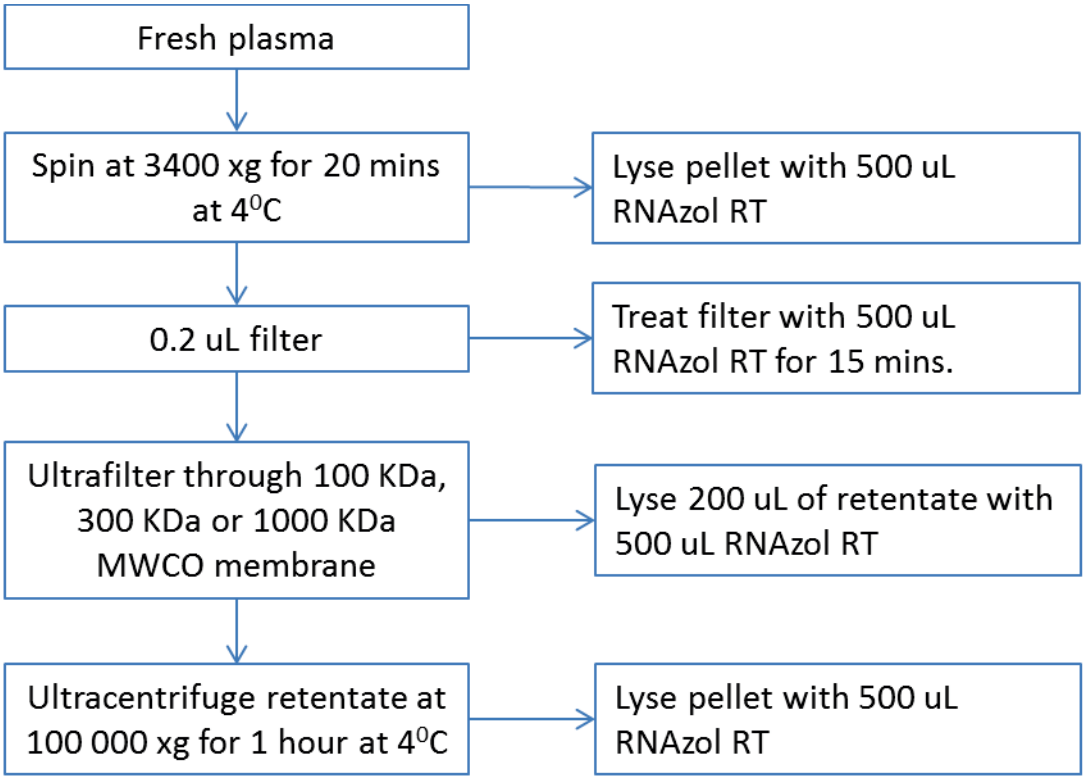

Figure. 3.10. Optimising exosome isolation for maximum RNA yield from plasma.

A large volume (10 mL) of Plasma was selected to begin this analysis. The first platelet pelleting step was performed at 3400 x g for 20 mins at 4^{0}C. The resulting pellet was lysed in RNAzol. Next the supernatant was filtered and the filter was incubated with RNAzol-RT at RT for 15 minutes. At this point, different ultrafilter pore sizes were used (100 KDa, 300 KDa and 1000 KDa). 200 µL of retentate from each pore size condition was lysed with 500 µL RNAzol. Some retentates were not lysed, but were instead added to 22 mL ultracentrifuge tubes, topped up with 1x DPBS and centrifuged at 100 000 x g for 1 hour at 4^{0}C. The resulting pellets were lysed. Note that in every experiment, flow throughs and supernatants were ignored in order to avoid fractions which may have contained free floating AGO2 bound miRNAs.

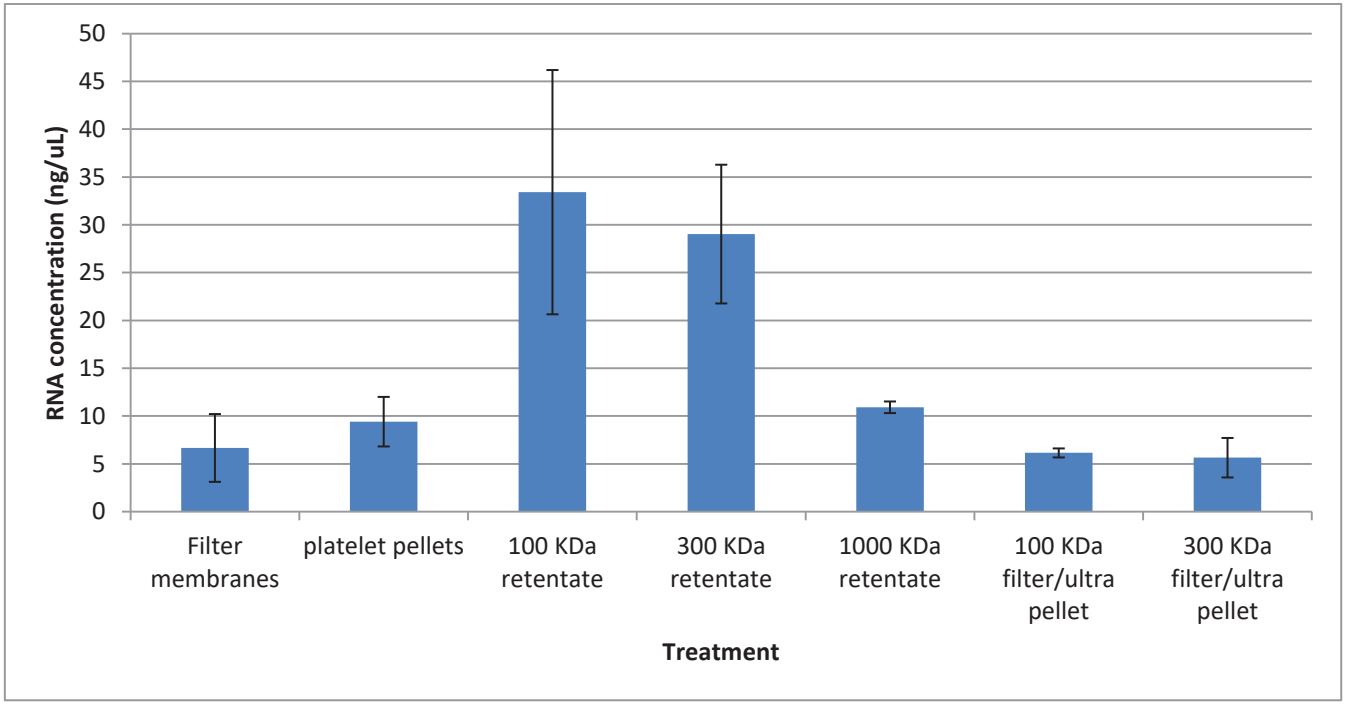

Figure 3.11. Comparison of RNA yields from plasma exosomes using different exosome isolation methods.

RNA isolation performed at each step of Plasma processing beginning with basic filtration of the Plasma and ending with ultracentrifugation. RNA isolations were performed at each step of exosome isolation from Plasma beginning with the filter membranes used to clear larger particles before samples were frozen at -80^{0}C. A new technique was also used in which retentates were taken and subjected to ultracentrifugation at 100 000 x g for 1 hour at 4^{0}C. Very little RNA can be recovered from any of the sources besides 100 KDa and 300 KDa retentate. In line with previous experiments, the yields from these sources is highly variable, showing that either method is still unsuitable for isolation of exosomes from Plasma. 3 biological replicates were performed for each condition.

3.4.5. Optimising exosomal RNA isolation from Plasma exosomes: Ultracentrifugation-Ultrafiltration (UC-UF)

Given the inconsistent RNA isolation efficiencies obtained using the ultrafiltration protocol, the failure of ultracentrifugation to produce RNA samples with a concentration suitable for qPCR and the contamination with Plasma proteins, a new method was developed. The purpose of this method was to take a larger volume of Plasma to start with and deplete most Plasma proteins using ultracentrifugation. This would be followed by the removal of the rest of these contaminant proteins by ultrafiltration through a 100 KDa MWCO ultrafiltration unit. This process would hopefully increase the yield of exosomal RNA and enhance the purity of the exosome samples it was being extracted from. This new method began with ultracentrifugation at 100 000 x g of a large (10 mL) sample of Plasma which caused the particles to precipitate while most of the Plasma proteins remained in solution. These proteins could then be poured off with the supernatant leaving a crude sample of particles and any Plasma proteins that co-precipitated with them. This was followed by resuspension of the crude pellet in DPBS which was then ultrafiltered to try and remove these contaminant proteins. The full method used to perform this optimisation attempt is summarised in Figure 3.12.

The final samples resulting from this UC-UF technique were then subjected to DELFIA Europium assay looking for the markers CD9, TSG101 and AGO2 in accordance with guidelines that had just been released by the International Society for Extracellular Vesicles (ISEV). This body is the world's foremost authority on exosomes and all extracellular vesicles, and their 2014 paper titled "Minimal experimental requirements for definition of extracellular vesicles and their functions: a position statement from the International Society for Extracellular Vesicles" suggested using these three markers as the best possible indicators of exosome sample quality (203). If the samples acquired by Ultracentrifugation-Ultrafiltration contained mostly exosomes, both CD9 and TSG101 had to be present and AGO2 was expected to be absent to exclude the possibility that miRNAs from outside the exosomes were contributing to the RNAs isolated from the exosome samples. The Ultracentrifugation-Ultrafiltration samples were also subjected to Nanosight analysis to determine particle size and quantity.

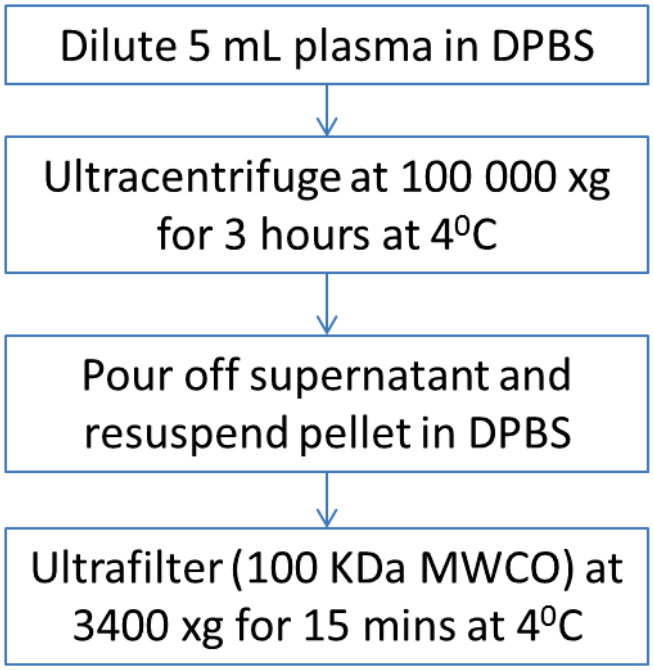

Figure 3.12. Ultracentrifugation-Ultrafiltration methodology for plasma exosome isolation.

5 mL of Plasma was added to a 22 mL ultracentrifuge and topped up with 1x DPBS. This was then centrifuged at 100 000 x g for 3 hours at 4^{0}C. The supernatant was removed and the pellet was resuspended in 200 µL of 1x DPBS. This was added to an Amicon ultrafiltration unit which was topped up to its full volume of 15 mL with 1x DPBS. The tubes were then centrifuged at 3400 x g for 15 minutes at 4^{0}C. Retentates were used for RNA isolation or DELFIA/Nanosight protocols. The DELFIA protocol was performed in technical duplicate as per section 3.1.2. The Nanosight methodology was performed in biological triplicate on all samples as per section 3.1.3.

Unfortunately, this technique was also highly unsuccessful, with issues of contamination still persisting in spite of the extra processing steps. AGO2 contamination was completely absent from the samples, but given that the TRF values were massively lower even than the background control, this suggests some kind of interference from the Plasma itself. The fact that the levels of CD9 and TSG101 were inconsistent between identically processed samples also suggests this. Particle size was also still an issue as it was consistently less than the 100 -120 nm expected for a pure exosome sample. The markers assessed on the exosomal surface were also unreliably detectable amongst the healthy donor samples as seen in Figure 3.13. Figure 3.14. contains the Nanosight data.

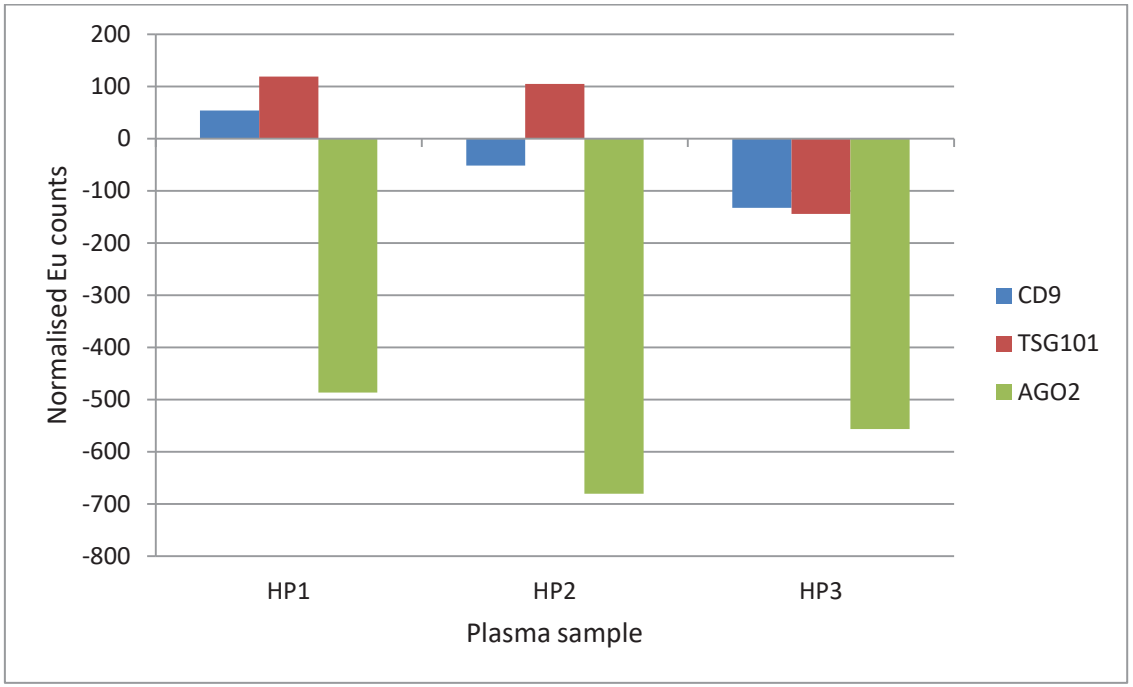

Figure 3.13. Detecting the presence of exosomal markers in UC-UF processed plasma exosome samples.

Qualitative analysis of exosome samples isolated from different fluids by Ultracentrifugation-Ultrafiltration (HP1 = healthy Plasma). Exosomes were isolated from 10 mL Plasma samples (n = 3) by ultracentrifugation at 100 000 x g for 1 hour at 4^0C. This was followed by resuspension of the exosome sample in 15 mL of DPBS and ultrafiltration using and Amicon 100 KDa filtration device spun at 3400 x g for 15 mins. The retentate was diluted to a final volume of 820 µL and split into one 20 µL fraction reserved for Nanosight analysis, and 8x 100 µL volumes which were added to a Perkin-Elmer high-bind Optiplate and incubated over night at 4^0C. The DELFIA Europium assay protocol was then followed as per section 3.2.2. Exosomal markers CD9, TSG101 and AGO2. AGO 2 is not detectable in any samples which suggests that Ultracentrifugation-Ultrafiltration is effective at eliminating this contaminant. However CD9 and TSG101 are not detectable in all samples which strongly suggests that Ultracentrifugation-Ultrafiltration is an ineffective method for isolating exosomes from Plasma.

a) HP1	
Particle count per mL	Mode particle size (nm)
2.68xE^8	65.6

b) HP2	
Particle count per mL	Mode particle size (nm)
2.51xE^8	72.1

c) HP3	
Particle count per mL	Mode particle size (nm)
5.37xE^9	67.8

Figure 3.14. Purity of exosome samples acquired by UC-UF from Plasma.

Exosomes were isolated from 10 mL Plasma samples (n = 3) by ultracentrifugation at 100 000 x g for 1 hour at 4^0C. This was followed by resuspension of the exosome sample in 15 mL of DPBS and ultrafiltration using and Amicon 100 KDa filtration device spun at 3400 x g for 15 mins. The retentate was diluted to a final volume of 820 µL and split into one 20 µL fraction reserved for Nanosight analysis, and 8x 100 µL volumes which were added to a Perkin-Elmer high-bind Optiplate and incubated over night at 4^0C. **a)** Nanosight data for Healthy Plasma sample 1 (HP1). Reasonable particle count, but smaller than expected particle size. **b)** Nanosight data for HP2. Reasonable particle count, but smaller than expected particle size. **c)** Nanosight data for HP3. Reasonable particle count, but smaller than expected particle size.

3.4.6. Optimising exosomal RNA isolation from Plasma exosomes: Comparison of RNA yield and quality between ExoRNeasy and UC-UF

ExoRNeasy is a kit released by Qiagen late in 2014. The kit promised a simple, short and well optimised protocol for the isolation of exosomes that required no ultracentrifugation. From a diagnostic standpoint, the advantages of this are obvious as there is little need for advanced laboratory skills and a faster method would allow more samples to be processed per day. For this reason, a head to head comparison between this kit and our Ultracentrifugation-Ultrafiltration technique was devised. To be considered successful, samples isolated using ExoRNeasy had to meet at least the same RNA quantity and quality acquired by Ultracentrifugation-Ultrafiltration. Both methodologies provided roughly the same concentration of exosomal RNA (14 ng/µL) measured by Nanodrop. However using exoRNeasy to purify exosomes provided a sample of much higher quality. In fact the UC-UF sample was so contaminated with protein and trace amounts of RNA isolation reagent that the concentration provided by the Nanodrop was likely a substantial overestimate. Also of note was the fact that the exosome purification with ExoRNeasy required only 1 mL of plasma compared to the 10 mL of plasma that were used in the UC-UF protocol. This experiment was performed in biological quadruplicate.

3.4.7. Measuring expression levels of biomarker candidate miRNAs in Plasma exosomes

With a consistent method for isolating Plasma exosome RNA now available, isolations were performed on our initial cohort of 5 PCa patients and compared to 6 healthy donor Plasma samples. Cel-miR-39 was used as a spike-in control to act as an endogenous control, and also to confirm that miR-92b* is an appropriate endogenous control for comparisons between exosomes of healthy controls or PCa patients. Early results were somewhat encouraging as 3 exomiRs (let-7i, miR-126*, miR-1228*) were significantly (>2-fold) enriched in all of our patients compared to the control group. A further 3 of our candidates biomarkers (miR-106b, miR-22, miR-25) were significantly enriched in 4 out of 5 samples. Unfortunately, miR-1228, miR-149* and miR-125b-2* were not significantly enriched. This data is presented in Figure 3.16.

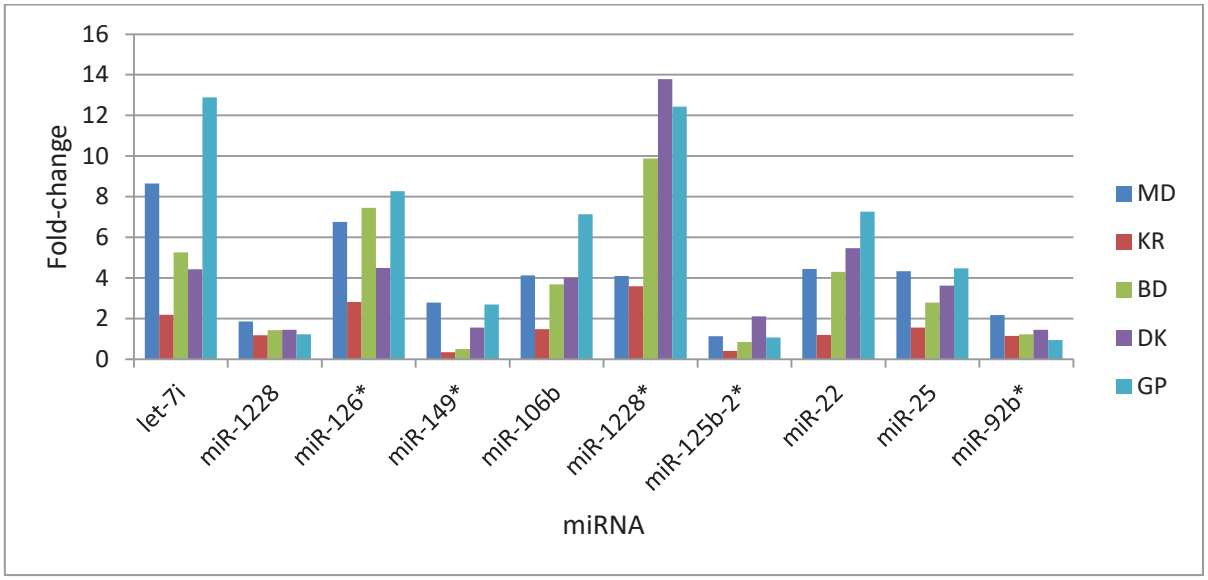

Figure 3.16. Comparison of exomiR expression levels between healthy and PCa plasma exosomes.

Plasma exosome samples were isolated from 1 mL starting volumes using the Qiagen exoRNeasy kit according to the manufacturer's instructions, including the optional cel-miR-39 spike in step. RNA samples were then normalised to 50 ng/µL using a Thermo-fisher Nanodrop. Samples were reverse transcribed for let-7i, miR-1228, miR-126*, miR-149*, miR-106b, miR-1228*, miR-125b-2*, miR-22, miR-25, miR-92b* and cel-miR-39 using the Applied Biosystems high capacity reverse transcriptase kit. qPCR was then performed on each miRNA and their levels were assessed in 5 PCa Plasma exosomal RNA samples versus a control group of normal Plasma exosomes provided by healthy volunteers. All exomiR levels were normalised to cel-miR-39 (to calculate ΔCt), then the PCa expression levels were were calculated using the ΔΔCt method (ΔCt[PCa patient sample] – ΔCt[control samples0]). Let-7i, miR-126* and miR-1228* all performed exceptionally well as they were significantly Enriched (>2 fold) in all patient samples. MiR-106b, miR-22 and miR-25 are also very promising biomarker candidates as they were significantly Enriched in most of the samples. MiR-1228, miR-149* and miR-125b-2* however were not significantly Enriched as the microarray suggested. MiR-92b* remained stably expressed across all samples even relative to the exogenous spike in gene (cel-miR-39), suggesting that miR-92b* is an appropriate endogenous control for exosomes. The initials on the right hand side indicate PCa patient samples.

Knowing that some of these biomarker candidates were significantly enriched in PCa Plasma exosomes harvested from patients, the qPCR data were subjected to Hierarchical clustering analysis using DataAssist software (Applied Biosystems). This would determine whether the expression levels of these exomiRs as a group supplied enough information to wholly differentiate healthy from PCa patients. Unfortunately, this was not the case. Although three out of five patients clustered very closely (Figure 3.17), the healthy patients didn't form their own cluster and were quite scattered amongst the six (numbered 1 – 6 on Figure 3.17.) healthy volunteer samples. However, upon looking at the data, several miRNAs seemed more highly Enriched in the PCa patient samples.

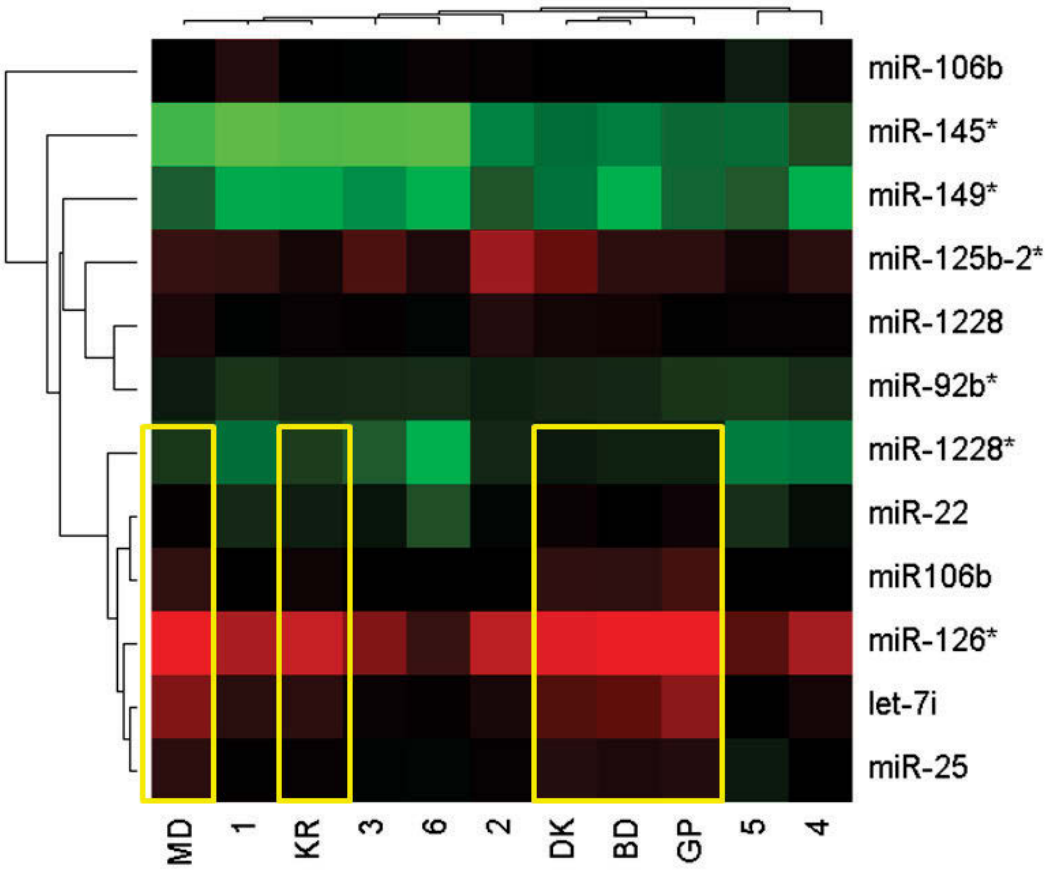

Figure 3.17. Hierarchical clustering analysis of differentially expressed exomiRs between PCa and healthy plasma samples.

Heat map produced from qPCR data. Data from previous Figure were re-analysed using hierarchical clustering analysis. Patient samples don't cluster entirely separately from control samples, but miR-126*, let-7i, miR-25, miR-106b and miR-22 are all more highly expressed in the patient samples only. These miRNAs are highlighted in the yellow boxes. On the X-axis, the numbers represent healthy plasma exomiR samples, the initials represent PCa patient exomiR samples.

3.5. Optimisation of Exosomal RNA Isolation From Human Urine

3.5.1. Optimising exosomal RNA isolation from urine exosome samples

The optimization steps required to obtain pure exosomes from Urine were much simpler, given the quite high quality of exosome samples isolated using ultrafiltration as evidenced by Figure 3.6. However, the issues in obtaining reliable yields of exosomal RNA persisted and required optimization. Fortuitously, simply using more Urine and ultrafilter units sufficed in producing pure, concentrated samples of exosomes as shown by the high count of particles of approximately 100 nm with high levels of exosomal marker protein (as unpublished data from our lab confirms). These exosome samples also consistently gave RNA yields sufficient for qPCR and microarray analysis (≥ 20 ng/µL) (Table 3.4.). Most of the 260/230 and 260/280 ratios (ratios indicative of RNA sample quality on the Nanodrop) were outside of normal parameters. However, an application note released by Norgen Biotek reveals that these ratios are to be expected when dealing with exosomal RNA samples (224).

Table 3.4. RNA yields obtained for all Urine exosome isolations

Sample ID	Nucleic Acid Conc. (ng/uL)	yield (ng)	260/280	260/230
MG19550901 PU	19.15	191.5	1.455	0.4
MG19550901 PxU	61.65	616.5	1.605	0.81
MJ19530831 PU	24.05	240.5	1.455	0.255
MJ19530831 PxU	87.65	876.5	1.65	0.74
MG19520301 PU	33.25	332.5	1.495	0.445
MG19520301 PxU	21.8	218	1.445	0.235
GP19650926 PU	21.15	211.5	1.465	0.37
MD19390904 PU	27.45	274.5	1.495	0.355
JA19450328 PU	30.55	305.5	1.505	0.4
WS19671017 PU	21.85	218.5	1.47	0.41
JP19521114 PU	22.45	224.5	1.48	0.33
DK19541003 PU	31.85	318.5	1.56	0.445
PW19470610 PU	35.55	355.5	1.63	0.52
BD19510912 PU	10.05	100.5	1.49	0.345
MA1971112 HU	29.25	292.5	1.505	0.465
RK19560620 HU	20.55	205.5	1.49	0.44
BW19510831 HU	26.7	267	1.48	0.34
SG19560229 HU	22.2	222	1.475	0.365

3.5.2. Measuring the levels of exomiR biomarker candidates in Urine before and after radical prostatectomy

Patients recruited for this study had samples taken both before they had a prostatectomy (complete removal of prostate) and after this surgery was performed, which allowed for longitudinal analysis of biomarker exomiR levels in Urine exosomes before and after removal of the cancer. Three groups were looked at in this experiment. The first was a control group made up of Urine exomiRs from healthy patients (HU = Healthy Urine exosomes). The other two groups were made up of patient samples taken before (PU = PCa Urine exosomes) and after their prostatectomy (PxU = PCa urine exosomes after surgery). Only a small number of samples were available for processing (2 HU, 2 PU and 2 PxU) but they did provide an interesting picture. The three groups clustered near to one another, However they did not segregate into distinct hierarchical clusters as evidenced by the dendrogram on the X-axis in Figure 3.18. There were also substantial observable differences in expression levels between the two post surgery samples as seen below in Figure 3.18. These three conditions would be better resolved with a much larger samples size but this work has yet to be done.

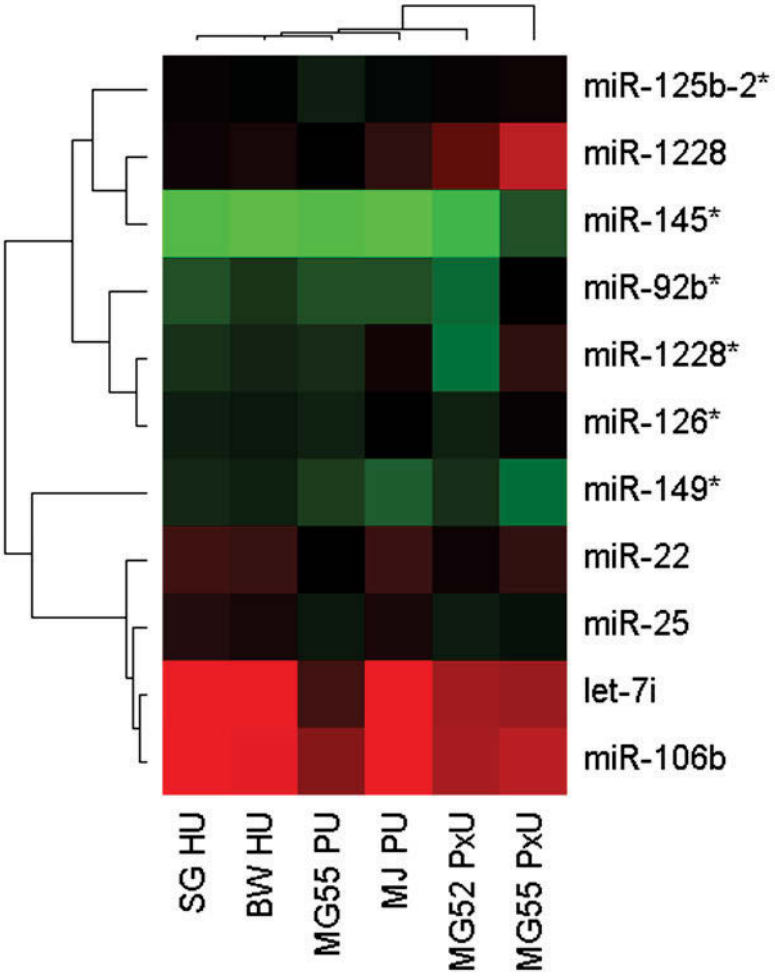

Figure 3.18. Hierarchical clustering analysis of differentially expressed exomiRs between PCa and healthy urine samples.

The suffix HU indicates a sample obtained from a healthy volunteer (n = 2). PU indicates a sample from a PCa patient prior to radical prostatectomy (n = 2) and PxU indicates a sample from the same PCa patient post-surgery (n = 2). Although the expression profiles from each group do cluster close to one another, they do not cluster together perfectly. There are also quite obvious visual differences between the two PxU samples. For example, miR-1228*, miR-22 and miR-1228 are expressed at substantially higher levels in MG55 PxU than MG 52 PxU.

3.6. Discussion

3.6.1. The effectiveness of ultrafiltration of human body fluids for exomiR isolation

Because PCa is such a common malignancy throughout the world, any diagnostic technique used in a screening program would have to be high throughput and robust to meet existing needs and to cope with the increasing incidence of PCa in the western world, due to the aging population. With the increasing number of techniques that are suitable for isolation of exosomes from body fluids, it was necessary to determine which technique was most suitable for each bodily fluid. As noted in the ultrafiltration description above, it should come as no surprise that we adopted this technique for our Urine samples. However, we did not use DTT because the DELFIA assay employed to fully characterise our exosome samples requires proteins in their native states. Use of DTT may have lowered detection of exosomal markers and falsely lead us to believe that our samples did not contain exosomes. We also introduced an extra ultracentrifugation step after the ultrafiltration to enhance purity of our samples, and to increase the RNA yield to meet minimum standards required for input into qPCR.

Ultrafiltration was used for Plasma exosome isolation, although the techniques we tried to develop in our own lab were unable to isolate pure exosome samples or exosomal RNA of acceptable yield and quality for qPCR analysis. The Qiagen exoRNeasy protocol was the only technique capable of isolating sufficient quantities of RNA for qPCR in a reliable manner. However, at the time these experiments were performed, releasing and quantifying exosomes bound by the column could not be done which made exosome quality control impossible. Furthermore, as described in the ultrafiltration section, the population of particles isolated using exoRNeasy is not limited to exosomes. The filtration through a 0.2 µm filter prior to starting the protocol is likely to have increased the purity of the samples we acquired using exoRNeasy, but once again, the inability to assess the quality of these exosomal samples acquired using exoRNeasy has prevented us from assessing this fully.

Lastly, Saliva samples were not followed up for exomiR expression given the fact that let-7i could not be detected at all in Salivary exosomes. This exomiR is associated with exosomes of prostate origin, and even more so with PCa (129, 222, 223). Nonetheless, exosomes can be isolated from human Saliva samples using ultrafiltration, albeit in small quantities, and these samples contain enough RNA to be suitable for qPCR. It is possible therefore that Salivary exosomes may have diagnostic potential for cancers of the head and neck.

Apart from RNA yield and qPCR concerns, exosome samples also needed to be uncontaminated with other particles and excessive soluble proteins. The choice of ultrafiltration proved most effective at removing contaminants from Urine and Saliva samples as evidenced by the particle size and tetraspanin expression profiles seen in Figure 3.5. Unfortunately, the same cannot be said for Plasma which showed smaller than expected particle size and CD63 could not be detected in these samples. Even after a great deal of optimisation, Plasma samples could not be fully and reliably cleaned up asCD9 and TSG101 could not always be detected. However, AGO2 was consistently absent across all samples confirming that ultrafiltration was suitable for removing all of this protein, and presumably their non-exosomal miRNA cargo. However, this experiment should be further optimised as the highly negative results for AGO2 in the DELFIA assay were unexpected. Unfortunately positive controls for the AGO2 antibody were not possible given the significant expense of buying the purified protein.

3.6.2. Effectiveness of exomiR biomarker candidates in human Plasma

ExomiRs have come under great scrutiny in recent years for their potential to detect PCa with much higher sensitivity and specificity than is currently available. For example, high exosomal miR-141 expression in serum has been associated with PCa, and this exomiR even exhibited some ability to differentiate between PCa, benign prostatic hypertrophy (BPH) and healthy volunteer patients (125). Furthermore, high serum miR-141 also indicated a higher chance of advanced metastatic disease (approximately 70% chance), a pathological feature that is currently very difficult to predict.

miR-375 is also an excellent serum/Plasma based exomiR for diagnosing PCa. It has been shown to be 8 times more expressed in serum exosomes from PCa compared to healthy volunteers (126). MiR-375 and miR-1290 are also associated with advanced androgen independent PCa and are indicators of poor overall survival as 80% of patients with high levels of both exomiRs were dead at 24 months after diagnosis (127). Given both the diagnostic and prognostic potential of this exomiR, it may also become a powerful tool for clinicians administering care to PCa patients throughout the course of their treatment.

Unfortunately, our small patient cohort and short study duration prevented us from assigning any prognostic value to our biomarker panel just yet. However, there does appear to be some diagnostic potential, given that 3 out of 5 patients did cluster together, largely thanks to the expression profile of miR-126*. But overall, the performance of the biomarker panel was unable to differentiate PCa patients from healthy people and will most likely require the inclusion of more established Plasma exomiR biomarkers such as miR-141 and miR-375. More patients also need to be recruited in order to grasp the broader trends in the expression of the biomarker candidates. Other PCa clinicopathological metrics such as Gleason score, T-stage, PSA levels should also be included to fully assess the usefulness of the biomarker panel. The other option is to simply profile Plasma exomiRs directly from different patient cohorts. For example, a healthy volunteer group, a BPH group, a PCa patient group, the same patient group after radical prostatectomy and an advanced metastatic group. This would allow for stratification of these patients into risk groups and provide some evidence of prognostic ability. Unfortunately in this study the number of patients and volunteers that were recruited was insufficient to answer these questions.

3.6.3. Diagnostic potential of urinary exomiR biomarkers

Another extensively investigated area of exomiR cancer diagnostics is in cancers of the urogenital system, in particular bladder and prostate cancer. Armstrong et al identified an enriched exomiR signature consisting of five miRNAs, isolated from human Urine. This group showed that miRNAs usually found in the tumours themselves could be assayed for in urinary exosomes and buffy coat cells. Importantly, they also showed that these exomiRs positively correlate with cancer presence and the same exomiRs are not detectable in blood Plasma alone (199). However, this group used a Norgen kit to isolate their exosomes and did not include any quality control assessment at all, so the purity of their exosome samples is unknown. A further seven exomiR biomarker candidates have also been put forward by De Long et al who did perform surface marker analysis of their exosome samples. Very high sensitivity (88%) and specificity (78%) were reported using this panel of exomiRs for the diagnosis of bladder cancer (225). Unfortunately there was no overlap in reported exomiR biomarker candidates, but as was the case previously, different exosome isolation methods were used, which may explain this variation.

Urinary exosomes have also been useful in diagnosing prostate cancer (PCa), with an exomiR signature of three miRNAs being recently discovered (124). This group gave the highest standard of exosomal quality control seen in the literature so far, having performed Atomic Force Microscopy (AFM) and Dynamic Light Scattering (DLS) assays to check the size and morphology, and looked at the presence of CD9 and TSG101 while demonstrating the absence of free floating AGO2 which may carry contaminating, non-exosomal miRNA. They also demonstrated high specificity and sensitivity for miR-574-3p being ROC=0.85 and 71% respectively. miR-141 also performed admirably with sensitivity at ROC=0.86 and sensitivity at 66%. MiR-141 is of particular interest because it is also associated with Plasma exosomes in PCa patients as described in the previous section.

Again, the small patient cohort we had access to at this stage of the experiment did limit the conclusions that could be made. Nevertheless, it is highly encouraging that qPCR ready quantities of exosomal RNA could be acquired from all patient samples (table 3.1) albeit with some RNA quality issues. However, the most interesting Urine exomiR, miR-1228 actually increased in expression after radical prostatectomy (Figure 3.18.), and the other exomiRs failed to exhibit clear trends. This raised the unfortunate possibility that the exomiR biomarker candidates identified using cell culture are not very effective in actual patient samples. There were also ongoing problems with recovering qPCR ready amounts of exosomal RNA from patient samples. Further experiments were planned to further increase exosome yield from Urine and to discover more exomiR biomarker candidates by directly comparing PCa patient Urine exomiRs to normal urine exomiRs.

Chapter 4 abstract:

Given the immense difficulties in optimising exosome isolation procedure for bodily fluids and the mixed success using our original panel of biomarker candidates identified using cell culture exosomes, a second round of biomarker discovery was undertaken. Using our optimised exosome isolation procedures, we produced sufficiently concentrated exosomal RNA samples from Urine samples and discovered that Plasma exosomal RNA isolated using ExoRNeasy was insufficient for further analysis. The Urine samples were then analysed on the Taqman based OpenArray platform. The Taqman Megaplex pool A and pool B primer sets were chosen for their ability to identify expression levels of 754 mature human miRNAs in each sample. This analysis produced miRNA expression profiles for PCa patients before and after the cancer was removed surgically, as well as for a healthy control group. This facilitated the identification of exomiRs that are elevated in PCa and also allowed us to determine whether these exomiRs drop once the cancer is removed. The expression profiles were then subjected to functional analysis using Cytoscape to ascertain whether the new PCa exomiR profile had the same potential to interact with the immune system that was seen in Chapter 1 when looking at the microarray exomiR profiles.

4.1. Methods

4.1.1. Pre-processing, storage conditions and sample tracking

All Urine samples were stored at -80^{0}C as soon as they reached the lab. Urine was thawed as needed at 37^{0}C, then centrifuged at 2000 x g for 20 mins at 4^{0}C to remove any cells or large debris. The supernatant was then vacuum filtered using a 0.2 µm PES filter membrane. The filtrate was then pipetted into 45 mL aliquots for freezing until ready for use. These aliquots were then thawed as needed to prevent wastage of precious patient samples and kept the number of freeze thaw cycles to a minimum.

Plasma samples were stored at -80^{0}C as soon as they reached the lab and were thawed at 37^{0}C until ready for use. The small aliquots of plasma acquired from patients (typically 10 mL) were then syringe filtered through a 0.2 µm PES filter membrane which removed cells and other large particles. These samples were then analysed straight away.

Patient sample details were also recorded and stored in Excel documents for later interrogation. The sample details were stored using an alphanumeric identifier such as: BW19510831 HU. The BW indicates the patients/volunteers initials and the numbers that follow represent the patient's date of birth. The HU indicates healthy urine. Similarly a PU suffix indicates a sample from a PCa patient while PxU indicates a sample taken from a PCa patient after removal of the cancer. Some healthy plasma samples were acquired in bulk volumes of approximately 250 mL. These plasma samples had no patient details attached to them and were simply termed HP1, HP2 etc where HP indicates healthy plasma.

4.1.2. Exosomal RNA isolation from Urine

Urine is a much more dilute fluid than Plasma, which necessitated use of larger starting volumes. 135 mL of pre-filtered Urine was chosen for this reason.

To begin, 5x Amicon Ultra-15 ultrafiltration units (Sigma) were set up and 15 mL of pre-filtered Urine was added to each. These tubes were centrifuged at 3400 x g for 10 minutes at 4^0C. Then, each tube was topped up with a further 15 mL volume of pre-filtered Urine and the centrifugation was repeated. The retentate was removed from each ultrafiltration unit and added to a 2.0 mL ultracentrifuge tube (Beckman Coulter Inc.). Each ultrafiltration unit was extensively washed with 600 µL of 1x DPBS and this volume was added to another 2.0 mL ultracentrifuge tube. These tubes were then centrifuged at 100 000 x g for 1 hour at 4^0C. All pellets derived from the same sample were lysed directly in 500 µL of RNAzol, or resuspended in 400 µL of 1x DPBS for DELFIA/nanosight protocols.

4.1.3. Accurate exosomal RNA quantification using the Agilent Bioanalyzer Pico detection kit

The RNA 6000 Pico kit (138) was chosen for exosomal RNA analysis as it was able to provide accurate estimates of very low RNA concentrations which was necessary after the abnormal ratios seen on the Nanodrop in chapter 3. The RNA 6000 Pico kit was also able to estimate a RIN, but as only exosomal RNA samples were acquired in these experiments, the RIN was disregarded given the unreliable quantities of the 18s and 28S ribosomal subunits in exosomal samples reported in previous chapters.

4.1.4. DELFIA Europium assay to detect canonical exosomal marker proteins

This was performed exactly as described in section 3.2.2 without modification. The antibodies used in this chapter can be found in table 4.1.

Table 4.1. Antibodies Used.

Antibody	Primary or Secondary	Catalog No.	Dilution Used
Rabbit monoclonal [EPR5702] to CD63	Primary	ab134045	1:1000
Rabbit monoclonal [EPR2949] to CD9	Primary	ab92726	1:1000
Rabbit monoclonal [EPR7130(B)] to TSG101	Primary	ab30871	1:1000
Rabbit monoclonal [EPR10411] to Ago2 / eIF2C2	Primary	ab186733	1:1000
Goat anti-rabbit H&L (biotin)	Secondary	ab97049	1:5000

4.1.5. Nanosight methodology for exosome sample quality control.

This protocol was performed as described in section 3.2.3.

4.1.6. Pre-amplification of urinary exosomal RNA prior to OpenArray analysis

Because the concentrations of urinary exosomal RNA were so low, a miRNA pre-amplification step was required to amplify these samples before they could be assessed on the Applied Biosystems OpenArray platform. This process was performed in accordance with the protocol supplied by the manufacturer. In brief, exosomal RNA samples were normalised to approximately 1 ng/µL using the Agilent Bioanalyzer RNA Pico chips. Next, Reverse transcription reactions were performed using the reagents as laid out in Table 4.2.

Table 4.2. 1x Pre-amplification reaction.

Component	Volume (µL) for 1x reaction
Total RNA (1 ng/µL)	3.00
Megaplex RT Primers (Pool A or B)	0.75
dNTPs with dTTP (100 mM)	0.15
MultiScribe Reverse Transcriptase (50 U/µL)	1.50
10x RT Buffer	0.75
$MgCl_2$ (25 mM)	0.90
RNAse Inhibitor (20 U/µL)	0.09
Nuclease Free Water	0.36
Total	7.50

Following the reverse transcription reaction over 40 cycles of amplification, the Low Sample Input (LSI) Megaplex PreAmp reaction was performed for 16 cycles. Reagents were laid out as seen in the Table below.

Table 3.3. 1x LSI Megaplex PreAmp reaction.

Component	Volume (µL) for 1x reaction
Reverse Transcription Product	7.5
Taqman PreAmp Master Mix	20
Megaplex PreAmp Primers (Pool A or B)	4.0
Nuclease Free Water	8.5
Total	40

The PreAmp product was then diluted 1:20 with Nuclease free water and either used directly or stored at -20^{0}C for later use.

4.1.7. OpenArray qPCR protocol

Once samples had gone through the reverse transcriptase and PreAmp phases, they were ready to be profiled using OpenArray plates pre-coated with Megaplex human miRNA pools A and B, which are a set of 377 Taqman human mature miRNA probes each. The samples were loaded onto the plate as per the protocol supplied by the manufacturer. Briefly, PreAmp products were loaded into the 384 well sample plate in the desired orientation (format 168), along with the necessary master mix and other components. The 384 well sample plate was then loaded into the OpenArray AutoLoader, which loaded the OpenArray plate with the samples. Once loaded, the OpenArray was sealed with an OpenArray case and loaded with immersion fluid. The sealed OpenArray plate was then put into the Quantstudio 12k Flex system and the qPCR was performed.

4.1.8. Cytoscape methods for the discovery of potential urine exomiR functions in PCa biology

This was performed as described in section 2.1.12.

4.2. Results

4.2.1. Exosome quality assessment from Urine samples using exosomal surface markers and nanoparticle tracking analysis

The first step in performing exomiR profiling in Urine was to ensure that exosome samples met the minimum experimental requirements for the identification of exosomes, which was released by ISEV several months before this work was performed (203). In brief, this involved looking at 3 exosomal surface markers. CD9 and TSG101 were selected as positive markers given their strong association with the exosomal surface. AGO2 was selected as a negative marker as it occurs only on the inside of exosomes and thus would not be detectable if our exosome samples were intact and free from contaminating AGO2 also suspended in the Urine. Besides assessment of these marker proteins, Nanoparticle Tracking Analysis (NTA, Nanosight) was performed to ensure that all particles were within exosomal size ranges. Figure 4.2. shows that CD9 and TSG101 could be detected in all urinary exosome samples, and Figure 4.3. shows that all samples contained large numbers of particles falling within expected exosomal size ranges.

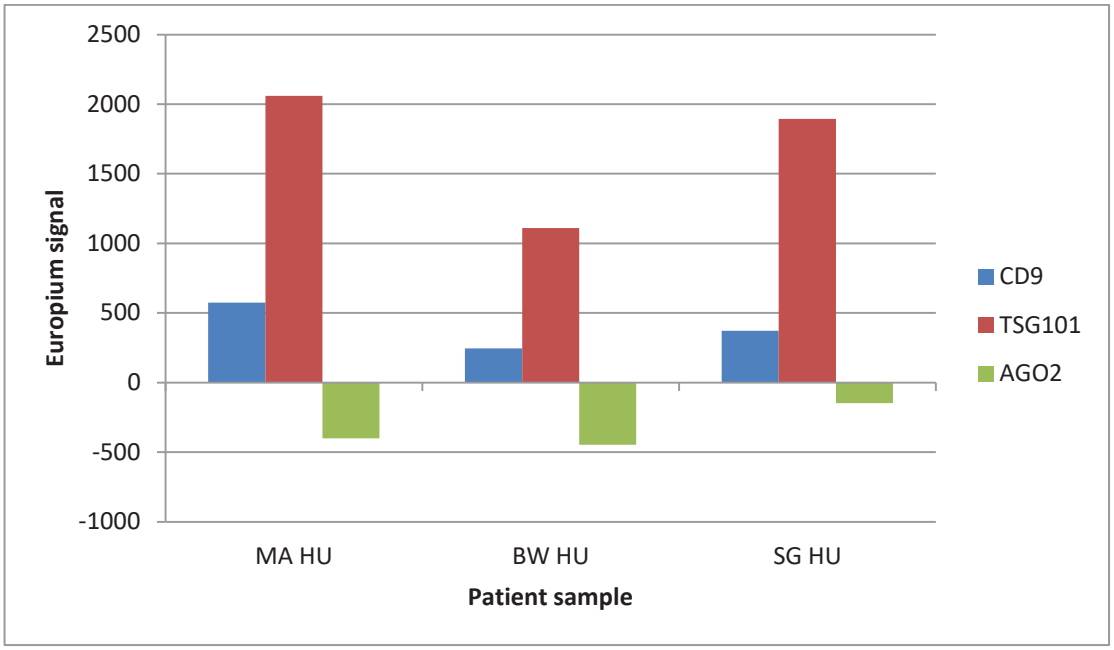

Figure 4.2. Exosome quality assessment using Exosomal marker proteins.

Exosomes were isolated from three biological replicates (MA HU, BW HU and SG HU) of healthy Urine using ultrafiltration/ultracentrifugation. DELFIA Europium assay was then performed on the resulting exosome samples using rabbit derived CD9, TSG101 or AGO2 primary antibodies. MA, BW and SG refer to the first and last initials of the patients name. HU refers to the fact that these are healthy samples of urine. CD9 and TSG101 are high in all samples, but AGO2 could not be detected in any samples and often fell below background levels.

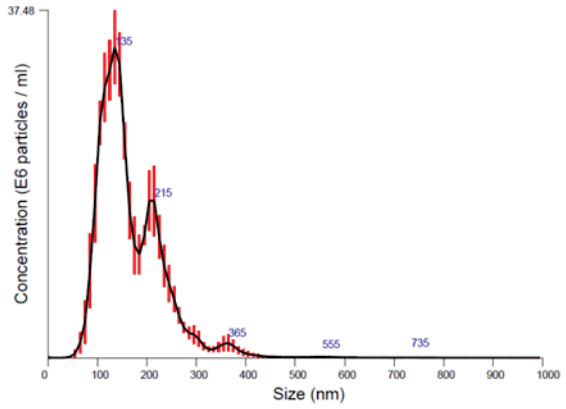

MA19711112 HU	
Particle count per mL	Mode particle size (nm)
3.58xE^8	135.7

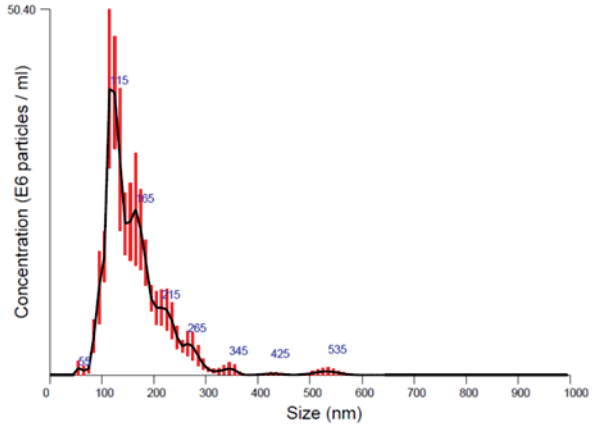

BW19510831 HU	
Particle count per mL	Mode particle size (nm)
3.2xE^8	119.8

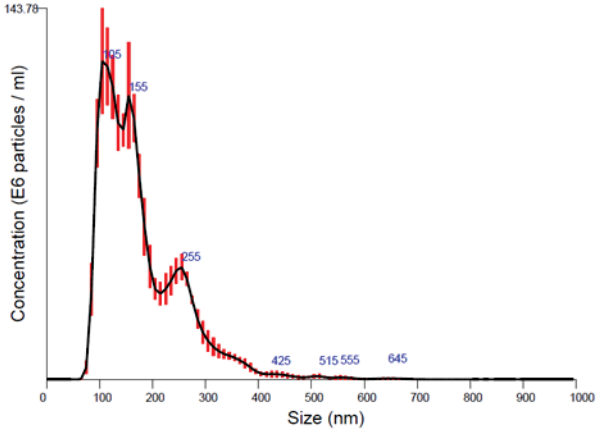

SG19560229 HU	
Particle count per mL	Mode particle size (nm)
1.53xE^9	109.3

Figure 4.3. Exosome quality assessment using Nanosight.

The exosome samples taken from three biological replicates of healthy urine (indicated by the HU suffix) were resuspended in 1x DPBS prior to analysis using exosomal surface markers. A 1 µL aliquot of each sample was taken and diluted in 1 mL of of 1x DPBS. Each diluted sample was then analysed using a Nanosight LM-14 instrument as per section 4.1.5. The sample name refers to the patients initials followed by their date of birth. HU indicates that the samples are of healthy urine. The small blue numbers indicate the size in nm of the most concentrated particles. Mode particle size and particle count were within acceptable limits.

4.2.2 Exosomal RNA quality assessment using Nanodrop and Bioanalyzer 2100 Pico ships

Before any high throughput expression profiling could be performed from Urine or Plasma, the methods for isolating exosomal RNA from these fluids needed to be validated. The first and most important requirement was that enough RNA could be isolated from the source material. This was relatively simple for Plasma as the manufacturers protocol could be followed exactly (226). The Urine protocol however was developed within our lab and required more extensive validation, the first being RNA yield.

RNA quality assessment was performed using a combination of Nanodrop and RNA Pico chips for the Agilent Bioanalyzer 2100. RNA could be isolated from both Plasma and Urine as confirmed by both the Nanodrop and Pico Chips. The Nanodrop data showed that RNA could be isolated from both sources with a minimum of contaminants as defined by Norgen (224). The Pico chip analysis also confirmed that the majority of RNA isolated from both Urine and Plasma consists of small RNAs of <200 nt as indicated by the small single peak between this region in Figure 4.4. However the yields of RNA reported by both methods differed hugely from one another, by several orders of magnitude. These data are shown in Table 4.4.

Table 4.4. Exosomal RNA concentrations as measured by the Nanodrop and RNA 6000 Pico chip.

Sample ID	Nanodrop RNA concentration (ng/uL)	Pico chip RNA concentration (pg/uL)
BW19510831 HU	72.25	161
RK19560620 HU	22.05	246
SG19560229 HU	59.2	176
HP1	8.2	20
HP2	20.9	28
HP3	30.65	49

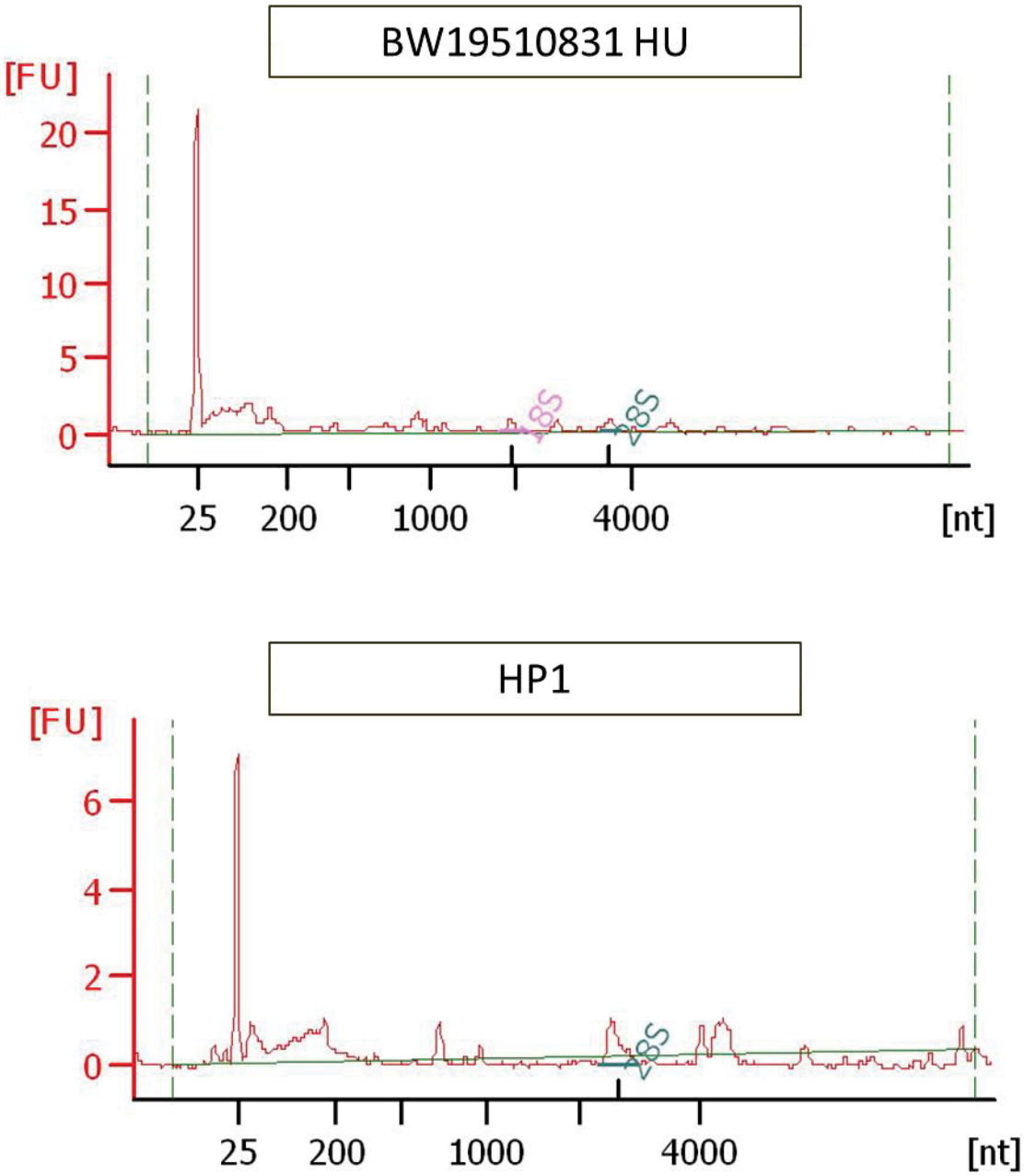

Figure 4.4. Representative data of Bioanalyzer 2100 RNA Pico 6000 analysis of exosomal RNA samples from Urine and Plasma.

RNA quality readouts using the Nanodrop and the RNA Pico chip, representative data. Exosomal was isolated using either the pooled ultrafiltration/ultracentrifugation-RNAzol RT technique for Urine or the exoRNeasy protocol for Plasma. RNA concentrations were assessed using the Thermo-fisher Nanodrop and the Agilent BioanalyzerRNA Pico chip. The first image shows representative Pico chip results for the healthy Urine samples (designated by the HU suffix). The single peak between 25 and 200 nt indicates the dominance of small RNAs in these samples. The second image shows representative Pico chip results from healthy Plasma samples. Similar to the Urine samples, the largest peak is between 25 and 200 nt suggesting that small RNAs predominate in these samples also.

4.2.3. OpenArray pre-amplification with Low Sample Input (LSI) protocol for Urine derived exosomes

OpenArray analysis can be performed from starting RNA concentrations of above 100 ng/µL using the standard openarray reverse transcriptase protocol. However, given the extremely low yields of RNA obtained from Urine exosomes samples, a different protocol was required. The LSI protocol, also available from Applied Biosystems (227) allowed us to perform successful reverse transcriptase reactions from as little as 1 ng of template RNA. Before running the cDNA product on the Openarray however, it was necessary to run standard qPCRs to confirm that the amplification process was successful. To do this, miRNAs from each Megaplex primer pool were selected, and standard qPCRs were performed in all relevant samples. MiR-106b was chosen to probe all samples with pool A megaplex primers, while miR-126* and miR-125b-2* were selected to probe samples with pool B megaplex primers.

The results of this show that all samples were positive for the relevant miRNA(s), confirming that the LSI preamplification was successful. Furthermore, the NTC showed no amplification, indicating negligible contamination. The no reverse transcriptase control (NRT) also showed no amplification, showing that there was no contamination from genomic sources. These data are presented in Table 4.5.

Table 4.5. LSI PreAmp cDNA quality control prior to OpenArray analysis.

Sample	miRNA	MEGAplex Pool	Ct average	Standard Deviation
SG HU	miR-106b	A	19.053	0.03888845
SG HU	miR-126*	B	25.629	0.040550095
SG HU	miR-125b-2*	B	23.894	0.121410033
BW HU	miR-106b	A	19.808	0.005507835
BW HU	miR-126*	B	24.885	0.03605528
BW HU	miR-125b-2*	B	24.406	0.189088525
MA HU	miR-106b	A	18.323	0.031097023
MA HU	miR-126*	B	24.969	0.186039026
MA HU	miR-125b-2*	B	23.209	0.236747647
NTC	miR-106b	A	Undetermined	NA
NTC	miR-126*	B	Undetermined	NA
NTC	miR-125b-2*	B	Undetermined	NA
NRT	miR-106b	A	Undetermined	NA
NRT	miR-126*	B	Undetermined	NA
NRT	miR-125b-2*	B	Undetermined	NA

Amplification data from cDNA samples. Exosomal RNA was isolated from three biological replicates of healthy urine (MA HU, BW HU and SG HU) using RNAzol RT and normalised to 1 ng/µL using the Agilent Bioanalyzer RNA Pico chip. RNA then underwent pre-amplification as per the Applied Biosystems low sample input protocol for reverse transcription using human miRNA primer pools A and B. qPCR was then performed on miR-106b (pool A), miR-126* (pool B) and miR-1265b-2* (pool B) in all samples. The blue, green, and red flat lines on figure a and b indicate CT cut-offs for each of these miRNAs **A)** Amplification curves for all pool A and pool B miRNAs in healthy urine samples **B)** No amplification recorded in no template controls (NTC) or No reverse transcriptase (NRT) controls.

4.2.4. Identification of Differentially expressed urinary exomiRs associated with PCa, using the Taqman OpenArray platform

With all quality control steps now performed with satisfactory results as defined in section 4.2.2, the Openarray analysis was finally performed on the urinary exosomal RNA samples. The first analysis performed on this data was to identify new biomarker candidates, by comparing the profiles from the prostate cancer patient Urine (PU; three biological replicates) with those from the health volunteer Urine (HU; three biological replicates). This analysis revealed 22 exomiRs that were significantly enriched (≥2 fold higher, $P<0.05$) in prostate cancer urinary exosomes. These results are summarised in the volcano plot and accompanying Table in Figure 4.6. and table 4.5. respectively.

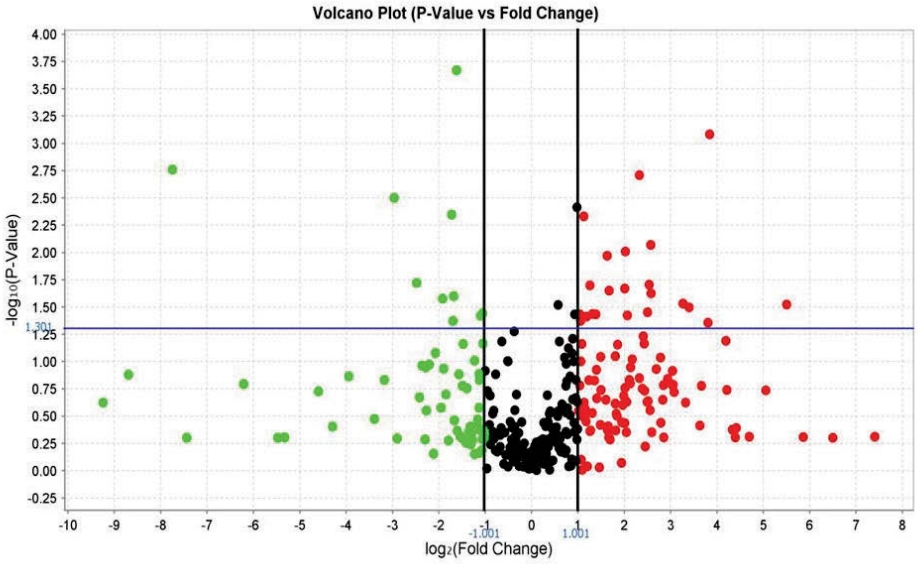

Figure 4.6. Volcano plot of exomiR expression from PCa patient urine compared to healthy urine

Exosome samples were isolated from three biological replicates of healthy Urine and PCa patient urine using the pooled ultrafiltration/ultracentrifugation technique. RNA was then isolated using RNAzol RT and normalised to 1 ng/µL using the Agilent Bioanalyzer RNA Pico chip. RNA then underwent pre-amplification as per the Applied Biosystems low sample input protocol for reverse transcription using human miRNA primer pools A and B. qPCR was then performed using the Applied Biosystems miRNA OpenArray. To be considered statistically significant enrichment in PCa exosomes, an exomiR had to be expressed at >2 (greater than 1 on X-axis) fold higher in PCa samples with P-value < 0.05 (above 1.301 on Y-axis). There are 22 exomiRs that meet these criteria. Green dots represent exomiRs that are packaged at lower concentrations in PCa urine exosomes compared to healthy urine exosomes. Red dots indicate exomiRs that are enriched in PCa urine compared to healthy urine. Black dots indicate exomiRs that are not differentially expressed between these two conditions.

Table 4.5. Statistically significant enriched PCa exomiRs

miRNA	fold-change (PU vs HU)	P-value
miR-375	45.397	0.03
miR-20b	14.301	0.001
miR-215	13.986	0.044
mmu-miR-187	10.573	0.032
miR-216b	9.609	0.029
miR-193b	5.982	0.024
miR-886-3p	5.936	0.009
miR-149	5.813	0.02
miR-484	5.649	0.035
miR-744	5.011	0.002
miR-324-3p	4.194	0.038
miR-10b	4.069	0.01
miR-17	4.02	0.0021
miR-106a	3.193	0.022
miR-532-3p	3.095	0.011
miR-664	2.61	0.037
miR-425*	2.494	0.037
miR-29a	2.396	0.02
mmu-miR-93	2.273	0.039

miR-455	2.18	0.005
miR-196	2.078	0.042
miR-628-3p	2.058	0.037

The next step was to identify a urinary exomiR profile in the same patients once the cancer was removed by radical prostatectomy (samples designated PxU; 3 biological replicates). This profile was then compared to the previous analysis (PU vs HU) to identify exomiRs that were high while the PCa was untreated, but dropped significantly (≤2 fold lower, $P<0.05$) once the cancer was removed. Again, volcano plot analysis was performed to identify exomiRs packaged at lower concentrations in PxU urine samples. Eleven exomiRs were identified and four of these were significantly higher in the previous analysis. These data are presented in Figure 4.7.

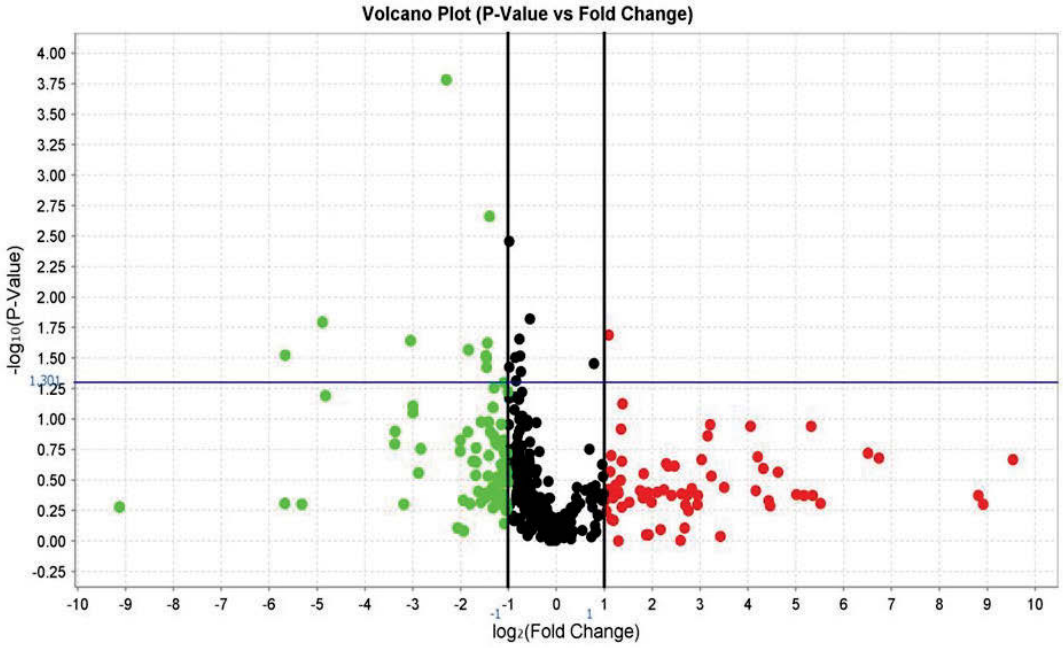

Figure 4.7. Volcano plot of exomiR expression from PCa patient urine before prostatectomy compared to the same patients post-surgery.

Exosome samples were isolated from three biological replicates of healthy Urine and PxU patient urine using the pooled ultrafiltration/ultracentrifugation technique. RNA was then isolated using RNAzol RT and normalised to 1 ng/µL using the Agilent Bioanalyzer RNA Pico chip. RNA then underwent pre-amplification as per the Applied Biosystems low sample input protocol for reverse transcription using human miRNA primer pools A and B. qPCR was then performed using the Applied Biosystems miRNA OpenArray. To be considered a statistically significant decreased in exomiR level, an exomiR had to be expressed at < -2 (lass than -1 on X-axis) fold higher in PCa samples with P-value < 0.05 (above 1.301 on Y-axis). There are 11 exomiRs that meet these criteria, 4 of which were highly enriched in urinary PCa exosomes compared to healthy urine exosomes. Green dots represent exomiRs that are packaged at lower concentrations in PCa urine exosomes compared to healthy urine exosomes. Red dots indicate exomiRs that are enriched in PCa urine compared to healthy urine. Black dots indicate exomiRs that are not differentially expressed between these two conditions.

Table 4.6. Statistically significant exomiRs that were enriched at time of diagnosis, but dropped once the cancer was removed.

miRNA	fold-change (PxU vs PU)	P-value
miR-375	-50	0.03
miR-20b	-4.902	0
miR-149	-2.74	0.038
miR-106a	-2.132	0.05

4.2.5. Discovering the potential functional significance of enriched urinary exomiRs using Cytoscape

Having identified a number of highly enriched exomiRs in PCa patient Urine, this data set was interrogated for functional significance using the Cytoscape platform. This analysis was again performed under the assumption that enriched exomiRs are most likely to be functional, and that recipient cells absorb these exomiRs which then down-regulate target mRNAs in that cell. The population of potential target mRNAs was generated by finding the top 100 target genes (according to context score) of the top ten most enriched exomiRs. These genes were pooled into one large super-list, which was then organised into a protein interaction network. Sub-networks were then produced using the MCODE algorithm, and the genes in these sub-networks were used to produce gene ontologies using the BiNGO plugin. Seven sub-networks were built in total, and of this group clusters 1, 3 and 4 were particularly interesting (Figures 4.8., 4.9., and 4.10, respectively). This is because these groups contained many ontological terms that are related to immune evasion (Tables 4.7., 4.8., and 4.9. respectively) which has been a theoretical cancer exosome function for some time and is discussed in detail in chapter 2.

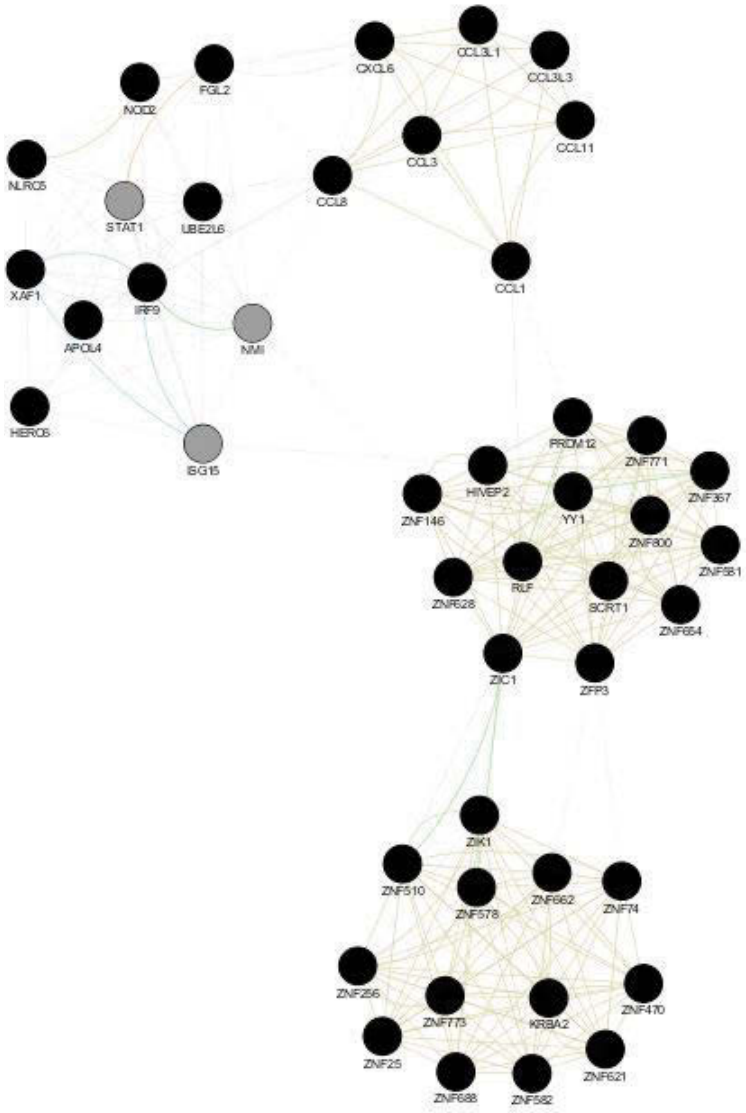

Figure 4.8. MCODE PU vs HU Cluster 1, target genes of exomiRs found to be highly Enriched in PCa patient urine compared to normal patient urine.

Interaction hub taken from a larger network of genes using the MCODE algorithm. The top ten miRNAs most highly enriched in PCa exosomes were merged with their most likely target genes using TargetScan 5.2. The top 100 target genes of each exomiR were then selected using the context score. This large list (approximately 900 potential target genes) was then interrogated for interactions using GENEMania, a Cytoscape plugin. Black nodes represent genes that are known or predicted targets of exomiRs enriched in PCa exosomes. Grey nodes are genes known to interact heavily with genes in the black nodes and were selected for inclusion in the network using the GeneMANIA plugin. PU vs HU indicates that the proteins in this network are targets of exomiRs enriched in PCa urine (PU) compared to healthy urine (HU). There are a total of 45 nodes (proteins likely to be down-regulated by the absorption of exomiRs secreted by androgen independent PCa) in the network. There are 280 edges (lines between the nodes that represent protein-protein interactions) amongst these genes. Different line colours indicate different types of protein-protein interactions.

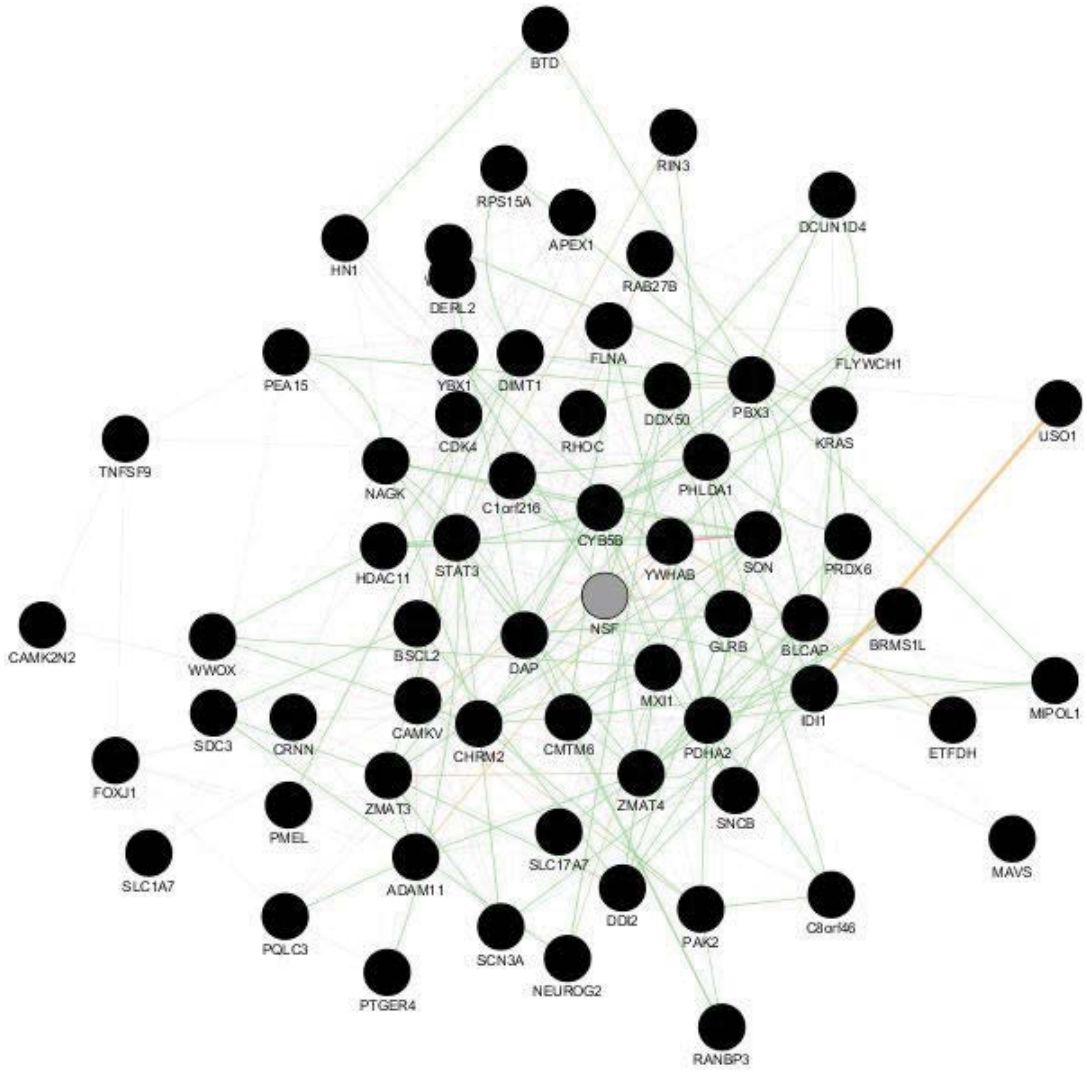

Figure 4.9. MCODE PU vs HU Cluster 2, target genes of exomiRs found to be highly Enriched in PCa patient urine compared to normal patient urine.

Interaction hub taken from a larger network of genes using the MCODE algorithm. The top ten miRNAs most highly enriched in PCa exosomes were merged with their most likely target genes using TargetScan 5.2. The top 100 target genes of each exomiR were then selected using the context score. This large list (approximately 900 potential target genes) was then interrogated for interactions using GENEMania, a Cytoscape plugin. Black nodes represent genes that are known or predicted targets of exomiRs enriched in PCa exosomes. Grey nodes are genes known to interact heavily with genes in the black nodes and were selected for inclusion in the network using the GeneMANIA plugin. PU vs HU indicates that the proteins in this network are targets of exomiRs enriched in PCa urine (PU) compared to healthy urine (HU). There are a total of 65 nodes (proteins likely to be down-regulated by the absorption of exomiRs secreted by androgen independent PCa) in the network. There are 327 edges (lines between the nodes that represent protein-protein interactions) amongst these genes. Different line colours indicate different types of protein-protein interactions.

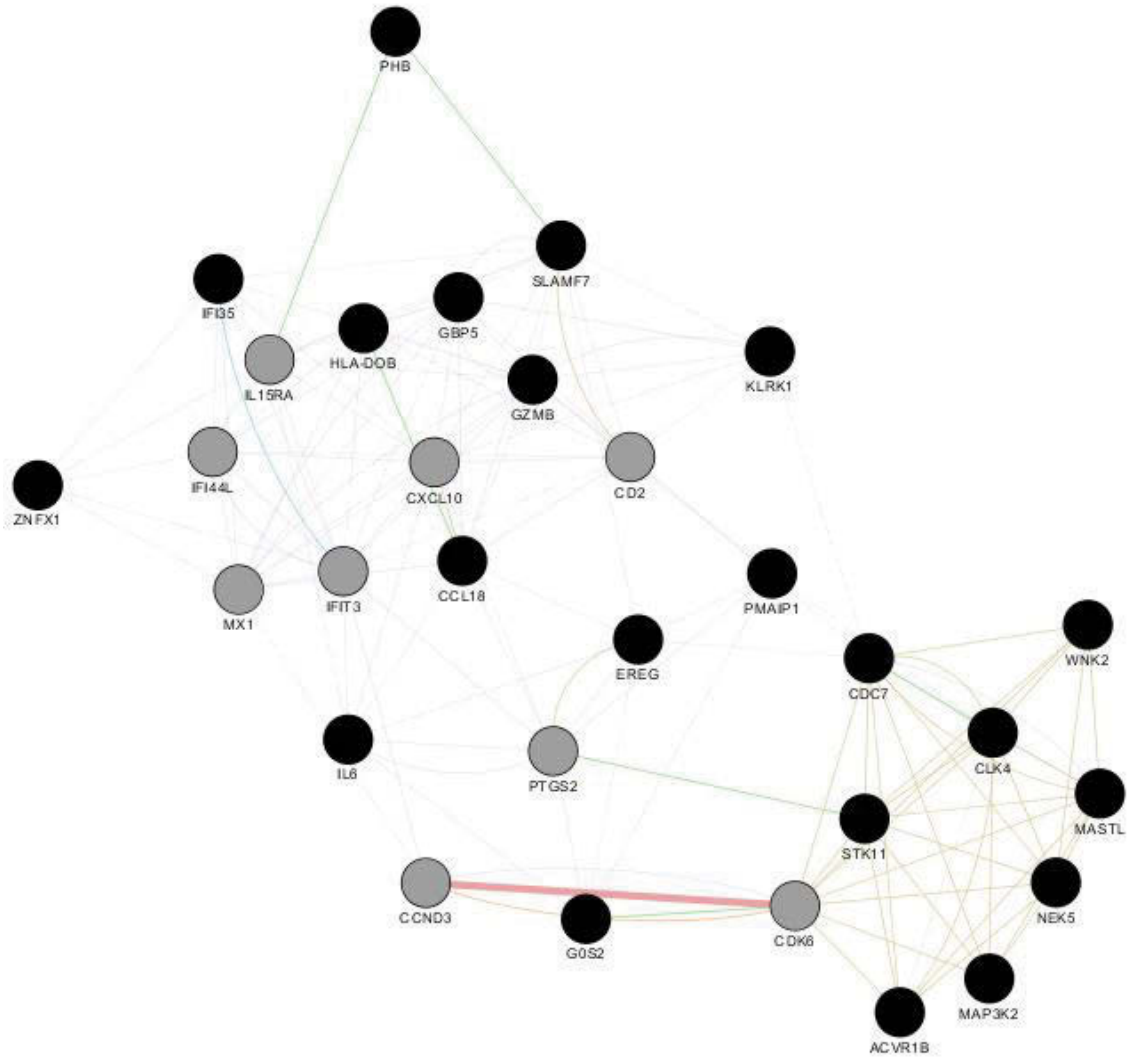

Figure 4.10. MCODE PU vs HU Cluster 4, target genes of exomiRs found to be highly Enriched in PCa patient urine compared to normal patient urine.

Interaction hub taken from a larger network of genes using the MCODE algorithm. The top ten miRNAs most highly enriched in PCa exosomes were merged with their most likely target genes using TargetScan 5.2. The top 100 target genes of each exomiR were then selected using the context score. This large list (approximately 900 potential target genes) was then interrogated for interactions using GENEMania, a Cytoscape plugin. Black nodes represent genes that are known or predicted targets of exomiRs enriched in PCa exosomes. Grey nodes are genes known to interact heavily with genes in the black nodes and were selected for inclusion in the network using the GeneMANIA plugin. PU vs HU indicates that the proteins in this network are targets of exomiRs enriched in PCa urine (PU) compared to healthy urine (HU). There are a total of 65 nodes (proteins likely to be down-regulated by the absorption of exomiRs secreted by androgen independent PCa) in the network. There are 327 edges (lines between the nodes that represent protein-protein interactions) amongst these genes. Different line colours indicate different types of protein-protein interactions.

Table 4.7.MCODE Cluster 1 gene ontology analysis

Type I Interferon Signalling Pathway
Response to Type I Interferon
Cellular Response to Type I Interferon
Negative regulation of Type I interferon Production

Table 4.8. MCODE Cluster 3 gene ontology analysis

Negative Regulation of NF-KappaB Transcription Factor Activity
Positive Regulation of Extrinsic Apoptotic Signalling
Cytoplasmic Sequestering of Protein

Table 4.9. MCODE Cluster 4 gene ontology analysis

Nitric Oxide Biosynthetic processes
Positive Regulation of Nitric Oxide Biosynthetic Process
Regulation of Nitric Oxide Biosynthetic Process
Regulation of Acute Inflammatory Response
Positive Regulation of Smooth Muscle Cell Proliferation
Natural Killer Cell Activation
Localization Within Membrane

The functional analysis performed using the OpenArray qPCR data as a template broadly agreed with the analysis performed on the Affymetrix miRNA microarray in that immunomodulatory processes are targeted for interference, albeit with a different set of miRNAs as input. This is not surprising given the functional crossover of many miRNAs. However, this analysis did yield some contradictory data as well, as seen in Cluster 6 (Figure 4.11.) and Table 4.10. The functions highlighted in this analysis indicate that any immune cells able to absorb PCa exomiRs would experience disinhibition of proliferative pathways.

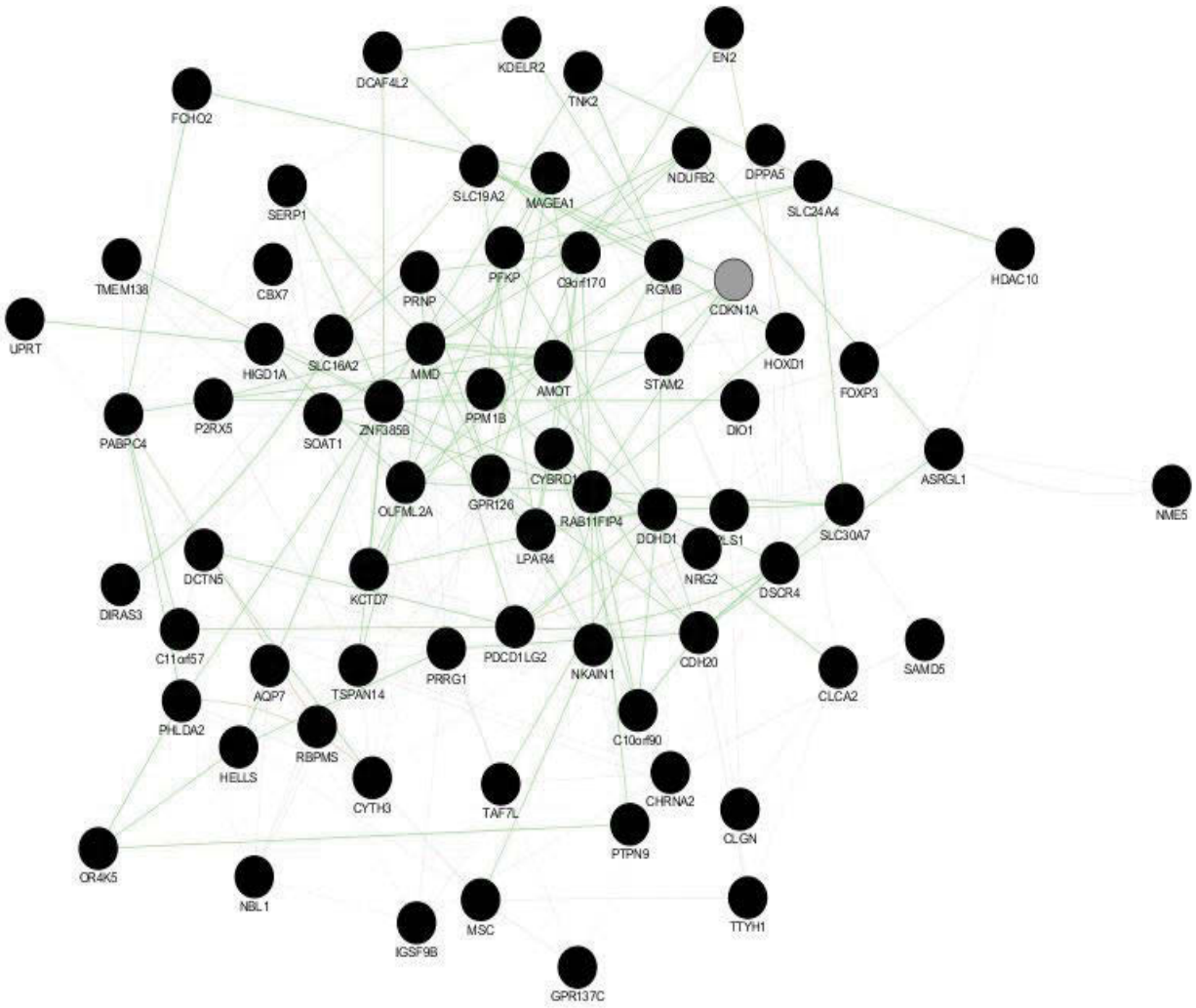

Figure 4.11. MCODE PU vs HU Cluster 6, target genes of exomiRs found to be highly Enriched in PCa patient urine compared to normal patient urine.

Interaction hub taken from a larger network of genes using the MCODE algorithm. The top ten miRNAs most highly enriched in PCa exosomes were merged with their most likely target genes using TargetScan 5.2. The top 100 target genes of each exomiR were then selected using the context score. This large list (approximately 900 potential target genes) was then interrogated for interactions using GENEMania, a Cytoscape plugin. Black nodes represent genes that are known or predicted targets of exomiRs enriched in PCa exosomes. Grey nodes are genes known to interact heavily with genes in the black nodes and were selected for inclusion in the network using the GeneMANIA plugin. PU vs HU indicates that the proteins in this network are targets of exomiRs enriched in PCa urine (PU) compared to healthy urine (HU). There are a total of 72 nodes (proteins likely to be down-regulated by the absorption of exomiRs secreted by androgen independent PCa) in the network. There are 243 edges (lines between the nodes that represent protein-protein interactions) amongst these genes.

Table 4.10. MCODE Cluster 6 gene ontology analysis

Negative Regulation of T Cell Proliferation
Negative Regulation of T Cell Activation
Negative Regulation of Leukocyte Proliferation
Negative Regulation of Mononuclear Cell Proliferation
Negative Regulation of Lymphocyte Proliferation

4.3. Discussion

4.3.1. An optimised ultrafiltration protocol for the isolation of urinary exosomes and their RNA

Even though our earlier Urine exosome isolation method was effective (see section 3.3.1.), it required further optimisation to reliably obtain RNA yields suitable for qPCR, a fundamental aspect of a reliable diagnostic test system. Our own method differed from that popularised by Cheruvanky et al (196) and Chanavajjhalaa et al (197) in several important respects. Firstly, DTT was not used to detect CD9, TSG101 and AGO2 in their native state on the surface of the exosome, in order to validate our technique. Unfortunately, this meant that a substantially larger amount of Urine (135 mL) was required to isolate a suitable amount of exosomes because so many exosomes are lost due to interference by Tamm-Horstfall protein (228). The large Urine volume requirement did not prove to be a barrier as the Urine collection process occurred over 2 or more days allowing ample time to collect sufficient amounts.

Given the larger amounts of Urine used in our experimental protocol, it was also necessary to pool retentates. The retentates were then subjected to a short ultracentrifugation to remove any remaining contaminants and to make RNA isolation easier by beginning the extraction from the solid pellet instead of a liquid retentate sample as was done previously. The exosomal markers shown in Figure 4.1 leave no doubt that the particles isolated by our method are positive for the expected markers, and there is no contamination with free-floating AGO2. The nanosight data also confirm that all particles are within accepted size parameters and contain a reasonably high number of particles.

The need for ultracentrifugation however may be a complicating factor if our technique were to be used in a pathology laboratory scenario. This is not a very common piece of equipment and is not a very high throughput instrument either. For these reasons, further development of this technique should include a simpler clean up step in place of the ultracentrifugation. As discussed in the previous chapter, there exists a wealth of techniques available for exosome isolation from bodily fluids. A very promising avenue is the recent emergence of a lectin based agglutination method proposed by Samsonov et al (124). In brief, this technique involves an initial spin at 20 000 x g for 45 minutes at 4^0C to remove cell debris and non-exosomal particles. Then Concanavalin A is added and incubated at 4^0C overnight, followed by a centrifugation at 20 000 x g for 90 minutes at 4^0C. This produces a THP free exosome sample (229) that yields exosomal RNA suitable for qPCR, without the use of an ultracentrifuge. However, this method is likely slower than our ultrafiltration method thanks to the overnight incubation, but higher throughput thanks to the use of lower speed centrifugations. It may prove to be a useful adjunct technique post ultrafiltration to precipitate exosomes without ultracentrifugation.

4.3.2. Low Sample Input Openarray facilitated the discovery of a new PCa exomiR profile derived from Urine

After the realisation that our exomiR isolation method gives only miniscule amounts of RNA (see Table 4.4), a new method was required to amplify cDNA samples in order to compensate for the low sample input. We applied the Low Sample Input (LSI) method from Applied Biosystems to meet this requirement. Using this method we were able to confirm that inputs as low as 1 ng of total exosomal RNA were enough to amplify and detect exomiRs in standard qPCR (Figure 4.5.). Importantly, the LSI method produced cDNA that was free from genomic or other contamination which is always a concern when a pre-amplfication step is involved (Figure 4.5.).

Having confirmed the suitability of the LSI method as an exomiR amplification technique (Figure 4.5.), miRNA profiling was performed using the Applied Biosystems Openarray human miRNA panel. This panel consisted of 754 mature human miRNA sequences, from which we expected a detection rate of about 62% (227). Once the data was obtained, it was normalised using global normalisation as this is the most suitable method for normalising very large data sets such as this one (230). The data were then compared to find differential expression under two conditions, **i)** PU vs HU; to identify exomiRs that are enriched in patient urinary exosomes compared to healthy urinary exosomes and **ii)** PU vs PxU; to identify exomiRs that decrease in response to removal of the prostatic tumour. The first analysis identified 22 exomiRs that were enriched in patient urinary exosomes, and this enrichment was statistically significant ($P<0.05$, Figure 4.6.). Unfortunately, there was no cross-over between this panel and the panel previously identified using cell-culture exosomes which casts further doubt on the suitability of using cell culture exosome samples to identify potential biomarkers.

The most important results obtained from this experiment however came from looking at the PU vs PxU comparison (Figure 4.7.). This shows that most exomiR levels decreased in patient urine once the prostate tumour is removed. Most importantly, miR-375, miR-20b, miR-149 and miR-106a were all initially enriched in PCa urine exomiRs, but their expression levels decreased sharply after radical prostatectomy. This suggests that these exomiRs are highly secreted by PCa cells, and given the decrease in expression post-RP, they may even be useful tumour response markers or prognostic indicators. MiR-375 shows particular promise in this area given its association with exosomes isolated from metastatic PCa patients (126, 127).

The next step in using this newly identified PCa exomiRs profile is validation. To validate the diagnostic potential of this profile, a very large number of patients will need to be recruited for future studies to increase the statistical power of the data set. For example to achieve the approximately 70% sensitivity reported by Wolf et al (6), assuming the 80% prevalence rate in men 70 years and over (9), 976 men of this age group would be required according to guidelines published by Karimollah Hajian-Tilaki (231). Furthermore, this patient group will have to be tracked during the course of their progression in order to find the prognostic/treatment-response marker potential as well.

4.3.3 Potential role in regulating gene expression for enriched PCa exomiRs discovered in urine

The functional analysis performed on the target genes of the top 10 enriched PCa patient exomiRs revealed a propensity for immune evasion related processes. These processes mainly involved the Type I interferon pathway, NF-KappaB signalling, the Nitric oxide pathway and NK cell activation.

It has been known for some time that the Type I interferon pathway is fundamental to host initiated anticancer responses (232), and it has been suggested that type I interferons are effectors in an immunosurveillance network imposed on developing tumour cells by the immune system (233). This immunosurveillance consists of three phases. **Phase 1:** malignant cells are eliminated as they emerge by the immune system, **Phase 2:** equilibrium is established between emerging malignant cells and the immune system. **Phase 3:** low immunogenic variants of malignant cells escape destruction by the immune system and initiate tumour formation. Together these phases are termed cancer immunoediting (234), and type I interferons are known to intervene at each phase (235-237). Therefore, any uptake of PCa exomiRs by cells of the immune system is likely to result in a decreased ability to remove or control malignant cell growth by the immune system.

The potential target cells for these PCa exosomes are many. Obviously they include cells of the immune system such as conventional and Plasmacytoid DC's which are known to secrete large quantities of type I interferons in response to viral infections (238, 239). More specifically, tumour infiltrating CD11c+ DCs have been shown to produce type I interferons in response to tumour derived DNA (240). PCa exosomes may also interact downstream with cytotoxic T lymphocytes (CTLs) and NK cells, as a loss of type I interferons may result in a decreased expression of perforin 1 and granzyme B (241), cytotoxic proteins required for anticancer cytotoxicity. Furthermore, a decrease of type I interferons may also foster conditions in which NK cells actually attack and destroy CTLs that are mounting a specific response against tumour cells, as type I interferons are known to reduce the amount of NK cell activator molecules presented on the surface of the CTL (242, 243). Macrophage function could also be inhibited by a decrease in type I interferon expression, as they are responsible for stimulating the release of the pro-inflammatory IL-18 and IL-1b (244).

Disinhibition of the NF-KappaB pathway may also aid in cancer cell survival (see (245) for review). This hypothesis however revolves around the idea that PCa exosomes secreted in to the tumour microenvironment are re-absrobed by PCa cells in times of crisis. There is some precedent for this as it has been shown that HeLa cells access Survivin, an anti-apoptotic protein, on the surface of exosomes secreted by the HeLa cells themselves (246, 247). Survivin has since been suggested to operate in a similar manner in PCa as well, given that Survivin is significantly more expressed on the surface of exosomes isolated from PCa patients compared to healthy controls (248). If negative regulators of NF-KappaB such as BRMS1L (249), DAP and FOXJ1 (250) (the exomiR targets that contribute to this ontology) can be suppressed as needed by PCa cells via exosomal re-uptake, this may help explain the resistance of PCa to apoptosis.

The Nitric Oxide (NO) pathways named in Table 4.9. offer a further enticing explanation of how PCa cells may avoid death signals from their surroundings and enhance their own survival. For example, it is well known that low NO levels are associated with angiogenesis and tumour proliferation, while higher levels are associated with the formation of peroxynitrite which induces apoptosis of tumour cells (251). It is possible that PCa exosomes are taken up by immune cells within the tumour and surrounding tissue which results in decreased NO production by these cells thanks to the suppressive actions of the PCa exomiRs. This would then lead to lower levels of NO that are more conducive to angiogenesis and tumour proliferation.

Although the evidence here is interesting, it is still incomplete without performing actual *in vitro* or *in vivo* experiments for confirmation. Furthermore, the bioinformatics data presented here does not contain gene ontologies that were relevant to the tissue and cell types of interest, and occasionally even produced contradictory evidence such as that seen in cluster 6 (Figure 4.11.). Therefore, to test the applicability of the cancer biomarkers detected so far in actual PCa related processes, a set of exomiRs was identified with potential roles in tumour stroma formation. This data is presented in the next chapter.

Chapter 5 abstract:

The data available from the first round of microarrays revealed several highly Enriched microRNAs with known or potential roles in fibroblast differentiation, an important process in prostate tumour progression. Firstly, we isolated highly pure exosomes from the very aggressive DU145 prostate cancer cell line using gradient density ultracentrifugation. It was confirmed by Nanosight and DELFIA assay that pure exosomes were isolated, and RNA was isolated from the exosomal samples. Using qPCR, it was shown that the microRNAs of interest were abundant in these exosomes. Primary fibroblast cells were then differentiated over 72 hours using either DU145 exosomes or soluble TGFB. The hypothesis being tested was that DU145 exosomes would carry their unique cargo of exomiRs to fibroblast cells, detectably increasing the levels of these exomiRs in the recipient cells. The exomiRs would then lead to down-regulation of target genes in the recipient cells that would aid in fibroblast to myofibroblast transdifferentiation. Although the cells differentiated into myofibroblast as expected, it seems that exosomal microRNA does not contribute to this process, given that none of the exomiRs became enriched in response to exosome treatment.

5.1. Methods

5.1.1. Integra bioreactor setup and maintenance

Standard tissue culture techniques provided only minimal amounts exosomes and their RNA. This was not suitable for functional experiments or several other types of qualitative analyses presented in this thesis. However, the Integra bioreactor system is able to concentrate exosomes secreted from a very large cell population, and massively increase the Exosomal yield.

To setup an Integra bioreactor flask, the desired cell population must first be expanded using standard tissue culture techniques up to between 2.5 x 10^7 and 3.0 x 10^7 cells. The cells also had to be harvested during their exponential growth phase. To meet these requirements, cells were passaged into 5x T175 flasks and allowed to reach approximately 70% confluency before they were harvested using TrypLE reagent (Life Technologies). Next, the cells were pooled from each flask and centrifuged at 1000 rpm for 5 minutes at RT. The supernatant was drained off and the cells were resuspended in 15 mL of exosome depleted media. Once resuspended, this suspension was drawn into a 20 mL syringe (Terumo Corporation, Tokyo, Japan) using a drawing up needle (Terumo). The cells were then pushed into the cell chamber of the bioreactor flask via the injection port. 250 mL of full media was then added into the main chamber. All bubbles were then removed from the cell chamber using a drawing up needle via the injection port. With all bubbles removed, a further 250 mL of full media was added to the main chamber. The bioreactor flask was then stored in an incubator at 37^0C and 5% CO_2. After 2 weeks, the cells are fully established and the media must be regularly changed after this time. To change the media, firstly the full media in the main chamber was removed by decanting. Then, the supernatant was removed from the cell chamber using a 20 mL syringe and drawing up needle. This supernatant was highly enriched with exosomes, other particles and cell debris and was stored briefly at 4^0C until ready to be processed.

The cell chamber was then washed thoroughly to remove dead cells and cell debris. This involved injecting 10 mL of media containing only 5% pen/strep and rocking the flask back and forth. This process is repeated 3 times before adding 15 mL of media (RPMI, 5% v/v exosome depleted foetal calf serum, 5% v/v penicillin/streptomycin/glutamine) into the cell chamber and 500 mL of media (RPMI, 5% v/v foetal calf serum, 5% v/v penicillin/streptomycin/glutamine) to the main chamber. Once again, all bubbles were removed from the cell chamber and the flask was returned to the incubator until the next week when the media had to be changed again. Cell populations were maintained in this manner for no more than 6 months. A schematic view of the Integra bioreactor flask is shown in Figure 5.1.

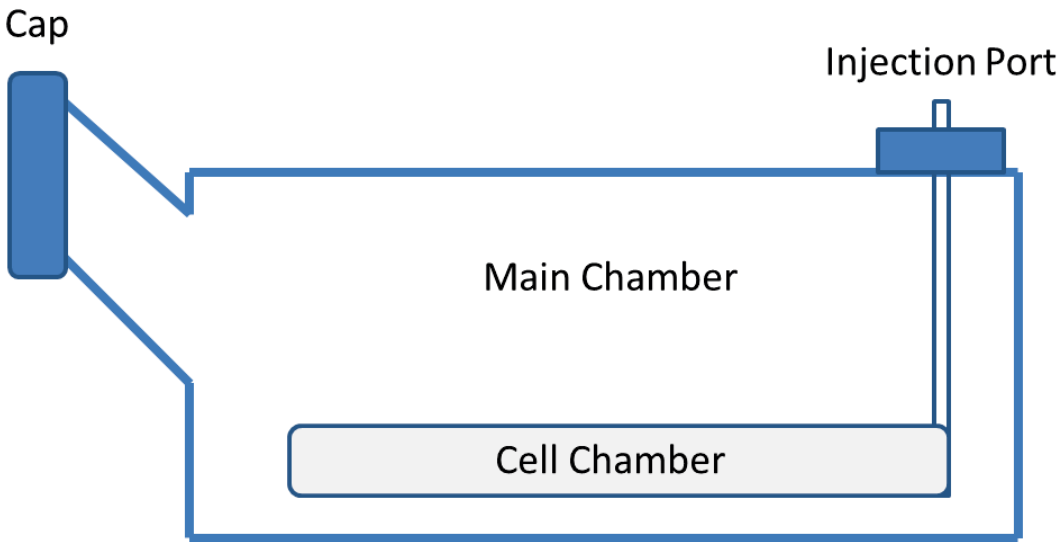

Figure 5.1. Schematic view of Integra bioreactor flask.

The initial cell population is seeded into the cell chamber via syringe in 15 mL media containing exosome-depleted FCS. The main chamber is then filled with 500 mL of media containing regular FCS. Once the cell population is established on the membrane held within the cell chamber (approximately 2 weeks), the media is changed in the cell chamber via the injection port, and the main chamber by decanting the old media out and pouring fresh new media in. After this time, the media is changed weekly in both chambers. Any media recovered from the cell chamber is enriched with exosomes secreted by the cell population. This media is stored at -80^{0}C until ready for further processing.

5.1.2. Processing of Integra supernatants

Once the supernatant was recovered from the Integra bioreactor, they were centrifuged at 1000 rpm for 5 minutes at 4^0C. The supernatant was transferred to a new tube and the pellet was discarded. The supernatant was then spun at 2000 x g for 15 minutes at 4^0C. The supernatant was transferred to a syringe fitted with a 200 µm PES filter membrane and the supernatant was filtered. This filtered supernatant was then stored at -80^0C until ready for use.

5.1.3. Gradient ultracentrifugation

Prior to putting a sample of exosomes onto a sucrose gradient, the exosome sample had to first be precipitated from its original fluid (culture supernatant, urine, plasma etc.). This was done by centrifuging the original sample at 100 00 x g for 1 -3 hours at 4^0C. Once finished, the supernatant was poured off or drawn out with a pipette. The pellet was then resuspended in 300 µL of 1x DPBS and stored at 4^0C until ready for use.

To prepare the gradient, 2 different sucrose solutions were prepared in sterile dH_2O. The first sucrose solution was prepared at 0.19M (the light solution) and the other at 2.5M (the heavy solution). At this point a gradient maker was employed to make the sucrose gradient. The gradient maker was stood atop a magnetic stirring apparatus and a small magnetic flea was added to each well of the gradient maker. 2.5 mL of the light solution was then added to the well nearest the output port on the gradient maker, while 2.5 mL of the heavy solution was added to the well furthest from the output port. A spinal needle (Beckton Dickinson, Franklin Lakes, NJ, USA) was then attached to the output port and bent so that it touched the bottom of the gradient ultracentrifuge tube (Beckman Coulter inc., Pasadena, CA, USA). The magnetic stirrer was activated and both taps on the gradient maker were opened simultaneously. The tube was allowed to fill until a small amount of fluid remained in both wells. Both taps were closed at the same time and the gradient maker was gently lifted away from the ultracentrifuge tube. It was crucial not to disturb the ultracentrifuge tube from this point, as any disturbance would spoil the gradient.

Once the gradient was poured, the 300 µL sample of exosomal material was then layered on top of the gradient very gently using a pipette. The tubes were then transferred to an MLS-50 (Beckman Coulter Inc.) swing out rotor. A speed ramping protocol was employed which would ramp up to 210 000 x g and hold at this speed for a total of 14 hours The rotor was then allowed to coast to stop . Once the protocol was finished, the tubes were carefully removed to avoid disturbing the gradient. 16x 300 µL fractions were taken from each tube and stored at 4^0C until ready for further analysis.

5.1.4. Density determination

Exosomes are known to float between 1.1 and 1.2 g/mL density in a sucrose gradient. To determine this, a refractometer was used to measure the refractive index (RI) of each fraction. Afterwards, the RI could be used to calculate the density of each fraction and the exosome rich fractions could be inferred from this data.

Operation of the refractometer (J577WR-SV, Rudolph Research) was performed as follows: 200 µL of the first (and least concentrated) fraction was loaded onto the refractometer lens and the lens chamber was closed. The reading was taken and recorded and the sample was pipetted back into the sample tube. The lens was washed three times with dH_2O and the next sample was read. This process continued until RI values were obtained for all fractions. The calculation, $y = -0.592x^2 + 4.2944x - 3.6748$ was used to convert RI (x) to density. The exosomes are now ready to be purified by a second round of ultracentrifugation.

5.1.5. Obtaining pure exosomes from sucrose gradient fractions

At this point in the process, there are pure exosomes in several fractions, which are still full of sucrose. To remove the sucrose, all fractions were subjected to a second round of ultracentrifugation. All 300 µL fractions were transferred to fresh 1.8 mL ultracentrifuge tubes (Beckman Coulter Inc.) which were topped up with 1x DPBS. These tubes were then centrifuged in a Beckman TLA110 rotor at 100 000 x g for 1 hour at 4^0C. The supernatant was then removed using a syringe and 21G needle (Terumo Corporation). All pellets were resuspended in 300 µL of 1x DPBS and stored at 4^0C until ready for use.

5.1.6. Obtaining pure exosomes using sucrose cushion isolation

For experiments that required large amounts of functionally intact exosomes, this method was chosen as per previous work published by the Clayton lab (252) based on a procedure originally designed by Lamparski et al (253). The protocol itself begins with the isolation of a crude exosome sample from an Integra bioreactor supernatant. This is done simply by ultracentrifugation at 100 000 x g for 1 hour at 4^0C, then resuspending the pellet in 20 mL of 1x DPBS and added to a fresh Beckman SW28 ultracentrifuge tube. Next, the sucrose cushion is prepared to the following specifications: 20 mM Tris, 30% sucrose in D_2O (Sigma-Aldrich). 4 mL of sucrose cushion solution is then poured into the bottom of the SW28 ultracentrifuge tube using a spinal needle (Beckton-Dickinson). The sample is then ultracentrifuged at 100 000 x g for 75 mins at 4^0C. The bottom 4 mL of of the tube was collected via syringe after this ultracentrifugation. The sample was diluted to fill another ultracentrifuge tube with 1x DPBS and again ultracentrifuged at 100 000 x g for 1 hour at 4^0C. The pellet was then resuspended in the desired volume of 1x DPBS.

5.1.7. Accurate exosomal RNA quantification using the Agilent Bioanalyzer Pico detection kit

This was performed as described in section 4.1.3.

5.1.8. Quantitative Real Time Polymerase Chain Reaction (qPCR) Methods

This was performed as described as in section 2.1.6 but with some differences in volume. These differences can be found in Table 5.1. All Taqman probes used in this chapter are detailed in Table 5.2.

Table 5.1. Standard method used for 1x qPCR reaction

Reagent	Volume (µL)
Taqman master mix (2x)	5
Taqman probe	0.5
cDNA	2
dH_2O	2.5
Total	10

Table 5.2. Taqman primers/probes used for qPCR

Taqman Primer/Probe Name	Assay ID
miR-125b	000449
miR-92b*	002343
Let-7i	002221
miR-22	000398
miR-25	000403
miR-106b	002380
SMAD2	Hs00998187_m1
SMAD7	Hs00998193_m1
MEF2D	Hs00954735_m1
MECP2	Hs04187588_m1

All other steps were performed in accordance with the manufacturers protocol (139). Each gene expression assay was performed in triplicate, and the average Ct was calculated from the three Ct values. Next, the delta Ct (ΔCt) value was calculated which is a measure of the difference in expression levels between the gene of interest (GOI) and the endogenous control (EC). Once the ΔCt was calculated, the ΔΔCt was calculated which measures the difference in expression levels between two cell types/experimental conditions. In this experiment, the difference measured was between the GOI in PCa exosomes versus the same GOI in PNT2 (normal prostate exosomes). The formula used to calculate the ΔΔCt was: ΔCt(PCa exosomes) – ΔCt (PNT2 exosomes). Fold-changes were then calculated between PCa exosomes and PNT2 exosomes using the formula $2^{-\Delta\Delta Ct}$.

However, for some experiments presented in this chapter, neither a ΔCt or ΔΔCt was necessary. This is because these experiments were qualitative only, looking for the detection or lack thereof of certain exomiRs. For these experiments, the Level Above Detection Threshold (LAD) was calculated. The threshold for the positive detection of an exomiR of interest was set at Ct 35, with any amplification after this point being considered unreliable/artefactual. Hence, to determine the LAD, the following formula was used: LAD = Ct(exomiR of interest) – 35.

5.1.9. DELFIA Europium assay to detect canonical exosomal marker

This was performed as described in section 3.2.2 using a Wallac Victor^2 1420 plate reader (Perkin Elmer) instead of the Tecan m100. The antibodies used in this chapter can be found in table 5.3.

Table 5.3. Antibodies Used.

Antibody	Primary or Secondary	Catalog No.	Dilution Used
Rabbit monoclonal [EPR2949] to CD9	Primary	ab92726	1:1000
Goat anti-rabbit H&L (biotin)	Secondary	ab97049	1:5000

5.1.10. Nanosight methodology for exosome sample quality control.

This was performed as described in section 3.2.3.

5.1.11. Inducing fibroblast to myofibroblast transdifferentiation through exposure to DU145 exosomes and soluble TGFβ

In order to identify the role of DU145 exomiRs on myofibroblast transdifferentiation, primary fibroblasts (AG2262, Coriell Cell bank) needed to be transdifferentiated into myofibroblasts in line with previous experiments performed in the Clayton lab where this research took place (252). Firstly, the cells were allowed to grow to 70 – 80% confluency in cell culture media containing 10% exosome depleted FCS. The cells were then growth arrested for 72 hours by growing them in serum free media. The fibroblasts were then treated with either **i)** 10 µg of soluble TGFβ, **ii)** DU145 exosomes (normalised to 10 µg total protein by microBCA assay, Thermo-Fisher Scientific) isolated using the Sucrose cushion method (section 5.1.5.) **iii)** no treatment. The cells and their culture media were harvested at 8, 27 and 72 hours. The culture media was used to perform the HGF assay, and the cells were lysed in RNAzol RT at 8, 27 and 72 hours after exosome exposure. RNA was isolated and normalised to 100 ng/µL prior to reverse transcription. miR-106b, let-7i, miR-125b, miR-22 and miR-25 primers were used for this reverse transcription to test the hypothesis that exposure to exosomes would increase the levels of these exomiRs in the recipient cells. Each miRNA is also known to be highly expressed in PCa exosomes (see appendix Table 2) and are potentially involved in Epithelial to Mesenchymal transition (EMT). MiR-92b* was used as the endogenous control as per previous chapters. Several target genes of these exomiRs were also reverse transcribed from the transdifferentiated myofibroblast RNA as they are known or suspected to be involved in this process. These target genes are MECP2, MEF2D, SMAD2 and SMAD7.

5.1.12. Immunofluorescence analysis of α-SMA expression to confirm fibroblast to myofibroblast transdifferentiation

After growth arrested fibroblast cells were incubated with DU145 exosomes for the required amount of time (8 hrs, 27 hours and 72 hours), they were subjected to fixation in ice-cold acetone:methanol mixed in a 1:1 v/v ratio. The cells were left covered in this solution for 20 minutes at -20^{0}C. After fixation was complete, the cells were incubated in blocking agent (1x PBS, 5% normal goat serum, 0.3% Triton-X) for 60 minutes at room temperature. The blocking buffer was then discarded and the cells were washed three times with 1X PBS, and the primary antibody (mouse monoclonal α-SMA antibody, sc-130616, diluted to 1:500, Santa Cruz Biotechnology) was introduced and incubated overnight at 4^{0}C. This antibody was chosen as α-SMA is a canonical marker for myofibroblasts and was used in previous experiments in the Clayton lab (252). The following day, the primary antibody was washed off over three rinses with 1x PBS and the secondary antibody was applied (goat anti-mouse antibody conjugated to Alexa-488, A32723, diluted 1:500) and incubated for 1 hour at room temperature. Cells were then visualised using a light microscope at 200x magnification and photographed using the attached Canon PowerShot G6 (exposure time = 0.6 sec).

5.1.13. HGF secretion assay to identify different myofibroblast phenotypes using DuoSet ELISA Development system

After transdifferentiation was complete (72 hours after initial exposure), the culture media was harvested from the cells prior to cell fixation for immunofluorescence. The culture media was then assayed for the amount of HGF secretion using the DuoSet ELISA Development System according to the manufacturer's protocol (254).

5.2. Results

5.2.1. Isolation of pure PCa exosomes containing microRNAs of interest from sucrose gradient fractions

In order to prove that exosome samples contained our microRNAs of interest, pure exosome samples had to be obtained and probed for miRNAs of interest using qPCR. The first step in obtaining pure exosome samples was to find which fractions that contained exosomes after gradient density ultracentrifugation was complete. Once the density of each fraction was acquired using refractometry and the exosomes were separated from their sucrose solution, they were analysed using the Nanosight. In parallel to this, the remainders of each fraction were used to begin the DELFIA assay to identify canonical exosomal markers and isolate RNA.

Particle size was fairly consistent across all fractions and each particle size recorded was within acceptable size limits to be considered exosomes. Particle count, CD9 expression levels and RNA yields all peak between fractions 10 and 12, indicating the presence of pure exosomes. This analysis was performed on three biological replicates and representative data can be found in Figure 5.2.

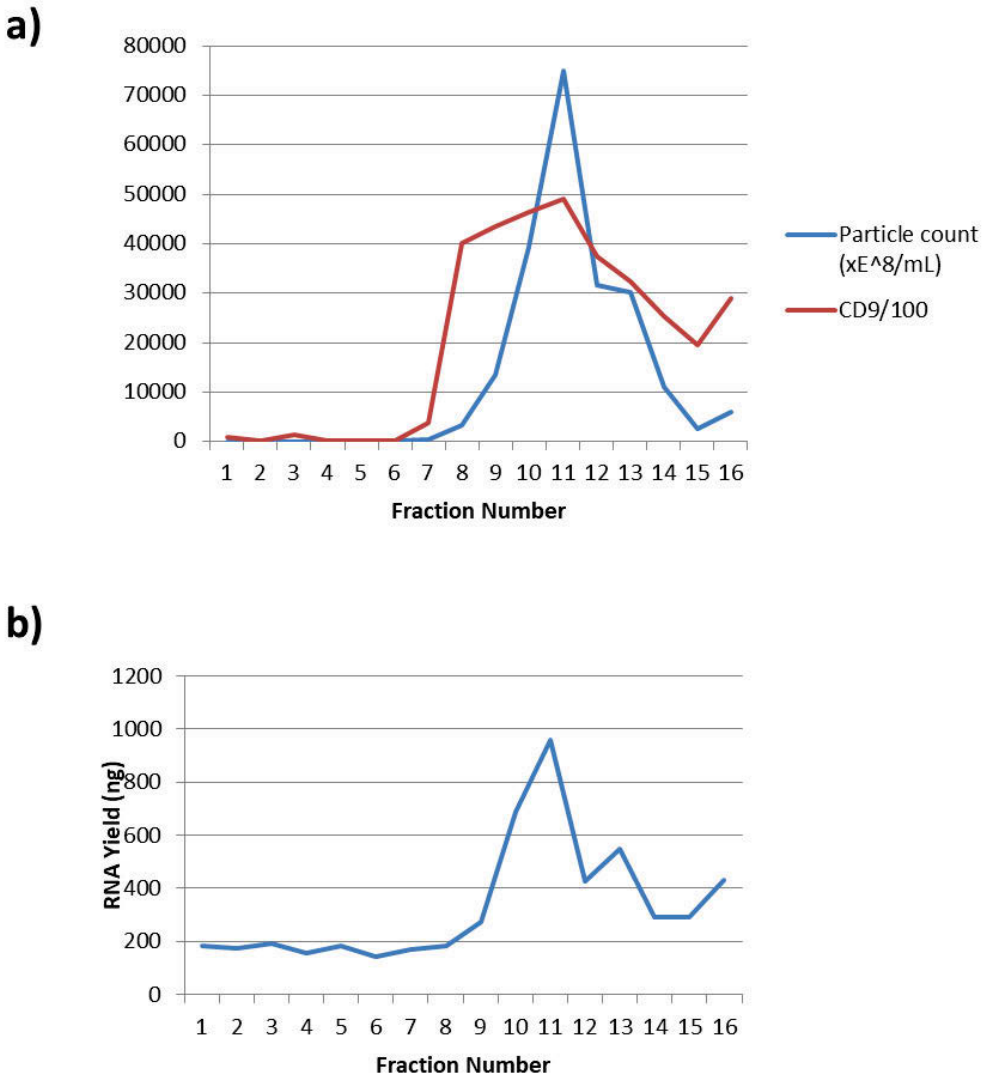

Figure 5.2. Identifying exosome rich sucrose gradient fractions using particle count, CD9 expression and RNA yield assessment.

Representative data from Qualitative analysis of exosome fractions acquired from gradient density ultracentrifugation. Exosomes were isolated from DU145 cells grown in Integra bioreactor flasks. Culture supernatants were first centrifuged at 100 000 x g for 1 hour at 4^0C to isolate a crude pellet. This pellet was then resuspended in 200 µL of DPBS and layered on to a sucrose gradient. Gradient ultracentrifugation was performed at 200 000 x g for 16 hours at 4^0C. 16 fractions were then taken from the gradient and density was calculated by determining the refractive index. Each fraction was then subjected to a second ultracentrifugation at 100 000 x g for 1 hour at 4^0C and the resulting pellets were resuspended in 200 µL of DPBS. Particles were then enumerated and qualitatively assessed using the Nanosight, and DELFIA europium assays were performed on each fraction looking at CD9. The values reported on the graph are CD9 counts /100 as the raw CD9 counts were too high to fit on the graph. RNA was also isolated from each fraction using RNAzol RT and RNA concentration was assessed using a Thermo-fisher Nanodrop. **a)** Particle count and CD9 concentration in each fraction. **b)** RNA yields isolated from each fraction.

qPCR reactions were then performed using 100 ng of total RNA as a template from each fraction. The two probes selected for use were miR-92b* given its excellent performance as an endogenous control for exosomal RNA (used in chapters 2,3 and 4) and let-7i given its association with PCa exosomes, DU145 in particular (222). Relative expression level was not calculated in this experiment. Instead, the level above detection threshold (LAD) was calculated using the formula: $LAD = 2^{(35-\Delta Ct)}$, to measure how high above the detection threshold of Ct 35 the signal was. Both of these exomiRs were expressed at their highest levels in fractions 10, 11 and 12. Importantly, each of these fractions were located between 1.1 and 1.2 g/mL, the density at which exosomes are known to settle in a gradient (137). These data are presented in Figure 5.3.

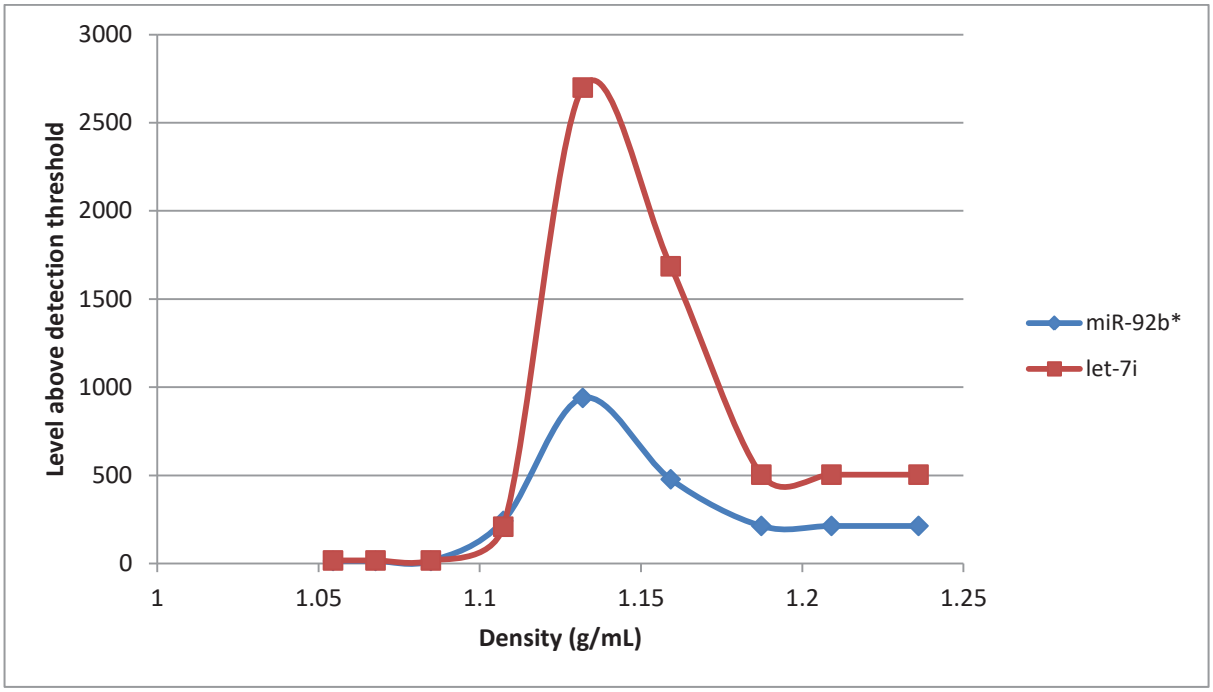

Figure 5.3. Identification of exomiRs in sucrose gradient fractions by qPCR.

MiRNA expression profile from fractions taken from gradient density ultracentrifugation of exosome sample. RNA extracted from density gradient ultracentrifugation was amplified using the Applied Biosystems high capacity reverse transciptase kit. miR-92b* and let-7i levels were then assessed by qPCR using Taqman reagents. The aim of this experiment was detection of miRNAs at different densities and no endogenous control was used to calculate relative expression levels. However, the fold above background was calculated by using the formula: LAD = Ct(exomiR of interest) – 35, as any result after Ct 35 was considered below detection threshold. Exosomes are known to settle out at densities between 1.1 and 1.2 g/mL of sucrose (137) and it is within this region that the greatest signal from miR-92b* and let-7i was recorded.

5.2.2 Fibroblast to Myofibroblast differentiation is induced by exposure to PCa exosomes

It was known that PCa exosomes can cause primary fibroblast cells to differentiate into Myofibroblast cells and that this process is dependent on exosomal TGFβ (252, 255, 256). However, inducing differentiation using soluble TGFβ as opposed to exosomal TGFβ does not produce an identical myofibroblast phenotype. For example, exosome differentiated myofibroblasts (EDMs) secrete large amounts of HGF while soluble TGFβ differentiated myofibroblasts (STDMs) secrete very little (Figure 5.4.). This is important because the HGF/c-met pathway is strongly implicated in regulating PCa progression and metastasis (257). Furthermore, the fact that a different and more complicated phenotype is observed in EDMs suggests that exosomal TGFβ is not solely responsible for this differentiation.

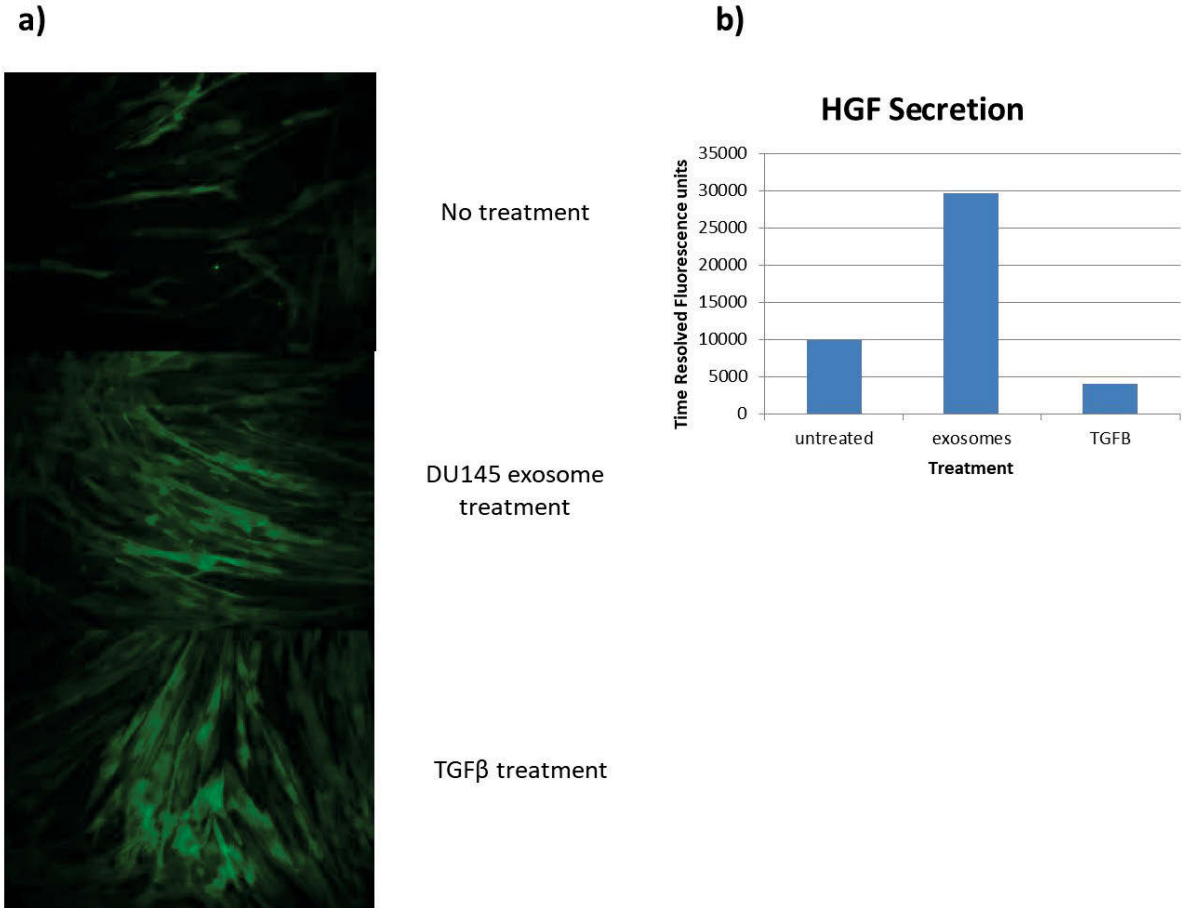

Figure 5.4. DU145 exosomes cause fibroblast to myofibroblast transdifferentiation and induce secretion of HGF from the myofibroblasts.

Primary fibroblasts were grown for 3 days, then subjected to growth arrest. DU145 Exosomes were then applied to these cells for 24 hours and α-SMA(252) levels were assessed using fluorescence microscopy. HGF levels were assessed in the culture supernatant by DELFIA Europium assay. **a)** Untreated cells show only background levels of α-SMA. Exosome treated and soluble TGFB treated cells show similarly elevated levels of α-SMA. **b)** Exosome treated cells secrete much higher levels of HGF than untreated cells. In fact, TGFB seems to slightly inhibit secretion of HGF. This experiment was performed on only once but is corroborated by evidence published by Clayton et al.

5.2.3. qPCR confirms that all functional exomiR candidates are detectable in DU145 exosomes

The first step in testing whether or not DU145 exomiRs play a role in producing the EDM phenotype was to ensure that all DU145 exomiRs of interest could be detected in DU145 exosomes (Figure 5.5.). This clearly showed that all exomiRs are expressed between sucrose gradient fractions 9, 10 and 11 as expected from previous experiments, and that this expression is at a high level with most exomiRs being detected 40 000 fold higher than background level, which was set at cycle 35. This was performed on one exosome sample.

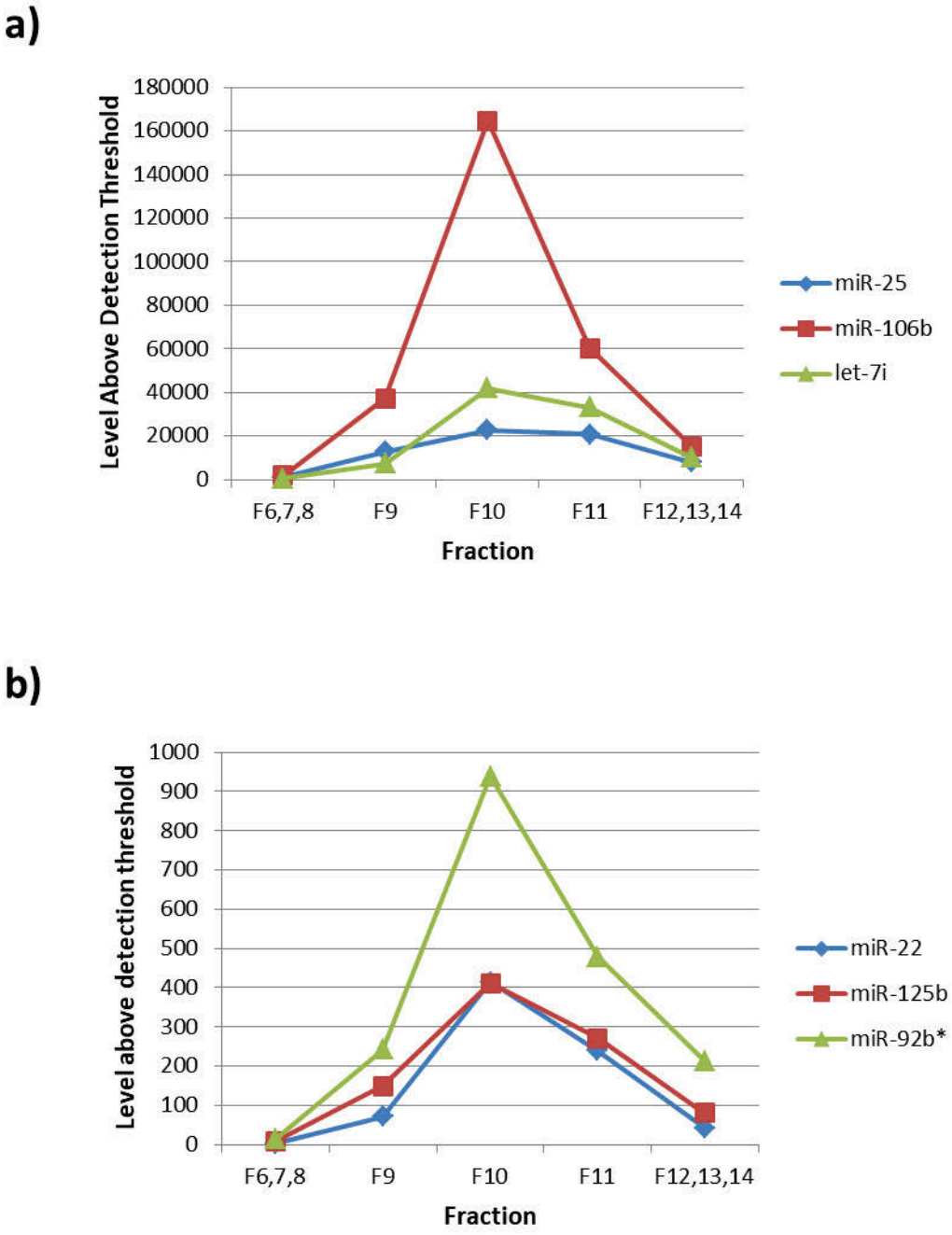

Figure 5.5. Detection of functional exomiR candidates in DU145 exosomes by qPCR.

Exosomes were isolated from Integra bioreactor culture supernatants and subjected to Sucrose gradient ultracentrifugation. Sucrose was washed off each fraction by ultracentrifugation and RNA was isolated from each sample. Fractions 1 to 5 contained no RNA, fractions 6,7 and 8 were pooled to reach an appropriate concentration for reverse transcription (100 ng total) as were fractions 12, 13 and 14. Fractions 9, 10 and 11 contained sufficient quantities of RNA already. All samples were normalised to 100 ng and subjected to reverse transcription followed by qPCR. Level above detection threshold (LAD) was calculated for each exomiR. All exomiRs were at their most concentrated in fractions 9, 10 and 11. **A)** LAD for the three most highly expressed DU145 exomiRs. **B)** LAD for the three lesser expressed DU145 exomiRs.

5.2.4. qPCR shows no variation in levels of exomiRs or potential target genes in response to DU145 exosome treatment

Exosomes were then added to the growth arrested primary fibroblasts for 8, 27 and 72 hours. At each time point, the cells were lysed with RNAzol RT and analysed for significantly increased levels of the functional exomiR candidates (> 2-fold increase after exosome treatment) as well as corresponding significant decreases in known or putative target genes (<-2 fold decrease after exosome treatment) which would indicate uptake of exomiRs and exomiR function respectively. Unfortunately, the microRNA levels did not change significantly relative to the control at any time point selected for this experiment, and none of the target gene levels changed significantly either (Figure 5.6.). This experiment had only one biological sample per time point.

a)

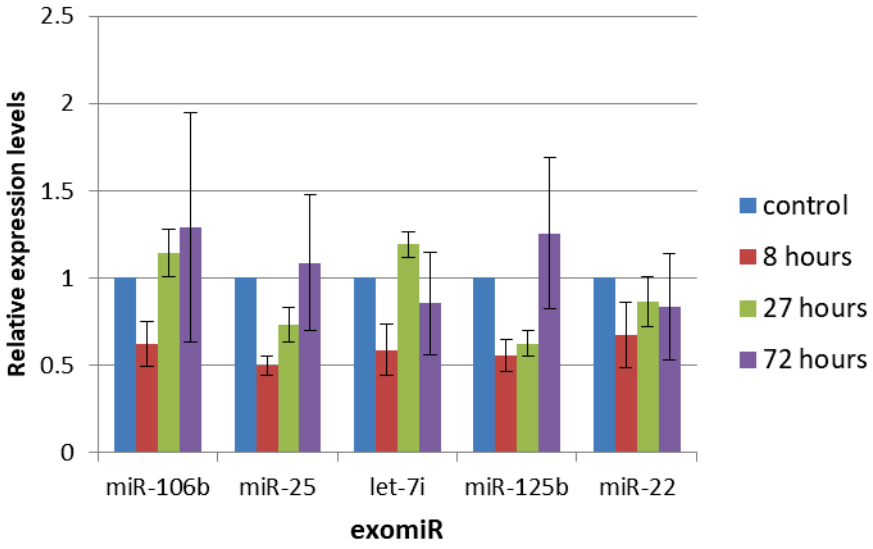

b)

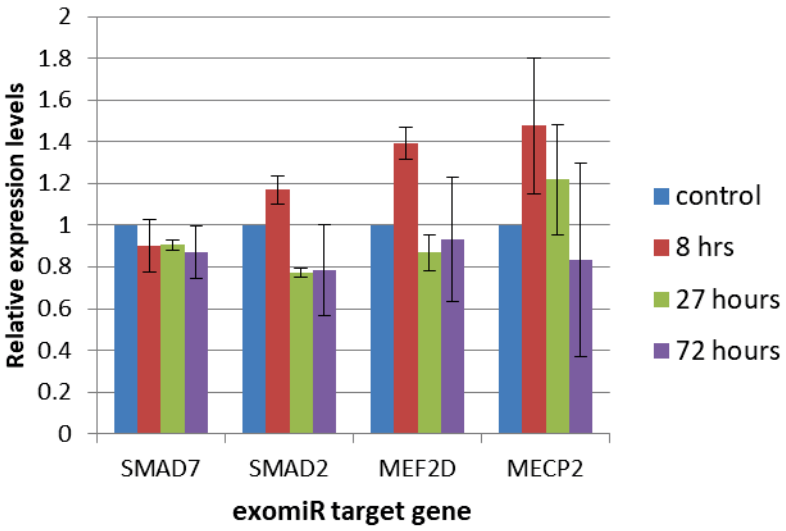

Figure 5.6. Expression levels of exomiRs and their target genes are not significantly changed during 72 hours of exposure to DU145 exosomes.

RNA samples were taken at 8, 27 and 72 hours post treatment and amplified using the Applied Biosystems high capacity reverse transcriptase kit. MiRNAs and their potential target genes were then assessed using relevant Taqman probes by qPCR. **A)** DU145 exomiRs do not become significantly enriched (>2-fold increase) in fibroblasts receiving DU145 exosomes. None of these exomiRs became significantly enriched in the fibroblasts at any point in the experiment, suggesting that they were not absorbed in significant quantities. **b)** ExomiR target genes are not down-regulated by exposure to DU145 exosomes. None of these genes were significantly down-regulated (<-2-fold decrease) at any point during the experiment.

5.3. Discussion

5.3.1. Exosomes initiate epithelial to mesenchymal transition in the tumour microenvironment which enhances metastatic potential

It is beyond doubt that cancer exosomes can profoundly effect the microenvironment surrounding the primary tumour, as well as prime distal sites for later metastasis (258). It is also important to note that exosomes have been implicated in tumour microenvironment modification across all 10 established and emerging hallmarks of cancer (18).

Apart from the immune system modulating effects discussed at length in previous chapters, it is also known that exosomes can activate a metastatic cascade in the tumour microenvironment beginning with epithelial to mesenchymal transition (EMT) (259, 260). EMT allows the tumour cells to invade surrounding tissue and intravasate into the circulation (261, 262). In the case of PCa, it is TGF-β on the exosome surface that is largely responsible for EMT (252, 255, 256). Reaching beyond the site of the primary tumour, cancer exosomes can also prime distant sites where metastatic deposits can later develop. Exosomes can facilitate this by altering elements of the extracellular matrix (ECM) in these pre-metastatic niches and enhance angiogenesis to support growing metastatic deposits (263-265).

This metastatic niche formation also offers an enticing explanation for the organ specificity of metastases. For example, B16-F10 melanoma cells were shown to be retained in the local lymph nodes of mice, while similarly sized liposomes diffused throughout the mouse. This is the exact pattern of organotropic metastasis expected for this type of cancer (266), which suggests that specific exosomal surface molecules were responsible for this affinity (264). It is currently thought that several adhesion and ECM related proteins are responsible for this pre-metastatic niche formation, including Integrins $\alpha_6\beta_1$, $\alpha_6\beta_4$ and $\alpha_V\beta_5$ (267), Wnt-PCP signalling proteins (268) and tetraspanins CD151 and Tspan8 (269).

To begin exploring the potential role of exomiRs in altering tumour microenvironment, several exomiRs were selected from our previous analyses with relevance to Myofibroblast formation, a crucial part of EMT. The selected exomiRs are outlined in section 5.3.2.

5.3.2. Selection of exomiRs and target mRNA candidates with potential roles in fibroblast to myofibroblast transdifferentiation

Target exomiRs were selected based on existing literature that placed them in the EMT pathway, or gave them some type of relevance to Myofibroblast specific gene expression. These processes became the focus because of the well documented role of myofibroblasts in EMT, and the importance of EMT in cancer progression (270). The first exomiRs selected were miR-106b and miR-25 as they are transcribed from the same cluster. MiR-106b in particular was very highly expressed, being 160 000 times higher than background levels in DU145 exosomes. These miRNAs have several associations with EMT, and the role of this miRNA varies considerably depending on cellular context. For example, In breast cancer cells the miR-106b-25 cluster targets SMAD7, activates the TGFβ signalling pathway and induces EMT (271). MiR-106b is also associated with a high breast cancer recurrence risk (272) and it enhances the invasiveness and cell migration in H1299 NSCLC cells and may enhance the metastatic potential of lung cancer (273). However, miR-106b can also inhibit EMT as was the case when looking at Human kidney tubular epithelial cells (HK-2). These cells actually reduced their expression of α-SMA when miR-106b was induced by salvianolic acid (274). Therefore, we hypothesise that the more likely scenario for miR-106b as an exomiR is to target SMAD7 and enhance the fibroblast response to the TGFβ found on the exosomal surface.

MiR-25 also targets MEF2D, with 2 highly conserved 8-mer binding sites for this miRNA in the 3'UTR of this gene (275). MEF2D was selected as a potential target of interest because of its known role in hepatocellular carcinoma (276, 277) and colorectal carcinoma (278) as a supporting agent of EMT. This feature is in opposition to the previous hypothesis as a knockdown of MEF2D by exosomal miR-25 could potentially decrease the fibroblasts ability to undergo transdifferentiation. MEF2D was included to ensure that PCa exomiRs do not inhibit the Myofibroblast transdifferentiation process by targeting this gene.

miR-22 was chosen for its role in triggering EMT (279). MiR-22 also has a negative correlation with E-cadherin and a positive correlation with Vimentin in hepatocellular carcinoma (280). This pattern of gene expression matches that found in myofibroblasts (281, 282). However, MECP2 contains a miR-22 and miR-106b binding site in it's 3'UTR (275). This is important because MECP2 is an important gene in the myofibroblast transdifferentiation pathway during fibrosis (283, 284). This was another area which could potentially inhibit Myofibroblast transdifferentiation so levels of this gene were assessed throughout the experiment.

MiR-125b was chosen for its known role in fibroblast to Myofibroblast transition in cardiac fibrosis (285). However, in cancer cells themselves, it seems that this miRNA is actually antagonistic towards EMT as seen in breast cancer cells (286, 287), liver cancer cells (288) and melanoma cells (289). This leads to the hypothesis that miR-125b is removed from the PCa cells via exosomes in order to escape repression of EMT, a process known to occur in PCa cells (290, 291). The exosomes can then fuse with nearby fibroblasts and aid in inducing EMT in these cells, ultimately aiding in the progression of the cancer. However, there is a known anti-apoptotic role for miR-125b in PCa as well (292), so this balance may be important and will require further study.

Lastly, let-7i was chosen for its known high expression in PCa exosomes (222, 223), making this exomiR a good indicator of uptake by the fibroblasts should these levels become increased during the experiment. However, let-7i (with miR-125b) also potentially targets SMAD2, a known enhancer of TGFβ signalling in certain cell types (293-295). This gene was included to ensure that there were no off-target effects induced by exomiR uptake.

5.3.3. Exosomes isolated by gradient density ultracentrifugation are intact and induce fibroblast to myofibroblast transdifferentiation

The isolation of functionally intact exosomes in the quantities required to elicit a response from target cells was a substantial challenge. This was mainly because of the small quantities of exosomal material obtained from standard cell culture supernatants. To improve this situation, CELLine CL 1000 bioreactor flasks were used to grow DU145 PCa cells. This system is normally used to isolate large volumes of monoclonal antibodies from hybridoma cell lines (296) and involves the high density, long-term culture of these cells. DU145 cells were grown in this manner and allowed to produce exosomes for 7 days at a time until the media was removed and the exosomes were isolated by sucrose gradient ultracentrifugation. This method was performed according to the protocol described by Théry et al (137).

The first step in showing that exosome samples were sufficiently pure for functional analysis was to isolate the sucrose fractions which contained exosomes. These fractions were defined as those which contained particles of a size somewhere between 100 and 140 nm, high expression levels of CD9, the highest particle counts and also which fractions contained the most RNA. It can be seen from Figure 5.1 that the fractions that met these criteria were 9,10, 11 and 12 only. The RNA from all fractions was then reverse transcribed and analysed by qPCR for the presence of the reference miRNA (miR-92b*) and a miRNA of interest known to be associated with PCa exosomes (let-7i) (222, 223). This showed that our exomiRs of interest were truly exosomal and not evenly distributed throughout all fractions. This analysis also showed that the vast majority of qPCR amplification occurred from fractions of density between 1.1 and 1.2 g/mL sucrose, which is exactly where exosomes are known to congregate along a sucrose gradient (137).

The final step was to show that these DU145 exosomes were able to induce fibroblast to Myofibroblast differentiation, a critical component of EMT (252, 255, 256).The target cells chosen for this experiment were primary fibroblasts that were growth arrested by FBS starvation for 72 hours prior to exosome exposure. The fibroblasts were then exposed to either **i)** FBS deprived media, **ii)** 10 ng/mL soluble TGFβ, or **iii)** DU145 exosomes containing a total load of 10 ng/mL TGFβ. The results show quite clearly that DU145 exosomes induce the Myofibroblast specific alpha Smooth Muscle Actin (α-SMA) as expected (see Figure 5.3.a). This analysis also showed that exosomes induce the secretion of Hepatocyte Growth Factor (HGF), while soluble TGF-β at the same concentration actually reduced HGF levels below the control. This is also in line with previous observations (252).

All this evidence taken together illustrates that the exosomes isolated from the bioreactors were of high purity and contained exomiRs of interest in high concentrations. These exosomes were also able to induce fibroblast to Myofibroblast differentiation. The remaining question was, do these PCa exomiRs influence this process at all?

5.3.4. The PCa exomiRs analysed in this study do not influence myofibroblast transdifferentiation

Unfortunately, there were no observable trends found in the expression of any of the exomiRs or their putative target genes, as the expression levels never reached the 2-fold increase cut-off for significance. The lack of any change in expression levels implies that PCa exomiRs are simply not absorbed in significant numbers by the transdifferentiating fibroblast cells. Although there are a number of published works that suggest functional miRNAs can be delivered through exosomes and influence cell behaviour (100, 297-299), exomiRs are available in exosomes in a very low stoichiometric ratio (<1 copy per exosome) (300). It is therefore possible that the concentration of exosomes was too low to have an effect on transdifferentiation of the fibroblast cells. This raises further questions as to what is a "physiological" concentration of exosomes? There is currently no answer to this question and there will likely be no one size fits all answer. Exosome secretion is governed by many different factors among which is malignancy of cells and hypoxia (301). However, this will likely vary from patient to patient and there is no data regarding this from PCa patients. The bioavailability of exosomes in the PCa microenvironment is also questionable and again could vary enormously between patients. All of these questions remain to be answered before the role of PCa exomiRs in EMT can be truly understood.

Another complicating factor regarding exosomal uptake is the fact that exosomes can be targeted to lysosomes after being endocytosed (302). Endocytosed exosomes were shown to be targeted to the lysosome within 6 hours of exposure, resulting in the breakdown of the exosomes in this compartment. In this case, the exosomal TGFβ would be able to act on target cells during the first few minutes of exosomal exposure as exosomes become adsorbed onto the target cell surface. Then, over the next 6 hours the exosomes would be degraded along with their cargo of exomiRs.

Unfortunately, neither the low stoichiometric ratio of exosome:miRNA or the potential digestion of endocytosed exosomes and their content provides any insight regarding the increased secretion of HGF from exosome treated fibroblasts. Despite the fact that HGF is known to increase cancer cell invasion in the PCa tumour microenvironment (303, 304), the stimulus for its secretion is unknown. This study suggests that at least one factor for HGF secretion originates from PCa exosomes, but the exosomal molecule responsible for this effect has yet to be identified.

5.3.5. Exosomes may remove miRNAs that are inhibitory to PCa growth and progression

Given that exposure of fibroblasts to PCa exosomes did not lead to increased expression of known PCa exomiRs, another hypothesis is needed to explain why certain miRNAs are packaged into exosomes. Apart from the potential immunological roles discussed in chapters 2 and 4, the PCa cells may simply be eliminating miRNAs that are inhibitory to processes that aid in tumour survival and expansion.

Once again focusing on MECP2 it can be seen that the loss of miRNAs that would normally repress this gene in PCa cells would enhance the growth and progression of PCa cells. MECP2 is a methyl binding protein known to repress transcription at methylated sites in DNA. Yaqinuddin et al have reported that down-regulation of this gene by siRNA knockout in PC3 cells results in poor proliferation, increased apoptosis and inhibited invasive/migratory abilities *in vitro* (305). This is supported by earlier studies in which a recombinant retroviral vector for MECP2 was able to induce ectopic expression of this gene in LNCaP cells. The result was increased cell proliferation under androgen negative conditions (306), which is important as LNCaP cells are known to be androgen dependent. Further evidence for the importance of MECP2 in prostate cancer is witnessed in the anti-cancer mechanism of curcumin. This potent chemotherapeutic agent prevents MECP2 binding the promoter of neurog1, de-repressing this gene whose absence is normally an indicator of the presence of PCa (307) and also early stage colon cancer (308). MECP2 de-repression may also aid in the formation of PCa metastases, as it has been reported that promoter methylation of the KAI1 gene by MECP2 is a feature of both metastatic PCa cell lines and metastases isolated from PCa patients (309). This gene is targeted by both miR-106b and let-7i, the two most prevalent miRNAs identified in DU145 exosomes There were also a large number of exomiRs identified by microarray that can also target MECP2 (275).

However, several questions remain regarding this potential mechanism of PCa exomiR function. Firstly, how are certain miRNAs selected for inclusion into exosomes and subsequent elimination. It is possible that they are absorbed by lncRNAs whose expression is triggered by hypoxia, nutrient starvation or immunological attack for example. Then the lncRNAs and their miRNA passengers are loaded into the exosomes via recognition of signal motifs as suggested by Ahadi et al (129). This has yet to be tested experimentally however. Given the incredibly small stoichiometric ratio of exosome:miRNA it may also be possible that these miRNAs are passively picked up during exosome synthesis in the multivesicular body, but the overall loss of these miRNAs is enough to de-repress certain oncogenes. This must also be tested experimentally.

6. Discussion

6.1. Identifying exomiR biomarker candidates in human body fluids

6.1.1. Urine is the best source of PCa exomiRs for PCa biomarker development

At the start of this project, it was decided to identify potential RNA biomarkers for PCa using human PCa cell lines. This was an attractive idea as it was a much simpler process to isolate exosomes from tissue culture supernatants, and the risks of contamination with other non-exosomal particles was minimal. However these biomarker candidates were unable to differentiate PCa patient samples from healthy ones. This necessitated a second round of biomarker discovery this time beginning with PCa patient samples. Exosome isolation from human body fluids also required much optimisation. In fact, exosome isolation from human bodily fluids proved to be the most challenging aspect as each fluid required quite different protocols to acquire exosomes of sufficient quantity and purity. For example, exosome isolation from human urine required pre-filtration of large urine volumes through a 0.2 µm filter membrane to remove as many non-exosomal particles as possible before beginning the isolation. In contrast, plasma was stored in much smaller aliquots which were syringe filtered (0.2 µm) in 4 – 8 mL volumes as needed, as filtering large volumes of plasma clogged the larger filters almost immediately. This also raised the issue of contamination with significant quantities of non-exosomal protein. Tamm-Horsfall Protein (THP) was the main issue with urine as it is known to sequester exosomes, which ultimately lowers the yield of exosomes and therefore exomiRs that can be obtained from urine samples (229). In plasma the main issue was Albumin which is at an extremely high concentration (310), and it was difficult to remove in a manner that left exosomes intact.

The approach chosen for urine was to simply isolate exosomes from a greater volume of urine (135 mL versus the 15 mL used in the pilot study (Figure 3.1.), in order to compensate for the loss of exosomes caused by THP sequestration. This approach was successful in isolating sufficient quantities of intact exosomes that expressed the correct exosomal marker proteins. It may be possible in future to isolate sufficient volumes of exosomes from smaller amounts of urine (40 mL) with the use of DTT (196, 197). However this will make it impossible to assay exosomal surface markers in their native state, as DTT is a powerful denaturant. DTT treatment may not be needed in large scale implementation of this diagnostic procedure given the high quality exosome identifications performed during this project (203).

Plasma contained a much greater concentration of protein and lipid macromolecules that needed to be removed to acquire exosome samples of comparable purity to what we acquired from Urine. The most robust method to perform this task was the ExoRNeasy kit from Qiagen. Using this kit, exosomal RNA was isolated in a matter of hours instead of the 1 – 2 day procedure utilised for urine. This is important from a diagnostic screening perspective as it will increase the rate at which patient samples can be processed and will prevent backlogs of samples forming in diagnostic pathology labs. However, this kit did not isolate pure exosomes as shown by Enderle et al (198). In fact, it isolated a broader vesicle population termed "extracellular vesicles (EV)" by the authors. This is problematic because the origin of these non-exosomal EVs is unknown, and their co-isolation with exosomes will produce RNA samples of mixed origin. It is also possible that the ratio of exosomal to non-exosomal EVs may shift in different disease states which will require thorough characterisation prior to use in any kind of diagnostic assay. To overcome this issue, plasma samples were subjected to filtration through a 0.2 µm filter instead of the 0.8 µm filter suggested in the manufacturer's protocol. It should be noted that doing this resulted in very low yields of RNA.

With these considerations in mind, urine is currently the most promising fluid for the design of a non-invasive diagnostic test for PCa. The fact that urine is in constant contact with the prostate and that the glomerulus does not allow exosomes through under normal conditions guarantees that a large number of exosomes isolated from urine originate from the prostate. Urine can also be given more frequently than blood, and it is known that urine exosomes are very stable, and that intact RNA can be isolated from urine exosomes that have undergone multiple freeze thaw cycles (311, 312). This feature will allow patient samples to be transported long distances without damaging the exomiR diagnostic signature. Remote communities will then be able to access state-of-the-art diagnostic techniques for this common cancer.

However, as exosomes are too large to cross the glomerular filtration membrane, it is unlikely that urinary exosomes will be very effective at identifying the presence of metastatic deposits elsewhere in the body. For this reason, plasma exosomes may still have substantial diagnostic value for this condition but there are several important questions that must be addressed first. For example, the contribution of exosomes from other tissues could generate a misleading exomiR signature. The answer to this will most likely be found by exhaustive profiling of metastatic PCa patients to identify accurate exomiR signatures. A technique for estimating the proportion of an exosome sample originating from a PCa metastasis would also be an effective method, but would require prior knowledge of the contents of an exosome originating from a particular type of PCa metastasis. This would produce a more targeted search instead of the broad profiling ability discussed so far. This has already proven an effective strategy in the diagnosis of ovarian cancer (209).

6.1.2. Selecting appropriate exosomal reference genes for PCa exomiR biomarker development

The use of reference genes in any qPCR based assay is vital for the correct interpretation of experimental results. They act as loading controls to ensure that two samples can be directly compared, and clinical use of qPCR is no exception (147, 148). However, finding appropriate reference genes was a difficult task throughout this project. MiR-92b* was selected after much trial and error in cell culture exosomes given that it can be detected at very similar levels (within 2-fold difference)in both PCa cell lines and in the PNT2 cell line (see Figure 2.19.). However, the expression levels of this miRNA were not as uniform when looking at exomiR expression in human bodily fluids and was dropped in favour of a spike-in control, cel-miR-39, which proved to be very uniformly detected across patient samples that received the spike-in. Cel-mir-39 was not used in the OpenArray experiment because the probe for this miRNA was not a component of the Human pool A or pool B Megaplex primer pools available at the time, and an experiment with this many miRNAs required the use of global normalisation anyway. However, for the use of any of the biomarker candidates proposed in chapter 4, cel-miR-39 is highly recommended as a reference gene to ensure that exosomal RNA sample input is the same and that RNA extraction efficiency is consistent. This will be the norm in any future experiments arising from these discoveries.

6.2. Use of exomiRs as diagnostic, prognostic and treatment response markers

6.2.1. Utility of exomiRs as diagnostic, prognostic and/or treatment response markers for organ confined and advanced PCa

There are extensive constraints on the effectiveness of existing diagnostic biomarkers for PCa such as the limited ability of PSA to accurately and sensitively identify the presence of primary and metastatic tumours at early stage of disease (313). PSA is also unreliable in tracking the progression of the disease, and it gives little prognostic information (313). Another issue making PCa diagnosis and prognosis difficult is the requirement for invasive procedures such as the prostate biopsy, which is often accompanied by a transrectal ultrasound. This process may even be repeated multiple times on a patient (314). These pieces of information taken together are indicative of the need to develop a less invasive, more accurate and sensitive diagnostic/prognostic workflow for the clinical care of PCa patients.

6.2.2. ExomiR biomarker candidates are promising PCa diagnostics

The second stage in developing this workflow is identifying markers that can identify the presence of PCa as early as possible. The first efforts made towards this goal described in chapters 2 and 3 were not very successful given the poor ability of our tissue culture identified exomiR panel to identify PCa at all. The urine exomiR panel (Table 4.5.); however, has strong potential for this given the proximity of urine to the prostate. Also, urine analysis is the least invasive method available for sample collection. Of the diagnostic marker panel revealed in chapter 4, miR-375 is the most outstanding biomarker candidate. It was highly Enriched in the PCa patients with high statistical significance which suggests that it is likely to be easily detectable in urinary exomiRs from PCa patients. However given the age range of our cohort (63 – 76 years old) and the mixed blood PSA concentrations at time of diagnosis, it is not possible to make any conclusions regarding the effectiveness of our exomiRs panel at diagnosing early stage disease.

However, Stuopelyte et al have recently shown that miR-375 expression in the urine of PCa patients is a strong indicator of PCa, increasing the sensitivity of diagnosis from 64% for PSA alone up to 84% when combined with miR-375. The specificity of diagnosis also jumped from 52% when using PSA alone to 76% when miR-375 was included (315). Most importantly, this study showed that clinically lower grade PCa had high levels of miR-375 in the urine, while miR-148 was expressed more in the urine of higher grade PCa patients (315), which suggests that miR-375 is an appropriate early biomarker for PCa. Koppers-Lalic et al, went on to show that miR-375 is associated with extracellular vesicles in patient urine (316), as does the work presented in this thesis. However, the former do suggest that 3´ end truncated miR-375 is the true biomarker in urinary EVs. Gao et al also highlight the use of miR-375 as a sensitive and accurate biomarker for early PCa as they were able to differentiate between Benign Prostatic Hypertrophy (BPH) and PCa with 87.7% sensitivity and 75% specificity when looking at miR-375, miR-21 and PSA levels in patient serum (317).

PCa Urinary exosome expression levels of miR-106a may also be a useful early diagnostic as it is strongly associated with solid prostate tumours and is involved in RB1 down-regulation (318), which is a known early event in PCa development (319) occurring often through loss of heterozygosity of the gene from chromosome 13 (320, 321). The loss of RB1 by deletion has become much more associated with castration resistant, aggressive and likely to recur PCa (322, 323). However, Sharova et al have recently used miR-106a alongside miR-130b and miR-223 to differentiate between BPH and PCa (324), an indicator of the utility of this miRNA as an early diagnostic. However this group utilised circulating serum miRNAs and did not perform any EV isolations to demonstrate exosomal association.

miR-149 was also detected at high levels in PCa urine exosomes and it became significantly down-regulated once the cancerous prostate was removed (table 4.5. and table 4.6.) . This miRNA is associated with advanced Castration Resistant Prostate Cancer (CRPC) (325) and is responsible for Syndecan-1 dependent PCa cell growth at high levels (326) however this may lead to a decreased invasive ability of PCa cells (327). This suggests that miR-149 is more likely to be useful as an indicator of advanced PCa, but further studies will be required to validate this hypothesis.

Unfortunately, miR-20b has no association with early PCa. However, miR-20b is a candidate PCa oncomiR because it targets the tumour suppressor PTEN (328). MiR-20b performs this function alongside miR-106a which may indicate its potential as a biomarker given the association of miR-106a to differentiate between BPH and PCa as described above.

6.2.3. ExomiR biomarker candidates are promising prognostic and treatment response markers for PCa

The urine exomiR panel presented in chapter 4 offers the most exciting prospects for the clinical care of PCa patients. It is currently very difficult to give accurate prognoses for PCa using PSA (313), and other techniques rely on taking biopsies of the prostate or imaging the affected areas with various staining techniques to stage the cancer. None of these techniques are particularly good at predicting that a cancer will become more invasive and metastasize, nor can they predict the likelihood of recurrence. Imaging can be used to track the size and distribution of tumours throughout a patient providing very coarse treatment response information (i.e. has the tumour load decreased, stayed stable or increased), but imaging techniques only provide information on one feature of the cancer at a time, it's ability to uptake the radioactive substrate. ExomiRs could provide details of several aspects of tumour biology at once if multiple exomiR biomarkers are measured and the biological roles of these exomiRs is well understood in the context of PCa. Given the expression pattern described in chapter 4, it is likely that the levels of miR-375, miR-106a, miR-149 and miR-20b can be used to track the progression of disease. For example, if levels of these urinary exomiRs rises in the weeks/months after a treatment, it is likely that the cancer is returning, requiring further imaging and potentially further therapies.

There is also the association of our urinary exomiR panel with particular types of PCa. For example, miR-375 has been associated with early organ confined cancers as well as more advanced cancers. This was shown by Hart et al using deep sequencing to analyse solid tumour samples. They were able to reveal that miR-375 expression increases in organ confined cancer, then increases again when the cancer metastasises to the lymph nodes (329). Others have also used serum levels of miR-375 (alongside several other serum miRNAs/proteins) to differentiate between organ confined PCa and disseminated PCa (330), hormone responsive PCa from CRPC (331) and to separate T3-T4 cancers from T1-T2 cancers (332). Huang et al then demonstrated that serum exosomal miR-375 (with miR-1290) could be used to identify CRPC patients with poor overall survival (127). As yet, no studies have linked urinary exomiR-375 to PCa or to different stages or grades of PCa.

Unfortunately, at the time of writing, there are no prognostic implications for miR-106a, miR-149 or miR-20b in the literature. However, with further validation, hopefully these candidates can be used to garner prognostic information, and given their expression pattern they are likely to be useful treatment response markers.

A final consideration for the use of exomiRs as prognostic/treatment response markers is the presence or absence of metastatic deposits. If the cancer has become sufficiently invasive and aggressive enough to form metastases outside of the urinary tract, it is likely that exosomes secreted from these areas will fail to enter the urine given the small filter size of the glomerulus. At the time of writing, there is no data regarding the ability of blood borne exosomes to cross the glomerulus, although it seems likely in cases of kidney-related pathology that can damage the glomeruli.

6.3. Understanding the role of exosomal RNAs in PCa tumour biology

6.3.1. Challenges to understanding the roles of lncRNAs in tumour exosome biology

The exact roles of lncRNAs in exosome biology are currently unknown. Certainly as biomarkers they showed little promise from the earliest experiments performed in this project given their limited expression in exosomes, a phenomenon which has since been observed in several other studies (333-335). However, exosomal lncRNAs still have the potential to be considered as cancer biomarkers. For example, Gezer et al showed that the small number of lncRNAs that can be isolated from exosomes exhibit higher expression in the exosomes compared to the parent cell line (336). Furthermore, three of the most well studied lncRNAs, HOTAIR, MALAT1 and MEG3, have been identified as exosomal biomarkers for cervical cancer (337). As for PCa, Ahadi et al have revealed that PCa exosomes contain unique lncRNAs that are expressed at much higher levels than their parent cells (338). It has also been shown that exosomal lncRNA-p21 isolated from patient urine can differentiate BPH from PCa with 94% specificity when combined with PSA. However this combination was not very sensitive with a reported value of only 52% (128).

The functional relevance of lncRNA in exosome biology also remains mostly unexplored. Nonetheless, some studies have discovered roles for exosomal lncRNA in various disease states. For example, linc-VLDLR has been identified as a component of EVs shed in response to chemotherapeutic agents in Hepatocellular carcinoma cell lines. Linc-VLDLR can then be reabsorbed into HCC cells via EVs resulting in attenuation of chemotherapy induced cell death (339). CD90+ liver cancer stem cells have also been shown to induce a pro-angiogenic phenotype in surrounding endothelial cells via the action of H19 lncRNA that is transferred via exosomes (340). In renal cancer, lncARSR has been shown to operate as molecular decoys that divert miRNAs from their intended mRNA targets, allowing these targets to be translated. In this case, lncARSR is transmitted to chemotherapy sensitive cells where it sequesters miR-34 and miR-449, enhancing the ability of these cells to resist the effects of Sunitinib (341).

There are several reasons for the sparse data regarding exosomal lncRNA biomarker utility and function. First of all, the origin of a particular lncRNA can be difficult to pin down compared to a small RNA thanks to extensive editing of RNA sequence such as the reasonably common Adenosine to Inosine (A-to-I) substitution (342, 343). This plasticity in lncRNA sequence means that a lncRNA may appear with altered sequence depending on any number of factors including cell type, disease states/mutations and it may increase or decrease the affinity of a lncRNA for absorbing miRNAs and/or incorporation into exosomes. The recent discovery of ecircRNA is another complicating factor as current techniques are limited in their ability to define the conformation of an RNA, and accurate definition and mapping to the genome of an RNA in this unconventional conformation requires use of global nonco-linear sequencing, a relatively new technique developed specifically to sequence ecircRNA (344).

The sheer number of lncRNA transcripts is also a substantial barrier to elucidating the functions of specific transcripts. There are currently 133 361 human lncRNA transcripts recorded on lncRBASE, an online repository of identified human and murine lncRNA (345). Annotating this many transcripts is a major task requiring vast amounts of research hours before functions can be definitively ascribed in normal and disease states. However, new techniques are emerging to speed up this process such as the recently described RACE-seq, a method for determining gene structure and boundaries which is very useful for elucidating the origin of a lncRNA as well as any exon-intron type maturation (346). lncRNAs can also contain long repetitive sequences that many sequencing techniques edit out as part of their analytical pipeline in order to cope with the dense data sets generated by high-throughput sequencing (347). This may require further optimisation of *in silico* analytical techniques to not miss this feature of any lncRNAs.

6.3.2. Comparison between microarray and OpenArray exomiR profiles reveals a potential interplay between PCa exosomes and the tumour microenvironment

Both of these techniques proved to be extremely powerful to identify differential expression in exosomes or in cells but each had both advantages and disadvantages. For example, the microarray was able to give full coverage of all known human mature miRNAs whereas the OpenArray was only capable of profiling 784 previously identified human miRNAs. However, the microarray has a lower reproducibility than the OpenArray as the OpenArray utilises qPCR as its detection method which is the best available method for RNA profiling technology. The LSI method used to amplify low yield samples in chapter 4 can also fail to detect up to 38% of miRNAs giving this method a fairly high false negative rate, limiting the possible discoveries from the pool of 784 miRNAs for which probes are available (227).

Given the differences between RNA profiling techniques as well as the significantly different inputs (Exosomes isolated from cell lines versus exosomes from patient body fluids), it is unsurprising that exomiR expression profiles from chapters 2 and 4 do not match one another. Despite the lack of miRNA expression similarity between cell culture and patient exosomes, the target genes of the highly expressed exomiRs from the microarray analysis (chapter 2) and the OpenArray analysis (chapter 4) had similar biological roles, mainly in regulating the immune system.

Highly expressed exomiRs from the microarray and OpenArray analyses targeted genes relevant to Natural Killer (NK) cell and Dendritic Cell (DC) activation, proliferation and cancer killing ability. For example, the microarray analysis highlighted exomiRs potentially capable of abrogating the production/secretion of cytokines IL-2 and IL-10. IL-2 is required to induce IL-10 secretion from NK cells (348), which enhances the cytolytic functions of NK cells (349, 350). The loss of either cytokine could therefore inhibit the NK cells natural tumour killing ability and this has been demonstrated by Zheng et al (351). Comparably, the OpenArray on PCa urine implicated several exomiRs that target Type I interferons IFN-γ and TNF-α) which are also known to enhance the killing ability of NK cells and CD8+ Cytotoxic T Lympyocytes (CTLs) (241).

These cytokines are also relevant to DCs in cancer because there are extensive and highly pleiotropic interactions between NK cells and DCs via the 4 cytokines described above. For instance, IL-2 is in use as a cancer therapeutic when it is combined with mAb complexes (termed IL-2c) and administered in conjunction with DCs. This results in increased numbers of CD8+ CTLs and NK cells as well as enhancing the killing ability of these cells (352). Furthermore, IL-2 is required to stimulate adequate production of IFN-γ that is essential for both DC maturation into the potent antigen presenting form (353) as well as enhancing the killing ability of NK cells (241, 354). TNF-α also exerts a pronounced effect on DC maturation and survival in cancer. For example, patients who were subjected to pulses of tumour antigens accompanied with TNF-α exhibited an approximately 10% higher maturation rate of their DC populations accompanied by enhanced secretion of IFN-γ and IL-22 (355). Furthermore, PCa is known to cause the death of DCs when the two cell types are co cultured and addition of TNF-α to the co-culture is able to prevent DC death (356).

When this bioinformatic data and its interpretations are combined with the findings regarding tumour stroma impact described in chapter 5, it paints a picture in which exosomes modulate the invasive potential of the prostate tumour through protein-protein interactions at the surface without any influence by exomiRs. However, the exomiRs may be able to exert influence over immunological processes resulting in increased immune evasion. This data is summarised in Figure 6.1.

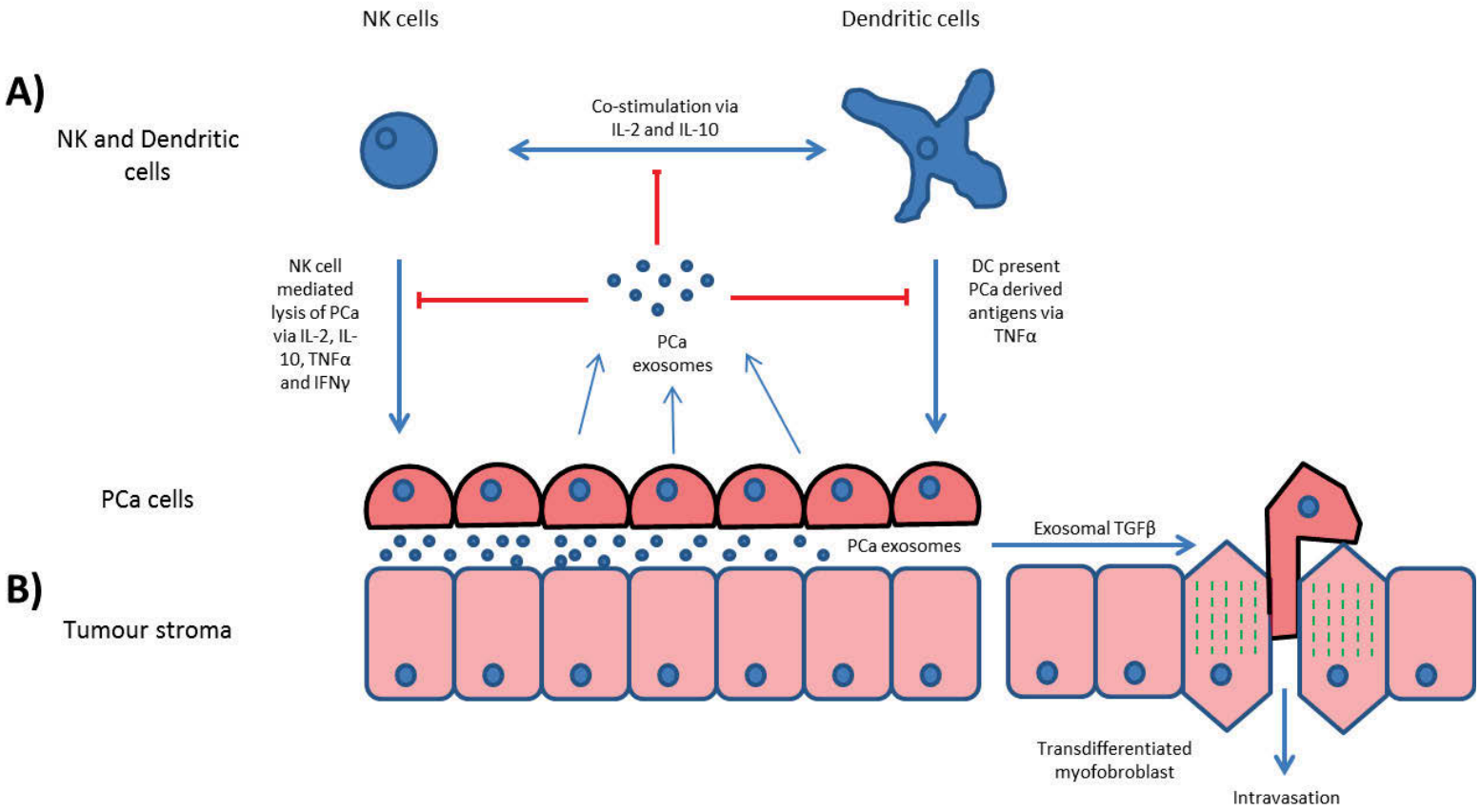

Figure 6.1. Potential ExomiR functions in PCa tumour stroma.

A) based on the results presented in chapters 2, 4 and 5, we hypothesise the following model. The exosomes secreted by the PCa cells contain exomiRs with potential to attenuate these processes. **B)** The findings presented in chapter 5 revealed that PCa exosomes induce transdifferentiation of myfibroblasts which in turn support invasion and intravasation of PCa cells

6.4. Future directions

6.4.1. Requirements for validating exomiRs as diagnostic, prognostic and treatment response markers

Despite the fact that our microarray based biomarker panels were able to be validated by qPCR *in vitro*, their expression profile showed very little promise in actual human bodily fluids as a diagnostic. This would suggest that exosomes derived from tissue culture are a poor indicator of the type of exomiRs likely to be found in the more complicated bodily fluid samples. However, OpenArray analysis performed on human urine proved to be an excellent way of discovering new biomarkers and will also be explored in future studies using plasma exosomes to identify early diagnostic PCa exomiRs as well as exomiRs that would indicate metastasis. As for the potential of urinary exomiRs as early diagnostic biomarkers, they will be validated in a much larger sample of men both before and after PCa in much the same manner as was presented in this project.

Validation on a larger sample size will have the following range of challenges that must be overcome. Unlike plasma, urine samples are not routinely stored by hospitals so gaining access to large numbers of urine samples is an essential phase of experimental planning. The next consideration is the number of patients required to confirm or deny the diagnostic potential of the biomarker panel presented in chapter 4. Although the prevalence in men over 70 is well known, the prevalence in other age groups is not. This leads to two possible experimental designs for future validation experiments. The first option is to simply set the prevalence estimate low so that the biomarker panel can be assessed for diagnostic potential in male volunteers of any age. The second option is to stratify patients into age groups with increasing assumed prevalence as age increases. The first option will lead to the most robust test, but the second option will produce results that aid in targeting particular patients with extreme sensitivity and specificity. Regardless of the approach used, an estimated minimum of 491 patient samples will be required to assess specificity and sensitivity simultaneously assuming a 30% prevalence rate in the population, according to guidelines laid out by Li and Fine (357).

As for determining the prognostic capabilities of the biomarker panel presented in chapter 4, the same patient sample group will need to be followed up for survival at regular intervals. This will allow for ROC curve analysis to determine which exomiRs correlate with poor survival rate and which (if any) correlate with a high survival rate. If follow up with the patients is frequent enough, it may even be possible to identify particular exomiRs as increasing or decreasing with particular interventions whether they are surgery based therapies, chemotherapies or radiation therapies. However this will require further division of the patient population based on severity of cancer as well as the treatment administered which may undermine the test power requiring yet more patient recruitment.

6.4.2. Investigating the roles of PCa exomiRs in the immune system and tumour microenvironment *in vitro*

It is worth investigating exomiRs for their potential as effectors of immune evasion. Given the network of likely interactions presented in Figure 6.1 NK and DCs are the most likely targets for exomiR interaction. In order to test this hypothesis, NK and DCs will need to be exposed to PCa exosomes as well as normal exosomes. Tissue culture of PCa and normal prostate cells in Integra bioreactors is an ideal way to achieve the concentrations necessary for this type of work. Different concentrations of exosomes should be added to identify the concentration at which any observed effects of exosome exposure are most pronounced, and all cell populations exposed to normal prostate exosomes must maintain uninhibited cell functions to prove that it is a feature of PCa exosomes causing changes in immune cell activity. The cell functions to be measured will include cell killing ability and IL-10, TNFα and IFNγ secretion into culture media. DC maturation and cell viability will be the parameters measured for DCs.

In order to prove that it is exomiRs responsible for any changes observed, the expression profile of the top ten exomiRs from microarray analysis and the top ten exomiRs from OpenArray analysis will be measured in NK and DCs before and after exosome treatment. To be considered effective, exomiR levels must rise significantly in the target cells, coupled with down-regulation of target genes identified by bioinformatic analysis. In order to confirm that it is the exomiRs of interest playing a role in any observed NK and/or DC dysfunction, antagomiRs against these exomiRs will be transfected at the same time as exosome exposure. If exomiR levels rise significantly in the target cell lines coupled with loss of immune functions, and the transfection of antagomiRs reverses or at least attenuates this process, the experiment will have revealed an immune evasion mechanism made possible by PCa exomiRs.

However, failure of this experiment is a distinct possibility given the findings presented in chapter 5. Despite high levels of exomiRs being present in DU145 exosomes, these exomiRs were not absorbed in significant quantities and their target genes were not down-regulated. It is possible that the exomiR-target combinations were not relevant to the cell/tissue types being analysed, but this seems unlikely given the level of evidence available in literature. However, the ratio of miRNA per exosome may be the cause of this apparently low uptake as Chevilet et al revealed that this ratio is very low (300).

Appendix

Appendix Table 1. miRNAs exosomes vs cells

miRNA ID	Fold-Change(Exosomes vs. Cells)
miR-1246	285.353
miR-3197	21.7462
miR-1224-5p	16.0435
miR-149-star	10.0557
miR-1290	9.505
miR-3154	7.46796
miR-663	7.0489
miR-1469	5.97319
miR-1228-star	5.20707
miR-1225-5p	4.97022
miR-762	4.86686
miR-92b-star	4.85077
miR-1915	4.84523
miR-638	4.81284
miR-4281	4.72225
miR-1975	4.0344
miR-2861	3.98567
miR-1908	3.77794
miR-150-star	3.57006
miR-1207-5p	2.90629
miR-572	2.85105
miR-3196	2.83651
miR-665	2.77309
miR-596	1.78942
miR-135a-star	1.57219
miR-103	-1.57042
miR-107	-1.58131
miR-1973	-1.62834
miR-3130-5p	-1.66191
miR-2276	-1.66661
miR-93-star	-1.91203
miR-378b	-1.92862
miR-15b	-2.19782
miR-550	-2.27656
miR-30a-star	-2.28677
miR-378-star	-2.34493
miR-501-5p	-3.00845
miR-1287	-3.07032
miR-574-3p	-3.08095

miR-4298	-3.87653
miR-550-star	-3.92619
miR-1260b	-4.37247
miR-149	-8.57514
miR-193a-5p	-10.1434
miR-4284	-10.3694
miR-935	-10.8695
miR-1180	-13.8032

Appendix Table 2. ExomiRs in Pca exosomes compared to PNT2 exosomes

miRNA ID	Fold-Change(PCa exosomes vs. PNT2 exosomes)
miR-125b	325.851
miR-663	214.85
miR-22	159.457
miR-320d	120.739
let-7i	116.249
miR-1246	100.872
miR-1469	83.8582
miR-106b	78.9743
miR-4281	69.4543
miR-3178	65.1041
miR-3196	55.28
miR-25	49.577
miR-1268	48.8538
miR-378	47.1211
miR-30b	45.084
miR-423-5p	44.662
let-7g	41.1015
miR-140-3p	39.9845
miR-106b*	39.5281
miR-345	36.498
miR-3185	35.8042
miR-1228*	34.7484
miR-183	31.5237
miR-3197	28.8875
miR-19b	27.7434
miR-378c	27.1062
miR-744	25.2063
miR-455-3p	21.9051
miR-151-3p	21.3418
miR-92b*	18.8951
miR-423-3p	18.2816
miR-425	16.6314
miR-1908	14.1672
miR-30a	13.9974
miR-93*	13.5886
miR-532-5p	12.8495
miR-128	11.4093
miR-339-3p	10.8206
miR-324-5p	10.7643

miR-1224-5p	9.73745
miR-15b	9.1299
miR-671-5p	7.52676
miR-301a	6.966
miR-4270	6.32711
miR-422a	5.8539
miR-500	4.70366
miR-1207-5p	4.63582
miR-185	4.32854
miR-877	2.88459
miR-574-3p	2.80559
miR-660	2.36278
miR-4306	1.70289
miR-3116	-1.51323
miR-508-5p	-1.51791
miR-548n	-1.52137
miR-199b-5p	-1.52241
miR-2116*	-1.52932
miR-454*	-1.56996
miR-2114	-1.57871
miR-767-3p	-1.58649
miR-3186-3p	-1.5991

miR-518c	-1.62831
miR-609	-1.66058
miR-409-5p	-1.6712
miR-770-5p	-1.67977
miR-675*	-1.69843
miR-634	-1.71703
miR-147	-1.75554
miR-1251	-1.76206
miR-103-as	-1.81159
miR-548e	-1.81167
miR-605	-1.81923
miR-1243	-1.86112
miR-646	-1.8765
miR-559	-1.94184
miR-624*	-2.11438
miR-154*	-2.17654
miR-107	-2.18362
miR-365	-2.21709
miR-7-2*	-2.29572
miR-103	-2.3495
miR-4258	-2.36598
miR-433	-2.40786

miR-410	-2.46232
miR-1913	-2.55219
miR-631	-2.70937
miR-548g	-2.85246
miR-1234	-7.75761
miR-1281	-16.3563

Appendix Table 3. ExomiRs from androgen independent cells compared to androgen responsive cells

miRNA ID	Fold-Change(androgen independent vs. androgen dependent)
miR-194	36.5564
miR-1979	29.0628
miR-27b	28.2926
miR-126	27.3805
miR-30c	19.0578
miR-200a	16.485
let-7f	16.4588
miR-28-3p	16.2222
miR-28-5p	13.3214
miR-15a	12.7876
miR-132	12.3354
miR-21	11.6908
miR-652	11.5556
miR-339-5p	9.48923
miR-331-3p	9.22667
miR-200b	8.89961
miR-320e	8.63309
miR-3195	8.37708
miR-128	7.44532
miR-324-3p	5.97323
miR-1263	2.97357
miR-362-5p	2.7414
miR-665	2.44907
miR-198	1.53077
miR-1203	-1.53493
miR-3163	-1.81294
miR-664	-1.98665
miR-1249	-2.4728
miR-1228	-4.91072

Appendix Table 4. PCa exosomal versus Cellular mRNA profile

Gene Symbol	Fold-Change(PCa exo vs. PCa cell)
SAR1B	81.6745
PODXL	64.091
RAD51	51.9288
OR52R1	14.4986
OR8D1	14.3261
OR1N2	13.9839
STRADA	12.7068
SRGAP3	12.5377
RAPGEF4	11.3984
IFT74	10.6407
PRAMEF11	10.4164
ZNF652	9.54544
SAA2	9.54013
SENP8	9.46884
HEATR7B2	9.03649
IL10	8.52399
PDHA2	8.39402
SULT1B1	8.13544
LIPT1	8.02531
OTC	7.94523
UBA5	7.15196
LMO1	7.04882
PRG2	6.87555
SHC1	6.82594
COL11A1	6.49707
MORN4	6.47707
CPA6	6.38828
LAT2	6.266
ALDH1A2	6.02078
SCN2A	5.85422
ODZ1	5.82304
LIN54	5.80393
PLEKHG5	5.76439
COL11A1	5.65463
TEX13A	5.24356
TAC4	5.19287
TLR8	5.00306
OR6S1	4.9277
IGDCC4	4.85645

SORBS1	4.7466
MAGEA10	4.69953
MFAP2	4.69439
STK24	4.6096
MAPK7	4.42145
PTCH1	4.29945
TSKS	4.12638
SNUPN	4.0948
RAI2	4.08628
DNAI1	4.06565
ZNF473	3.97976
PGC	3.97229
SYBU	3.94734
LARGE	3.88755
ALAS2	3.77399
UACA	3.65211
TLR3	3.33019
ZBTB20	3.13842
SNX5	3.11135
NM_024016	3.0626
NM_002148	2.96695
ABCB5	2.80368

ASB16	2.16031
BCL2L15	-2.00021
SCN11A	-2.13371
RHOBTB1	-2.34467
SYT4	-2.34955
DIO2	-2.4195
LRRC3B	-2.42305
PLCL1	-2.42563
ACTR3C	-2.48817
TCF7	-2.52282
RNASE12	-2.67555
RORA	-2.69935
TGIF2LX	-2.72446
TMEM57	-2.75664
SLC6A12	-2.7817
TM4SF4	-2.79729
PRR20B	-2.82197
ARPM1	-2.82238
MS4A3	-2.91959
CLEC4A	-2.97043
MAP2K2	-3.03336
TTLL3	-3.1886

OR4M1	-3.25503
C5orf49	-3.33592
CTNS	-3.33735
AGTRAP	-3.33866
ASXL2	-3.34354
CD99	-3.34446
CD99L2	-3.36366
RASSF5	-3.36711
NOL6	-3.38684
NOC2L	-3.39965
BTBD19	-3.45619
GSTA3	-3.45773
OR6P1	-3.46484
ACTL8	-3.47037
HCN3	-3.51817
PTPRR	-3.56523
GRHL3	-3.56563
CDK15	-3.58044
PGA3	-3.60628
PAICS	-3.61579
WBP2NL	-3.63871
LST-3TM12	-3.64172

USP29	-3.64759
NUP188	-3.66087
C9orf163	-3.66427
C19orf45	-3.69603
SLC6A7	-3.69618
KLF15	-3.73153
NR4A3	-3.76231
WHSC1	-3.8233
OR7D4	-3.86866
ABCC9	-3.89104
C6orf47	-4.0186
YIPF7	-4.06521
SYT14	-4.09132
FANCB	-4.11973
SASH1	-4.12761
FAM151B	-4.16173
DEFB116	-4.17329
OTX2	-4.1762
DEFB134	-4.18488
CALHM3	-4.19138
ELF3	-4.23158
HIST1H4G	-4.2488

SOAT2	-4.24908
PCDH11X	-4.25486
CEP68	-4.28597
AARSD1	-4.32487
GDI1	-4.43215
PALM2	-4.44795
RAB40AL	-4.53696
NGFRAP1	-4.55779
PLEKHA1	-4.56075
TBX22	-4.60533
SMC1B	-4.62456
ACP1	-4.7106
WDR85	-4.74836
TAS2R60	-4.76147
GRINA	-4.83062
TACC1	-4.90001
OR52L1	-4.90325
IL22RA1	-4.90561
IP6K1	-4.9282
THEMIS	-4.9408
NRD1	-4.98167
C3orf71	-4.99461

FAM108B1	-5.02868
PHTF2	-5.10639
ZNF430	-5.11483
IREB2	-5.14844
CCR5	-5.178
ETV1	-5.22375
ANKHD1	-5.24751
NM_152739	-5.36061
ITGB3	-5.36149
OR2C1	-5.36444
TBC1D12	-5.37108
GPR26	-5.41528
COL6A6	-5.43167
OPRD1	-5.50041
ZER1	-5.51106
C20orf132	-5.51555
TSGA10	-5.55527
C5orf13	-5.55564
TMEM174	-5.57184
PCDH11X	-5.59988
MYO5C	-5.61486
DISC1	-5.71955

SLC1A3	-5.78621
PRPS1L1	-5.81886
GCET2	-5.82976
XAB2	-5.83126
C1QTNF5	-5.83348
TEX264	-5.86927
PLTP	-5.89783
IGF2BP2	-6.05434
C4BPB	-6.1159
ZSCAN20	-6.16041
DENND4B	-6.20453
CPNE1	-6.21558
APBA3	-6.27934
VPS53	-6.32248
URM1	-6.62463
DHX30	-6.72432
VASH1	-6.73676
LY6G5B	-6.74399
MED23	-6.81074
LIMD1	-6.83252
TNS3	-6.8392
C1orf213	-6.84815

PHKG1	-6.88624
RGPD5	-7.05844
NPAT	-7.16553
EXTL3	-7.2237
CPNE1	-7.26757
PGRMC2	-7.32929
LRRC52	-7.48553
OR1N1	-7.58851
CDC14A	-7.67421
ABHD13	-7.74093
RHD	-7.82256
C12orf53	-7.8269
PPARD	-7.85765
BCO2	-7.89641
TOMM22	-7.95941
CAMTA2	-7.97067
RBL1	-8.33015
REEP6	-8.43096
FPR2	-8.44394
SOS1	-8.55345
TMPRSS5	-8.68984
FSCN3	-8.7733

RCC1	-8.77866
SMARCC2	-8.81653
AGT	-8.91086
FAM111A	-8.99597
RAMP3	-9.00209
JOSD2	-9.0154
PPOX	-9.121
SLCO1C1	-9.15733
HYAL3	-9.19585
SYT1	-9.20029
PCDHA1	-9.34711
INPP4A	-9.37218
MYL1	-9.40675
ANUBL1	-9.67261
PCDHB13	-9.9723
AGPAT4	-10.2704
RLF	-10.5595
USP54	-10.6845
HGSNAT	-10.9184
TMPPE	-11.091
PGM1	-11.1629
HDAC8	-11.2957

C16orf5	-11.5018
FBXL4	-11.8949
RAB4B	-12.2028
DBF4B	-13.1374
HIST1H2BD	-13.1835
CATSPER2	-13.3526
ABCC4	-13.8522
SPEF2	-13.9349
C21orf58	-14.2033
SELO	-14.5245
SLC12A2	-15.6005
NFATC1	-15.9359
MDM2	-16.6221
TMEM39B	-17.0526
HPS5	-17.6926
FGFR1	-18.327
PIGO	-18.9654
DTWD1	-19.0311
BTN2A1	-19.5005
PRDM12	-23.1288
C6orf26	-23.702
ADAT2	-28.0205

Appendix Table 5. PCA Exosomal versus Cell lncRNA profile

seqname	Fold-Change(PCa exo vs. PCa cell)
uc010bys.1	53.3522
uc010mkn.1	46.1077
ENST00000452932	29.5269
ENST00000442733	29.137
uc002xjn.1	21.0517
ENST00000428191	20.1523
chr6:49286902-49299646+	19.8825
BC070394	19.6058
ENST00000430456	18.8062
ENST00000430398	17.8248
BC065517	17.364
ENST00000439406	17.3115
G36533	15.5821
NR_024479	15.5364
uc002yys.2	15.5355
BC040994	14.9685
AF116719	14.6102
ENST00000423086	14.4292
ENST00000422141	14.4181
ENST00000431108	14.2887
ENST00000403497	14.093
ENST00000418640	14.0179
ENST00000448534	13.9123
BC127937	13.7894
uc.374+	13.7478
ENST00000366185	13.7378
AK022254	13.4942
BU619016	13.2818
ENST00000441208	13.098
ENST00000428537	12.8417
ENST00000504977	12.8399
AY927529	12.8262
uc001qoa.2	12.6314
ENST00000506227	12.5756
ENST00000412038	12.345
ENST00000451327	12.1976
ENST00000453459	11.9744
uc003dqh.1	11.9544
N39059	11.8874

HIT000044961	11.8659
uc001uvi.1	11.8402
ENST00000433817	11.8031
NR_001538	11.6843
ENST00000504494	11.6109
CR623181	11.226
NR_027916	11.1841
uc.276+	11.0912
ENST00000503181	10.9988
ENST00000505498	10.6791
ENST00000449766	10.4088
ENST00000441468	10.3794
ENST00000442031	10.3101
AF086403	10.1981
uc.26+	10.1529
ENST00000452888	9.88249
AK024579	9.76463
ENST00000501886	9.68869
ENST00000431034	9.6582
ENST00000508336	9.57937
ENST00000441316	9.51288
ENST00000462801	9.50743

uc004coj.1	9.50432
ENST00000404577	9.46023
chr7:152312201-152329460+	9.45553
uc003krz.2	9.4247
chr17:4292077-4301447+	9.24402
ENST00000512969	9.20484
ENST00000437611	9.04813
ENST00000429864	8.90834
BC045182	8.705
uc003yso.1	8.66965
ENST00000504161	8.61692
ENST00000421074	8.52424
chrX:152738361-152755601+	8.46231
AA868791	8.36407
ENST00000411341	8.35332
uc.301+	8.26196
ENST00000437466	8.23958
chr6:49286902-49299646-	8.04661
chr1:145399645-145402747-	7.99466

BC043219	7.9392
U10515	7.90107
ENST00000425717	7.90067
ENST00000427095	7.89677
ENST00000503589	7.88616
ENST00000414401	7.78795
NR_024580	7.76135
BC039108	7.7161
ENST00000412133	7.37422
ENST00000421336	7.37147
ENST00000411156	7.29127
chr21:15789329-15846029-	7.22535
chrX:105625324-105639025-	7.13808
chr1:214288602-214300602+	7.10152
NR_024369	7.04034
ENST00000443032	7.02127
BC095534	6.92685
ENST00000438849	6.89669
chr20:56035583-56041187-	6.82421

NR_002808	6.74758
ENST00000436766	6.6887
ENST00000435770	6.60306
chr12:29230483-29281008-	6.59767
ENST00000453078	6.55637
NR_026590	6.55432
ENST00000450891	6.51137
ENST00000425861	6.50276
chr11:27331250-27336865-	6.44557
BC043237	6.35872
ENST00000442161	6.32717
AK123811	6.31079
ENST00000452911	6.1505
BX648212	6.09563
BE254096	6.03148
NR_026542	5.9854
uc001upm.2	5.97725
uc002myf.2	5.97506
ENST00000493149	5.9607
ENST00000366212	5.77947
ENST00000420172	5.76447

ENST00000453648	5.74779
ENST00000420606	5.72565
ENST00000422231	5.70842
ENST00000446543	5.70642
NR_002787	5.68068
ENST00000505832	5.62928
ENST00000442180	5.56086
AK056971	5.53771
ENST00000429008	5.51639
ENST00000406616	5.48843
AK000864	5.43136
ENST00000439788	5.40884
chr6:3481226-3495626+	5.40359
ENST00000415159	5.39015
BI460894	5.37501
AF086093	5.31404
ENST00000412712	5.28733
ENST00000398618	5.26721
AY094612	5.25994
AA601390	5.13754
NR_024063	5.12041
AK129734	5.10116

Negative012	5.04754
chr5:78812894-78817242+	5.01375
NR_028063	5.01364
BG258490	5.00886
NR_026544	4.98726
ENST00000426609	4.96675
ENST00000441056	4.94329
ENST00000453073	4.93881
ENST00000515703	4.91735
exon1963+	4.88756
BC007809	4.86595
ENST00000404226	4.84685
ENST00000514216	4.8195
DB489328	4.79821
ENST00000441632	4.67308
uc001glm.2	4.66931
ENST00000512746	4.60654
BC024158	4.60488
chr6:164571914-164609149-	4.60088
BX098284	4.58735
ENST00000468470	4.56572

ENST00000439751	4.52188
uc004asr.3	4.46359
NR_024518	4.45697
ENST00000436121	4.43303
ENST00000470758	4.4304
ENST00000377168	4.42796
AK128801	4.42297
uc004del.1	4.41414
ENST00000508873	4.41299
AK023784	4.33387
ENST00000402084	4.3237
ENST00000511281	4.28517
BC033547	4.24523
ENST00000457809	4.24063
ENST00000501525	4.20684
ENST00000427009	4.20188
ENST00000502948	4.19924
ENST00000503783	4.14696
AK093174	4.13744
ENST00000432928	4.11414
NR_033119 NR_033119 NR_033119	4.09505

AF143878	4.03526
AK055000	4.02112
AL706118	4.0141
uc.43+	4.00656
ENST00000489016	3.99751
G36583	3.97264
uc003ozv.1	3.91026
ENST00000451349	3.89089
ENST00000422116	3.88892
uc002lax.3	3.88301
BC020462	3.86914
chr4:24135775-24143921+	3.85495
ENST00000445967	3.80352
uc003bih.2	3.79898
BC062454	3.77985
ENST00000504478	3.69856
ENST00000433167	3.59974
uc.384-	3.58288
AK097999	3.56779
NR_003506	3.54838
uc.243-	3.54721

X78261	3.47852
AK023501	3.47507
uc003hlv.2	3.42738
BF907292	3.34803
ENST00000433943	3.32395
ENST00000425185	3.32047
AB175890	3.31607
AF119867	3.29977
uc011bny.1	3.29793
DQ655975	3.28436
Negative051	3.25439
ENST00000454320	3.23119
AL044425	3.17783
ENST00000437347	3.16236
BC045633	3.14137
AI525920	3.10333
ENST00000467154	3.10148
ENST00000455299	3.07019
ENST00000398690	3.05543
uc010kfv.2	3.03162
ENST00000511484	3.01526
AK124797	2.92883

NR_026856	2.91915
CA423547	2.89273
G65701	2.89196
chr1:159599976-159620426-	2.83996
ENST00000463255	2.83906
ENST00000363328	2.83152
CR611965	2.82374
uc002oes.1	2.81356
NR_033352	2.79695
ENST00000429458	2.79019
ENST00000432706	2.75685
uc.21-	2.75085
ENST00000495088	2.72958
ENST00000444765	2.72427
G65651	2.69795
ENST00000455845	2.68574
ENST00000426903	2.63391
G43576	2.60971
chr6:159287212-159291153-	2.60121
ENST00000448783	2.59671
ENST00000431691	2.59613

ENST00000441768	2.5949
uc003jgy.2	2.56614
CK299764	2.53568
ENST00000505898	2.5337
nc-HOXA1-53-	2.49823
ENST00000416078	2.49318
uc.448+	2.42028
ENST00000430064	2.39185
ENST00000451439	2.38651
AF113684	2.37523
ENST00000366209	2.3524
CK905565	2.33782
uc001dfx.2	2.18535
ENST00000428023	2.07075
ENST00000501602	2.05264
ENST00000429730	2.04208
chr2:68206296-68223571-	-2.03375
ENST00000480493	-2.03879
AK026459	-2.09662
ENST00000509483	-2.13548
ENST00000492683	-2.15231

G36761	-2.16312
uc.266+	-2.17357
ENST00000454780	-2.18526
ENST00000455174	-2.2863
NR_027954	-2.28634
G43609	-2.29346
AF146695	-2.33391
NR_002935	-2.37493
uc001ikd.1	-2.38332
chr14:54676002-54680773-	-2.40413
AF116657	-2.46168
ENST00000412941	-2.46761
chr4:158983666-159005030+	-2.47433
AJ001890	-2.4785
ENST00000504210	-2.48116
ENST00000428642	-2.48154
DR423683	-2.50705
ENST00000479841	-2.52928
BI464915	-2.57531
ENST00000505645	-2.57746
CN479707	-2.5875

AK127532	-2.59699
AI671175	-2.61059
AY927569	-2.6328
ENST00000398120	-2.65977
ENST00000442867	-2.66771
ENST00000429227	-2.6948
ENST00000438855	-2.77013
NR_028596	-2.79416
ENST00000502570	-2.80526
ENST00000503616	-2.81501
ENST00000506803	-2.84896
AJ431618	-2.88685
BU681290	-2.89743
uc003adf.1	-2.89958
ENST00000503870	-2.90242
chr4:60340905-60362455-	-2.90351
ENST00000426709	-2.90462
exon394-	-2.90629
ENST00000456493	-2.91765
uc003idd.2	-2.92925
DA233116	-2.95194
ENST00000502140	-2.95458
BC063881	-2.96543
ENST00000406807	-2.98048
ENST00000427446	-2.98597
HIT000332671	-2.99109
ENST00000445936	-2.99147
AY339211	-3.00915
ENST00000418161	-3.01238
AI149906	-3.02264
ENST00000513032	-3.02602
BC036238	-3.03242
uc002obw.1	-3.0365
ENST00000507682	-3.0384
ENST00000395232	-3.05935
nc-HOXA9-79-	-3.06074
chr3:58165366-58172726-	-3.06331
ENST00000423162	-3.07501
uc.469-	-3.08966
ENST00000504852	-3.09302
AK094428	-3.10205
ENST00000443514	-3.11541

nc-HOXA5-67+	-3.1243
chr9:21753446-21790681+	-3.1245
chr3:118559485-118571910-	-3.13326
ENST00000503778	-3.13419
NR_024259	-3.13529
ENST00000451869	-3.1376
ENST00000424662	-3.13823
AB019562	-3.14018
ENST00000501748	-3.14528
ENST00000505828	-3.1511
ENST00000441399	-3.15596
ENST00000417697	-3.1814
ENST00000416385	-3.18325
ENST00000418624	-3.19125
ENST00000444014	-3.19693
ENST00000424290	-3.21278
ENST00000431500	-3.21814
ENST00000415016	-3.21851
uc002gwy.2	-3.21912
AY927604	-3.22012
ENST00000424940	-3.22079
ENST00000451575	-3.22873
ENST00000451718	-3.23676
ENST00000443179	-3.23827
ENST00000446621	-3.24472
ENST00000417498	-3.24759
ENST00000419904	-3.25328
uc.120+	-3.25587
CR621247	-3.25703
ENST00000434081	-3.25942
exon113-	-3.28212
uc002rhy.1	-3.28493
AL137472	-3.31216
chr15:63377715-63386763-	-3.31728
chr7:10142050-10160500+	-3.31898
chr5:67603294-67617869-	-3.33816
uc.244-	-3.33893
AK123329	-3.34219
DB317657	-3.348
ENST00000489449	-3.36066
ENST00000435157	-3.36638

uc.159+	-3.3665
uc.354+	-3.40576
ENST00000487580	-3.40659
AK124473	-3.42476
uc009xjd.1	-3.43404
BF356369	-3.43673
ENST00000440725	-3.44655
AB032363	-3.45125
chr13:69265749-69290074+	-3.45343
exon2911-	-3.45704
uc001cyw.1	-3.48518
NR_024009	-3.50954
AF070579	-3.51168
chr6:105939837-105951212-	-3.52823
chr4:177356004-177360135-	-3.52946
uc001ysx.1	-3.53552
ENST00000452667	-3.55514
nc-HOXC5-253-	-3.55754
ENST00000414424	-3.567
ENST00000472120	-3.56729
ENST00000421821	-3.56922
BE588180	-3.59013
uc002ump.1	-3.61481
ENST00000322493	-3.62503
ENST00000505741	-3.62552
CD357052	-3.6278
AF113697	-3.63628
uc.50+	-3.64351
BC041999	-3.64357
uc002rvb.2	-3.65424
BG188549	-3.67319
ENST00000513771	-3.6776
ENST00000434300	-3.67876
DB319310	-3.68381
ENST00000447309	-3.68413
ENST00000440241	-3.68414
ENST00000462083	-3.70815
ENST00000433876	-3.71954
ENST00000503675	-3.72528
ENST00000458718	-3.73089
chr11:57057697-57066754-	-3.73319

chr15:46971964-46982563+	-3.74397
ENST00000510485	-3.76122
uc001iuq.1	-3.78365
NR_028351	-3.79375
NR_003491	-3.8065
AW511194	-3.80969
ENST00000515105	-3.81179
uc003ebo.1	-3.82066
AK024389	-3.84026
uc003ibp.1	-3.88991
AK056959	-3.90844
AK098409	-3.91452
AW167909	-3.91476
ENST00000447646	-3.92631
NR_033265	-3.93487
chr3:24636446-24699146+	-3.96038
chr2:187731830-187759380-	-3.97421
ENST00000510016	-3.97919
BC037343	-3.99764
ENST00000444831	-4.01609
uc004aex.2	-4.01711
ENST00000422359	-4.02479
AA496137	-4.04022
ENST00000415019	-4.06024
NR_028044	-4.06062
BC034798	-4.06393
ENST00000402490	-4.06557
AK024231	-4.06622
CA395304	-4.07219
ENST00000449634	-4.08245
ENST00000505488	-4.11592
ENST00000479785	-4.12872
chr20:56692619-56702994+	-4.14383
uc.304+	-4.16158
AK096780	-4.16718
ENST00000457725	-4.1724
ENST00000306515	-4.18781
uc003jgj.2	-4.19542
ENST00000410913	-4.20409
ENST00000443031	-4.22106
BG619841	-4.23488

chr2:204428779-204440326-	-4.23651
ENST00000435632	-4.26905
uc001hbp.1	-4.27874
CR611171	-4.28106
ENST00000506476	-4.28469
BC009864	-4.29047
ENST00000334118	-4.29534
ENST00000434306	-4.29746
uc003kkq.1	-4.31707
BX648639	-4.32291
ENST00000416712	-4.35337
uc003udn.2	-4.36717
ENST00000508072	-4.38287
AK125824	-4.39747
DA204380	-4.40157
BC038756	-4.41337
BC042854	-4.42121
AK056676	-4.42519
uc003wpy.1	-4.42735
NR_033184	-4.44998
uc001ibs.1	-4.46768

chr10:31568469-31585244+	-4.47753
uc.81+	-4.48669
ENST00000504585	-4.49954
chr13:73819474-73846199+	-4.50024
BC028406	-4.52459
uc.121+	-4.55449
AF090887	-4.56438
uc001gmw.2	-4.57553
AK097966	-4.58517
ENST00000418615	-4.59068
AF052119	-4.60205
uc.102-	-4.61042
AK123376	-4.62738
chr4:25443352-25460177+	-4.63928
ENST00000511660	-4.69915
G36612	-4.70079
HIT000295253	-4.70251
AK091371	-4.70542
NR_027269	-4.7076
chr4:71997061-	-4.76914

72013886+	
uc002goe.1	-4.78199
ENST00000433396	-4.78275
ENST00000510564	-4.81093
ENST00000478982	-4.82078
ENST00000448961	-4.83567
ENST00000456384	-4.84014
G30803	-4.86439
ENST00000413993	-4.86925
NR_033438	-4.87766
ENST00000318406	-4.88418
ENST00000430364	-4.88797
AK126527	-4.88993
AF305819	-4.89313
uc001uoi.2	-4.89962
ENST00000451415	-4.9116
ENST00000439450	-4.9165
NR_026900	-4.92442
AF130065	-4.92935
ENST00000419158	-4.93187
ENST00000513330	-4.94214
ENST00000434531	-4.94949

AJ238554	-4.9511
AK057018	-4.9748
AK056943	-4.97834
G65607	-4.98375
ENST00000510845	-4.991
ENST00000442984	-4.99487
ENST00000412680	-5.0042
ENST00000407522	-5.05562
AK293938	-5.06351
ENST00000331122	-5.0797
ENST00000454456	-5.09783
AK097187	-5.10643
ENST00000461229	-5.11991
G30761	-5.13918
NR_033266	-5.1452
uc004abv.1	-5.14822
ENST00000447057	-5.15038
AK02164	-5.16632
AW270097	-5.17662
ENST00000509057	-5.18337
ENST00000431981	-5.19661
ENST00000504408	-5.21519

AY927550	-5.23962
AF070586	-5.24503
ENST00000422460	-5.26662
uc.425+	-5.29913
NR_026937	-5.32366
uc.362+	-5.32496
AF147361	-5.34509
AK125870	-5.3477
M15530	-5.36672
ENST00000355132	-5.38653
BG254544	-5.40826
AK125235	-5.40991
ENST00000439182	-5.45355
BM912149	-5.46188
ENST00000422120	-5.46326
BC015852	-5.47176
uc003bpu.1	-5.50648
uc.33+	-5.52105
ENST00000424487	-5.53443
ENST00000449144	-5.53609
AK309134	-5.55834
AI767623	-5.57225

chr14:76020622-76030872+	-5.60123
NR_027119	-5.61745
ENST00000406944	-5.62527
AK024621	-5.62822
NR_024388	-5.63766
HIT000395606	-5.70247
BC037882	-5.70562
ENST00000478814	-5.73842
ENST00000434601	-5.7451
NR_026803	-5.77491
ENST00000445083	-5.783
uc001wvl.1	-5.80588
uc004erg.1	-5.81287
ENST00000448700	-5.83252
AX810724	-5.86061
BC042023	-5.86317
BX648197	-5.87796
CR608123	-5.89663
uc.419+	-5.94888
uc002nrv.1	-5.95123
ENST00000420585	-5.96816

AK124863	-5.97759
ENST00000510759	-5.9778
uc004eqv.2	-5.98201
AX747038	-5.98269
BC014866	-5.98564
AK091880	-6.00629
uc.12-	-6.07495
CB857271	-6.08225
chr7:73684091-73687309-	-6.08283
AW516314	-6.08299
NR_026674	-6.10692
ENST00000508840	-6.18466
G36872	-6.20543
BX648207	-6.21708
uc001dnu.1	-6.23286
NR_002998	-6.23439
uc010kkf.1	-6.23752
AF130075	-6.26765
uc002jyv.1	-6.30105
ENST00000437831	-6.30498
AK022134	-6.30804

uc001omv.1	-6.31953
NR_002833	-6.35148
uc001gvu.2	-6.38862
ENST00000425763	-6.41572
AK001998	-6.41725
G36665	-6.42387
ENST00000425559	-6.44461
ENST00000426148	-6.4535
N36328	-6.49819
ENST00000506373	-6.531
AK126785	-6.53747
AW572416	-6.54543
ENST00000444137	-6.57357
NR_003149	-6.5924
ENST00000449485	-6.59718
uc003vcg.2	-6.62831
ENST00000474769	-6.63625
ENST00000512498	-6.64693
AF359416	-6.74124
uc.2+	-6.74938
AF119898	-6.76361
ENST00000439844	-6.76806

DB239440	-6.77059
CR595419	-6.78452
ENST00000454331	-6.78806
ENST00000435243	-6.79435
CR623291	-6.82164
ENST00000404529	-6.85222
BX477169	-6.88916
ENST00000437925	-6.90838
AL355738	-6.95226
ENST00000416584	-6.95419
ENST00000416959	-6.99476
uc.462+	-7.00657
ENST00000503681	-7.00802
ENST00000423712	-7.02252
NR_026885	-7.17058
ENST00000508209	-7.18313
CR613504	-7.21664
BC023650	-7.21987
ENST00000429099	-7.22601
ENST00000454260	-7.25225
AK022255	-7.27432
NR_002788	-7.36216

ENST00000401555	-7.37502
AK026750	-7.39118
ENST00000433131	-7.43542
NR_003934	-7.46131
AK000151	-7.51947
ENST00000509197	-7.60163
AK095147	-7.60814
G36663	-7.69696
ENST00000502685	-7.75249
AK130823	-7.76372
NR_033269	-7.7923
uc003eub.2	-7.80222
ENST00000501627	-7.877
uc.92-	-7.89494
ENST00000438808	-7.92469
CR598366	-7.96324
uc004aes.1	-7.98543
AI859713	-8.04549
uc.195+	-8.05196
AF143322	-8.08668
uc011dmf.1	-8.11601
uc001llv.1	-8.12935

ENST00000422521	-8.14032
AK021614	-8.17533
NR_027270	-8.20336
uc002ade.1	-8.28201
NR_024283	-8.32098
NR_024253	-8.33806
ENST00000420365	-8.34679
BC092457	-8.39414
DQ655957	-8.41223
HIT000089567	-8.45689
HIT000046399	-8.53483
CR624430	-8.58545
AF088026	-8.60001
uc010nwj.2	-8.63763
uc004aaw.1	-8.69232
CV370110	-8.71258
ENST00000431361	-8.74389
ENST00000431924	-8.88643
uc010kkv.1	-8.91304
ENST00000441336	-8.92729
AK055670	-8.937
AF075028	-8.94616

NR_024533	-8.96246
ENST00000508288	-8.97316
DA267910	-9.01531
ENST00000414365	-9.07442
ENST00000504219	-9.08288
uc002edy.2	-9.14326
DA195606	-9.16579
BC015876	-9.17933
HIT000047782	-9.26507
ENST00000417716	-9.31262
AF338234	-9.36677
AK022473	-9.40718
ENST00000454137	-9.43833
U58664	-9.50024
ENST00000452466	-9.52312
ENST00000436266	-9.54572
NR_024413	-9.5581
AF086156	-9.83921
ENST00000377547	-9.93108
AK090797	-9.95145
AK055194	-9.95214
ENST00000417888	-10.001

NR_004855	-10.142
ENST00000499988	-10.3254
ENST00000456053	-10.3366
ENST00000438935	-10.3654
AK128410	-10.3858
ENST00000509666	-10.6146
uc003kjh.3	-10.7375
AK024206	-10.8391
ENST00000439244	-10.967
AF090094	-11.2787
AK057933	-11.4695
uc001ihe.3	-11.5026
AK021415	-11.5866
uc001jei.2	-11.6271
ENST00000436802	-11.6422
X92110	-11.7399
ENST00000515247	-11.8846
AK023938	-11.9461
ENST00000514010	-12.1777
ENST00000450880	-12.2646
ENST00000485582	-12.2968
AK123944	-12.3108

NR_033322	-12.4909
AF070595	-12.5853
chr17:55283426-55307276+	-12.6654
ENST00000420330	-12.7373
ENST00000422088	-12.744
NR_024606	-12.8288
ENST00000438347	-12.9033
NR_027046	-13.1019
ENST00000379928	-13.2863
NR_026770	-13.7583
uc003mzj.1	-14.0818
AB073353	-14.1417
ENST00000453157	-14.2538
NR_026813	-14.3714
AL080082	-14.9627
AK125997	-15.2371
ENST00000363006	-15.6894
AK021572	-15.6954
AF086424	-16.1428
AK096084	-16.3892
uc.63-	-16.57

uc010lhv.1	-17.3019
HIT000028608	-17.4033
uc003ene.2	-17.4155
BQ187752	-17.4368
AL832122	-17.4601
ENST00000430825	-17.5465
ENST00000435945	-17.5616
uc001ich.2	-17.8736
NR_027294	-18.4032
NR_026657	-18.4755
AK021432	-19.0677
ENST00000419236	-19.3885
ENST00000503579	-19.938
NR_030697	-21.072
ENST00000421848	-21.9785
AK098399	-24.4871
AK055958	-25.3913
ENST00000504019	-28.8129
AK024988	-43.8012

Appendix Table 6. mRNA in PCa Exosomes

GeneSymbol	Fold-Change(PCa vs. PNT2)
GSPT2	38.167
SPIRE2	12.2856
ATP8B1	7.84979
NMNAT3	6.1734
ZNF256	5.04894
ZNF789	4.15442
ARPC1A	4.06565
CLDN2	3.86678
FOXD4	3.86626
SORBS1	3.86125
TRPC5	3.84404
LMBR1L	3.81486
SLC23A3	3.62524
PDIA5	3.27423
ADCK2	3.25236
P2RX4	3.16056
WDR85	2.91702
RNF31	2.9016
CD59	2.86484
ZNF655	2.68282
ZNF24	2.41066
PYCR1	2.36136
BDNF	2.35315
IGF2BP2	2.05556
HDHD1A	2.00357
TNFRSF19	-2.00294
IL23R	-2.03477
EVI2B	-2.04378
CNST	-2.06092
KCTD4	-2.0683
TCEB3B	-2.06873
C20orf85	-2.07736
FKBP5	-2.08621
CCL15	-2.09185
CPEB2	-2.10147
OR13C3	-2.11241
KLHDC8A	-2.11534
MS4A6E	-2.14013
ZNF98	-2.16606
DNAJB3	-2.18214

PLCXD2	-2.18251
XPR1	-2.20751
AGPAT1	-2.21682
LIMD1	-2.22778
PROM1	-2.23959
AKR1D1	-2.24058
LRRC48	-2.24975
PCDHGC5	-2.26155
OR5I1	-2.26452
ADAT2	-2.2824
HTN1	-2.33094
MGC87042	-2.3911
XAB2	-2.41242
UBAP1	-2.44268
PYDC2	-2.50678
IL13	-2.50996
ZNF784	-2.51762
ARPM1	-2.56773
SIRT2	-2.5783
ELN	-2.57925
TNF	-2.62617
CHD2	-2.65855

VPS53	-2.69034
IQCB1	-2.7477
NGFRAP1	-2.77649
SLC15A2	-2.83629
CLSPN	-2.83762
PPIL3	-2.84276
SMC1A	-2.85099
PLAC8	-2.85597
DCAF17	-2.89789
PIRT	-2.90278
SLC30A8	-2.92024
FANCB	-2.93321
DUSP10	-2.93498
EFCAB3	-2.94133
AURKC	-2.94617
NARFL	-2.94857
TMOD2	-2.98549
ZNF25	-3.10297
EGR4	-3.15635
LY6G5B	-3.29634
KIF24	-3.34197
ZNF484	-3.34302

IPO7	-3.37588
TYR	-3.39046
SLC37A3	-3.40833
OR10R2	-3.44147
BANF2	-3.49262
TMEM30A	-3.53151
ABCC4	-3.59636
CBLN1	-3.62419
IL11RA	-3.649
PIN4	-3.72473
ZNF99	-3.83394
ZNF673	-3.93605
OPA1	-3.98524
RBBP9	-4.11929
ZNF623	-4.18766
ZAR1	-4.19192
TAT	-4.6304
ANO6	-4.74982
MIER1	-4.9044
LYN	-4.92292
HPS5	-5.08229
RNF222	-7.03283

CRYGN	-7.65475
WNT4	-8.00456
MRGPRX3	-8.04255
PRAMEF10	-8.44867
GAL3ST4	-9.63308
CXorf59	-10.4702
CLVS2	-18.9929
P2RY10	-20.21
KIF5C	-24.682
TNFSF13B	-42.6385
CYP2F1	-48.701
PRG3	-50.8842
FXYD3	-60.2503
PRCP	-84.1002
PDE4B	-84.766

Appendix Table 7. lncRNA in PCa Exosomes

Sequence Name	Fold-Change(PCa exo vs. PNT2 exo)
uc003tje.3	9.26199
ENST00000427447	8.70007
BX648801	8.07532
ENST00000448271	6.43048
ENST00000412208	5.59751
NR_002158	3.44294
ENST00000506769	3.36333
uc.338+	2.75096
ENST00000427917	2.65833
AY927482	2.1943
G42927	2.0479
uc002lbc.1	-2.00361
AL133075	-2.00586
AF130063	-2.01543
chr8:20669795-20684520-	-2.01862
AI830440	-2.02593
ENST00000449714	-2.0267
L32786	-2.02684
AY927555	-2.02723
ENST00000474156	-2.03659
uc003jms.1	-2.03871
BQ187752	-2.03926
ENST00000430468	-2.05125
ENST00000416930	-2.05308
ENST00000514459	-2.05518
ENST00000451601	-2.06171
ENST00000429307	-2.06528
NR_026674	-2.06591
ENST00000513127	-2.07616
ENST00000504996	-2.08424
NR_027100	-2.08688
ENST00000449581	-2.089
ENST00000444110	-2.09195
chr18:22001892-22005509-	-2.09599
ENST00000442197	-2.09861
G36586	-2.10683
ENST00000442866	-2.10864

ENST00000473299	-2.11009
chr3:188617206-188630328-	-2.11955
ENST00000401029	-2.12016
BE792654	-2.13108
uc.450+	-2.13699
exon113+	-2.13825
BC047538	-2.14149
nc-HOXC8-148-	-2.14579
ENST00000453068	-2.15029
ENST00000404109	-2.15649
AF086275	-2.16049
ENST00000404428	-2.16191
BC092461	-2.18609
BC033941	-2.19615
uc.8-	-2.20273
G65622	-2.20886
NR_027918	-2.21582
ENST00000433227	-2.22147
ENST00000456526	-2.22687
uc.158+	-2.22887
DB197298	-2.22927

AK056398	-2.23463
ENST00000504752	-2.23617
AF113684	-2.23749
chr19:6516276-6522541-	-2.23974
AK025129	-2.24432
ENST00000515805	-2.27613
ENST00000428211	-2.29612
ENST00000417390	-2.3012
ENST00000445465	-2.30883
ENST00000447985	-2.31118
uc.386+	-2.32066
ENST00000435210	-2.32098
AK126826	-2.32171
ENST00000505632	-2.33325
ENST00000428581	-2.33376
chr2:130534055-130541005+	-2.33724
ENST00000475129	-2.33843
AK097189	-2.34129
ENST00000443897	-2.34974
G65645	-2.37871
ENST00000422483	-2.38332

uc.60+	-2.39705
chr4:10120852-10137502-	-2.40527
ENST00000420896	-2.40581
CR602329	-2.40653
ENST00000504399	-2.41006
G36761	-2.41008
chr15:67094324-67136376-	-2.41098
uc001zeh.1	-2.41858
AK123329	-2.43483
ENST00000381143	-2.44919
ENST00000366376	-2.45542
BC062796	-2.47843
ENST00000428146	-2.50302
AF070571	-2.52292
ENST00000455257	-2.52325
ENST00000460993	-2.52391
BX538340	-2.5324
uc001kgy.2	-2.53291
CR748447	-2.53909
uc.306-	-2.54835
ENST00000507497	-2.55347
ENST00000510570	-2.55443
BC127931	-2.55881
AK024988	-2.56414
AK023843	-2.56839
BC007917	-2.57104
ENST00000453474	-2.58844
ENST00000439077	-2.59144
uc001lxi.1	-2.59526
ENST00000450068	-2.59538
ENST00000417335	-2.59566
NR_001569	-2.59816
AK097620	-2.60584
AK098585	-2.60797
BC011242	-2.61798
uc.149+	-2.61826
ENST00000419614	-2.63837
uc.466-	-2.65149
NR_002725	-2.65939
BX648121	-2.67635
AF009305	-2.68724
DA833286	-2.6955
ENST00000407745	-2.72029

ENST00000425971	-2.76241
ENST00000480018	-2.77086
ENST00000503863	-2.78274
ENST00000368895	-2.7881
ENST00000442796	-2.79017
uc001ytz.1	-2.79957
U86813	-2.81162
ENST00000429657	-2.82359
uc010fdb.1	-2.87262
ENST00000402173	-2.88233
ENST00000505636	-2.89693
uc003ike.2	-2.90059
ENST00000448783	-2.95206
BC037791	-2.95699
ENST00000417727	-2.95749
BC043575	-2.96101
ENST00000501930	-2.96714
ENST00000380981	-2.97216
ENST00000446698	-2.98607
AF085943	-3.03865
AK054937	-3.0762
NR_027850	-3.08878

ENST00000439244	-3.12938
ENST00000428516	-3.1304
ENST00000413093	-3.14071
AA417063	-3.19442
nc-HOXA1-59-	-3.2008
ENST00000509327	-3.20739
HIT000089567	-3.22283
chr12:38744956-38769831+	-3.24436
AV731116	-3.31492
ENST00000432815	-3.33754
CV417507	-3.36589
AJ001889	-3.38052
AW809121	-3.42102
ENST00000426475	-3.42995
AF130056	-3.43806
ENST00000418161	-3.43974
BX647986	-3.44228
ENST00000419236	-3.44675
AK022441	-3.44915
NR_028412	-3.4544
chr7:80952564-80965489+	-3.54877

AF116656	-3.57457
AF086224	-3.62243
NR_026995	-3.62968
uc003iij.1	-3.67279
ENST00000417016	-3.70043
NR_027317	-3.71755
uc.409-	-3.77053
DA808840	-3.87343
BC073933	-3.89033
ENST00000440522	-3.89592
AK094677	-3.90568
NR_024481	-3.9057
AK000151	-3.91737
NR_002927	-3.94072
ENST00000509483	-3.98804
AK128149	-4.0331
ENST00000430825	-4.13813
NR_002825	-4.18153
NR_027237	-4.22333
CR627028	-4.28373
uc001plh.1	-4.36362
ENST00000448117	-4.42726

ENST00000423333	-4.54735
ENST00000420395	-4.6355
nc-HOXB2-162+	-4.93638
ENST00000439846	-5.09287
ENST00000426716	-5.1089
ENST00000437408	-5.11273
uc.313-	-5.19555
AK027393	-5.47274
AK097597	-5.56629
ENST00000436249	-5.72767
AK094780	-5.94621
U52051	-5.99218
AK057050	-6.13382
ENST00000508851	-6.15519
NR_026813	-6.33289
BG399904	-6.56025
AK097674	-7.7479
AK024690	-8.40351
BC042005	-9.84665
ENST00000428945	-10.9344
ENST00000454643	-11.717
ENST00000510579	-13.823

NR_024433	-14.1165
ENST00000419852	-14.7888
uc003myo.1	-16.8065
ENST00000418297	-19.6748
DB321928	-19.8717
ENST00000508179	-24.3901
AK098800	-35.8698
ENST00000405929	-37.134
ENST00000366160	-38.5479
ENST00000360436	-40.6836
AK130411	-53.2045
NR_002833	-59.0077
CR604021	-59.9725
BC131500	-246.807

Appendix Table 8. mRNAs secreted in exosomes by Androgen Independent PCa Cells

Gene Symbol	Fold-Change(AI exo vs. AD exo)
FDX1	14.9325
POLR3H	4.06399
GAS2L1	3.59606
PXN	2.8188
AKT1S1	2.39709
SRCAP	2.09299
NCEH1	-2.00869
FCGRT	-2.08575
TEKT3	-2.56002
NF2	-2.57631
MUC7	-2.60494
NAIP	-2.64492
RREB1	-2.65368
MAPK7	-2.66623
SUN1	-2.68173
GPR111	-2.68295
UQCC	-2.83566
GATM	-2.85684
FCHO2	-2.8835
SYTL2	-3.06934
CD8B	-3.34324
HOXD3	-3.40483
MCM8	-3.54894
GRIA4	-3.59164
MDC1	-3.6644
SMPD1	-3.74732
XAGE3	-3.79029
SPATA3	-3.92035
C17orf108	-3.9219
OR2D2	-4.24609
PTER	-5.19454
CREM	-5.20067

Appendix Table 9. lncRNAs secreted in exosomes by Androgen Independent PCa Cells

seqname	Fold-Change(AI exo vs. AD exo)
ENST00000426397	4.58268
ENST00000392635	3.87529
uc001asy.1	3.52296
AI638100	2.5926
uc002nrw.1	2.40564
ENST00000361653	2.32979
uc.35-	-2.0766
chr13:31090534-31097634+	-2.30112
G36703 G36703	-2.38398
BC113046	-2.38566
BC047494 BC047494	-2.45273
ENST00000435988	-2.53389
AK026449 AK026449	-2.66065
ENST00000414071	-2.80679
AK124842 AK124842 AK124842	-2.8262

BC016684	-2.86779
BF330770	-2.86811
chr20:541348-562112-	-2.8792
ENST00000411328	-2.88555
AL157490	-2.92292
ENST00000490865	-3.14601
ENST00000505053	-3.24769
ENST00000511596	-3.27181
ENST00000510469 ENST00000510469 ENST00000510469 ENST00000510469	-3.46581
DA877320 DA877320	-3.69623
ENST00000434988	-3.96562
ENST00000402263 ENST00000402263	-3.97844
BF223372	-4.54345
AF370371	-4.73942
ENST00000338236	-4.89949
ENST00000439443 ENST00000439443	-5.13883
chr5:20531868-20547218+	-5.37251

ENST00000449462	-5.41231
ENST00000443479	-5.63409

Bibliography

1. Porth CM (2007) *Essentials of Pathophysiology: Concepts of Altered Health States* (Lippincott Williams & Wilkins, Philadelphia) 2nd Ed p 1148.
2. Levine MA, Ittman M, Melamed J, & Lepor H (1998) Two consecutive sets of transrectal ultrasound guided sextant biopsies of the prostate for the detection of prostate cancer. *Journal of Urology* 159(2):471-476.
3. Eichler K*, et al.* (2006) Diagnostic Value of Systematic Biopsy Methods in the Investigation of Prostate Cancer: A Systematic Review. *Journal of Urology* 175(5):1605-1612.
4. Thompson IM*, et al.* (2009) Adjuvant Radiotherapy for Pathological T3N0M0 Prostate Cancer Significantly Reduces Risk of Metastases and Improves Survival: Long-Term Followup of a Randomized Clinical Trial. *Journal of Urology* 181(3):956-962.
5. Network AC (2010) *Localised Prostate Cancer - a guide for men and their families* 3rd Ed p 130.
6. Wolf AMD*, et al.* (2010) American Cancer Society guideline for the early detection of prostate cancer: Update 2010. *CA Cancer Journal for Clinicians* 60(2):70-98.
7. Catalona WJ*, et al.* (1998) Use of the percentage of free prostate-specific antigen to enhance differentiation of prostate cancer from benign prostatic disease: A prospective multicenter clinical trial. *Journal of the American Medical Association* 279(19):1542-1547.
8. Kawakami J, Siemens DR, & Nickel JC (2004) Prostatitis and prostate cancer: Implications for prostate cancer screening. *Urology* 64(6):1075-1080.
9. Haas GP & Sakr WA (1997) Epidemiology of prostate cancer. *Ca-A Cancer Journal for Clinicians* 47(5):273-287.
10. Loeb S, Carter HB, Berndt SI, Ricker W, & Schaeffer EM (2011) Complications after prostate biopsy: Data from SEER-Medicare. *Journal of Urology* 186(5):1830-1834.
11. Epstein JI, Walsh PC, Carmichael M, & Brendler CB (1994) Pathologic and Clinical Findings to Predict Tumor Extent of Nonpalpable (Stage T1 c) Prostate Cancer. *JAMA: The Journal of the American Medical Association* 271(5):368-374.
12. Wilt TJ*, et al.* (2008) Systematic review: Comparative effectiveness and harms of treatments for clinically localized prostate cancer. *Annals of Internal Medicine* 148(6):435-448.
13. Harris R & Lohr KN (2002) Screening for prostate cancer: An update of the evidence for the U.S. Preventive Services Task Force. *Annals of Internal Medicine* 137(11):917-929.
14. Stanford JL*, et al.* (2000) Urinary and sexual function after radical prostatectomy for clinically localized prostate cancer: The prostate cancer outcomes study. *Journal of the American Medical Association* 283(3):354-360.
15. Draisma G*, et al.* (2009) Lead time and overdiagnosis in prostate-specific antigen screening: Importance of methods and context. *Journal of the National Cancer Institute* 101(6):374-383.
16. Mitchell PS*, et al.* (2008) Circulating microRNAs as stable blood-based markers for cancer detection. *Proceedings of the National Academy of Sciences of the United States of America* 105(30):10513-10518.
17. Balzano F*, et al.* (2015) MiRNA stability in frozen plasma samples. *Molecules* 20(10):19030-19040.
18. Hanahan D & Weinberg Robert A (2011) Hallmarks of Cancer: The Next Generation. *Cell* 144(5):646-674.
19. Brenner S (1974) The Genetics of Caenorhabditis elegans. *Genetics* 77:71-94.

20. Lee RC, Feinbaum RL, & Ambros V (1993) The Heterochronic Gene lin-4 Encodes Small RNAs With Antisense Complimentarity to lin-14. *Cell* 75:843-855.
21. Reinhart BJ & Slack FJ (2000) The 21-nucleotide let-7 RNA regulates developmental timing in Caenorhabditis elegans. *Nature* 403(6772):901.
22. Roush S & Slack FJ (2008) The let-7 family of microRNAs. *Trends in Cell Biology* 18(10):505-516.
23. Lagos-Quintana M, Rauhut R, Lendeckel W, & Tuschl T (2001) Identification of novel genes coding for small expressed RNAs. *Science* 294(5543):853-858.
24. Lau NC, Lim LP, Weinstein EG, & Bartel DP (2001) An abundant class of tiny RNAs with probable regulatory roles in Caenorhabditis elegans. *Science* 294(5543):858-862.
25. Lee RC & Ambros V (2001) An extensive class of small RNAs in Caenorhabditis elegans. *Science* 294(5543):862-864.
26. Zhang B, Pan X, Cobb GP, & Anderson TA (2007) microRNAs as oncogenes and tumor suppressors. *Developmental Biology* 302(1):1-12.
27. Lee Y*, et al.* (2004) MicroRNA genes are transcribed by RNA polymerase II. *EMBO Journal* 23(20):4051-4060.
28. Yoontae L*, et al.* (2003) The nuclear RNase III Drosha initiates microRNA processing. *Nature* 425:415.
29. Tomari Y & Zamore PD (2005) MicroRNA Biogenesis: Drosha Can't Cut It without a Partner. *Current Biology* 15(2):R61-R64.
30. Han J*, et al.* (2004) The Drosha-DGCR8 complex in primary microRNA processing. *Genes and Development* 18(24):3016-3027.
31. Lund E, Güttinger S, Calado A, Dahlberg JE, & Kutay U (2004) Nuclear Export of MicroRNA Precursors. *Science* 303(5654):95-98.
32. Bernstein E, Caudy AA, Hammond SM, & Hannon GJ (2001) Role for a bidentate ribonuclease in the initiation step of RNA interference. *Nature* 409(6818):363.
33. Djuranovic S, Nahvi A, & Green R (2011) A Parsimonious Model for Gene Regulation by miRNAs. *Science* 331:550-553.
34. Wilczynska A & Bushell M (2015) The complexity of miRNA-mediated repression. *Cell Death and Differentiation* 22(1):22-33.
35. Fabian MR, Sonenberg N, & Filipowicz W (2010) Regulation of mRNA Translation and Stability by microRNAs. *Annual Review of Biochemistry* 79(1):351-379.
36. Piao X, Zhang X, Wu L, & Belasco JG (2010) CCR4-NOT Deadenylates mRNA Associated with RNA-Induced Silencing Complexes in Human Cells. *Mol. Cell. Biol.* 30(6):1486-1494.
37. Rouya C*, et al.* (2014) Human DDX6 effects miRNA-mediated gene silencing via direct binding to CNOT1. *RNA* 20(9):1398-1409.
38. Mathys H*, et al.* (2014) Structural and Biochemical Insights to the Role of the CCR4-NOT Complex and DDX6 ATPase in MicroRNA Repression. *Molecular Cell* 54(5):751-765.
39. Khavejian A, Svitkin YV, Sukarieh R, M'Boutchou MN, & Sonenberg N (2005) Mammalian poly(A)-binding protein is a eukaryotic translation initiation factor, which acts via multiple mechanisms. *Genes and Development* 19(1):104-113.
40. Roy G*, et al.* (2002) Paip1 interacts with poly(A) binding protein through two independent binding motifs. *Molecular & Cellular Biology* 22(11):3769-3782.
41. Martineau Y*, et al.* (2008) Poly(A)-binding protein-interacting protein 1 binds to eukaryotic translation initiation factor 3 to stimulate translation. *Molecular and Cell Biology* 21:6658-6667.
42. Craig AWB, Haghighat A, Yu ATK, & Sonenberg N (1998) Interaction of polyadenylate-binding protein with the eIF4G homologue PAIP enhances translation. *Nature* 392(6675):520-523.

43. Uchida N, Hoshino S, Imataka H, Sonenberg N, & Katada T (2002) A novel role of the mammalian GSPT/eRF3 associating with poly(A)-binding protein in Cap/Poly(A)-dependent translation. *Journal of Biological Chemistry* 277(52):50286-50292.
44. Chen C-YA, Zheng D, Xia Z, & Shyu A-B (2009) Ago–TNRC6 triggers microRNA-mediated decay by promoting two deadenylation steps. *Nature Structural & Molecular Biology* 16(11):1160-1166.
45. Coller J & Parker R (2004) EUKARYOTIC mRNA DECAPPING. *Annual Review of Biochemistry* 73(1):861-890.
46. Eichhorn SW*, et al.* (2014) MRNA Destabilization Is the dominant effect of mammalian microRNAs by the time substantial repression ensues. *Molecular Cell* 56(1):104-115.
47. Elbashir SM, Lendeckel W, & Tuschl T (2001) RNA interference is mediated by 21- and 22-nucleotide RNAs. *Genes and Development* 15(2):188-200.
48. Hutvágner G & Zamore PD (2002) A microRNA in a multiple-turnover RNAi enzyme complex. *Science* 297(5589):2056-2060.
49. Yekta S, Shih IH, & Bartel DP (2004) MicroRNA-Directed Cleavage of HOXB8 mRNA. *Science* 304(5670):594-596.
50. Liu J*, et al.* (2004) Argonaute2 Is the Catalytic Engine of Mammalian RNAi. *Science* 305(5689):1437-1441.
51. Tang G, Reinhart BJ, Bartel DP, & Zamore PD (2003) A biochemical framework for RNA silencing in plants. *Genes and Development* 17(1):49-63.
52. Iorio MV & Croce CM (2012) MicroRNA dysregulation in cancer: Diagnostics, monitoring and therapeutics. A comprehensive review. *EMBO Molecular Medicine* 4(3):143-159.
53. Calin GA & Croce CM (2007) Chromosomal rearrangements and microRNAs: A new cancer link with clinical implications. *Journal of Clinical Investigation* 117(8):2059-2066.
54. Medina PP, Nolde M, & Slack FJ (2010) OncomiR addiction in an in vivo model of microRNA-21-induced pre-B-cell lymphoma. *Nature* 467(7311):86-90.
55. Kozomara A & Griffiths-Jones S (2011) MiRBase: Integrating microRNA annotation and deep-sequencing data. *Nucleic Acids Research* 39(SUPPL. 1):D152-D157.
56. Cheng H*, et al.* (2011) Circulating plasma MiR-141 is a novel biomarker for metastatic colon cancer and predicts poor prognosis. *PLoS ONE* 6(3).
57. Catto JWF*, et al.* (2011) MicroRNA in Prostate, Bladder, and Kidney Cancer: A Systematic Review. *European Urology*:671 - 681.
58. Chang YL*, et al.* (2015) MicroRNA-7 inhibits the stemness of prostate cancer stem-like cells and tumorigenesis by repressing KLF4/PI3K/Akt/p21 pathway. *Oncotarget* 6(27):24017-24031.
59. Coppola V, De Maria R, & Bonci D (2010) MicroRNAs and prostate cancer. *Endocrine-Related Cancer* 17(1):F1-F17.
60. Cai S*, et al.* (2015) Downregulation of microRNA-23a suppresses prostate cancer metastasis by targeting the PAK6-LIMK1 signaling pathway. *Oncotarget* 6(6):3904-3917.
61. Cheng CY*, et al.* (2014) MiR-34 Cooperates with p53 in Suppression of Prostate Cancer by Joint Regulation of Stem Cell Compartment. *Cell Reports* 6(6):1000-1007.
62. Schaefer A*, et al.* (2010) Diagnostic and prognostic implications of microRNA profiling in prostate carcinoma. *International Journal of Cancer* 126(5):1166-1176.
63. Sun D*, et al.* (2011) miR-99 family of microRNAs suppresses the expression of prostate-specific antigen and prostate cancer cell proliferation. *Cancer Research* 71(4):1313-1324.
64. Xu B*, et al.* (2015) Hsa-miR-146a-5p modulates androgen-independent prostate cancer cells apoptosis by targeting ROCK1. *Prostate* 75(16):1896-1903.
65. Musiyenko A, Bitko V, & Barik S (2008) Ectopic expression of miR-126*, an intronic product of the vascular endothelial EGF-like 7 gene, regulates prostein translation and

invasiveness of prostate cancer LNCaP cells. *Journal of Molecular Medicine* 86(3):313-322.
66. Wei JJ*, et al.* (2011) Regulation of HMGA1 expression by MicroRNA-296 affects prostate cancer growth and invasion. *Clinical Cancer Research* 17(6):1297-1305.
67. Leite KRM*, et al.* (2011) MicroRNA-100 expression is independently related to biochemical recurrence of prostate cancer. *Journal of Urology* 185(3):1118-1122.
68. Dalmay T & Edwards DR (2006) MicroRNAs and the hallmarks of cancer. *Oncogene* 25(46):6170-6175.
69. Qihong H*, et al.* (2008) The microRNAs miR-373 and miR-520c promote tumour invasion and metastasis. *Nature Cell Biology* 10(2):202-210.
70. Leite KRM*, et al.* (2009) Change in expression of miR-let7c, miR-100, and miR-218 from high grade localized prostate cancer to metastasis. *Urologic Oncology: Seminars and Original Investigations*:265-269.
71. Kouzarides T (2007) Chromatin Modifications and Their Function. *Cell* 128(4):693-705.
72. Tsai MC*, et al.* (2010) Long noncoding RNA as modular scaffold of histone modification complexes. *Science* 329(5992):689-693.
73. Feng J*, et al.* (2006) The Evf-2 noncoding RNA is transcribed from the Dlx-5/6 ultraconserved region and functions as a Dlx-2 transcriptional coactivator. *Genes & Development* 20(11):8-8.
74. Moran VA, Perera RJ, & Khalil AM (2012) Emerging functional and mechanistic paradigms of mammalian long non-coding RNAs. *Nucleic Acids Research* 40(14):6391-6400.
75. Bernstein BE, Meissner A, & Lander ES (2007) The Mammalian Epigenome. *Cell* 128(4):669-681.
76. Khalil AM & Rinn JL (2011) RNA–protein interactions in human health and disease. *Seminars in Cell & Developmental Biology* 22(4):359-365.
77. Lamond AI & Spector DL (2003) Nuclear speckles: a model for nuclear organelles. *Nature Reviews Molecular Cell Biology* 4(8):605-612.
78. Nakagawa S & Hirose T (Paraspeckle nuclear bodies—useful uselessness? *Cellular and Molecular Life Sciences*:1-10.
79. Prasanth KV*, et al.* (2005) Regulating Gene Expression through RNA Nuclear Retention. *Cell* 123(2):249-263.
80. Tripathi V*, et al.* (2010) The Nuclear-Retained Noncoding RNA MALAT1 Regulates Alternative Splicing by Modulating SR Splicing Factor Phosphorylation. *Molecular Cell* 39(6):925-938.
81. Clemson CM*, et al.* (2009) An Architectural Role for a Nuclear Noncoding RNA: NEAT1 RNA Is Essential for the Structure of Paraspeckles. *Molecular Cell* 33(6):717-726.
82. Sharma S*, et al.* (2011) Dephosphorylation of the nuclear factor of activated T cells (NFAT) transcription factor is regulated by an RNA-protein scaffold complex. *Proceedings of the National Academy of Sciences of the United States of America* 108(28):11381-11386.
83. Beltran M*, et al.* (2008) A natural antisense transcript regulates Zeb2/Sip1 gene expression during Snail1-induced epithelial-mesenchymal transition. *Genes and Development* 22(6):756-769.
84. Kino T, Hurt DE, Ichijo T, Nader N, & Chrousos GP (2010) Noncoding RNA gas5 is a growth arrest- and starvation-associated repressor of the glucocorticoid receptor. *Sci Signal* 3(107).
85. Cesana M*, et al.* (2011) A Long Noncoding RNA Controls Muscle Differentiation by Functioning as a Competing Endogenous RNA. *Cell* 147(2):358-369.
86. Salzman J, Gawad C, Wang PL, Lacayo N, & Brown PO (2012) Circular RNAs are the predominant transcript isoform from hundreds of human genes in diverse cell types. *PLoS ONE* 7(2).

87. Jeck WR*, et al.* (2013) Circular RNAs are abundant, conserved, and associated with ALU repeats. *RNA* 19(2):141-157.
88. Wang PL*, et al.* (2014) Circular RNA is expressed across the eukaryotic tree of life. *PLoS ONE* 9(3).
89. Memczak S*, et al.* (2013) Circular RNAs are a large class of animal RNAs with regulatory potency. *Nature* 495(7441):333-338.
90. Hansen TB*, et al.* (2013) Natural RNA circles function as efficient microRNA sponges. *Nature* 495(7441):384-388.
91. Chung S*, et al.* (2011) Association of a novel long non-coding RNA in 8q24 with prostate cancer susceptibility. *Cancer Science* 102(1):245-252.
92. Clarke RA*, et al.* (2009) New genomic structure for prostate cancer specific gene PCA3 within BMCC1: Implications for prostate cancer detection and progression. *PLoS ONE* 4(3).
93. Ifere GO & Ananaba GA (2009) Prostate Cancer Gene Expression Marker 1 (PCGEM1): A patented prostate- specific non-coding gene and regulator of prostate cancer progression. *Recent Patents on DNA and Gene Sequences* 3(3):151-163.
94. Srikantan V*, et al.* (2000) PCGEM1, a prostate-specific gene, is overexpressed in prostate cancer. *Proceedings of the National Academy of Sciences of the United States of America* 97(22):12216-12221.
95. Laner T, Schulz WA, Engers R, Müller M, & Florl AR (2005) Hypomethylation of the XIST gene promoter in prostate cancer. *Oncology Research* 15(5):257-264.
96. Yap KL*, et al.* (2010) Molecular Interplay of the Noncoding RNA ANRIL and Methylated Histone H3 Lysine 27 by Polycomb CBX7 in Transcriptional Silencing of INK4a. *Molecular Cell* 38(5):662-674.
97. Cui Z*, et al.* (The prostate cancer-up-regulated long noncoding RNA PlncRNA-1 modulates apoptosis and proliferation through reciprocal regulation of androgen receptor. *Urologic Oncology: Seminars and Original Investigations*:1117-1123.
98. Kosaka N*, et al.* (2010) Secretory mechanisms and intercellular transfer of microRNAs in living cells. *Journal of Biological Chemistry* 285(23):17442-17452.
99. Montecalvo A*, et al.* (2012) Mechanism of transfer of functional microRNAs between mouse dendritic cells via exosomes. *Blood* 119(3):756-766.
100. Kogure T, Lin WL, Yan IK, Braconi C, & Patel T (2011) Intercellular nanovesicle-mediated microRNA transfer: A mechanism of environmental modulation of hepatocellular cancer cell growth. *Hepatology* 54(4):1237-1248.
101. Mathivanan S & Simpson RJ (2009) ExoCarta: A compendium of exosomal proteins and RNA. *Proteomics* 9(21):4997-5000.
102. Bhowmick NA & Moses HL (2005) Tumor–stroma interactions. *Current Opinion in Genetics & Development* 15(1):97-101.
103. Lobb RJ, Lima LG, & Möller A (2017) Exosomes: Key mediators of metastasis and pre-metastatic niche formation. *Seminars in Cell and Developmental Biology*:3-10.
104. Kucharzewska P*, et al.* (2013) Exosomes reflect the hypoxic status of glioma cells and mediate hypoxia-dependent activation of vascular cells during tumor development. *Proceedings of the National Academy of Sciences of the United States of America* 110(18):7312-7317.
105. Umezu T*, et al.* (2014) Exosomal miR-135b shed from hypoxic multiple myeloma cells enhances angiogenesis by targeting factor-inhibiting HIF-1. *Blood* 124(25):3748-3757.
106. Meacham CE & Morrison SJ (2013) Tumour heterogeneity and cancer cell plasticity. *Nature* 501(7467):328-337.
107. Xiao D*, et al.* (2016) Melanoma cell-derived exosomes promote epithelial-mesenchymal transition in primary melanocytes through paracrine/autocrine signaling in the tumor microenvironment. *Cancer Letters* 376(2):318-327.

108. Beckler MD*, et al.* (2013) Proteomic analysis of exosomes from mutant KRAS colon cancer cells identifies intercellular transfer of mutant KRAS. *Molecular and Cellular Proteomics* 12(2):343-355.
109. Hiratsuka S*, et al.* (2002) MMP9 induction by vascular endothelial growth factor receptor-1 is involved in lung-specific metastasis. *Cancer Cell* 2(4):289-300.
110. Kaplan RN*, et al.* (2005) VEGFR1-positive haematopoietic bone marrow progenitors initiate the pre-metastatic niche. *Nature* 438(7069):820-827.
111. Zhou W*, et al.* (2014) Cancer-Secreted miR-105 destroys vascular endothelial barriers to promote metastasis. *Cancer Cell* 25(4):501-515.
112. Zheng H*, et al.* (2006) Expressions of MMP-2, MMP-9 and VEGF are closely linked to growth, invasion, metastasis and angiogenesis of gastric carcinoma. *Anticancer Research* 26(5 A):3579-3583.
113. Grange C*, et al.* (2011) Microvesicles released from human renal cancer stem cells stimulate angiogenesis and formation of lung premetastatic niche. *Cancer Research* 71(15):5346-5356.
114. Andreola G*, et al.* (2002) Induction of lymphocyte apoptosis by tumor cell secretion of FasL-bearing microvesicles. *Journal of Experimental Medicine* 195(10):1303-1316.
115. Huber V*, et al.* (2005) Human colorectal cancer cells induce T-cell death through release of proapoptotic microvesicles: Role in immune escape. *Gastroenterology* 128(7):1796-1804.
116. Jeong WK*, et al.* (2005) Fas ligand-positive membranous vesicles isolated from sera of patients with oral cancer induce apoptosis of activated T lymphocytes. *Clinical Cancer Research* 11(3):1010-1020.
117. Yu S*, et al.* (2007) Tumor exosomes inhibit differentiation of bone marrow dendritic cells. *Journal of Immunology* 178(11):6867-6875.
118. Xiang X*, et al.* (2009) Induction of myeloid-derived suppressor cells by tumor exosomes. *International Journal of Cancer* 124(11):2621-2633.
119. Peinado H, Lavotshkin S, & Lyden D (2011) The secreted factors responsible for pre-metastatic niche formation: Old sayings and new thoughts. *Seminars in Cancer Biology* 21(2):139-146.
120. Valenti R*, et al.* (2006) Human tumor-released microvesicles promote the differentiation of myeloid cells with transforming growth factor-β-mediated suppressive activity on T lymphocytes. *Cancer Research* 66(18):9290-9298.
121. Mitchell PJ*, et al.* (2009) Can urinary exosomes act as treatment response markers in prostate cancer? *Journal of Translational Medicine* 7.
122. Muralidharan-Chari V, Clancy JW, Sedgwick A, & D'Souza-Schorey C (2010) Microvesicles: Mediators of extracellular communication during cancer progression. *Journal of Cell Science* 123(10):1603-1611.
123. Ratajczak J, Wysoczynski M, Hayek F, Janowska-Wieczorek A, & Ratajczak MZ (2006) Membrane-derived microvesicles: Important and underappreciated mediators of cell-to-cell communication. *Leukemia* 20(9):1487-1495.
124. Samsonov R*, et al.* (2016) Lectin-induced agglutination method of urinary exosomes isolation followed by mi-RNA analysis: Application for prostate cancer diagnostic. *Prostate* 76(1):68-79.
125. Li Z*, et al.* (2015) Exosomal microRNA-141 is upregulated in the serum of prostate cancer patients. *OncoTargets and Therapy* 9:139-148.
126. Li M*, et al.* (2015) An optimized procedure for exosome isolation and analysis using serum samples: Application to cancer biomarker discovery. *Methods* 87:26-30.
127. Huang X*, et al.* (2015) Exosomal miR-1290 and miR-375 as prognostic markers in castration-resistant prostate cancer. *European Urology* 67(1):33-41.
128. Işin M*, et al.* (2015) Exosomal lncRNA-p21 levels may help to distinguish prostate cancer from benign disease. *Frontiers in Genetics* 6(MAY).

129. Ahadi A, Brennan S, Kennedy PJ, Hutvagner G, & Tran N (2016) Long non-coding RNAs harboring miRNA seed regions are enriched in prostate cancer exosomes. *Scientific Reports* 6:24922.
130. Umezu T, Ohyashiki K, Kuroda M, & Ohyashiki JH (2013) Leukemia cell to endothelial cell communication via exosomal miRNAs. *Oncogene* 32(22):2747-2755.
131. Théry C, Amigorena S, Raposo G, & Clayton A (2006) Isolation and Characterization of Exosomes from Cell Culture Supernatants and Biological Fluids. *Curr Protoc Cell Biol* 30.
132. Horoszewicz JS*, et al.* (1980) The LNCaP cell line--a new model for studies on human prostatic carcinoma. *Progress in clinical and biological research* 37:115-132.
133. Stone KR, Mickey DD, Wunderli H, Mickey GH, & Paulson DF (1978) Isolation of a human prostate carcinoma cell line (DU 145). *International Journal of Cancer* 21(3):274-281.
134. Kaighn ME, Shankar Narayan K, & Ohnuki Y (1979) Establishment and characterization of a human prostatic carcinoma cell line (PC-3). *Investigative Urology* 17(1):16-23.
135. Korenchuk S*, et al.* (2001) VCaP, a cell-based model system of human prostate cancer. *In Vivo* 15(2):163-168.
136. Berthon P, Cussenot O, Hopwood L, Le Duc A, & Maitland NJ (1995) Functional expression of SV40 in normal human prostatic epithelial and fibroblastic cells: Differentiation pattern of non-tumorigenic cell lines. *International Journal of Oncology* 6(2):333-343.
137. Théry C, Amigorena S, Raposo G, & Clayton A (2006) Isolation and characterization of exosomes from cell culture supernatants and biological fluids. *Current protocols in cell biology / editorial board, Juan S. Bonifacino ... [et al.]* Chapter 3.
138. Agilent Technologies I (2013) Agilent Small RNA Kit Guide. (Agilent Technologies, Waldbronn).
139. Technologies L (2010) Taqman Gene Expression Assays Protocol. (Life Technologies, Carlsbad).
140. Smoot ME, Ono K, Ruscheinski J, Wang PL, & Ideker T (2011) Cytoscape 2.8: New features for data integration and network visualization. *Bioinformatics* 27(3):431-432.
141. Saito R*, et al.* (2012) A travel guide to Cytoscape plugins. *Nature Methods* 9(11):1069-1076.
142. Garcia DM*, et al.* (2011) Weak seed-pairing stability and high target-site abundance decrease the proficiency of lsy-6 and other microRNAs. *Nat Struct Mol Biol* 18(10):1139-1146.
143. Warde-Farley D*, et al.* (2010) The GeneMANIA prediction server: biological network integration for gene prioritization and predicting gene function. *Nucleic Acids Research* 38(suppl 2):W214-W220.
144. Bader GD & Hogue CW (2003) An automated method for finding molecular complexes in large protein interaction networks. *BMC Bioinformatics* 4(2):13.
145. Bindea G*, et al.* (2009) ClueGO: a Cytoscape plug-in to decipher functionally grouped gene ontology and pathway annotation networks. *Bioinformatics* 25(8):1091-1093.
146. Milane L, Singh A, Mattheolabakis G, Suresh M, & Amiji MM (2015) Exosome mediated communication within the tumor microenvironment. *Journal of Controlled Release* 219:278-294.
147. Bustin SA (2010) Why the need for qPCR publication guidelines?—The case for MIQE. *Methods* 50(4):217-226.
148. Dooms M, Chango A, Barbour E, Pouillart P, & Abdel Nour AM (2013) Improving biological relevancy of transcriptional biomarkers experiments by applying the MIQE guidelines to pre-clinical and clinical trials. *Methods* 59(1):147-153.
149. Vlassov AV, Magdaleno S, Setterquist R, & Conrad R (2012) Exosomes: Current knowledge of their composition, biological functions, and diagnostic and therapeutic potentials. *Biochimica et Biophysica Acta - General Subjects* 1820(7):940-948.

150. Ji H*, et al.* (2013) Proteome profiling of exosomes derived from human primary and metastatic colorectal cancer cells reveal differential expression of key metastatic factors and signal transduction components. *Proteomics* 13(10-11):1672-1686.
151. Sánchez CA*, et al.* (2016) Exosomes from bulk and stem cells from human prostate cancer have a differential microRNA content that contributes cooperatively over local and pre-metastatic niche. *Oncotarget* 7(4):3993-4008.
152. Willms E*, et al.* (2016) Cells release subpopulations of exosomes with distinct molecular and biological properties. *Scientific Reports* 6.
153. Goswami S*, et al.* (2016) Differential Expression and Significance of Circulating microRNAs in Cerebrospinal Fluid of Acute Encephalitis Patients Infected with Japanese Encephalitis Virus. *Molecular Neurobiology*:1-11.
154. Coakley G, Maizels RM, & Buck AH (2015) Exosomes and Other Extracellular Vesicles: The New Communicators in Parasite Infections. *Trends in Parasitology* 31(10):477-489.
155. Berrone E*, et al.* (2015) Detection of cellular prion protein in exosomes derived from ovine plasma. *Journal of General Virology* 96(12):3698-3702.
156. Kanada M, Bachmann MH, & Contag CH (2016) Signaling by Extracellular Vesicles Advances Cancer Hallmarks. *Trends in Cancer* 2(2):84-94.
157. Meehan K & Vella LJ (2016) The contribution of tumour-derived exosomes to the hallmarks of cancer. *Critical Reviews in Clinical Laboratory Sciences* 53(2):121-131.
158. Hanahan D & Weinberg RA (The Hallmarks of Cancer. *Cell* 100(1):57-70.
159. Clayton A & Tabi Z (2005) Exosomes and the MICA-NKG2D system in cancer. *Blood Cells, Molecules, and Diseases* 34(3):206-213.
160. Clayton A*, et al.* (2008) Human tumor-derived exosomes down-modulate NKG2D expression. *Journal of Immunology* 180(11):7249-7258.
161. Hedlund M, Nagaeva O, Kargl D, Baranov V, & Mincheva-Nilsson L (2011) Thermal- and oxidative stress causes enhanced release of NKG2D ligand-bearing immunosuppressive exosomes in leukemia/lymphoma T and B cells. *PLoS ONE* 6(2).
162. Lundholm M*, et al.* (2014) Prostate tumor-derived exosomes down-regulate NKG2D expression on natural killer cells and CD8+ T cells: Mechanism of immune evasion. *PLoS ONE* 9(9).
163. Raulet DH (2003) Roles of the NKG2D immunoreceptor and its ligands. *Nature Reviews Immunology* 3(10):781-790.
164. Abusamra AJ*, et al.* (2005) Tumor exosomes expressing Fas ligand mediate CD8+ T-cell apoptosis. *Blood Cells, Molecules, and Diseases* 35(2):169-173.
165. Yang L, Wu X, Wang D, Luo C, & Chen L (2013) Renal carcinoma cell-derived exosomes induce human immortalized line of Jurkat t lymphocyte apoptosis in vitro. *Urologia Internationalis* 91(3):363-369.
166. Gabrilovich DI & Nagaraj S (2009) Myeloid-derived suppressor cells as regulators of the immune system. *Nat Rev Immunol* 9(3):162-174.
167. Ostrand-Rosenberg S & Sinha P (2009) Myeloid-Derived Suppressor Cells: Linking Inflammation and Cancer. *The Journal of Immunology* 182(8):4499-4506.
168. Gobbo J*, et al.* (2016) Restoring Anticancer Immune Response by Targeting Tumor-Derived Exosomes with a HSP70 Peptide Aptamer. *Journal of the National Cancer Institute* 108(3).
169. Zaidi MR & Merlino G (2011) The Two Faces of Interferon-γ in cancer. *Clinical cancer research : an official journal of the American Association for Cancer Research* 17(19):6118-6124.
170. Wang X & Lin Y (2008) Tumor necrosis factor and cancer, buddies or foes? *Acta pharmacologica Sinica* 29(11):1275-1288.
171. Lehrfeld TJ & Lee DI (Dendritic cell vaccines for the treatment of prostate cancer. *Urologic Oncology: Seminars and Original Investigations* 26(6):576-580.

172. Pampena MB & Levy EM (2015) Natural Killer Cells as Helper Cells in Dendritic Cell Cancer Vaccines. *Frontiers in Immunology* 6:13.
173. Boyman O & Sprent J (2012) The role of interleukin-2 during homeostasis and activation of the immune system. *Nature Reviews Immunology* 12(3):180-190.
174. Yu TK, Caudell EG, Smid C, & Grimm EA (2000) IL-2 activation of NK cells: Involvement of MKK1/2/ERK but not p38 kinase pathway. *Journal of Immunology* 164(12):6244-6251.
175. Rakoff-Nahoum S & Medzhitov R (2009) Toll-like receptors and cancer. *Nature Reviews Cancer* 9(1):57-63.
176. Razack AH (2007) Bacillus Calmette–Guerin and bladder cancer. *Asian Journal of Surgery* 30(4):302-309.
177. Zhang Y*, et al.* (2014) Systemic injection of TLR1/2 agonist improves adoptive antigen-specific T cell therapy in glioma-bearing mice. *Clinical Immunology* 154(1):26-36.
178. Li S, Sun R, Chen Y, Wei H, & Tian Z (2015) TLR2 limits development of hepatocellular carcinoma by reducing IL18-mediated immunosuppression. *Cancer Research* 75(6):986-995.
179. Mills IG (2014) Maintaining and reprogramming genomic androgen receptor activity in prostate cancer. *Nat Rev Cancer*:187-198.
180. Batra P & Sharma AK (2013) Anti-cancer potential of flavonoids: recent trends and future perspectives. *3 Biotech* 3(6):439-459.
181. Fantini M*, et al.* (2015) In vitro and in vivo antitumoral effects of combinations of polyphenols, or polyphenols and anticancer drugs: Perspectives on cancer treatment. *International Journal of Molecular Sciences* 16(5):9236-9282.
182. Yang H & Dou QP (2010) Targeting Apoptosis Pathway with Natural Terpenoids: Implications for Treatment of Breast and Prostate Cancer. *Current Drug Targets* 11(6):733-744.
183. Sundin T, Peffley DM, Gauthier D, & Hentosh P (2012) The isoprenoid perillyl alcohol inhibits telomerase activity in prostate cancer cells. *Biochimie* 94(12):2639-2648.
184. Ohlsson Å, Ullerås E, Cedergreen N, & Oskarsson A (2010) Mixture effects of dietary flavonoids on steroid hormone synthesis in the human adrenocortical H295R cell line. *Food and Chemical Toxicology* 48(11):3194-3200.
185. Laverdière I*, et al.* (2015) The UGT1 locus is a determinant of prostate cancer recurrence after prostatectomy. *Endocrine-Related Cancer* 22(1):77-85.
186. Pino-Lagos K, Benson MJ, & Noelle RJ (2008) Retinoic Acid in the Immune System. *Annals of the New York Academy of Sciences* 1143:10.1196/annals.1443.1017.
187. Geissmann F*, et al.* (2003) Retinoids Regulate Survival and Antigen Presentation by Immature Dendritic Cells. *The Journal of Experimental Medicine* 198(4):623-634.
188. Mohty M*, et al.* (2003) All-trans retinoic acid skews monocyte differentiationinto interleukin-12-secreting dendritic-like cells. *British Journal of Haematology* 122(5):829-836.
189. Taraboletti G*, et al.* (1997) Effect of all trans-retinoic acid (ATRA) on the adhesive and motility properties of acute promyelocytic leukemia cells. *International Journal of Cancer* 70(1):72-77.
190. Saurer L, McCullough KC, & Summerfield A (2007) In Vitro Induction of Mucosa-Type Dendritic Cells by All-Trans Retinoic Acid. *The Journal of Immunology* 179(6):3504-3514.
191. Bronte V, Serafini P, Apolloni E, & Zanovello P (2001) Tumor-induced immune dysfunctions caused by myeloid suppressor cells. *Journal of Immunotherapy* 24(6):431-446.
192. Huang X*, et al.* (2013) Characterization of human plasma-derived exosomal RNAs by deep sequencing. *BMC Genomics* 14(1):1-14.

193. Chen Y, Gelfond JAL, McManus LM, & Shireman PK (2009) Reproducibility of quantitative RT-PCR array in miRNA expression profiling and comparison with microarray analysis. *BMC Genomics* 10(1):1-10.
194. Git A*, et al.* (2010) Systematic comparison of microarray profiling, real-time PCR, and next-generation sequencing technologies for measuring differential microRNA expression. *RNA* 16(5):991-1006.
195. Wang B & Xi Y (2013) Challenges for MicroRNA Microarray Data Analysis. *Microarrays (Basel, Switzerland)* 2(2):10.3390/microarrays2020034.
196. Cheruvanky A*, et al.* (2007) Rapid isolation of urinary exosomal biomarkers using a nanomembrane ultrafiltration concentrator. *American Journal of Physiology - Renal Physiology* 292(5):F1657-F1661.
197. Channavajjhalaa SK*, et al.* (2014) Optimizing the purification and analysis of miRNAs from urinary exosomes. *Clinical Chemistry and Laboratory Medicine* 52(3):345-354.
198. Enderle D*, et al.* (2015) Characterization of RNA from exosomes and other extracellular vesicles isolated by a novel spin column-based method. *PLoS ONE* 10(8).
199. Armstrong DA, Green BB, Seigne JD, Schned AR, & Marsit CJ (2015) MicroRNA molecular profiling from matched tumor and bio-fluids in bladder cancer. *Molecular Cancer* 14(1).
200. Zlotogorski-Hurvitz A*, et al.* (2015) Human Saliva-Derived Exosomes: Comparing Methods of Isolation. *Journal of Histochemistry and Cytochemistry* 63(3):181-189.
201. Ravi RK, Khosroheidari M, & DiStefano JK (2015) A modified precipitation method to isolate urinary exosomes. *Journal of Visualized Experiments* (95).
202. Alvarez ML (2014) Isolation of urinary exosomes for RNA biomarker discovery using a simple, fast, and highly scalable method. in *Methods in Molecular Biology*, pp 145-170.
203. Lötvall J*, et al.* (2014) Minimal experimental requirements for definition of extracellular vesicles and their functions: a position statement from the International Society for Extracellular Vesicles. *Journal of Extracellular Vesicles; Vol 3 (2014) incl supplements*.
204. Rood IM*, et al.* (2010) Comparison of three methods for isolation of urinary microvesicles to identify biomarkers of nephrotic syndrome. *Kidney International* 78(8):810-816.
205. Muller L, Hong CS, Stolz DB, Watkins SC, & Whiteside TL (2014) Isolation of biologically-active exosomes from human plasma. *Journal of Immunological Methods* 411:55-65.
206. Böing AN*, et al.* (2014) Single-step isolation of extracellular vesicles by size-exclusion chromatography. *Journal of Extracellular Vesicles* 3:10.3402/jev.v3403.23430.
207. Zarovni N*, et al.* (2015) Integrated isolation and quantitative analysis of exosome shuttled proteins and nucleic acids using immunocapture approaches. *Methods* 87:46-58.
208. Kalra H*, et al.* (2013) Comparative proteomics evaluation of plasma exosome isolation techniques and assessment of the stability of exosomes in normal human blood plasma. *Proteomics* 13(22):3354-3364.
209. Taylor DD & Gercel-Taylor C (2008) MicroRNA signatures of tumor-derived exosomes as diagnostic biomarkers of ovarian cancer. *Gynecologic Oncology* 110(1):13-21.
210. Kim G*, et al.* (2012) Noble polymeric surface conjugated with zwitterionic moieties and antibodies for the isolation of exosomes from human serum. *Bioconjugate Chemistry* 23(10):2114-2120.
211. Mizutani K*, et al.* (2014) Isolation of prostate cancer-related exosomes. *Anticancer Research* 34(7):3419-3423.
212. Hong CS, Muller L, Boyiadzis M, & Whiteside TL (2014) Isolation and characterization of CD34+ blast-derived exosomes in acute myeloid leukemia. *PLoS ONE* 9(8).
213. Chen C*, et al.* (2014) Paper-based immunoaffinity devices for accessible isolation and characterization of extracellular vesicles. *Microfluidics and Nanofluidics* 16(5):849-856.

214. Chen C, Lin BR, Hsu MY, & Cheng CM (2015) Paper-based devices for isolation and characterization of extracellular vesicles. *Journal of Visualized Experiments* 2015(98).
215. Chen C*, et al.* (2010) Microfluidic isolation and transcriptome analysis of serum microvesicles. *Lab on a Chip - Miniaturisation for Chemistry and Biology* 10(4):505-511.
216. He M, Crow J, Roth M, Zeng Y, & Godwin AK (2014) Integrated immunoisolation and protein analysis of circulating exosomes using microfluidic technology. *Lab on a Chip - Miniaturisation for Chemistry and Biology* 14(19):3773-3780.
217. Kanwar SS, Dunlay CJ, Simeone DM, & Nagrath S (2014) Microfluidic device (ExoChip) for on-chip isolation, quantification and characterization of circulating exosomes. *Lab on a Chip - Miniaturisation for Chemistry and Biology* 14(11):1891-1900.
218. Zhao Z, Yang Y, Zeng Y, & He M (2016) A microfluidic ExoSearch chip for multiplexed exosome detection towards blood-based ovarian cancer diagnosis. *Lab on a Chip - Miniaturisation for Chemistry and Biology* 16(3):489-496.
219. Ltd. N (2012) nanosight LM10 HS Operating Manual. (Nanosight LTd., Wiltshire).
220. Ltd. N (2012) NanoSight NTA 2.3 Analytical Software. (Nanosight Ltd., Wiltshire).
221. Livak KJ & Schmittgen TD (2001) Analysis of Relative Gene Expression Data Using Real-Time Quantitative PCR and the 2−ΔΔCT Method. *Methods* 25(4):402-408.
222. Hessvik NP, Phuyal S, Brech A, Sandvig K, & Llorente A (2012) Profiling of microRNAs in exosomes released from PC-3 prostate cancer cells. *Biochimica et Biophysica Acta - Gene Regulatory Mechanisms* 1819(11):1154-1163.
223. Hessvik NP, Sandvig K, & Llorente A (2013) Exosomal miRNAs as biomarkers for prostate cancer. *Frontiers in Genetics* 4(MAR).
224. B. Lam MS, Y. Haj-Ahmad (2012) Revised Guidelines for RNA Quality Assessment for Diverse Biological Sample Input. (Norgen Biotek Corporation).
225. De Long J*, et al.* (2015) A non-invasive miRNA based assay to detect bladder cancer in cell-free urine. *American Journal of Translational Research* 7(11):2500-2509.
226. Qiagen (2015) ExoRNeasy Serum/Plasma Handbook. (Qiagen, Limburg).
227. Biosystems A (2011) Optimized protocol with low sample input for profiling human microRNA using the OpenArray platform. (Life Technologies).
228. Fernández-Llama P*, et al.* (2010) Tamm-Horsfall protein and urinary exosome isolation. *Kidney International* 77(8):736-742.
229. Kosanović M & Janković M (2014) Isolation of urinary extracellular vesicles from Tamm-Horsfall protein–depleted urine and their application in the development of a lectin-exosome-binding assay. *BioTechniques* 57(3):143-149.
230. D'haene B, Mestdagh P, Hellemans J, & Vandesompele J (2012) miRNA Expression Profiling: From Reference Genes to Global Mean Normalization. *Next-Generation MicroRNA Expression Profiling Technology: Methods and Protocols*, ed Fan J-B (Humana Press, Totowa, NJ), pp 261-272.
231. Hajian-Tilaki K (2014) Sample size estimation in diagnostic test studies of biomedical informatics. *Journal of Biomedical Informatics* 48:193-204.
232. Moschos S, Varanasi S, & Kirkwood JM (2005) Interferons in the treatment of solid tumors. *Cancer treatment and research* 126:207-241.
233. Schreiber RD, Old LJ, & Smyth MJ (2011) Cancer immunoediting: Integrating immunity's roles in cancer suppression and promotion. *Science* 331(6024):1565-1570.
234. Dunn GP, Old LJ, & Schreiber RD (2004) The three Es of cancer immunoediting. in *Annual Review of Immunology*, pp 329-360.
235. Dunn GP*, et al.* (2005) A critical function for type I interferons in cancer immunoediting. *Nature Immunology* 6(7):722-729.
236. Koebel CM*, et al.* (2007) Adaptive immunity maintains occult cancer in an equilibrium state. *Nature* 450(7171):903-907.
237. Chen HM*, et al.* (2009) Critical role for constitutive type I interferon signaling in the prevention of cellular transformation. *Cancer Science* 100(3):449-456.

238. Meixlsperger S*, et al.* (2013) CD141+ dendritic cells produce prominent amounts of IFN-α after dsRNA recognition and can be targeted via DEC-205 in humanized mice. *Blood* 121(25):5034-5044.
239. Reizis B, Bunin A, Ghosh HS, Lewis KL, & Sisirak V (2011) Plasmacytoid dendritic cells: Recent progress and open questions. in *Annual Review of Immunology*, pp 163-183.
240. Woo SR*, et al.* (2014) STING-dependent cytosolic DNA sensing mediates innate immune recognition of immunogenic tumors. *Immunity* 41(5):830-842.
241. Guillot B*, et al.* (2005) The expression of cytotoxic mediators is altered in mononuclear cells of patients with melanoma and increased by interferon-α treatment. *British Journal of Dermatology* 152(4):690-696.
242. Crouse J*, et al.* (Type I Interferons Protect T Cells against NK Cell Attack Mediated by the Activating Receptor NCR1. *Immunity* 40(6):961-973.
243. Xu Haifeng C*, et al.* (Type I Interferon Protects Antiviral CD8⁺ T Cells from NK Cell Cytotoxicity. *Immunity* 40(6):949-960.
244. Novikov A*, et al.* (2011) Mycobacterium tuberculosis triggers host type I IFN signaling to regulate IL-1β production in human macrophages. *Journal of Immunology* 187(5):2540-2547.
245. Nguyen DP, Li J, Yadav SS, & Tewari AK (2014) Recent insights into NF-κB signalling pathways and the link between inflammation and prostate cancer. *BJU International* 114(2):168-176.
246. Khan S*, et al.* (2009) Extracellular, cell-permeable survivin inhibits apoptosis while promoting proliferative and metastatic potential. *British Journal of Cancer* 100(7):1073-1086.
247. Khan S*, et al.* (2011) Survivin is released from cancer cells via exosomes. *Apoptosis* 16(1):1-12.
248. Khan S*, et al.* (2012) Plasma-Derived Exosomal Survivin, a Plausible Biomarker for Early Detection of Prostate Cancer. *PLoS ONE* 7(10).
249. Samant RS*, et al.* (2007) Breast cancer metastasis suppressor 1 (BRMS1) inhibits osteopontin transcription by abrogating NF-κB activation. *Molecular Cancer* 6(1):1-9.
250. Lin L, Spoor MS, Gerth AJ, Brody SL, & Peng SL (2004) Modulation of Th1 Activation and Inflammation by the NF-κB Repressor Foxj1. *Science* 303(5660):1017-1020.
251. Lee SY, Rim Y, McPherson DD, Huang SL, & Kim H (2014) A novel liposomal nanomedicine for nitric oxide delivery and breast cancer treatment. *Bio-Medical Materials and Engineering* 24(1):61-67.
252. Webber J, Steadman R, Mason MD, Tabi Z, & Clayton A (2010) Cancer exosomes trigger fibroblast to myofibroblast differentiation. *Cancer Research* 70(23):9621-9630.
253. Lamparski HG*, et al.* (2002) Production and characterization of clinical grade exosomes derived from dendritic cells. *Journal of Immunological Methods* 270(2):211-226.
254. systems RD (2013) DuoSet ELISA Development Systems.
255. Chowdhury R*, et al.* (2015) Cancer exosomes trigger mesenchymal stem cell differentiation into pro-angiogenic and pro-invasive myofibroblasts. *Oncotarget* 6(2):715-731.
256. Webber JP*, et al.* (2015) Differentiation of tumour-promoting stromal myofibroblasts by cancer exosomes. *Oncogene* 34(3):290-302.
257. Varkaris A*, et al.* (2011) The role of HGF/c-Met signaling in prostate cancer progression and c-Met inhibitors in clinical trials. *Expert Opin Investig Drugs* 20(12):1677-1684.
258. Syn N, Wang L, Sethi G, Thiery JP, & Goh BC (2016) Exosome-Mediated Metastasis: From Epithelial-Mesenchymal Transition to Escape from Immunosurveillance. *Trends in Pharmacological Sciences* 37(7):606-617.
259. Jeppesen DK*, et al.* (2014) Quantitative proteomics of fractionated membrane and lumen exosome proteins from isogenic metastatic and nonmetastatic bladder cancer cells reveal differential expression of EMT factors. *Proteomics* 14(6):699-712.

260. Franzen CA*, et al.* (2015) Urothelial cells undergo epithelial-to-mesenchymal transition after exposure to muscle invasive bladder cancer exosomes. *Oncogenesis* 4:e163.
261. You Y*, et al.* (2015) Matrix metalloproteinase 13-containing exosomes promote nasopharyngeal carcinoma metastasis. *Cancer Science* 106(12):1669-1677.
262. Aga M*, et al.* (2014) Exosomal HIF1[alpha] supports invasive potential of nasopharyngeal carcinoma-associated LMP1-positive exosomes. *Oncogene* 33(37):4613-4622.
263. Costa-Silva B*, et al.* (2015) Pancreatic cancer exosomes initiate pre-metastatic niche formation in the liver. *Nat Cell Biol* 17(6):816-826.
264. Hood JL, San RS, & Wickline SA (2011) Exosomes Released by Melanoma Cells Prepare Sentinel Lymph Nodes for Tumor Metastasis. *Cancer Research* 71(11):3792-3801.
265. Peinado H*, et al.* (2012) Melanoma exosomes educate bone marrow progenitor cells toward a pro-metastatic phenotype through MET. *Nat Med* 18(6):883-891.
266. Rinderknecht M & Detmar M (2008) Tumor lymphangiogenesis and melanoma metastasis. *Journal of Cellular Physiology* 216(2):347-354.
267. Hoshino A*, et al.* (2015) Tumour exosome integrins determine organotropic metastasis. *Nature* 527(7578):329-335.
268. Luga V*, et al.* (Exosomes Mediate Stromal Mobilization of Autocrine Wnt-PCP Signaling in Breast Cancer Cell Migration. *Cell* 151(7):1542-1556.
269. Yue S, Mu W, Erb U, & Zöller M (2015) The tetraspanins CD151 and Tspan8 are essential exosome components for the crosstalk between cancer initiating cells and their surrounding. *Oncotarget* 6(4):2366-2384.
270. Radisky DC, Kenny PA, & Bissell MJ (2007) Fibrosis and Cancer: Do Myofibroblasts Come Also From Epithelial Cells Via EMT? *Journal of cellular biochemistry* 101(4):830-839.
271. Smith AL*, et al.* (2012) The miR-106b-25 cluster targets Smad7, activates TGF-[beta] signaling, and induces EMT and tumor initiating cell characteristics downstream of Six1 in human breast cancer. *Oncogene* 31(50):5162-5171.
272. Zheng R*, et al.* (2015) Prognostic value of miR-106b expression in breast cancer patients. *Journal of Surgical Research* 195(1):158-165.
273. Savita U & Karunagaran D (2013) MicroRNA-106b-25 cluster targets β-TRCP2, increases the expression of Snail and enhances cell migration and invasion in H1299 (non small cell lung cancer) cells. *Biochemical and Biophysical Research Communications* 434(4):841-847.
274. Tang Q*, et al.* (2014) Expression of miR-106b-25 induced by salvianolic acid B inhibits epithelial-to-mesenchymal transition in HK-2 cells. *European Journal of Pharmacology* 741:97-103.
275. Agarwal V, Bell GW, Nam J-W, & Bartel DP (2015) Predicting effective microRNA target sites in mammalian mRNAs. *eLife* 4:e05005.
276. Yu W*, et al.* (2014) MEF2 transcription factors promotes EMT and invasiveness of hepatocellular carcinoma through TGF-β1 autoregulation circuitry. *Tumor Biology* 35(11):10943-10951.
277. Hong X, Hong XY, Li T, & He CY (2015) Pokemon and MEF2D co-operationally promote invasion of hepatocellular carcinoma. *Tumor Biology* 36(12):9885-9893.
278. Su L*, et al.* (2016) MEF2D transduces microenvironment stimuli to ZEB1 to promote epithelial-mesenchymal transition and metastasis in colorectal cancer. *Cancer Research*:5050-5067.
279. Song SJ & Pandolfi PP (2014) miR-22 in tumorigenesis. *Cell Cycle* 13(1):11-12.
280. Ding L*, et al.* (2014) miR-22 expression in hepatocellular carcinoma: Correlation with E-cadherin and vimentin expression. *World Chinese Journal of Digestology* (21):3142-3147.

281. Baum J & Duffy HS (2011) Fibroblasts and Myofibroblasts: What are we talking about? *Journal of cardiovascular pharmacology* 57(4):376-379.
282. Willis BC, duBois RM, & Borok Z (2006) Epithelial Origin of Myofibroblasts during Fibrosis in the Lung. *Proceedings of the American Thoracic Society* 3(4):377-382.
283. Mann J*, et al.* (2010) MeCP2 Controls an Epigenetic Pathway That Promotes Myofibroblast Transdifferentiation and Fibrosis. *Gastroenterology* 138(2):705-714.e704.
284. Zhou P, Lu Y, & Sun XH (2011) Zebularine suppresses TGF-beta-induced lens epithelial cell- myofibroblast transdifferentiation by inhibiting MeCP2. *Molecular Vision* 17:2717-2723.
285. Nagpal V*, et al.* (2016) MiR-125b Is Critical for Fibroblast-to-Myofibroblast Transition and Cardiac Fibrosis. *Circulation* 133(3):291-301.
286. Yang Q*, et al.* (2015) MiR-125b regulates epithelial-mesenchymal transition via targeting Sema4C in paclitaxel-resistant breast cancer cells. *Oncotarget* 6(5):3268-3279.
287. Hong L*, et al.* (2016) miR-125b inhibited epithelial–mesenchymal transition of triple-negative breast cancer by targeting MAP2K7. *OncoTargets and Therapy* 9:2639-2648.
288. Zhou JN*, et al.* (2015) MicroRNA-125b attenuates epithelial-mesenchymal transitions and targets stem-like liver cancer cells through small mothers against decapentaplegic 2 and 4. *Hepatology* 62(3):801-815.
289. Zhang J*, et al.* (2016) MicroRNA-125b suppresses the epithelial–mesenchymal transition and cell invasion by targeting ITGA9 in melanoma. *Tumor Biology* 37(5):5941-5949.
290. Giannoni E*, et al.* (2010) Reciprocal Activation of Prostate Cancer Cells and Cancer-Associated Fibroblasts Stimulates Epithelial-Mesenchymal Transition and Cancer Stemness. *Cancer Research* 70(17):6945-6956.
291. Veveris-Lowe TL*, et al.* (2005) Kallikrein 4 (hK4) and prostate-specific antigen (PSA) are associated with the loss of E-cadherin and an epithelial-mesenchymal transition (EMT)-like effect in prostate cancer cells. *Endocrine-Related Cancer* 12(3):631-643.
292. Shi X-B*, et al.* (2011) miR-125b promotes growth of prostate cancer xenograft tumor through targeting pro-apoptotic genes. *The Prostate* 71(5):538-549.
293. Roach KM, Wulff H, Feghali-Bostwick C, Amrani Y, & Bradding P (2014) Increased constitutive αSMA and Smad2/3 expression in idiopathic pulmonary fibrosis myofibroblasts is K(Ca)3.1-dependent. *Respiratory Research* 15(1):155.
294. Heldin CH, Vanlandewijck M, & Moustakas A (2012) Regulation of EMT by TGFβ in cancer. *FEBS Letters* 586(14):1959-1970.
295. Phanish MK, Wahab NA, Colville-Nash P, Hendry BM, & Dockrell MEC (2006) The differential role of Smad2 and Smad3 in the regulation of pro-fibrotic TGFβ1 responses in human proximal-tubule epithelial cells. *Biochemical Journal* 393(2):601-607.
296. Baumann F (2005) Small-scale biomanufacturing benefits from disposable bioreactors. *BioPharm International* 18(12):22-25+30.
297. Butz H*, et al.* (2016) Exosomal MicroRNAs Are Diagnostic Biomarkers and Can Mediate Cell-Cell Communication in Renal Cell Carcinoma. *European Urology Focus* 2(2):210-218.
298. Franzen CA*, et al.* (2016) Urinary exosomes: The potential for biomarker utility, intercellular signaling and therapeutics in urological malignancy. *Journal of Urology* 195(5):1331-1339.
299. Liu Y*, et al.* (2016) STAT3-regulated exosomal miR-21 promotes angiogenesis and is involved in neoplastic processes of transformed human bronchial epithelial cells. *Cancer Letters* 370(1):125-135.

300. Chevillet JR*, et al.* (2014) Quantitative and stoichiometric analysis of the microRNA content of exosomes. *Proceedings of the National Academy of Sciences of the United States of America* 111(41):14888-14893.
301. King HW, Michael MZ, & Gleadle JM (2012) Hypoxic enhancement of exosome release by breast cancer cells. *BMC Cancer* 12(1):1-10.
302. Tian T*, et al.* (2013) Dynamics of exosome internalization and trafficking. *Journal of Cellular Physiology* 228(7):1487-1495.
303. Straussman R*, et al.* (2012) Tumour micro-environment elicits innate resistance to RAF inhibitors through HGF secretion. *Nature* 487(7408):500-504.
304. Knudsen BS & Edlund M (2004) Prostate Cancer and the Met Hepatocyte Growth Factor Receptor. *Advances in Cancer Research* 91:31-67.
305. Yaqinuddin A*, et al.* (2008) Silencing of MBD1 and MeCP2 in prostate-cancer-derived PC3 cells produces differential gene expression profiles and cellular phenotypes. *Bioscience reports* 28(6):319-326.
306. Bernard D*, et al.* (2006) The methyl-CpG-binding protein MECP2 is required for prostate cancer cell growth. *Oncogene* 25(9):1358-1366.
307. Shu L*, et al.* (2011) Epigenetic CpG Demethylation of the Promoter and Reactivation of the Expression of Neurog1 by Curcumin in Prostate LNCaP Cells. *BMC Biology*:1-9.
308. Herbst A*, et al.* (2011) Methylation of NEUROG1 in serum is a sensitive marker for the detection of early colorectal cancer. *American Journal of Gastroenterology* 106(6):1110-1118.
309. Lee J, Lee MS, Jeoung DI, Kim YM, & Lee H (2017) Promoter CpG-Site Methylation of the KAI1 Metastasis Suppressor Gene Contributes to Its Epigenetic Repression in Prostate Cancer. *Prostate* 77(4):350-360.
310. Hortin GL & Sviridov D (2010) The dynamic range problem in the analysis of the plasma proteome. *Journal of Proteomics* 73(3):629-636.
311. Zhou H*, et al.* (2006) Collection, storage, preservation, and normalization of human urinary exosomes for biomarker discovery. *Kidney International* 69(8):1471-1476.
312. Lv LL*, et al.* (2013) Isolation and quantification of MicroRNAs from urinary exosomes/microvesicles for biomarker discovery. *International Journal of Biological Sciences* 9(10):1021-1031.
313. Filella X & Foj L (2015) Emerging biomarkers in the detection and prognosis of prostate cancer. *Clinical Chemistry and Laboratory Medicine* 53(7):963-973.
314. Raja J, Ramachandran N, Munneke G, & Patel U (Current status of transrectal ultrasound-guided prostate biopsy in the diagnosis of prostate cancer. *Clinical Radiology* 61(2):142-153.
315. Stuopelyte K*, et al.* (2016) The utility of urine-circulating miRNAs for detection of prostate cancer. *British Journal of Cancer*.
316. Koppers-Lalic D*, et al.* (2016) Non-invasive prostate cancer detection by measuring miRNA variants (isomiRs) in urine extracellular vesicles. *Oncotarget* 7(16):22566-22578.
317. Gao Y*, et al.* (2016) Analysis of circulating miRNAs 21 and 375 as potential biomarkers for early diagnosis of prostate cancer. *Neoplasma* 63(4):623-628.
318. Volinia S*, et al.* (2006) A microRNA expression signature of human solid tumors defines cancer gene targets. *Proceedings of the National Academy of Sciences of the United States of America* 103(7):2257-2261.
319. Phillips SM*, et al.* (1994) Loss of the retinoblastoma susceptibility gene (RB1) is a frequent and early event in prostatic tumorigenesis. *British Journal of Cancer* 70(6):1252-1257.
320. Geck P, Szelei J, Jimenez J, Sonnenschein C, & Soto AM (1999) Early gene expression during androgen-induced inhibition of proliferation of prostate cancer cells: A new

suppressor candidate on chromosome 13, in the BRCA2-Rb1 locus. *Journal of Steroid Biochemistry and Molecular Biology* 68(1-2):41-50.
321. Li C*, et al.* (1998) Identification of two distinct deleted regions on chromosome 13 in prostate cancer. *Oncogene* 16(4):481-487.
322. Macleod KF (2010) The RB tumor suppressor: a gatekeeper to hormone independence in prostate cancer? *The Journal of Clinical Investigation* 120(12):4179-4182.
323. Sharma A*, et al.* (2010) The retinoblastoma tumor suppressor controls androgen signaling and human prostate cancer progression. *The Journal of Clinical Investigation* 120(12):4478-4492.
324. Sharova E*, et al.* (2016) A circulating miRNA assay as a first-line test for prostate cancer screening. *British Journal of Cancer* 114(12):1362-1366.
325. Zhu J*, et al.* (2015) Screening key microRNAs for castration-resistant prostate cancer based on miRNA/mRNA functional synergistic network. *Oncotarget* 6(41):43819-43830.
326. Fujii T, Shimada K, Tatsumi Y, Fujimoto K, & Konishi N (2015) Syndecan-1 responsive microRNA-126 and 149 regulate cell proliferation in prostate cancer. *Biochemical and Biophysical Research Communications* 456(1):183-189.
327. Zhao T & Liu J (2014) MiR-149 inhibition of cell growth and invasion by targeting FOXM1 in human prostate carcinoma. *Chinese Journal of Clinical Oncology* 41(17):1080-1083.
328. Dhar S, Hicks C, & Levenson AS (2011) Resveratrol and prostate cancer: Promising role for microRNAs. *Molecular Nutrition and Food Research* 55(8):1219-1229.
329. Hart M*, et al.* (2014) Comparative microrna profiling of prostate carcinomas with increasing tumor stage by deep sequencing. *Molecular Cancer Research* 12(2):250-263.
330. Haldrup C*, et al.* (2014) Profiling of circulating microRNAs for prostate cancer biomarker discovery. *Drug Delivery and Translational Research* 4(1):19-30.
331. Nguyen HCN*, et al.* (2013) Expression differences of circulating microRNAs in metastatic castration resistant prostate cancer and low-risk, localized prostate cancer. *Prostate* 73(4):346-354.
332. Wach S*, et al.* (2015) The combined serum levels of miR-375 and urokinase plasminogen activator receptor are suggested as diagnostic and prognostic biomarkers in prostate cancer. *International Journal of Cancer* 137(6):1406-1416.
333. Huang X*, et al.* (2013) Characterization of human plasma-derived exosomal RNAs by deep sequencing. *BMC Genomics* 14(1):319.
334. Lambertz U*, et al.* (2015) Small RNAs derived from tRNAs and rRNAs are highly enriched in exosomes from both old and new world Leishmania providing evidence for conserved exosomal RNA Packaging. *BMC Genomics* 16(1):151.
335. van Balkom BWM, Eisele AS, Pegtel DM, Bervoets S, & Verhaar MC (2015) Quantitative and qualitative analysis of small RNAs in human endothelial cells and exosomes provides insights into localized RNA processing, degradation and sorting. *Journal of Extracellular Vesicles; Vol 4 (2015) incl supplements*.
336. Gezer U, Özgür E, Cetinkaya M, Isin M, & Dalay N (2014) Long non-coding RNAs with low expression levels in cells are enriched in secreted exosomes. *Cell Biology International* 38(9):1076-1079.
337. Zhang J*, et al.* (2016) Exosomal Long Noncoding RNAs are Differentially Expressed in the Cervicovaginal Lavage Samples of Cervical Cancer Patients. *Journal of Clinical Laboratory Analysis*.
338. Ahadi A, Khoury S, Losseva M, & Tran N (2016) A comparative analysis of lncRNAs in prostate cancer exosomes and their parental cell lines. *Genomics Data* 9:7-9.
339. Takahashi K, Yan IK, Wood J, Haga H, & Patel T (2014) Involvement of extracellular vesicle long noncoding RNA (linc-VLDLR) in tumor cell responses to chemotherapy. *Molecular Cancer Research* 12(10):1377-1387.

340. Conigliaro A*, et al.* (2015) CD90+ liver cancer cells modulate endothelial cell phenotype through the release of exosomes containing H19 lncRNA. *Molecular Cancer* 14(1).
341. Qu L*, et al.* (2016) Exosome-Transmitted lncARSR Promotes Sunitinib Resistance in Renal Cancer by Acting as a Competing Endogenous RNA. *Cancer Cell* 29(5):653-668.
342. Yang Y, Zhou X, & Jin Y (2013) ADAR-mediated RNA editing in non-coding RNA sequences. *Science China Life Sciences* 56(10):944-952.
343. Picardi E, D'Erchia AM, Gallo A, Montalvo A, & Pesole G (2014) Uncovering RNA Editing Sites in Long Non-Coding RNAs. *Frontiers in Bioengineering and Biotechnology* 2:64.
344. Chen I, Chen CY, & Chuang TJ (2015) Biogenesis, identification, and function of exonic circular RNAs. *Wiley Interdisciplinary Reviews: RNA* 6(5):563-579.
345. Chakraborty S, Deb A, Maji RK, Saha S, & Ghosh Z (2014) LncRBase: An Enriched Resource for lncRNA Information. *PLoS ONE* 9(9):e108010.
346. Lagarde J*, et al.* (2016) Extension of human lncRNA transcripts by RACE coupled with long-read high-throughput sequencing (RACE-Seq). *Nature Communications* 7.
347. Chi KR (2016) Finding function in mystery transcripts. *Nature* 529(7586):423-425.
348. Mehrotra PT*, et al.* (1998) Production of IL-10 by Human Natural Killer Cells Stimulated with IL-2 and/or IL-12. *The Journal of Immunology* 160(6):2637-2644.
349. Park JY*, et al.* (2011) IL-15-Induced IL-10 Increases the Cytolytic Activity of Human Natural Killer Cells. *Molecules and Cells* 32(3):265-272.
350. Mocellin S*, et al.* (2004) IL-10 stimulatory effects on human NK cells explored by gene profile analysis. *Genes Immun* 5(8):621-630.
351. Zheng LM*, et al.* (1996) Interleukin-10 inhibits tumor metastasis through an NK cell-dependent mechanism. *Journal of Experimental Medicine* 184(2):579-584.
352. Kim MT*, et al.* (2015) Enhancing Dendritic Cell–based Immunotherapy with IL-2/Monoclonal Antibody Complexes for Control of Established Tumors. *The Journal of Immunology*.
353. Pan J*, et al.* (2004) Interferon-γ is an autocrine mediator for dendritic cell maturation. *Immunology Letters* 94(1–2):141-151.
354. He T, Tang C, Xu S, Moyana T, & Xiang J (2007) Interferon gamma stimulates cellular maturation of dendritic cell line DC2.4 leading to induction of efficient cytotoxic T cell responses and antitumor immunity. *Cellular & molecular immunology* 4(2):105-111.
355. Miwa S*, et al.* (2012) TNF-α and Tumor Lysate Promote the Maturation of Dendritic Cells for Immunotherapy for Advanced Malignant Bone and Soft Tissue Tumors. *PLoS ONE* 7(12).
356. Pirtskhalaishvili G, Shurin GV, Esche C, Trump DL, & Shurin MR (2001) TNF-α protects dendritic cells from prostate cancer-induced apoptosis. *Prostate Cancer and Prostatic Diseases* 4(4):221-227.
357. Li J & Fine J (2004) On sample size for sensitivity and specificity in prospective diagnostic accuracy studies. *Statistics in Medicine* 23(16):2537-2550.

Glossary

3'UTR: 3 Prime Untranslated Region

5'UTR: 5 Prime Untranslated Region

ADCC: Antibody Dependent Cell-Mediated Cytotoxicity

AFM: Atomic Force Microscopy

AGO1-4: Argonaute proteins 1-4

AI: Androgen Independent

AQP2: Aquaporin 2

AR: Aggregation Reagents

BAN: 4-Bromoanisole

BIM: BCL2-like 11 (apoptosis facilitator)

BMDC: Bone Marrow Derived Cell

BPH: Benign Prostatic Hyperplasia

BSA: Bovine Serum Albumin

C3PO: Component 3 Promoter of RISC

CAmiRs: Cancer Associated MicroRNAs

CCR4-NOT1: Carbon Catabolite Repression 4-Negative On TATA-less complex

CD9: Cluster Designation 9

CD34: Cluster Designation 34

CD63: Cluster Designation 63

CD44: Cluster Designation 44

CD81: Cluster Designation 81

CDK: Cyclin Dependent Kinase

cDNA: Complementary DNA

CLL: Chronic Lymphocytic Leukaemia

CRPC: Castration Resistant Prostate Cancer

CS: Culture Supernatant

CTL: Cytotoxic Lyphmocyte

DC: Dendritic Cell

DCP1/2: Decapping Complex

dNTPs: deoxynucleotide triphosphate

DPBS: Dulbecco's Phosphate Buffered Saline

DRE: Digital Rectal Examination

dsRNA: double stranded RNA

DTT: Dithiothreitol

DU: Differential Ultracentrifugation

E2F3: Transcription Factor E2F3

ECM: Extracellular Matrix

EDM: Exosome Differentiated Myofibroblast

EMT: Epithelial to Mesenchymal Transition

EpCAM: Epithelial Cell Adhesion Molecule

ESRRG: Estrogen receptor-related receptor gamma

EV: Extracellular Vesicle

ExomiR: Exosomal MicroRNA

exoRNA: exosomal RNA

FasL: Fas Ligand

FCS: Foetal Calf Serum

FDR: False Discovery Rate

GW182: Trinucleotide repeat-containing gene 6A protein

HCV: Hepatitis C Virus

HDAC4: Histone Deacetylase 4

HGF: Hepatocyte Growth Factor

HMGA2: High Mobility Group A2

HOTAIR: Hox Transcript Antisense RNA

HOXB8: homeobox B8

HU: Healthy Volunteer Urine

IA: Immunoaffinity

IA-MD: Immunoaffinity - Microfluidic hybrid Devices

IFNγ: Interferon Gamma

IL-2: Interleukin-2

IL-4: Interleukin-4

IL-10: Interleukin 10

IRES: Internal Ribosome Entry Site

ISEV: International SAociety for Extracellular Vesicles

KDa: Kilodaltons

lncARSR: lncRNA Activated in RCC with Sunitinib Resistance

lncRNA: Long Noncoding RNA

Ldbr: Lariat De-Branching Enzyme

LSI: Low Sample Input

M^7G: 5 prime methyl cap

MALAT1: metastasis associated lung adenocarcinoma transcript 1

MDSC: Myeloid Derived Suppressor Cell

MECP2: Methyl-CpG Binding Protein 2

MEF2D: myocyte enhancer factor 2D

MEG3: Maternally Expressed 3

miRNA: MicroRNA

mRNA: Messenger RNA

MVB: Multi-Vesicular Body

MWCO: Molecular Weight Cut-Off

MYC: proto-oncogene c-Myc

NK cell: Natural Killer cell

NKG2D: NK cell receptor D

NO: Nitric Oxide

NTA: Nanoparticle Tracking Analysis

NRT: No Reverse Transcriptase Control

NTC: No Template Control

OC2: ONECUT2

ORF: Open Reading Frame

p53: p53 tumour suppressor protein

PABP: Poly-A Binding Protein

PCa: Prostate Cancer

PCR: Polymerase Chain Reaction

PES: Polyethersulfone

PGE2: Prostaglandin E2

PIWI: P-element induced wimpy testis domain

PSA: Prostate Specific Antigen

PTEN: Phosphate and Tensin Homolog

PU: Prostate Cancer Patient Urine

PxU: Prostate Cancer Patient urine Taken After Radical Prostatectomy

qPCR: Quantitative Real Time Polymerase Chain Reaction

RA: Retinoic Acid

RAS: Rat Sarcoma small GTPase

RI: Refractive Index

RIN: RNA Integrity number

RISC: RNA Induced Silencing Complex

RLC: RISC Loading Complex

RNAi: RNA interference

ROC: Receiver Operating Characteristic

SCID: Severe Combined Immundoficiency

SEC: Size Exclusion Chromatography

SEM: Scanning Electron Microscope

siRNA: Small Interfering RNA

SMAD7: Mothers against decapentaplegic homolog 7

sp1: specificity protein 1

STDM: Soluble TGFβ Differentiated Myofibroblast

TEM: Transmission Electron Microscopy

Th1/2: T helper type 1 or 2

THP: Tamm-Horsfall Protein

TNFα: Tumour Necrosis Factor Aplha

TGFβ: Transforming Growth Factor Beta

TRAIL: TNF-related apoptosis-inducing ligand

TRBP: TAR RNA Binding Protein

TRF: Time Resolved Fluorescence

Treg: Regulator T cell

TSG101: Tumour Susceptibility Gene 101

UC: Ultracentrifugation

UF: Ultrafiltration

Xrn1: exoribonuclease 1 enzyme